ISSN: 2067 – 3809

ACTA TECHNICA CORVINIENSIS – BULLETIN of ENGINEERING

Tome IX [2016]
Fascicule 3
[July – September]

INDEXES & DATABASES

ACTA TECHNICA CORVINIENSIS – BULLETIN of ENGINEERINGis accredited and ranked in the "B+" CATEGORY Journal by CNCSIS – The National University Research Council's Classification of Romanian Journals, positionno. 940 (http://cncsis.gov.ro/).
ACTA TECHNICA CORVINIENSIS – BULLETIN of ENGINEERINGis a part of theSCIPIO - The Romanian Editorial Platform (http://www.scipio.ro/).

ACTA TECHNICA CORVINIENSIS – BULLETIN of ENGINEERINGis indexed, abstracted and covered in the world-known bibliographicaldatabases and directories including:
INDEX COPERNICUS – JOURNAL MASTER LIST
http://journals.indexcopernicus.com/
GENAMICSJOURNALSEEK Database
http://journalseek.net/
DOAJ – Directory of Open Access Journals
http://www.doaj.org/
EVISA Database
http://www.speciation.net/
CHEMICAL ABSTRACTS SERVICE (CAS)
http://www.cas.org/
EBSCO Publishing
http://www.ebscohost.com/
GOOGLE SCHOLAR
http://scholar.google.com
SCIRUS - Elsevier
http://www.scirus.com/
ULRICHSweb – Global serials directory
http://ulrichsweb.serialssolutions.com
getCITED
http://www.getcited.org
BASE - Bielefeld Academic Search Engine
http://www.base-search.net
Electronic Journals Library
http://rzblx1.uni-regensburg.de
Open J-Gate
http://www.openj-gate.com
ProQUEST Research Library
http://www.proquest.com
Directory of Research Journals Indexing
http://www.drji.org/
Directory Indexing of International Research Journals
http://www.citefactor.org/

ACTA TECHNICA CORVINIENSIS – BULLETIN of ENGINEERING is also indexed in the digital libraries of the following world's universities and research centers:
WorldCat – the world's largest library catalog
https://www.worldcat.org/
National Lybrary of Australia
http://trove.nla.gov.au/
University Library of Regensburg – GIGA German Institute of Global and Area Studies
http://opac.giga-hamburg.de/ezb/
Simon Fraser University – Electronic Journals Library
http://cufts2.lib.sfu.ca/
University of Wisconsin-Madison Libraries
http://library.wisc.edu/
University of Toronto Libraries
http://search.library.utoronto.ca/
The University of Queensland
https://www.library.uq.edu.au/
The New York Public Library
http://nypl.bibliocommons.com/
State Library of New South Wales
http://library.sl.nsw.gov.au/
University of Alberta Libraries - University of Alberta
http://www.library.ualberta.ca/
The University of Hong Kong Libraries
http://sunzi.lib.hku.hk/
The University Library - The University of California
http://harvest.lib.ucdavis.edu/

We are very pleased to inform that our international scientific journal ACTA TECHNICA CORVINIENSIS - Bulletin of Engineering completed its eight years of publication successfully [2008–2015, Tome I–VIII].
In a very short period the ACTA TECHNICA CORVINIENSIS - Bulletin of Engineering has acquired global presence and scholars from all over the world have taken it with great enthusiasm.
We are extremely grateful and heartily acknowledge the kind of support and encouragement from all contributors and all collaborators!

ACTA TECHNICA CORVINIENSIS
– Bulletin of Engineering
Tome IX [2016], Fascicule 4 [October – December]
ISSN: 2067 – 3809

AIMS, MISSION & SCOPE

General Aims

ACTA TECHNICA CORVINIENSIS – Bulletin of Engineering has been published since 2008, as an online supplement of the**ANNALS OF FACULTY ENGINEERING HUNEDOARA – International Journal Of Engineering**. Now, the **ACTA TECHNICA CORVINIENSIS – Bulletin of Engineering**is a free-access, online, international and multidisciplinary publication of the Faculty of Engineering Hunedoara. **ACTA TECHNICA CORVINIENSIS – BULLETIN OF ENGINEERING**exchange similar publications with similar institutions of our country and from abroad.

ACTA TECHNICA CORVINIENSIS – Bulletin of Engineeringis an international and interdisciplinary journal which reports on scientific and technical contributions. Every year, in four online issues (fascicules 1 – 4), **ACTA TECHNICA CORVINIENSIS – Bulletin of Engineering[e-ISSN: 2067-3809]** publishes a series of reviews covering the most exciting and developing areas of engineering. Each issue contains papers reviewed by international researchers who are experts in their fields. The result is a journal that gives the scientists and engineers the opportunity to keep informed of all the current developments in their own, and related, areas of research, ensuring the new ideas across an increasingly the interdisciplinary field. Topical reviews in materials science and engineering, each including:

- ✓ surveys of work accomplished to date
- ✓ current trends in research and applications
- ✓ future prospects.

As an open-access journal **ACTA TECHNICA CORVINIENSIS – Bulletin of Engineering** will serve the whole engineering research community, offering a stimulating combination of the following:

- ✓ Research Papers – concise, high impact original research articles,
- ✓ Scientific Papers – concise, high impact original theoretical articles,
- ✓ Perspectives – commissioned commentaries highlighting the impact and wider implications of research appearing in the journal.

ACTA TECHNICA CORVINIENSIS – Bulletin of Engineeringencourages the submission of comments on papers published particularly in our journal. The journal publishes articles focused on topics of current interest within the scope of the journal and coordinated by invited guest editors. Interested authors are invited to contact one of the Editors for further details.

Mission

ACTA TECHNICA CORVINIENSIS – Bulletin of Engineeringis an international and interdisciplinary journal which reports on scientific and technical contributions. The **ACTA TECHNICA CORVINIENSIS – Bulletin of Engineering** advances the understanding of both the fundamentals of engineering science and its application to the solution of challenges and problems in engineering and management, dedicated to the publication of high quality papers on all aspects of the engineering sciences and the management.

You are invited to contribute review or research papers as well as opinion in the fields of science and technology including engineering. We accept contributions (full papers) in the fields of applied sciences and technology including all branches of engineering and management. Submission of a paper implies that the work described has not been published previously (except in the form of an abstract or as part of a published lecture or academic thesis) that it is not under consideration for publication elsewhere. It is not accepted to submit materials which in any way violate copyrights of third persons or law rights. An author is fully responsible ethically and legally for breaking given conditions or misleading the Editor or the Publisher.

The Editor reserves the right to return papers that do not conform to the instructions for paper preparation and template as well as papers that do not fit the scope of the journal, prior to refereeing. The Editor reserves the right not to accept the paper for print in the case of a negative review made by reviewers and also in the case of not paying the required fees if such will be fixed and in the case time of waiting for the publication of the paper would extend the period fixed by the Editor as a result of too big number of papers waiting for print. The decision of the Editor in that matter is irrevocable and their aim is care about the high content-related level of that journal.

The mission of the **ACTA TECHNICA CORVINIENSIS – Bulletin of Engineering** is to disseminate academic knowledge across the scientific realms and to provide applied research knowledge to the appropriate stakeholders. We are keen to receive original contributions from researchers representing any Science related

field.
We strongly believe that the open access model will spur research across the world especially as researchers gain unrestricted access to high quality research articles. Being an Open Access Publisher, Academic Journals does not receive payment for subscription as the journals are freely accessible over the internet.

General Topics

ENGINEERING
- ✓ Mechanical Engineering
- ✓ Metallurgical Engineering
- ✓ Agricultural Engineering
- ✓ Control Engineering
- ✓ Electrical Engineering
- ✓ Civil Engineering
- ✓ Biomedical Engineering
- ✓ Transport Engineering
- ✓ Nanoengineering

CHEMISTRY
- ✓ General Chemistry
- ✓ Analytical Chemistry
- ✓ Inorganic Chemistry
- ✓ Materials Science & Metallography
- ✓ Polymer Chemistry
- ✓ Spectroscopy
- ✓ Thermo-chemistry

ECONOMICS
- ✓ Agricultural Economics
- ✓ Development Economics
- ✓ Environmental Economics
- ✓ Industrial Organization
- ✓ Mathematical Economics
- ✓ Monetary Economics
- ✓ Resource Economics
- ✓ Transport Economics
- ✓ General Management
- ✓ Managerial Economics
- ✓ Logistics

AGRICULTURE
- ✓ Agricultural & Biological Engineering
- ✓ Food Science & Engineering
- ✓ Horticulture

INFORMATION SCIENCES
- ✓ Computer Science
- ✓ Information Science

EARTH SCIENCES
- ✓ Geodesy
- ✓ Geology
- ✓ Hydrology
- ✓ Seismology
- ✓ Soil science

ENVIRONMENTAL
- ✓ Environmental Chemistry
- ✓ Environmental Science & Ecology
- ✓ Environmental Soil Science
- ✓ Environmental Health

BIOTECHNOLOGY
- ✓ Biomechanics
- ✓ Biotechnology
- ✓ Biomaterials

MATHEMATICS
- ✓ Applied mathematics
- ✓ Modeling & Optimization
- ✓ Foundations & methods

Invitation

We are looking forward to a fruitful collaboration and we welcome you to publish in our **ACTA TECHNICA CORVINIENSIS – Bulletin of Engineering**. You are invited to contribute review or research papers as well as opinion in the fields of science and technology including engineering. We accept contributions (full papers) in the fields of applied sciences and technology including all branches of engineering and management.
ACTA TECHNICA CORVINIENSIS – Bulletin of Engineeringpublishes invited review papers covering the full spectrum of engineering and management. The reviews, both experimental and theoretical, provide general background information as well as a critical assessment on topics in a state of flux. We are primarily interested in those contributions which bring new insights, and papers will be selected on the basis of the importance of the new knowledge they provide.
Submission of a paper implies that the work described has not been published previously (except in the form of an abstract or as part of a published lecture or academic thesis) that it is not under consideration for publication elsewhere. It is not accepted to submit materials which in any way violate copyrights of third persons or law rights. An author is fully responsible ethically and legally for breaking given conditions or misleading the Editor or the Publisher.

ACTA TECHNICA CORVINIENSIS
– Bulletin of Engineering
Tome IX [2016], Fascicule 4 [October – December]
ISSN: 2067 – 3809

ASSOCIATE EDITORS & REGIONAL COLLABORATORS

The Editor and editorial board membersdo not receive any remuneration. These positions are voluntary. The members of the Editorial Board may serve as scientific reviewers.

We are very pleased to inform that our journal **ACTA TECHNICA CORVINIENSIS – Bulletin of Engineering**is going to complete its eight years of publication successfully. In a very short period it has acquired global presence and scholars from all over the world have taken it with great enthusiasm. We are extremely grateful and heartily acknowledge the kind of support and encouragement from you.

ACTA TECHNICA CORVINIENSIS – Bulletin of Engineeringseeking qualified researchers as members of the editorial team. Like our other journals, **ACTA TECHNICA CORVINIENSIS – Bulletin of Engineering**will serve as a great resource for researchers and students across the globe. We ask you to support this initiative by joining our editorial team. If you are interested in serving as a member of the editorial team, kindly send us your resume to redactie@fih.upt.ro.

ACTA Technica CORVINIENSIS
BULLETIN OF ENGINEERING

ISSN:2067-3809

ACTA TECHNICA CORVINIENSIS
– Bulletin of Engineering
Tome IX [2016], Fascicule 4 [October – December]
ISSN: 2067 – 3809

INTERNATIONAL SCIENTIFIC COMMITTEE & SCIENTIFIC REVIEWERS

Manager & Chairman

Romania

Imre KISS , University Politehnica TIMISOARA, Faculty of Engineering HUNEDOARA, Department of Engineering & Management, General Association of Romanian Engineers (AGIR) – branch HUNEDOARA

International Scientific Committee Members &Scientific Reviewers from:

Slovakia

Štefan NIZNIK, Technical University of KOŠICE – KOŠICE
Karol VELIŠEK, Slovak University of Technology BRATISLAVA – TRNAVA
Juraj ŠPALEK, University of ŽILINA – ŽILINA
Ľubomir ŠOOŠ, Slovak University of Technology in BRATISLAVA – BRATISLAVA
Miroslav BADIDA, Technical University of KOŠICE – KOŠICE
Ervin LUMNITZER, Technical University of KOŠICE – KOŠICE
Ladislav GULAN, Slovak University of Technology – BRATISLAVA
Milan DADO, University of ŽILINA – ŽILINA
Miroslav VEREŠ, Slovak University of Technology in BRATISLAVA – BRATISLAVA
Milan SAGA,University of ŽILINA – ŽILINA
Imrich KISS, Institute of Economic & Environmental Security – KOŠICE
Michal CEHLÁR,Technical University KOSICE – KOSICE
Pavel NEČAS,Armed Forces Academy of General Milan Rastislav Stefanik – LIPTOVSKÝ MIKULÁŠ
Vladimir MODRAK, Technical University of KOSICE – PRESOV
Michal HAVRILA, Technical University of KOSICE – PRESOV
Dušan HUSKA,Slovak Agricultural University – NITRA

Romania

Teodor HEPUŢ, University Politehnica TIMIŞOARA – HUNEDOARA
Caius PĂNOIU, University Politehnica TIMIŞOARA – HUNEDOARA
Carmen ALIC, University Politehnica TIMIŞOARA – HUNEDOARA
Iulian RIPOŞAN, University Politehnica BUCUREŞTI – BUCUREŞTI
Ioan MĂRGINEAN, University Politehnica BUCUREŞTI – BUCUREŞTI
Victor BUDĂU, University Politehnica TIMIŞOARA – TIMIŞOARA
Liviu MIHON, University Politehnica TIMIŞOARA – TIMIŞOARA
Mircea BEJAN, Tehnical University of CLUJ-NAPOCA – CLUJ-NAPOCA
Ioan VIDA-SIMITI, Technical University of CLUJ-NAPOCA – CLUJ-NAPOCA
Csaba GYENGE, Technical University of CLUJ-NAPOCA – CLUJ-NAPOCA
Laurenţiu POPPER, University of ORADEA – ORADEA
Sava IANICI, "Eftimie Murgu" University of REŞIŢA – REŞIŢA
Ioan SZÁVA,"Transilvania" University of BRASOV – BRASOV
Liviu NISTOR, Technical University of CLUJ-NAPOCA – CLUJ-NAPOCA
Sorin VLASE,"Transilvania" University of BRASOV – BRASOV
Horatiu TEODORESCU DRĂGHICESCU,"Transilvania" University of BRASOV – BRASOV
Maria Luminita SCUTARU,"Transilvania" University of BRASOV – BRASOV

Italy

Alessandro GASPARETTO, University of UDINE – UDINE
Alessandro RUGGIERO, University of SALERNO– SALERNO
Adolfo SENATORE, University of SALERNO– SALERNO
Enrico LORENZINI, University of BOLOGNA – BOLOGNA

ACTA TECHNICA CORVINIENSIS – Bulletin of Engineeringis dedicated to publishing material of the highest engineering interest, and to this end we have assembled a distinguished Editorial Board and Scientific Committee of academics, professors and researchers. **ACTA TECHNICA CORVINIENSIS – Bulletin of Engineering** publishes invited review papers covering the full spectrum of engineering. The reviews, both experimental and theoretical, provide general background information as well as a critical assessment on topics in a state of flux. We are primarily interested in those contributions which bring new insights, and papers will be selected on the basis of the importance of the new knowledge they provide.

ACTA TECHNICA CORVINIENSIS – Bulletin of Engineeringencourages the submission of comments on papers published particularly in our journal. The journal publishes articles focused on topics of current interest within the scope of the journal and coordinated by invited guest editors. Interested authors are invited to contact one of the Editors for further details.

ACTA TECHNICA CORVINIENSIS – Bulletin of Engineeringaccept for publication unpublished manuscripts on the understanding that the same manuscript is not under simultaneous consideration of other journals. Publication of a part of the data as the abstract of conference proceedings is exempted.
Manuscripts submitted (original articles, technical notes, brief communications and case studies) will be subject to peer review by the members of the Editorial Board or by qualified outside reviewers. Only papers of high scientific quality will be accepted for publication. Manuscripts are accepted for review only when they report unpublished work that is not being considered for publication elsewhere. The evaluated paper may be recommended for:

- ✓ **Acceptance without any changes** – in that case the authors will be asked to send the paper electronically in the required .doc format according to authors' instructions;
- ✓ **Acceptance with minor changes** – if the authors follow the conditions imposed by referees the paper will be sent in the required .doc format;
- ✓ **Acceptance with major changes** – if the authors follow completely the conditions imposed by referees the paper will be sent in the required .doc format;
- ✓ **Rejection** – in that case the reasons for rejection will be transmitted to authors along with some suggestions for future improvements (if that will be considered necessary).

The manuscript accepted for publication will be published in the next issue of **ACTA TECHNICA CORVINIENSIS – Bulletin of Engineering** after the acceptance date.

All the authors and the corresponding author in particular take the responsibility to ensure that the text of the article does not contain portions copied from any other published material which amounts to plagiarism. We also request the authors to familiarize themselves with the good publication ethics principles before finalizing their manuscripts.

ACTA TECHNICA CORVINIENSIS
– Bulletin of Engineering
Tome IX [2016], Fascicule 4 [October – December]
ISSN: 2067 – 3809

TABLE of CONTENTS
ACTA TECHNICA CORVINIENSIS
– Bulletin of Engineering
Tome IX [2016] ,
Fascicule 4 [October – December]

Abstract: Mechanical vibration on the human body they represent a very dangerous factor, in fact they have been / and are considered by many researchers in the field, using various methods to reduce their dangerous values. In the field of automotive, mechanical vibration are induced by the tread and their functional mechanisms, it is transmitted to the human body mostly through the chassis and seats. Thus, in order to reduce dangerous values on while driving, as well as increasing the comfort were achieved various systems such as: magneto-rheological dampers to the vehicle structure and seat with air suspension, but can undertake research for development of new elements for amortization of shocks and vibrations at their level.
Keywords: magnets, neodymium, damper

Abstract: Five plies of Heliopol 9431ATYX_LSE/Stratimat300 glass fabric (300 g/m^2 specific weight), 6 mm thick laminate has been considered for experimental characterization using the three-point bend tests. Following distributions have been experimentally determined on five layers of Heliopol 9431ATYX_LSE/Stratimat300 glass fabric specimens using data recorded by the materials testing machine: Load (N)-deflection (mm), Stiffness (N/m) of each specimen, Young's Modulus of Bending (MPa) of each specimen, Flexural Rigidity (Nm^2) according to each specimen, Maximum Bending Stress at Maximum Load (MPa)-Maximum Bending Strain at Maximum Load, Work to Maximum Load (Nmm) of each specimen, Load at Break (kN)-Deflection at Break (mm), Maximum Bending Stress at Break (MPa)- Maximum Bending Strain at Break and Work to Break (Nmm) of each specimen.
Keywords: Heliopol 9431ATYX_LSE, Stratimat300, Three-point bend tests, Composite laminate, Glass fibers

Abstract: Electrics, hydraulics and pneumatics can be the main motion power of industrial robots. Pneumatic cylinders, pneumatic motors, pneumatic stepper motors and pneumatic bellows are widely used in industrial environment due to their power/weight ratio, power/volume ratio, strength, compactness, simplicity, reliability and cost. Disadvantages of pneumatic actuators can be summarized as follows: difficult to control accurately, air compressibility, compliance and noisiness. Relatively new type of the pneumatic actuators is the pneumatic artificial muscle (PAM) or pneumatic muscle actuator (PMA). Fluidic Muscle made by Festo Company is one of the most investigated commercially available PMA. Pneumatic muscle actuators can be used in industrial environment as well as in prosthesis or rehabilitation devices. In this paper a humanoid arm actuated by Fluidic Muscle is developed and presented.
Keywords: pneumatics, pneumatic muscle actuator, Fluidic Muscle, humanoid arm

Abstract: The humidity of the soil and the quality of seedbed preparation is an important factor influencing crop density and early establishment. It largely depends on weather conditions, but partly it can be controlled by soil management system. Field experiments of different soil tillage methods were carried out at Experimental Station of Aleksandras Stulginskis University in 2009. Treatments involved: 1) direct drilling, 2) shallow ploughing (10 cm depth), and 3) deep ploughing (20 cm depth). In the experiment spring barley (Hordeum vulgare L.) variety 'Simba' was cultivated. The soil of experimental site – Calc(ar)i-Endohypogleyic Luvisol (Drainic). The aim of the research was to estimate the influence of soil management system on seedbed parameters and crop density. It was estimated, that the highest roughness of the soil surface (31.8 mm) was, when the soil was ploughed at 20 cm depth, but contrarily the seedbed roughness was the lowest (15.2 mm). In ploughed soil at 20 cm depth the seeds were sown too deep – 88.4 % of them were below sowing depth. The highest accuracy was estimated in shallow ploughed soil – 43.8 % of the seeds were at sowing depth. Nevertheless in the dry weather conditions spring barley germinated faster when direct drilling was used, later on, experimental results showed, that spring barley crop density was significantly thinner (180 plants per m^2) compared to deep or shallow ploughing, whereas depth of the ploughing did not influence thickness of crop stand: it was 431–445 plants per m^2.
Keywords: deep and shallow ploughing, direct drilling, seedbed, crop stand density

Abstract: The progressive replacement of traditional methods with high-tech (complex) intelligent mechatronic systems, technologies and equipment is one of the most important aspects of the production processes evolution in all industrial fields. Due to accelerated progress of technology transferred in multiple technological innovations, extremely favorable conditions have been created for the development of production and thus of the manufacturing technologies and intelligent control on the automatization way of all subsystems constituting technological processes. New intelligent mechatronic technologies of 3D integrated control offer an integrated portfolio of software solutions and measurable difference for an enhanced quality by accelerating the time needed to produce the components, while the costs of new products are considerably reduced, but also for product development, fundamentally oriented towards ensuring a high level of efficiency in manufacturing and integrated control by increasing the profitability and satisfaction of product delivery requirements.
Keywords: auto industry, mechatronics, 3D integrated control, laser scanning, digitization

Abstract: The modern methods of mathematical theory of mathematical theory of elasticity permit to solve a large series of the problematic of bearings. In this study is presented the results of the use of plane theory of elasticity for study of the state of tensions in intern inner.The projection of the bearings elements, special the rolling bearings and the roller way is very important. It was studied the aspect of stresses in rolling with half-space method, finite elements (contact element), MathCad programmes. The compression of a cylinder in contact "nonconformist" with two surfaces, who are in opposition at the extremity of roles, can be analyses.
Keywords: numerical methods, finite elements, half-space, mathcad, bearings

Abstract: The purpose of this publication is to trace the supply chain of natural gas in Bulgaria. Is described his way - from the extraction in deposits of natural gas to distribution to the end user. Detail elucidated transmission of gas to Bulgaria from its neighboring countries. Is made overview of the types and storage facilities proposed are terms used for gas storage.
Keywords: natural gas, supply chain, gas distribution

Abstract: The article deals with the development of NC machines up to the most modern CNC machines. Automation in the production process provides a number of advantages. Great progress in the production process can deliver both quality products as well as saving time, which is nowadays one of the important aspects of production.
Keywords: geometric axis, synchronous axis, asynchronous axis

Abstract: One of the main stage of obtainig of castings is the pouring of the liquid alloy. Durring this process may occur a series of defects in the matherial structure or the configuration of the casting. According to the specialty literature the casting defects represent any deviation from the shape, dimensions, weight, the external aspect, macro and/or micro-structure and mechanical or chemical properties of the piece required by standards, norms or contractual technical conditions. The occurrence of these defects in castings can lead to increased the percentage registered with direct effects on company costs. For castings to obtain without defects Romanian foundries places great importances on the liquid alloy elaborating technology, moulding-cating technology and the materials used to achievement the moulds and cores. Thus, the development of the foundry department leads to a decrease in operations performed in the cutting processing department (by increasing the casting precision the allowances are smaller and share of the further processing will decrease). The paper presents the possibility of improving the quality of grey cast iron castings by moulding-casting technology optimization in order to decrease the percentage of rejects registered in industrial practice. Thus, the casting Supporting Roll-type is analyzed because it was registered a high percentage of defects (adherences, burrs and misalignment of the castings). These types of defects that lead to rejection of castings could be eliminated by changing the moulding technology, respectively by changing the way location of the

Abstract: The use of polymer matrix composites (PMC's) in the gas flow path of advanced turbine engines offers significant benefits for aircraft engine performance but their useful lifetime is limited by their poor environmental resistance. Flame sprayed NiCr graded coatings are being investigated as a method to address this technology gap by providing high temperature and environmental protection to polymer matrix composites. In this research coating was spread with two configuration, coating with bound coat and coating without bound coat. In general the coating with bound coat and coating without bound coat showed increase in micro hardness and adhesion temperature with increase curing temperature; this is due to the microstructural changes the physical splat structure of the coating also changes with heat treatment. All coating failed at the interface between the composites and the coating, failure occurs along the weakest plane within the system, some of the coating systems that have presented fracture at the bond coat/top coat interface. The surface topography of NiCr films was further examined by using AFM atomic force microscopy as a function of curing temperature at 100,200 and 300°C for 1 hour each, it can be clearly seen that the island structure was observed and the R_{max} increase, the surface became rougher with increasing curing temperature. The surface morphology and microstructure of the coating were examined using SEM.
Keywords: protective polymer fiber composites; polymer matrix composites in aerospace applications; high temperature flame spray coating; hard coating

Abstract: Through designing standards and technolgical development, electrical household appliances are manufactured by respecting well defined and regulated parameters. In order to fit into our courrent environment these appliances should be manufactured using efficient technologies that imply lower costs and lower amounts of energy. The performance of the appliances is targeted through continuous development and transformation. The quality of all electrical appliances is a decisive factor in creating the features that aim to make our life better. In this article, we present the intelligent appliance named – iron.
Keywords: Design, home appliances, iron, innovation, project

Abstract: The paper presents the results of the research conducted in order to reduce the hydrogen content from the steel designed for manufacturing pipes used to transport oil. The steel was produced in an electric arc furnace, type E.B.T. (Eccentric Bottom Tapping) 100t capacity, treated in L.F. (Ladle - Furnace) plants and V.D. (Vacuum -Degassing). In L.F. plants takes place a process of desulfurization and deoxidation with synthetic slag and steel heating plant for processing in vacuum without heat input (V.D.). This research was particularly aimed at explaining the influence of vacuuming parameters (during vacuuming, pressure vacuum system, and temperature of steel) over the hydrogen removal efficiency and hydrogen final content. The obtained data was processed in Excel program, the obtained correlations were analyzed from a technological standpoint and consequently the vacuum optimum parameters were established.
Keywords: Steel pipes, hydrogen content, electric arc furnace, E.B.T., L.F., V.D.

Abstract: In this paper is presented an advanced methodology for the analysis of stress and strain distribution (statical structural analysis using the finite element method) in the working bodies of agricultural cultivators for seedbed preparation in order to optimize them. The geometrical model of soil working body was develoepd in SolidWorks format before being taken and transferred to the program of analysis with finite elenets (ANSYS), in order to perform the necessary resistance calculations made in linear static domain. The obtained results provide valuable information on proper geometric dimensioning of the working bodies of agricultural cultivators.
Keywords: finite element method, structural statical analysis, working body, agricultural cultivator

Abstract: The aim of this article is to present the philosophy of kaizen, which may support the strategy for implementation of innovative changes, and thereby increase the innovativeness of Polish enterprises. The paper developed a theoretical and an empirical parts. The first part generally describes the core philosophy of kaizen and the second part shows the results of empirical studies conducted in the Polish enterprise which concern the state of employees' readiness and commitment to the implementation of kaizen.
Keywords: innovation, kaizen, employees, process of changes, polish enterprise

Abstract: The paper presents the research approach on the numerical simulation applicable to pressure relief valve on the bore gas evacuation device embedded on the high pressure barrels with special destinations. The numerical simulations were conducted in order to asses the behavior of the components elements of the pressure relief valve belonging to bore gas evacuation device. Consequently the present research could contribute at the problem of solving of an increased number of requirements with reduced resources in terms of functioning assessment of high pressure barrels with special destinations.
Keywords: High pressure barrels, bore gas evacuation and pressure relief valve

Abstract: This paper presents a brief statement of electromagnetic pollution generated by public sources of electromagnetic field, wich are distributed on the territory of City of Oradea, Bihor County, Romania. The Beginning of the paperwork is related to define and a general description of electromagnetic pollution. Followed by the description of the characteristics of public sources of electromagnetic field and finally the values of the electric field and magnetic induction in the vicinity of sources. These values were obtained by direct measurements made by the authors. With their help authors mapped and statistical analysis to prioritize city neighborhoods depending on the density of electromagnetic field sources and amplitude values for the electric and magnetic field.
Keywords: electromagnetic pollution, electric field strength, magnetic field density, electromagnetic map, electromagnetic field effects

Abstract: *Lobelia inflata* L. is a medicinally important species of the *Lobeliaceae* family. It is native to North America, it contains numerous piperidine alkaloids. The main alkaloid lobeline has been used as a respiratory stimulant. Recently, it has been come into the limelight due to research on CNS, drug abuse and multidrug resistance. It has been found that the plant can be successfully introduced (cultivated) and due to its favourable active principle production it can qualify for utilization. The outlined experiments have verified that N- and Mg-fertilization exerts a positive effect on plant production. The aim of this project was to examine the effect of magnesium and nitrogen fertilisation on the biomass and on the lobeline production of *in vitro* propagated *Lobelia inflata* in Hungary.
Keywords: *Lobelia inflata* (Indian tobacco), lobeline, biomass production, in vitro

Abstract: This study investigated the effects of heat treatment process on mechanical and microstructural properties of gray cast iron. The charged materials used were graphite, cast iron scraps and ferrosilicon which were subjected to chemical analysis using spectrometric analyzer, the charge calculation to determine the amount needed to be charged into the furnace was properly worked out and charged into the rotary furnace from which the as-cast was obtained. The as-cast was subjected to various degree of normalized heat treatment at different operating temperatures of 885°C, 893°C, 901°C, 909°C, 917°C and after which the mechanical properties of the gray cast iron produced were assessed by hardness, wear, tensile strength and microstructure tests. It was observed that hardness properties continued to increase as operating temperature increases and graphite flakes break the continuity of ferrite matrix results into an increase in hardness and tensile strength of the gray cast iron.
Keywords: Gray cast iron, Normalized, Hardness, Tensile strength, Wear, Temperature

Abstract: The paper presents the results of research conducted in the form of semi-finished steel casting for the manufacture of pipes that are intended to transport hydrocarbons. The research was aimed at determining the influence of the parameters that affect the process of cooling (hardening) on the liquid steel casting speed. Were included in the study the temperature of the steel at the entry into the cristalizor, steel overheating and cooling water flow in different areas, considered independent parameters and casting speed dependent parameter. The data obtained was processed in MATLAB, multiple correlations were obtained and are presented in both graphical and analytic form. The analysis conducted shows a comparison between the results obtained by three types of equations for each correlation which were analyzed from a technological point of view.
Keywords: steel casting, matlab, casting speed, steel cooling, pipes, EBT

Abstract: Teaching Finite Element Method (FEM) with Autodesk Inventor 2012, Statics and Strength of Materials we have collected a lot of sample how the lack of Statics knowledge and/or accurate FEM knowledge leads to incorrect results during stress analysis of Inventor. Our students use the 3D model part of the software really well but the application of Stress Analysis brings very often mistakes. Wrew are going to introduce the two most common problems that we could meet recently during the students' practice: choosing false constraints and leaving out of consideration the buckling.
Keywords: Finite Element Method, constraint, buckling

Abstract: In this study, some engineering parameters such as strength and deformation were determined for five standard varieties of Carnation stem. The experiments were conducted on samples selected from carnation greenhouses in Antalya. Strength parameters consisted of maximum and bio yield force in shearing, shearing and bio yield stress, maximum energy in maximum force, maximum energy in bio yield point and modulus of elasticity. Deformation parameters are also maximum bio yield deformation and maximum breaking dilatation. The tests were conducted at five moisture contents (89.90, 88.65, 90.08, 98.54 and 88.94% (dry basis) for five different varieties (Toldo, Betsy, Jack, Loris and Naxsos), respectively. It was found that, except bending stress, shearing force, bio yield force, bending force, shearing stress, bio yield stress, energy in bio yield point, and energy in shear point were statistically different at $P < 0.05$ whereas breaking dilatation and bio yield deformation were statistically different at $P < 0.001$.
Keywords: carnation; shearing force; bending force; dianthus; harvest; cutting comp

Abstract: This study examined the effect of cutting parameters on the surface roughness generated during face milling operation ofa pearlitic ductile iron using cemented carbide tool. The pearlitic ductile iron used for the study was prepared from scraps of ferrous metals using 100 kg rotary furnace at the Engineering Materials Development Institute (EMDI), Akure, Nigeria. Four cutting parameters were considered for the study, namely; cutting speed, feed rate, depth of cut and cutting fluid flow rate. The experimentation was based on Taguchi's design approach. The data collected were subsequently subjected to analysis of variance.The average surface roughness of machined surfaces, increased as depth of cut increased. The effect of increase in feed rate and cutting speed was to reducethe average surface roughness, though not statistically significant. On the other hand, surface roughness decreased significantly with increase in cutting fluid flow rate and depth of cut. The average surface roughness value was highest at zero fluid flow rate and lowest at the flow rate of 4 l/min. The study concluded that out of all four cutting parameters investigated, the cutting fluid flow rate had most considerable positive influence on the surface roughness of a machined pearlitic ductile iron.
Keywords: surface roughness, cutting parameters, face milling, pearlitic ductile iron

Abstract: The contamination of our living waters is a serious environmental issue in every corner of our world. The main polluting sources are the industry, the agriculture and the general population in their everyday life.

The **ACTA TECHNICA CORVINIENSIS – Bulletin of Engineering**,**Tome IX/2016, Fascicule 4 [October – December]** includes scientific papers presented in the sections of:

- **ISB–INMA TEH' 2015 International Symposium (Agricultural and Mechanical Engineering)**, organized by „Politehnica" University of Bucharest – Faculty of Biotechnical Systems Engineering, National Institute of Research–Development for Machines and Installations Designed to Agriculture and Food Industry – INMA Bucharest, EurAgEng – European Society of Agricultural Engineers and Romanian Society of Agricultural Engineers – SIMAR, in Bucharest, ROMANIA, between 29 – 31 October, 2015. The current identification numbers of the papers are # 8, 15, 17, 18 and 29, according to the present contents list.
- **International Conference on Science and Technique based on Applied and Fundamental Research – ICoSTAF 2016**, organized by University of Szeged, Faculty of Engineering, in Szeged, HUNGARY, 2 June 2016. The current identification numbers of the papers are # 24 and 27, according to the present contents list.
- **The 1st International Conference "Experimental Mechanics in Engineering"– EMECH 2016**, organized by Romanian Academy of Technical Sciences, Transilvania University of Brasov and Romanian Society of Theoretical and Applied Mechanics, in Brasov, ROMANIA, between 8 – 9 June 2016. The current identification numbers of the papers are # 1–2, 5–6 and 9–10, according to the present contents list.
- **STUDENTS ' SCIENTIFIC SYMPOSIUM – HD-46-STUD – 46 Years of Higher Education in Hunedoara – Doctoral Studies section (SD7)**, organized by University Politenica Timisoara, Faculty of Engineering Hunedoara and General Association of Engineers in Romania (AGIR) – Hunedoara brach, in Hunedoara, ROMANIA, between 20 – 21 May, 2016. The current identification numbers of the papers are # 16, 23 and 28, according to the present contents list.

Also, the **ACTA TECHNICA CORVINIENSIS – Bulletin of Engineering**, **Tome IX/2016, Fascicule 4 [October – December]**, includes original papers submitted to the Editorial Board, directly by authors or by the regional collaborators of the Journal.

ACTA Technica CORVINIENSIS
BULLETIN OF ENGINEERING

ISSN:2067-3809

ACTA TECHNICA CORVINIENSIS
– Bulletin of Engineering
Tome IX [2016], Fascicule 4 [October – December]
ISSN: 2067 – 3809

[1.]Horea SANDI, [2.]Ion VLAD, [3.]Nausica VLAD, [4.]Patricia MURZEA

A SUMMARY LOOK AT THE PERFORMANCE OFA LARGE SIZE STRUCTURE

[1.]Academy of Technical Sciences of Romania, ROMANIA
[2-3.] Technical University of Civil Engineering, Bucharest, ROMANIA
[4.] Technical Military Academy, Bucharest, ROMANIA

Abstract: The main objective of the paper is to present the results of the monitoring of the dynamic characteristics of the reinforced concrete infrastructure of the great hall of ROMEXPO, the main exhibition building in Bucharest. The monitoring included the initial stage and, thereafter, the stages post-earthquake and post-rehabilitation intervention, for the events of 1977.03.04, 1986.08.30, 1990.05.30 and 1990.05.31. The axial symmetry of the structure made it appropriate to use Fourier expansion techniques.
Keywords: dynamic characteristics, spectral densities, Fourier expansion, stages of performance

INTRODUCTION

The paper is concerned with a presentation of the main features and of the performance of a large size structure, namely the main hall of ROMEXPO in Bucharest, Romania. This paper includes:

- a brief presentation of some main characteristics of the structure dealt with;
- a brief presentation of the studies carried out;
- main results on the monitoring of the dynamic characteristics of the structure, at successive stages of the structural performances, before and after the earthquakes having occurred during the service period of the structure;
- references to the additional studies performed.

Other aspects dealt with, just briefly referred to due to the length restrictions of the paper, are mentioned in the references. The paper summarizes analytical and full scale experimental work carried out during two different periods:

- the period of analog recording (July 1976 to July 1993)during which Ioan Sorin Borcia (†), Mihail Stancu and Olga Stancu (†) had significant contributions;
- the period of digital recording (September 2011 to September 2012), during which Patricia Murzea (doctoral thesis [3] advised by the first author), Ion Vlad and Nausica Vlad (management and use of digital recording instrumentation, processing of records)had important contributions.

The first author developed and coordinated the analytical work and coordinated the experimental work and processing of records.

DATA OF THE PROBLEM AND APPROACH ADOPTED

The structure (lateral view: Figure 1, vertical section Figure 2) has an almost perfect axi-symmetrical layout and consists of a reinforced concrete infrastructure (mainly: 32 couples of 25m tall columns) and a steel dome. The initial network dome solution collapsed during the winter of 1963, due to strong non-symmetrical snow loading. The new solution adopted for the dome relies on 32 radial arches.

The diameter of the steel dome is 95 m and the altitude of the dome apex is 30 m. The external structure, which bears the dome, is separated from the internal structure, which bears the live loads determined by the service. An internal view of the dome is given in Figure 3, while a scheme of placing the instruments at the level at the main bearing ring in a horizontal plane view is given in Figure 4.

The earthquake of 1977.03.04 (which produced more than 30 cases of collapse of buildings in Bucharest [1]) damaged severely the structure. Some of the natural periods were seriously lengthened and the axial symmetry was obviously affected. The lateral glazing of the infrastructure was destroyed to more than 50%.

Figure 1: Lateral view from East. Main entrance

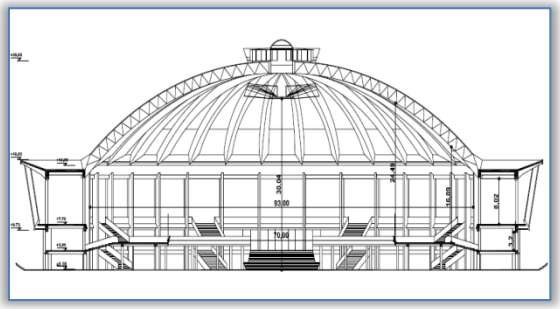

Figure 2: Vertical, central, section

Figure 3. Internal view of the dome

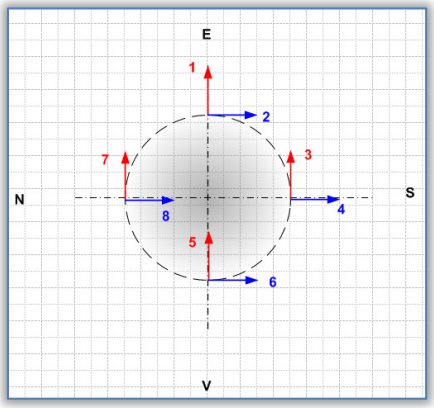

Figure 4. Degrees of freedom of condensed model

A first post-earthquake intervention was undertaken promptly and was adapted thereafter soon to more severe conditions, as required in order to increase the capacity of resistance of the structure to a level appropriate to the intensity of seismic hazard, as made obviously necessary by the experience of the 1977 event. A new rehabilitation and strengthening solution was developed after the occurrence of the subsequent events. Among other, the dynamic axial symmetry was thus rehabilitated. Note that the main reinforced concrete members were strengthened in comparison with their initial sizes.

The signals provided by the pickups used had to be combined in order to obtain the desired information on the deformation of the structure. During the period of analog recording the cables connected to the pickups were alternatively combined in field, in order to directly obtain the information of interest, namely time histories of the combinations referred to. During the period of digital recording just simple records of the reference variables were stored and the combinations of interest were obtained from the computer.

The reference model used for structural analysis is quite simple, due to the features of symmetry referred to. At the scale of the structure as a whole, it derives from a vertical macro-cantilever, placed at the central axis of the dome. Attention is paid to the horizontal local displacements at recording locations only, namely at the points of intersection of the EW and NS ring diameters with the (circular) axis of the main dome bearing ring (Figure. 4). The deformation of the structure is characterized on this basis by the horizontal components of displacements.

The systems of displacements corresponding to the natural oscillation shapes are ordered in principle as double sequences, depending on two variables. A first, basic variable corresponds to the order of natural macro-shape in the overall system. A second variable, representing the order of macro-shape in the detailed sequence of macro-shapes characterizing the deformation of the vertical bearing members, is not explicitly used in this frame. It is implicitly assumed that, in relation to this second variable, only the fundamental natural shape is considered. Two terms form a couple of identification symbols for the displacements of each order. In fact, only the fundamental term of the sequence corresponding to a term of the first sequence is used. The first sequence order concerning the infrastructure as a whole corresponds to following successive couples of terms:

- 0: ring dilatation and ring rotation around main structural axis;
- 1: rigid ring translation along a horizontal direction and along a direction orthogonal ($\pi/2$) to it;
- 2: basic (2^{nd} order) ovalization. oriented along the axes of coordinates and a couple of systems of displacements oriented at $\pi/4$ to it;
- 3^{rd}(3^{rd} order) ovalization oriented along the axes of coordinates and a couple oriented at $\pi/6$ to it etc.

To each of the coordinates referred to a couple of systems of displacements thus corresponds.

EXPERIMENTAL RESULTS

Monitoring at successive stages, analog results

A summary of results of analog recording is presented in Table 1.

Table 1. Dominant periods (s) revealed by ambient vibrations (analog recording)

Oscillation direction (DoF)	Recording moment: Before 1977.03.04 'quake (July '76)	After 1977.03.04 'quake (Mar.'77)	After provisional strengthening (steel bracing) (April '77)
In plane ring rotation	.41	.94	.59
E-W ring translation	.60	.98	.74
N-S ring translation	.60	1.08	.78
Ring ovalization	.35	.36	.36

Oscillation direction (DoF)	Recording moment: After final strengthening (r.c. spatial frame) (July '84)	After 1986.08.30 'quake (Sept. '86)	After 1990.05 'quakes (July '93)
In plane ring rotation	.43	.52	.52
E-W ring translation	.52	.65	.72
N-S ring translation	.55	.65	.66
Ring ovalization	.34	.39	.41

The peak frequency of oscillations along several (generalized) degrees of freedom of the structure is given. The cases, or moments, of loss of axial dynamic symmetry and of its recovery are made obvious. Some main remarks:

- the main dome bearing ring appears not to have been damaged by bending in the horizontal plane (the ovalization periods of the last row are practically unchanged), so it may be concluded that damage was practically confined to the vertical bearing members;
- the event of 1977 produced a strong loss of dynamic symmetry and, most obvious, a lengthening of the in plane ring rotation period corresponding to a loss of stiffness of about 80% (this led the first author to conclude and impose that the vertical bearing system of the structure is to be strengthened especially in the vertical tangent plane of the macro-cylindrical system built by the vertical bearing members);
- the strengthening intervention of 1984 brought the dynamic characteristics back close to the values of 1976 (pre-earthquake), but the subsequent earthquakes (1986, 1990) produced again a lengthening of natural periods that reveals some non-negligible damage.

Characteristics of the current stage of the structure, digital results

Segments of time histories of basic variables are given for illustration in Figures 5 (for displacements) and 6 (for velocities). The plots correspond respectively to the degrees of freedom defined in Figure 4. The plots reveal considerable differences between the various channels, from the points of view of spectral contents and amplitudes. These differences are on the other hand totally changed in case one looks at the plots corresponding to the various subspaces/ combinations of degrees of freedom involved by the structural dynamic symmetry characteristics. Some comments relying on the features of following combinations are presented subsequently.

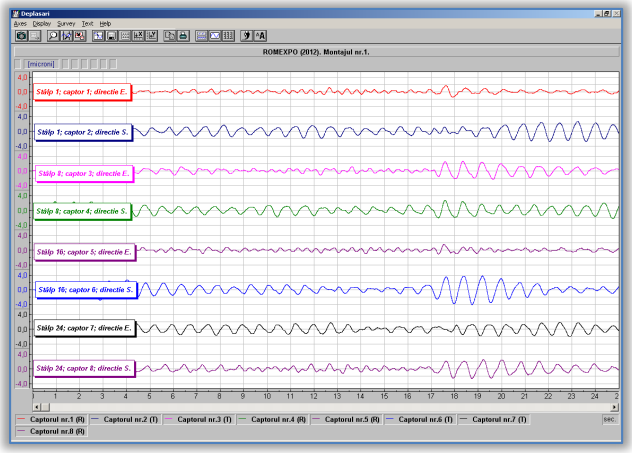

Figure 5: Time histories of displacements along condensed degrees of freedom

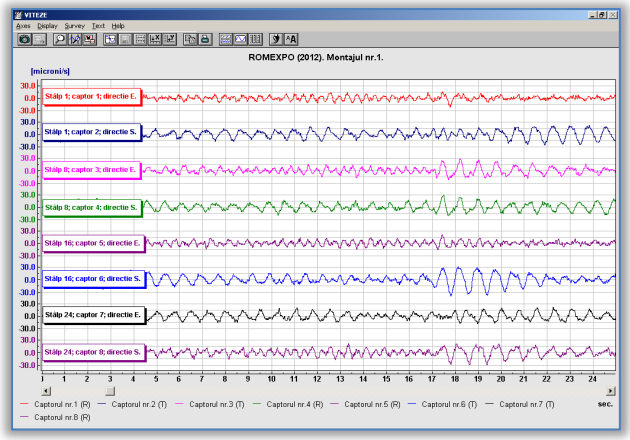

Figure 6: Time histories of velocities along condensed degrees of freedom

A first combination,

$$u_{rad} = (u_1 + u_4 - u_5 - u_8) / 4, \qquad (1)$$

is dealt with in Figures 7… 10. This corresponds to a superposition of symmetrical dilatation with values of a sequence of radial displacements corresponding to the 4-th, 8-th etc. normal mode. By difference to the other combinations dealt with, the sum thus defined does not reveal a clear spectral selectivity.

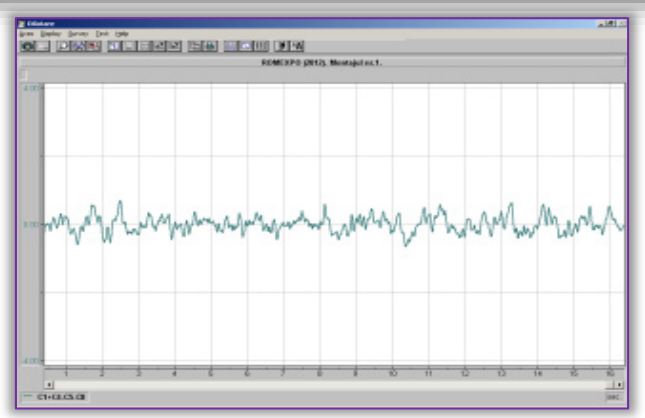

Figure 7: Time history of ring dilatation superposed with condensed coordinates of 4th, 8th etc. orders (displacements)

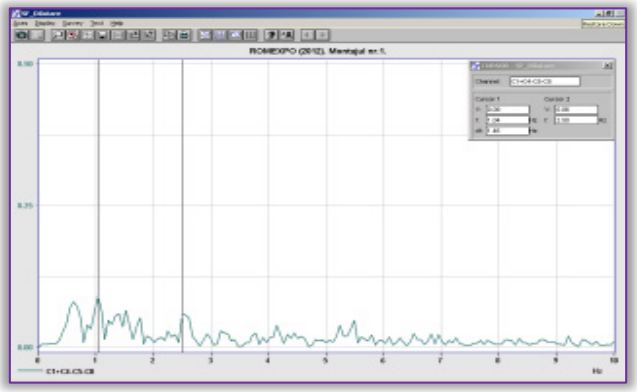

Figure 8: Fourier amplitude spectrum of time history of Figure 7

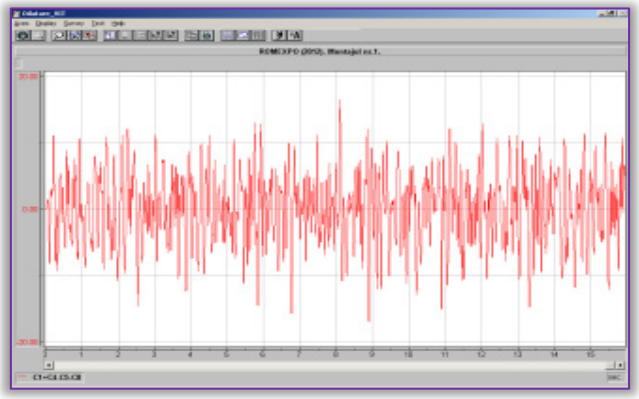

Figure 9: Time history of ring dilatation superposed with condensed coordinates of 4th, 8th etc. orders (velocities)

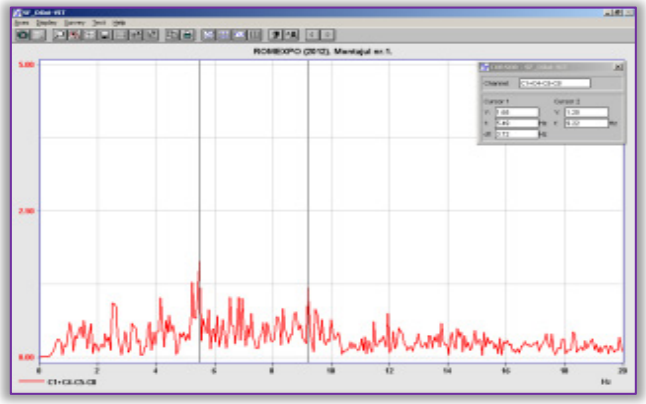

Figure 10: Fourier amplitude of time history of Figure 9

The combination corresponding to rigid rotation of the dome bearing ring around the axis of symmetry of the structure

$$u_{rot} = (u_3 - u_2 - u_7 + u_6) / 4 \qquad (2)$$

is dealt with in Figures 11… 14. This combination reveals a high spectral selectivity, as determined by the sharp peaks of the Fourier spectra.

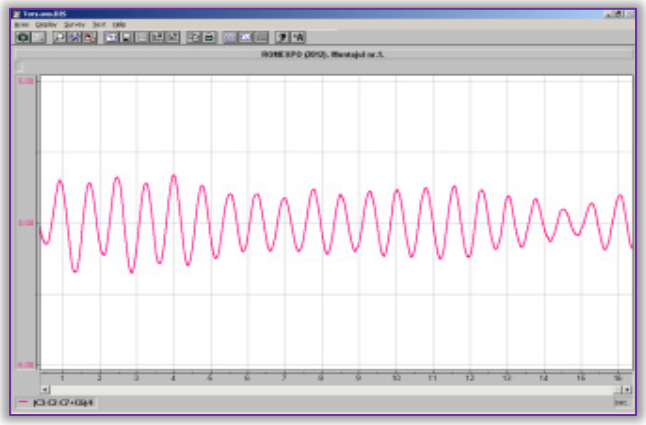

Figure 11: Time history of ring rotation around axis of symmetry of the structure (displacements)

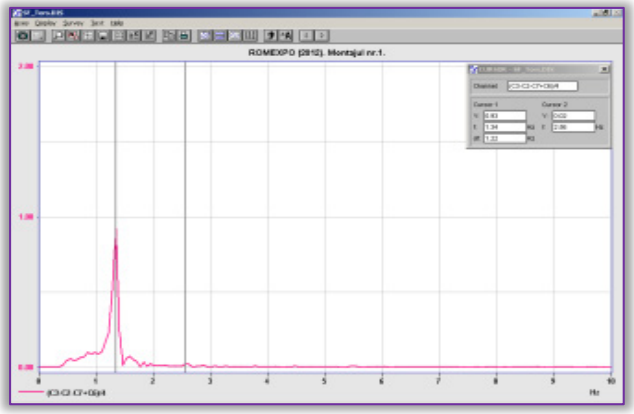

Figure 12: Fourier amplitude spectrum of time history of Figure 11

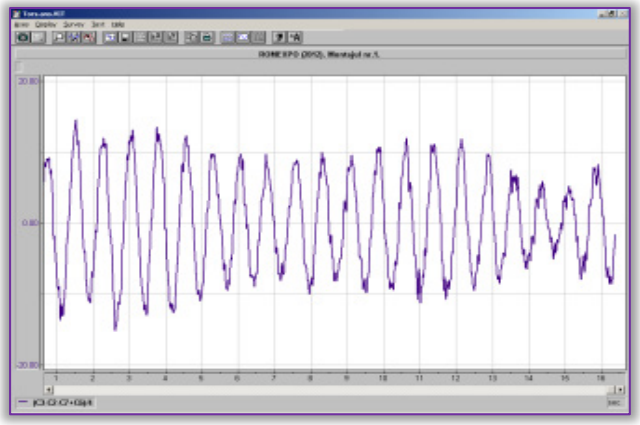

Figure 13: Time history of ring rotation around axis of symmetry of the structure (velocities)

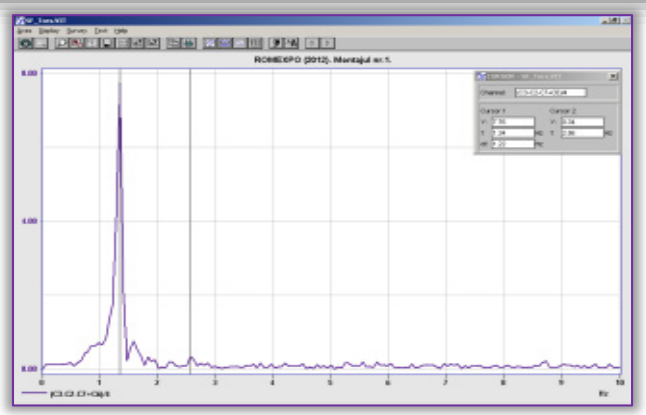

Figure 14: Fourier amplitude spectrum of time history of Figure13

The combination corresponding to rigid translation of the dome bearing ring along the E-W direction,

$$u_{EW} = (u_1 + u_3 + u_7 + u_8) / 4 \quad (3)$$

is dealt with in Figures 15...18. Here, also, the combination reveals a high selectivity (which is nevertheless lower than in case of the rotation motion).

The combination corresponding to rigid translation of the dome bearing ring along the N-S direction,

$$u_{NS} = (u_2 + u_4 + u_6 + u_8) / 4 \quad (4)$$

(see Figures 19 to 22) is comparable to the combination corresponding to the E-W combination.

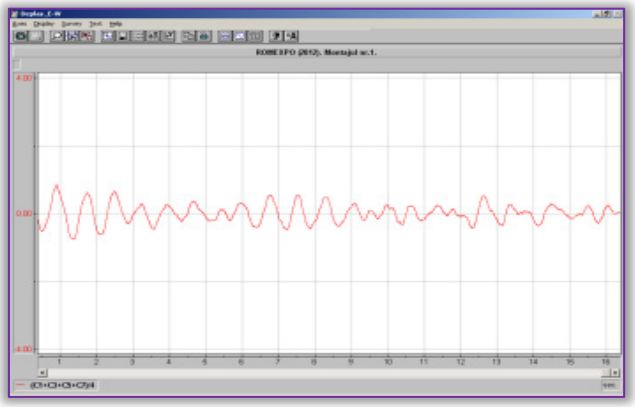

Figure 15: Time history of E-W ring translation (displacements)

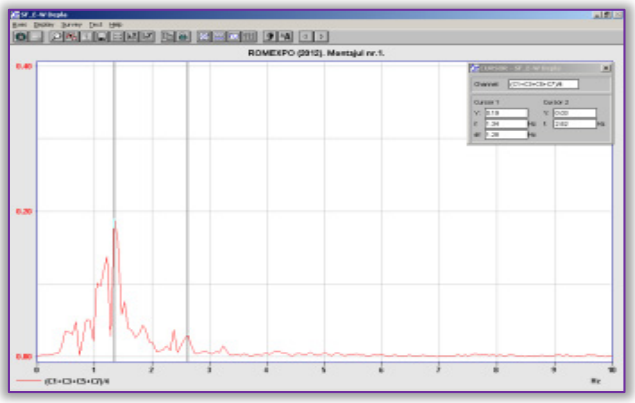

Figure 16: Fourier amplitude spectrum of time history of Figure15

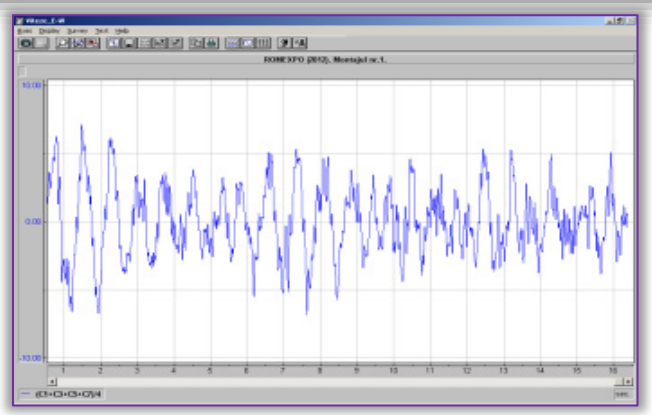

Figure 17: Time history of E-W ring translation (velocities)

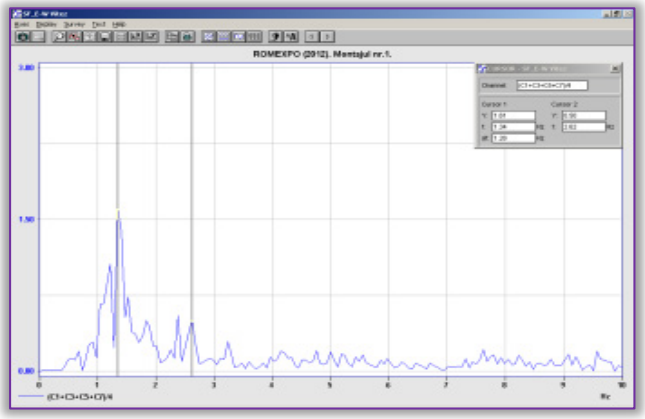

Figure 18: Fourier amplitude spectrum of time history of Figure17

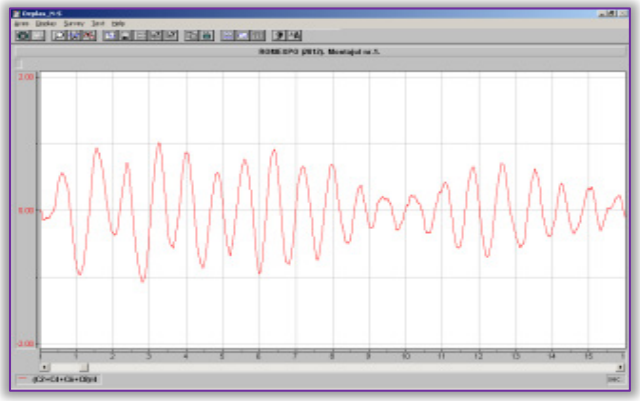

Figure 19: Time history of N-S ring translation (displacements)

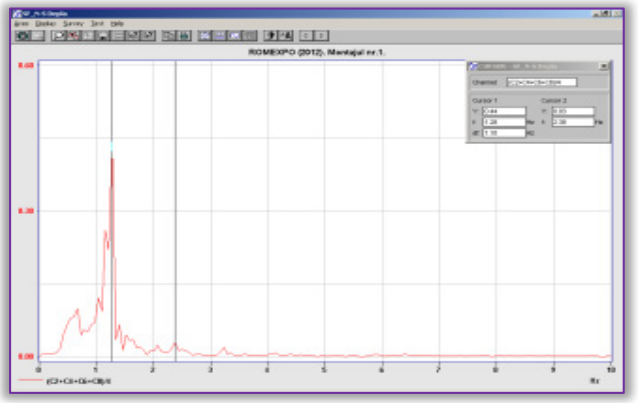

Figure 20: Fourier amplitude spectrum of time history of Figure 19

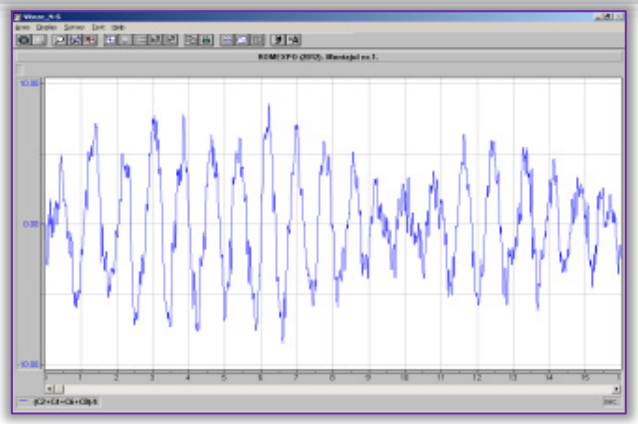

Figure 21: Time history of N-S ring translation (velocities)

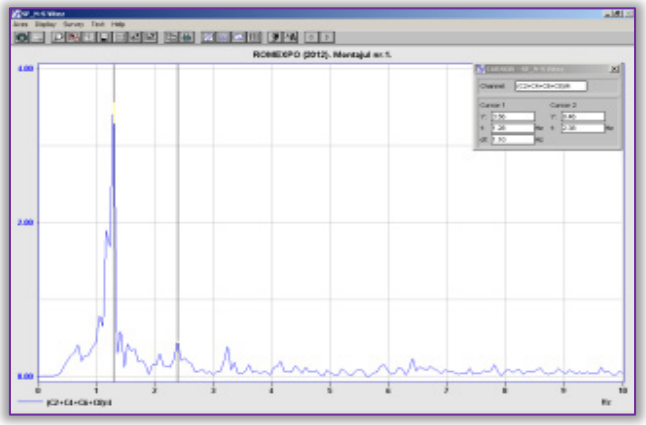

Figure 22: Fourier amplitude spectrum of time history of Figure21

The combination

$$u_{ov2} = (u_4 - u_1 - u_8 + u_5)/4 \quad (5)$$

corresponding to ovalization along the horizontal reference axes, is dealt with in Figures 23...26. The motion amplitude along this degree of freedom is high, as the spectral selectivity too.

The combination

$$u_{ov2'} = (u_1 - u_3 - u_7 - u_6)/4 \quad (6)$$

(see Figures 27 to 30) corresponding to ovalization along directions oriented at 45^0 with respect to horizontal axes, has characteristics that are quite similar to the previous ones.

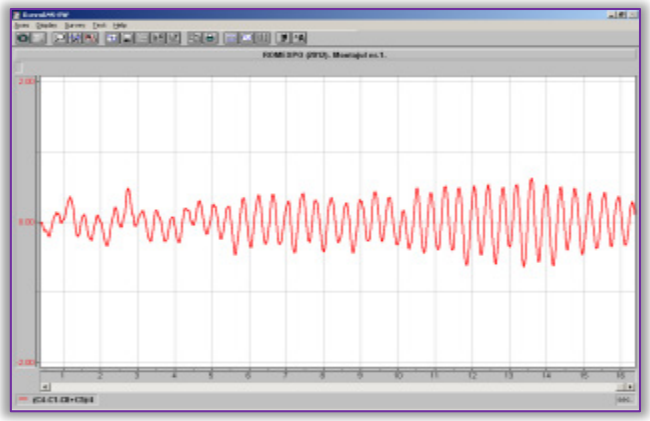

Figure 23: Time history of 2nd order ovalization along coordinate axes (displacements)

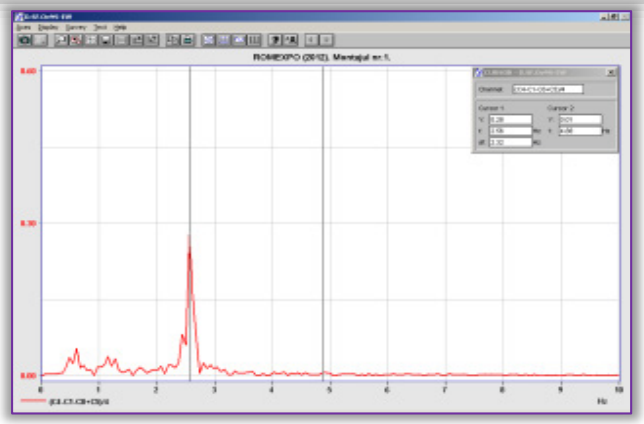

Figure 24: Fourier amplitude spectrum of time history of Figure 23

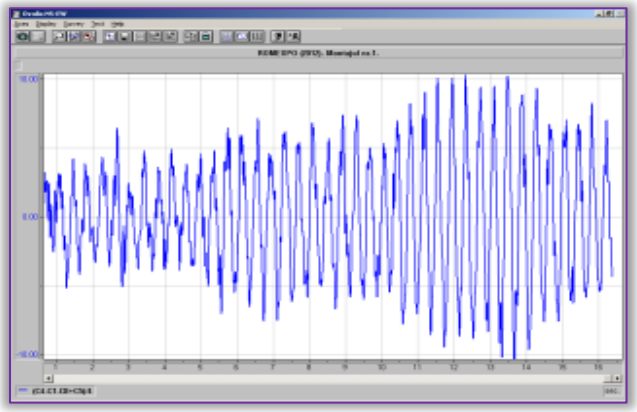

Figure 25: Time history of 2nd order ovalization along coordinate axes (velocities)

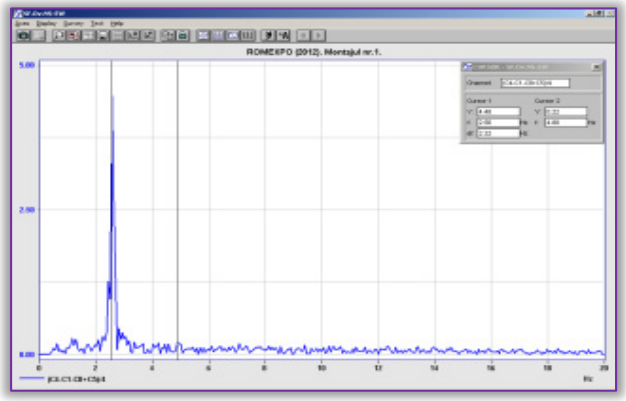

Figure 26: Fourier amplitude spectrum of time history of Figure 25

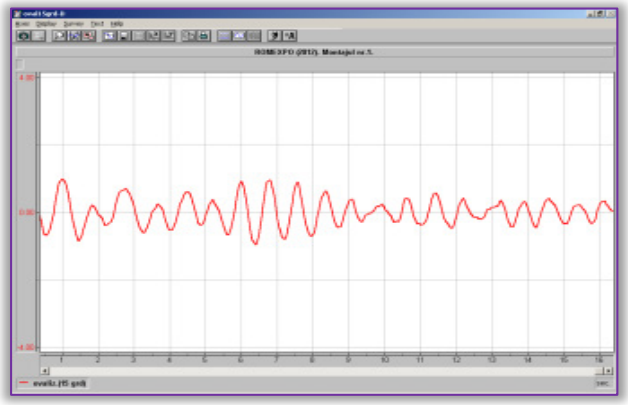

Figure 27: Time history of 2nd order ovalization 45^0 from coordinate axes (displacements)

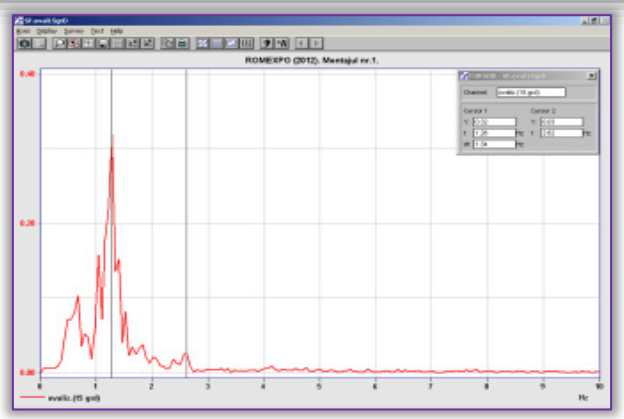

Figure 28: Fourier amplitude spectrum of time history of Figure 31

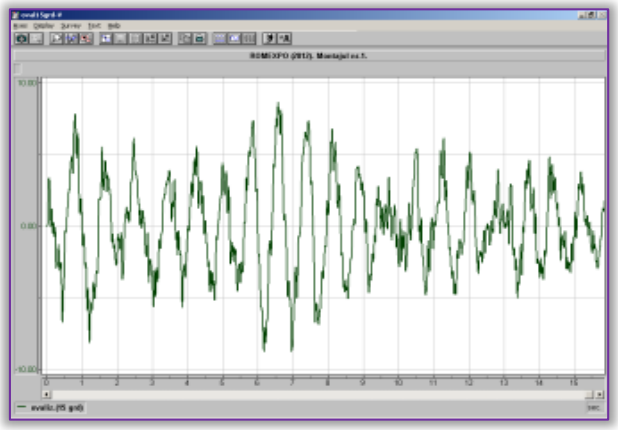

Figure 29: Time history 2nd order ovalization 45º from coordinate axes (velocities)

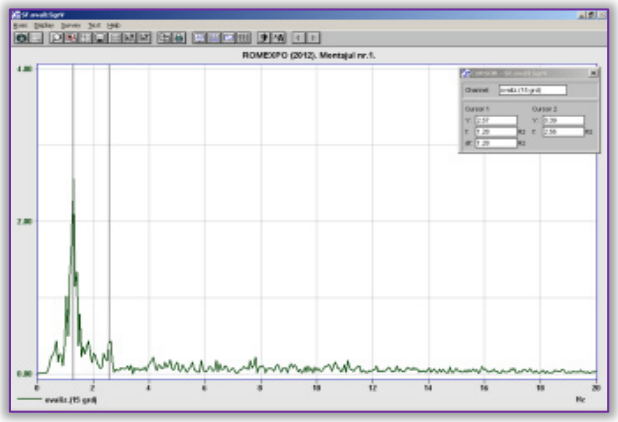

Figure 30: Fourier spectrum of time history of Figure 33

FINAL CONSIDERATIONS

The records obtained during the analog recording period (1976…1993) made it posible to determine a time history of occurrence of damage and of consequences of repair & rehabilitation interventions. They made it possible also to derive conclusions on the appropriate way to intervene.

The outcome of processing the digital basic information provided more detailed information about the features of dynamic deformation, including data on the dynamic seleectivity for the various deformation types.

The availability of the ROMEXPO structure and of the history of its performance offered a rare opportunity of obvious technical interest to combine the possibilities of joint analytical and experimental work in order to examine in depth the features of performance of a highly important structure and, moreover, to add to the knowledge and know how specific to the field of structural dynamics.

Given the currrent state of the art, it is desirable at present to use digital recording and processing techniques. This offers wide possibilities of investigation of various aspects of interest, as speciffic to the tasks dealt with.

This case study confirmed once more the possibilities offered by the combination of analytical and experimental work. A qualitative analytical grasping of the features of structural performance is necessary in order to adopt an efficient way to perform experimental work. On the other hand, the availability of appropriate experimental information offers the possibility of refining the analytical approach adopted.

The case study presented provided information about the influence of overloading upon the dynamic characteristics of the structure dealt with.It turns out that, even in the case in which the structure was not on the brink of collapse, some of the dynamic characteristics were quite strongly modified.

A look at the time histories of rigid risk translation, rigid risk rotation and (basic, second order) ovalization, given in previous figures, which are of comparable amplitudes, raises a problem of fundamental interest concerning the characterization of ground micro-tremors lying at the origin of ambient oscillations presented in the figures referred to. Given the strong dynamic symmetry of the structure dealt with, it turns out that the three categories of ambient oscillations referred to pertain to different, dynamically orthogonal, subspaces of the structure. This means that these three categories of oscillations must be due to different kinds of input ground motions. Consequently, the micro-tremors must consist basically of three corresponding homologous categories of components. This requires a revision of the usual approach to ground motion, which would take into account just rigid translation micro-tremors (and ground-structure interface motions). An approach proposed in this connection, [4], [6], [7], is to adopt a (stationary) random spatial model of micro-tremors and to consequently calibrate the correlation/coherence characteristics.

References

[1.] Șt. Bălan, V. Crisescu, I. Cornea (editors) : ”Cutremurul de pământ din Vrancea, de la 4 martie 1977” (The Vrancea earthquake of 4

March 1977). Editura Academiei, Bucharest, 1982.
[2.] G. Danci, D. Rădulescu, H. Sandi, M. Stancu: "Some first data on the Romania, 30/31 August 1986, earthquake". Proc. 8-th European Conf. on Earthquake Engineering, Lisbon, 1986.
[3.] P. Murzea: Studiu asupra specificării mărimilor de intrare privind acțiunea seismică asupra construcțiilor (Study on the specification of input on the seismic action upon structures). Doctoral Thesis. UTCB, 2012.
[4.] S. V. Pugachov: "Teoria sluchaynykh funktsiy" (Theory of random functions), GIFML, Moscow, 1960.
[5.] H. Sandi: "Siguranţa clădirilor de locuit. Invăţăminte rezultate din comportarea la cutremurul din 4 martie 1977". (Safety of residential buildings. Lessons from the performance during the 4 March 1977 earthquake). Construcţii, 12, 1981.
[6.] H. Sandi: "Stochastic models of spatial ground motions". Proc. 7-th European Conf. on Earthquake Engineering, Athens, 1982.
[7.] H. Sandi: "On the seismic input for the analysis of irregular structures". Proc. 4-th European Workshop on Irregular and Complex Structures, Thessaloniki, September 2005.
[8.] H. Sandi, M. Stancu, O. Stancu, I. S. Borcia: "A biography of a large-span structure, pre- and post- earthquake, after the provisional and final strengthening". Proc. 8-th European Conf. on Earthquake Engineering, Lisbon, 1986.
[9.] H. Sandi, G. Şerbănescu, T. Zorapapel: "Lessons from the Romania earthquake of 4 March 1977". Proc. 6-th European Conf. on Earthquake Engineering, Dubrovnik, 1978.
[10.] I. Vlad, H. Sandi, P. Murzea, O. Păucescu, N. Vlad: "An updated history of the earthquake performance of a large span structure" Proc. 15-th European Conference on Earthquake Engineering, Istanbul, 2014.

ACTA Technica CORVINIENSIS
BULLETIN OF ENGINEERING
ISSN:2067-3809

ACTA TECHNICA CORVINIENSIS
– Bulletin of Engineering
Tome IX [2016], Fascicule 4 [October – December]
ISSN: 2067 – 3809

[1.]Ionuţ DRAGOMIR, [2.]Nicolae–Doru STĂNESCU, [3.]Adrian CLENCI, [4.]Dinel POPA

RECOVERY OF A REAL CAM BY USING THE JARVIS MARCH

[1.] I AKKA ROMSERV, Bucharest, ROMANIA
[2-4.] University of Piteşti, Piteşti, ROMANIA

Abstract: In this paper the authors performed a comparison between the real shape of a cam and its convex cover. The goal is to highlight the advantages of using the Jarvis march in the synthesis of cams. The authors analyzed an intake cam used by the K7 engine manufactured by Renault Company, both from the constructive and variation of the dynamical parameters points of view.
Keywords: cam, Jarvis march, precision, K7 engine

INTRODUCTION

It is well known that the using the calculation programs that implement the Jarvis march offers the advantage of the possibility of the realization of a very precise and convex profile of the cam. The precision is practically limited to the precision of the computer. For instance, a precision of 0.1^0 is very usual in this case, comparing to the precision of 1^0 in the case of the classical methods.

Using such programs that implement the Jarvis march, the authors have as final goal to obtain a profile of the cam which modifies the functioning cycle of a typical K7 engine from Otto to an Atkinson type one. The Atkinson cycle is characterized by diminished polluting emissions and improved BSFC.

It was highlighted in some papers that the use of the Miller cycle for a Diesel leads to the decreasing of the polluting emissions and the increasing of the efficiency. Wang [1] applied the Miller for a Diesel engine, while Gonca [2–4] proved, by mathematical models, the increasing of the thermal efficiency with the aid of a cam obtained by mathematical calculation, which was implemented on a Diesel engine.

Li [5] studied the effective specific consumption of an Otto engine with direct injection obtaining, by using the Miller cycle, a decreasing of the BSFC by approximate 4.7 % for great loads and angular velocities.

In this paper, the authors recovered the cam of a K7 type engine by using the Jarvis march. They analyzed the camshaft of the engine from the point of view of the admission cam.

The distribution mechanism was simplified considering that the valve rocker is one with equal arms, directly acting upon the valve. In addition the surface of the valve rocker that is actuated by the cam is considered to be a plan one, so we discuss about a flat tappet.

EXPERIMENTAL DATA

The considered engine was a K7 type one manufactured by Dacia–Renault Company.

The experimental setup is described in Figure 1. On the camshaft we installed the device for the measurement of the variation of radius of the cam.

Figure 1: Determination of the dimensions of the cam

The rotational angle of the camshaft is determinate using a device to measure the angular displacement. In this way the dimension of the cam was measured using an angular step of 5^0, the value of this variation being read on a dial extensometer with a precision of 0.01 mm; the obtained data was used as input data in the calculation program that implements the Jarvis march. The obtained values are presented in Table 1. Separately we measured the radius of the base circle of the cam obtaining a value equal to 14.5 mm.

Table 1: Numerical values for the dimension of the cam

Angle of rotation of the camshaft	Valve's displacement	Angle of rotation of the camshaft	Valve's displacement
0	0	185	0
5	0.01	190	0
10	0.06	195	0
15	0.13	200	0
20	0.19	205	0
25	0.27	210	0
30	0.39	215	0
35	0.59	220	0
40	0.88	225	0
45	1.3	230	0
50	1.95	235	0
55	3.01	240	0
60	3.89	245	0
65	4.61	250	0
70	5.05	255	0
75	5.25	260	0
80	5.19	265	0
85	4.91	270	0
90	4.38	275	0
95	3.68	280	0
100	2.79	285	0
105	1.95	290	0
110	1.28	295	0
115	0.9	300	0
120	0.61	305	0
125	0.4	310	0
130	0.28	315	0
135	0.2	320	0
140	0.15	325	0
145	0.11	330	0
150	0.04	335	0
155	0.01	340	0
160	0	345	0
165	0	350	0
170	0	355	0
175	0	360	0
180	0		

In our assumptions presented in the first paragraph, the displacement of the valve lift is equal to the variation of the cam radius. This variation is graphically presented in Figure 2.

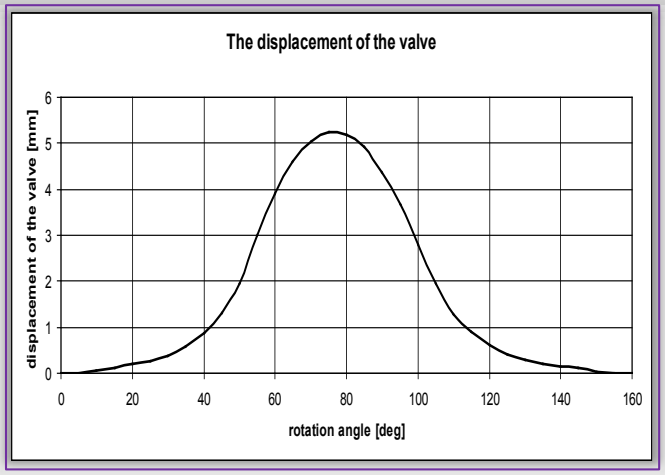

Figure 2: Variation of the displacement of the valve as function of the rotation angle of the camshaft

THE JARVIS MARCH

The Jarvis march is an algorithm that offers the convex cover of a finite set of planar points. The convex cover is obtained as a polygon having the apices among the original points.

If the original set of points form a convex set, then the convex cover consists in the set itself, the order of points being or not the same as in the original set.

Usually, the convex cover consists only in a part of the original set, the order of the points in the convex cover being not the same as in the original set.

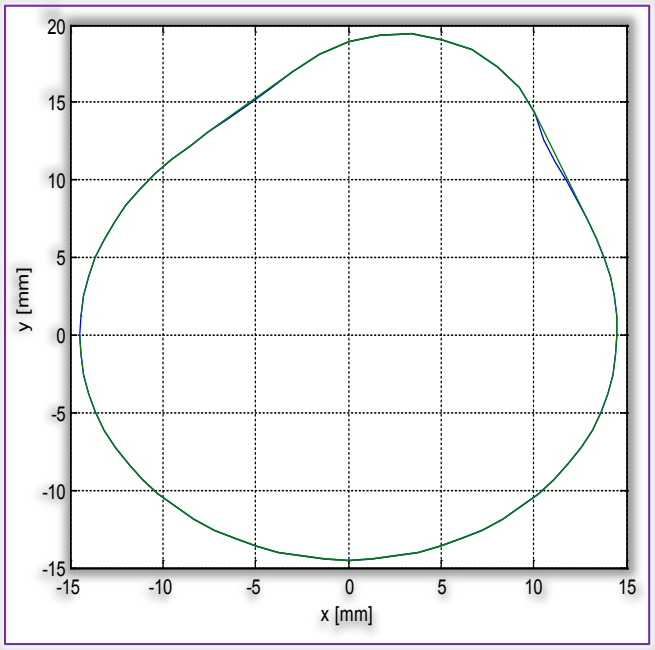

Figure 3: The original set of points and its convex cover for the cam

In our case we have 72 points which offer the profile of the original cam with a step of 5^0. The original polygon which passes through these 72 points is drawn with blue line in Figure 3. The convex cover of this set of points is drawn with green line in the same figure. Only 64 points out of

the original 72 are used. This non-conformity has as main causes by the great angular step (we have to consider a smaller one), and our assumption of a flat tappet of the distribution mechanism.
The reader can easily see that the differences between the real cam and the cam obtained by using the Jarvis march are small ones, so we may state the quasi coincidence of the two cams.

DYNAMICAL BEHAVIOR

It is interesting to see the dynamical behavior of the distribution mechanism in two situations. The first one is characterized by the use of approximation with a 5^0 angular step of the real cam, while the second one is characterized by the use of the cam obtained with the aid of the Jarvis march.

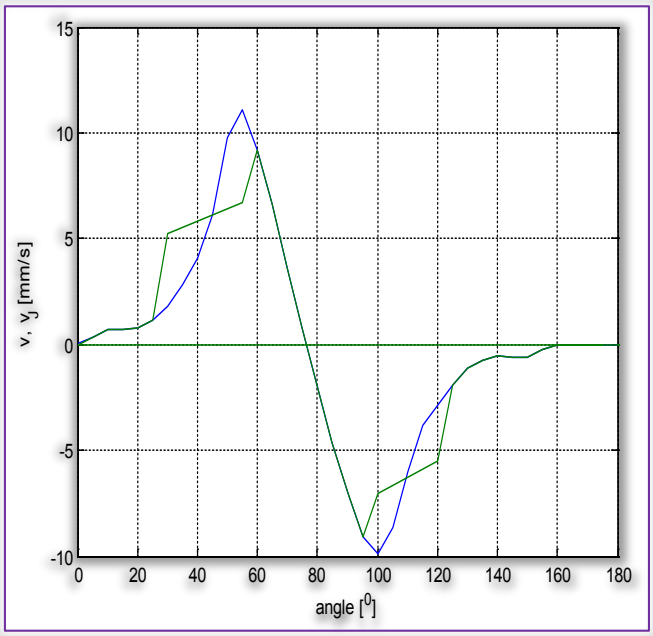

Figure 4: The variation of the valve's velocity

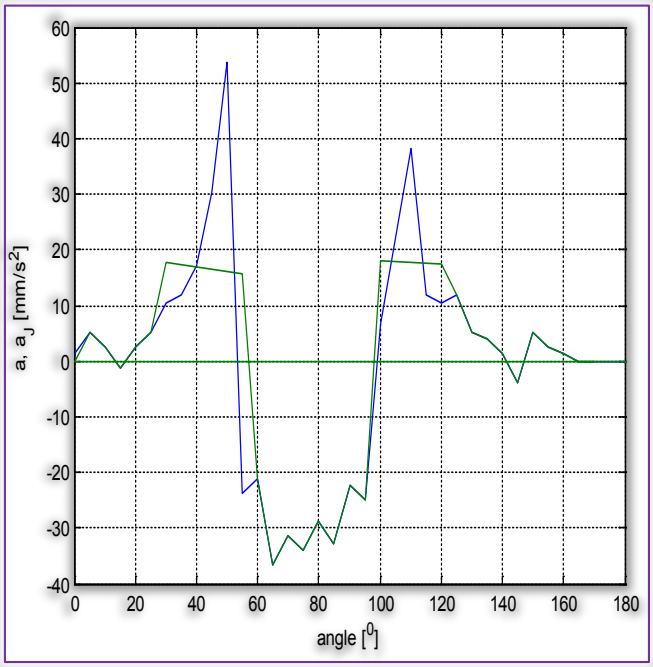

Figure 5: The variation of the valve's acceleration

In Figures 4 and 5 we presented the variations of two kinematic parameters: the velocity and the acceleration of the admission valve. In blue are plotted the variations of these parameters for the approximation of the real cam, while in green are plotted the variations of the same parameters for the cam obtained with the aid of the Jarvis march.
The graphics were obtained using the classical formula for the numerical derivation [6]. In the first situation (the approximation of the real cam) the angular step was a constant one and equal to 5^0. In the case of the second case (the cam obtained with the aid of the Jarvis march) the angular step was not a constant one, but depending on each point (some points are not found in the convex cover).
Analyzing these figures we may state that in the convex cam the velocity and the acceleration of the valve are smaller. The maximum value of the velocity decreases with approximate 25% comparing to the case of the approximation of the real cam. The changes are more dramatically for the acceleration when the maximum value is 3.5 lesser than that obtained in the first situation

CONCLUSION

Our paper demonstrates that the use of the convex cam obtained with the aid of the Jarvis march leads to smaller values for the velocity and acceleration of the valve. This thing implies an engine of smaller mass, increasing of the efficiency and reduction of the wear.
Our study will be extended in the following directions:

- different shapes of the follower not only the flat tappet which was used in the present paper;
- for a cam that characterizes the Miller–Atkinson cycle;
- practical validation of the theoretical aspects.

References

[1.] Wang Y, Zeng S, Huang J. Experimental investigation of applying Miller cycle to reduce NOx emission from diesel engine. Proc. IMechE, Part A: J. Power Energy 2005;219:631–8.
[2.] Gonca G, Kayadelen HK, Safa A. Comparison of diesel engine and Miller cycled diesel engine by using two zone combustion model. 1. In: INTNAM Symp 2011;17:681–97.
[3.] Gonca G, Sahin B, Ust Y, Parlak A. A study on late intake valve closing miller cycled diesel engine. Arab J Sci Eng 2013;38:383–93.
[4.] Gonca G, Sahin B, Ust Y, Parlak A, Safa A. Comparison of steam injected diesel engine and miller cycled diesel engine by using two zone combustion model. J Energy Inst, in press. http://dx.doi.org/10.1016/j.joei.2014.04.007.

[5.] Li T, Gao Y, Wang J, Chen Z. The Miller cycle effects on improvement of fuel economy in a highly boosted, high compression ratio, direct-injection gasoline engine: EIVC vs. LIVC. Energy Convers Manage 2014;79:59–65.
[6.] Teodorescu P.P., Stănescu N–D, Pandrea N, Numerical Analysis with Applications in Mechanics and Engineering, John Wiley & Sons, Hoboken, USA, 2013.

ACTA Technica CORVINIENSIS
BULLETIN OF ENGINEERING
ISSN:2067-3809

ACTA TECHNICA CORVINIENSIS
– Bulletin of Engineering
Tome IX [2016], Fascicule 4 [October – December]
ISSN: 2067 – 3809

[1.]István SZLUK, [2.]Gergely DEZSŐ, [3.]Ferenc SZIGETI

STUDY ON LOOSENING TORQUE OF THREADLOCKED BONDS

[1-3.] University of Nyíregyháza, Institute of Engineering and Agriculture, Department of Physics and Production Engineering, Nyíregyháza, HUNGARY

Abstract: One of the most important parameters of threadlocked bonds is loosening torque, which is a result of complex, time dependent chemical and physical, static and dynamical processes. Compliance of a threadlocker for a certain technical solution basically depends on it. In this paper we demonstrate results of experimental investigations on widely used threadlockers: Loctite 2400, 2700 and AJett 126.Loosening torque as function of curing time was measured on 8.8 galvanized steel screrws with three different threadlocker. Comprehension between thread surface cleaning, thread size, curing time and strength of thread bond was studied. It can be concluded that sensitivity of threadlockers for prior decontamination show significant difference, furthermore environmentally conscious materials saves costs of treatment, but may cause longer curing time, so deeper quantitative understanding of their functioning is needed for a competitive production design and optimization.
Keywords: threadlocking, loosening torque, production design, environmental consciousness

INTRODUCTION

Today adhesives are applied in a wide variety of industry fields like structure bonding, instant bonding, retaining, gasketing, threadlocking, thread sealing, lubrication and protection or surface treatment. In this study we focus on applications when adhesive makes a connection between two surfaces without any relative motion, like the first six item inthe previous list.

Threadlocking by adhesives has at least duplicate advantage in competitive manufacturing: on the one hand it lowers costs, on the other hand it has additional functions beyond preventing loosening, like protection from corrosion, sealing, reducing number of parts and space demand of the whole assembly. If the adhesive is environmentally friendly, this technology has no additional risk to nature and humans furthermore has no additional costs of safe disposal [8,9,10].

Adhesives function like chemical and mechanical bridge between surfaces to be connected. Strength and other features of glued bond are determined by adhesion between molecules of glue and surfaces, and cohesion between molecules of glue. Van der Waals intermolecular forces play key role in generating adhesive and cohesive forces.

Wettability is a highly important technical concept in adhesive technologies. When adhesives get in contact the surface, in ideal case the whole surface is covered by the liquid state adhesive, so after curing adhesive force arise along the total surface. This is the way of forming thebest, strongest bond. In reality this does not happen for at least three different reason.

1. Surface contaminations form a thin layer between the surface and adhesive preventing them from adhering.
2. Surface roughness, inequalities and porosity may also hamper spreading of adhesive even on a clean surface.For example pores can not be filled perfectly with adhesive. So voids may be formed between the surface and the adhesive, where of course adhesive force can not arise. This is related to the next reason.
3. The smaller the viscosity of the adhesive is, the faster and completer it covers the surface. In many cases viscosity of adhesive increases by time, so it loses gradually its ability to wet (maybe in second or minutes).

This is why surface energy of the adhesive and cleaning of surfaces before gluing or thereadlocking influences substantially the strength of the bond [1]. Adhesive strength is a highly complex quantity. Reference [6] describes a fuzzy logic system for estimeting adhesive strength of thin fil coatings of dynamically loaded machine parts. In this paper we consider a static problem, which

many parameters like frictional coefficient and relative speed plays no role in.

In our experiments we applied anaerobic threadlockers. Curing mechanism of anaerobic adhesives can be scetched as follows:

1. oxygen in the air inhibits the process of curing,
2. when the adhesive becomes occluded from air and get in contact with metal, peroxide molecules start to disintegrate to oxygen radicals,
3. which makes monomers to polymerize,
4. at the end adhesive turns to a solid state polymer which adheres strongly to the surfaces to be bonded together.

Polymerization is a time comnsuming process [2].

Objectives of our research are the followings.

1. Clarify the effect of cleaning (of absence of cleaning) to the strength of the bon din case of different threadlockers.
2. How loosening torque changes during the process of curing.
3. How size of thread influences the loosening torque.

EXPERIMENTAL PLAN AND METHODS

8.8 galvanized steel screws with sizes M10, M16 and M20 were used in our experiments. These are commonly and widely used bonding elements.

In experiments three different threadlockers were applied: a medium strength threadlocker Loctite 2400, and two high strength threadlocker Loctite 2700 and AJett 126.

Experiments were performed without prior cleaning of threads, and also applying cleaning with Loctite SF 7036 cleaner.

Figure 1. Screw and nut disassembled (example)

Loosening torque was measured after 6 different time intervals: 0.5h, 1h, 3h, 24h, 72h, 168h (h means hour). It means that threadlocked screw-nut pairsa were disassembled after a prescribed curing time (Figure 1). 12 measurements were performed for a certain threadlocker-thread size-curing time case. Salient values were omitted if existed, and mean value was calculated.

Experiments were performed at room temperature without termostating.

RESULTS

Results were taken into account if loosening torque exceeded 5 Nm. Under 5 Nm disassembling was possible by hand..Table 1 summarizes which cases were applicable for evaluation.

Before measurement results it is worth to mention two observations what are not studied here in details:

» During disassembly srew and nut heated up significantly. This is because of mechanical energy fed into the system during twisting away transformed to heat.

» Fracture of threadlocker gives qualitative information on relative strength of adhesive an cohesive forces. If cohesive forces are stronger then threadlocker separates from at least one of surfaces. If adhesive forces are stonger, then small pieces of threadlocker was observable on surfaces of both screw and nut.

Table 1. Threadlocker-thread size-curing time combinations resulting more than 5 Nm loosening torque. Letter „n" means that even after 168h (one week) loosening torque did not reach 5 Nm.

Threadlocker	Size	Without cleaning	With cleaning
Loctite 2400 (medium strength)	M10	n	n
	M16	24h, 72h, 168h	24h, 72h, 168h
	M20	0.5h, 1h, 3h, 24h, 72h, 168h	0.5h, 1h, 3h, 24h, 72h, 168h
Loctite 2700 (high strength)	M10	3h, 24h, 72h, 168h	1h, 3h, 24h, 72h, 168h
	M16	1h, 3h, 24h, 72h, 168h	1h, 3h, 24h, 72h, 168h
	M20	0.5h, 1h, 3h, 24h, 72h, 168h	0.5h, 1h, 3h, 24h, 72h, 168h
AJett 126 (high strength)	M10	not studied	not studied
	M16	1h, 3h, 24h, 72h, 168h	1h, 3h, 24h, 72h, 168h
	M20	not studied	not studied

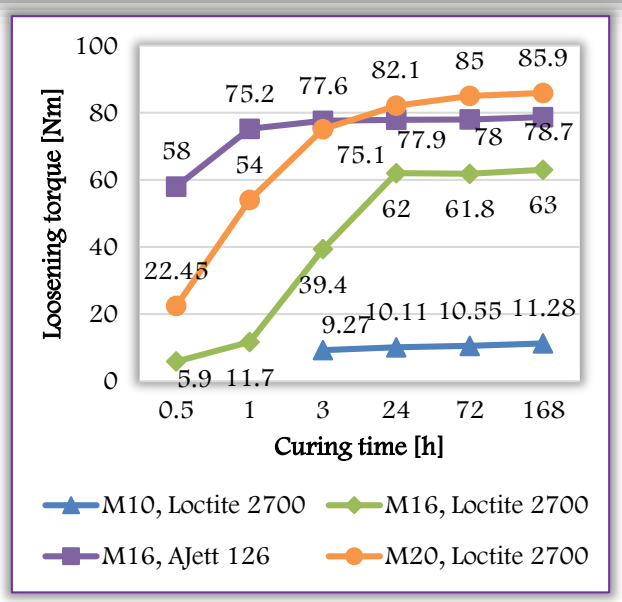

a)

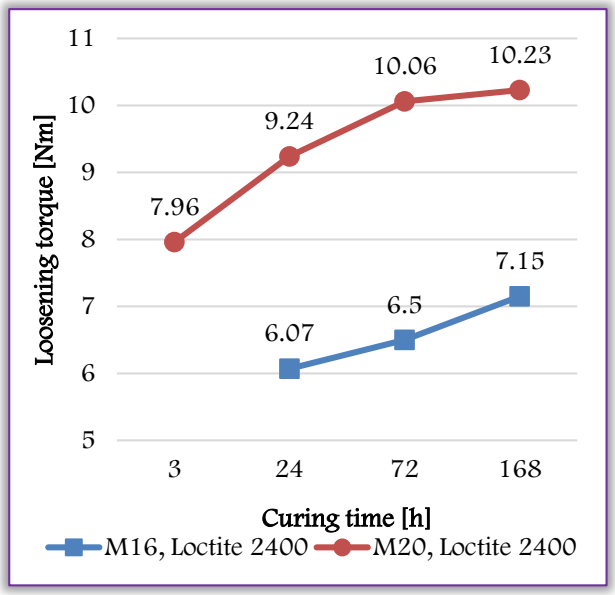

b)

Figure 2. Loosening torque in case of threadlocking without prior cleaning
a) High strength threadlockers,
b) Medium strength threadlockers

Figure 2 demonstrates mean values of loosening torques for experiments in which surface decontamination was not applied. Each curve shows that loosening torque increases with curing time. It is visible that medium strength threadlocker produces almost one magnitude less loosening torque than high strength threadlockers.

On Figure 3 same csases are demonstrated than on Figure 2., but with cleaning before locking with Loctite SF 7036 cleaner. Torques show higher values. Increase in loosening torque depeds on thread size and threadlocker.

At this point we can take some observations:

» Comparing the two high strength threadlocker, is can be stated that AJett 126 provides larger strength than Loctite 2700 in short curin times, but later strengths get close to each other. This can be explained with that Loctite Health and Safety threadlockers cure slower on inactive (e.g. galvanized, like our screws) surfaces.

» Loosening torque increases with thread size as it was expected.

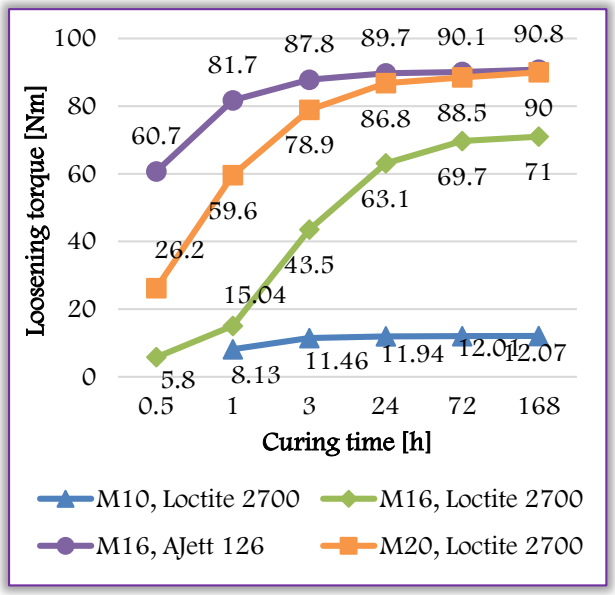

a)

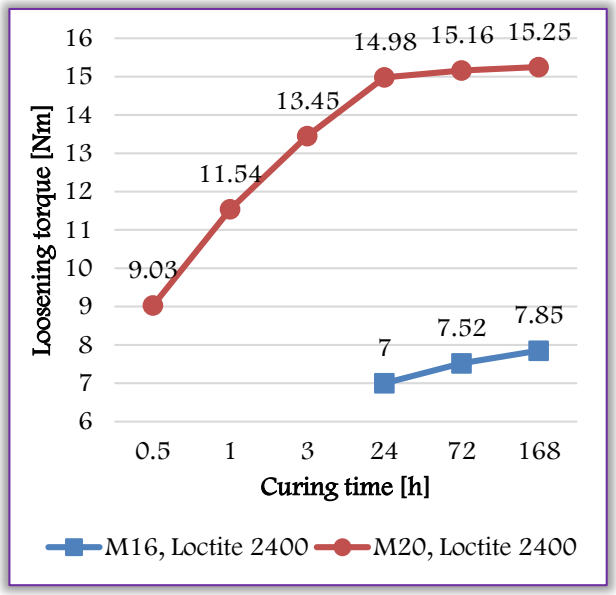

b)

Figure 3. Loosening torque in case of threadlocking with prior cleaning
a) High strength threadlockers,
b) Medium strength threadlockers

Shape of curves are different, but each of them can be more or less approximated with a logarithmic function:

$$f(t) = a \ln t + b, \quad (1)$$

where t is time in hours, a and b are fitting parameters. For high strength threadlockers and for larger thread sizes the approximation is better.

Curve fitting was performed by least square method for cases with at least 5 measurable losening torque. Table 2 shows parameters a, b and R^2, the coefficient of determination:

$$R^2 = \frac{\sum_i (x_i - \bar{x}) - \sum_i (x_i - \hat{x}_i)}{\sum_i (x_i - \bar{x})}, \quad (2)$$

where x_i are measured values at time instant t_i, $\bar{x}$ means average of x_i-s, and $\hat{x}_i$ denotes values of function resulted from regression. When regression can give account completely of the change of measured values, then $R^2=1$.

In Table 2. coefficients of determination changes from 0.78 to 0.98, five values reach 0.95. It means that our results of time dependency of curing and loosening torque can be well approximated by logarithmic funcion (1), and it is in good agreement with [2]. Generally it can be stated that each threadlockers reach strength guaranteed by manufacturer in 1 or 3 hours, and strength increases with a smaller but not negligible value till the end of one week after assembling.

Table 2. Regressed logarithmic function parameters and coefficient of determination for then selected cases from those demonstrated on Figures 1 and 2

Threadlocker and celaning		Size	a	b	R2
no cleaning	Loctite 2700	M10	2.11	7.78	0.98
	Loctite 2700	M16	37.51	0.50	0.90
	Loctite 2700	M20	36.83	27.04	0.95
	Loctite 2400	M20	3.39	4.39	0.95
	AJett	M16	10.71	62.49	0.78
decontaminated	Loctite 2700	M10	2.41	8.82	0.82
	Loctite 2700	M16	41.47	0.79	0.93
	Loctite 2700	M20	36.67	31.46	0.95
	Loctite 2400	M20	3.73	9.15	0.97
	AJett	M16	16.39	65.49	0.87

CONCLUSIONS

Generally, it is advisable to use cleaner before applying threadlockers. In case of AJett 126 threadlocker the mean value of loosening torque was approximately equal to Loctite 2700 with cleaning. So when using AJett 126 cleaning may be considered to be omitted for the sake of save time and energy.

Our experiments justified that loosening torque increases with thread size. This arises from the simple fact that the larger is the thread size the larger is the contacting surface.

For M16 thread AJett 126 threadlocker was also tested, and showed larger loosening torque.

AJett 126 has the shortest curing time, which has the advantage that curing finishes completely till the end of assembpling, so the bond will not be damaged during storage and transport.

Industrial users are more and more constrained by laws for applying health and safety (H&S) materials without any danger-signal on their data sheets instead of recently widely used materials with risks for health and environment. Loctite 2400 and Loctite 2700 are such H&S materials. The price of safety is usually the longer curing time especially on inactive (e.g. galvanized) surfaces, and any pollution makes weaker the strength of the bond.

References

[1.] Alphonsus Pocius: Adhesion and adhesives technology, Hanser publishers, Munich, 2012, ISBN 978-1-56990-511-1
[2.] HENKEL: Worldwide design handbook, Loctite, München, 1998, ISBN 096-5590-0-5
[3.] Loctite 2400 Data Sheet: http://tds.loctite.com/tds5/docs/2400-EN.PDF
[4.] Loctite 2700 Data Sheet: http://tds.loctite.com/tds5/docs/2700-EN.PDF
[5.] AJett 126 Data Sheet: http://www.ajett.com/AJett-126-TDS.pdf
[6.] Kharola Ashwani: Application of fuzzy logic reasoning model for determining adhesive strength of thin film coatings, Fascicule, International Journal of Engineering, 1Tome XIII [2015] p 217-221,ISSN: 1584-2665. ISSN: 1584-2673
[7.] HENKEL: Threadlocking, user's guide, Loctite, Budapest, 2008
[8.] threadlock.co.uk (downloaded 2016. 06. 20.)
[9.] bossard.com (downloaded 2016. 06. 20.)
[10.] Yubo Dong, Daniel P. Hess: Accelerated Vibration Life Tests of Threadlocking Adhesive, Journal of Aircraft 35(5):816-820 · September 1998

ACTA Technica CORVINIENSIS
BULLETIN OF ENGINEERING
ISSN:2067-3809

ACTA TECHNICA CORVINIENSIS
– Bulletin of Engineering
Tome IX [2016], Fascicule 4 [October – December]
ISSN: 2067 – 3809

[1.]Lukáš LIKAVČAN, [2.]Maroš MARTINKOVIČ

MATHEMATICAL MODELING OF FILLED POLYPROPYLENE BY MODIFIED CROSS MODEL

[1-2.]Slovak University of Technology Bratislava, Faculty of Materials Science and Technology in Trnava, SLOVAKIA

Abstract: The aim of this paper is to develop a mathematical model to investigate the rheological characteristics of short fibre reinforced thermoplastics. The rheological properties of this polypropylene were investigated using a capillary rheometer. Rheological characteristics of the composite components influence the development of resultant microstructures; this in turn affects mechanical characteristics of composites. The main rheological characteristics of polymer materials are viscosity and shear rate. They are the ones with fibre ratio changed. From the viscosity of unfilled material and 10% filled material, we can calculate viscosity for other filled materials. This mathematical formula is discussed in this paper.
Keywords: viscosity, reinforced thermoplastics, polypropylene, rheology, mathematical model

INTRODUCTION

Recently, fibre-reinforced thermoplastic composites have found wide application in structural and non-structural applications because of their excellent mechanical properties. Structural parts a prepared by injection moulding, where moulds are manufactured by machining – milling and grinding. For this application currently new polymer composites are developed [1]. But choice of processing conditions depends primarily on the rheological response of polymers. The incorporation of fillers into the thermoplastic melt viscosity increases. The rheological properties of sisal [3] pineapple and [2] the fibers have been studied, but not mathematically described. The mathematical behaviour of rheology of short fibre reinforced thermoplastics by Power-Law has been studied [5]. Viscosity of the fiber-reinforced thermoplastic fibers is affected by the weight ratio of a length of fiber greater at a lower shear rate than at a higher shear rate.

RHEOLOGY

Absolute viscosity provides a measure of a fluid's internal resistance to flow. However, viscosity of a the polymer melt depends on the concentration and the size (molecular weight) of dissolved polymer. By measuring the viscosity of the solution, we should be able to get an idea of the molecular weight [7]. Figure 1 shows a unit volume of the liquid moving speed of the shear deformation. Liquid viscosity is the ratio of shear stress to the resulting deformation speed (or equivalently, ratio of shear stress needed to move solution to a fixed strain rate given strain rate). Shear strain [4]:

$$\gamma = \frac{du}{dy} \tag{1}$$

where u is displacement in the x direction. The strain rate is therefore:

$$\dot{\gamma} = \frac{d}{dt} \cdot \frac{du}{dy} = \frac{dv_x}{dy} \tag{2}$$

where v_x is velocity in the x direction. The relations between viscosity (η), shear stress (τ), and shear rate ($\dot{\gamma}$) is:

$$\dot{\gamma} = \frac{\tau}{\eta} \tag{3}$$

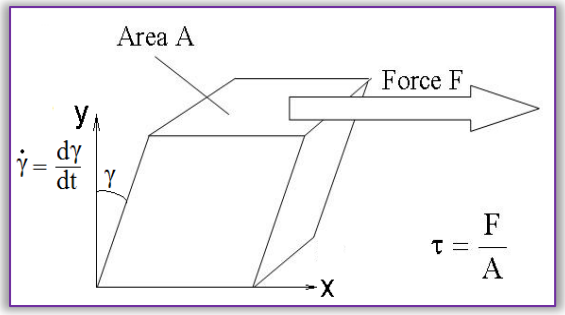

Figure 1. A volume unit of liquid moving at shear rate $\dot{\gamma}$ under the applied shear stress of τ

Newtonian fluid is one in which viscosity independents of shear rate. In other words, plot of shear stress versus shear strain rate is linear with a slope η. The Newtonian liquids, all of the energy passes through the molecules of sliding from each other. Liquids in which shear stress is proportional to the rate of strain are non-Newtonian flow. In the non-Newtonian fluids, relationship of shear stress /

strain rate is not linear. The viscosity varies with shear rate. Apparent viscosity is always defined by the relationship between shear stress and shear rate. Usually, the viscosity decreases at higher shear rates; This phenomenon is known as shear thinning. Real vs. shear forces shear rate to a non-Newtonian and Newtonian liquids are shown in Figure 2.

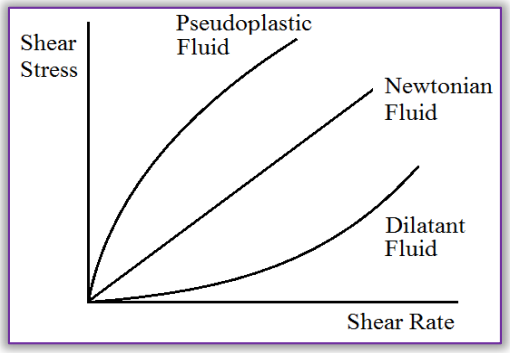

Figure 2. A schematic graph of shear stress to the shear rate for a Newtonian liquid Newton

The higher viscosity η of the polymer is generated by the higher resistance to flow of the melt. Otherwise, i.e. less resistance. The curves of viscosity of most thermoplastics exhibit the same dependence on shear rates, as shown in Figure 3.

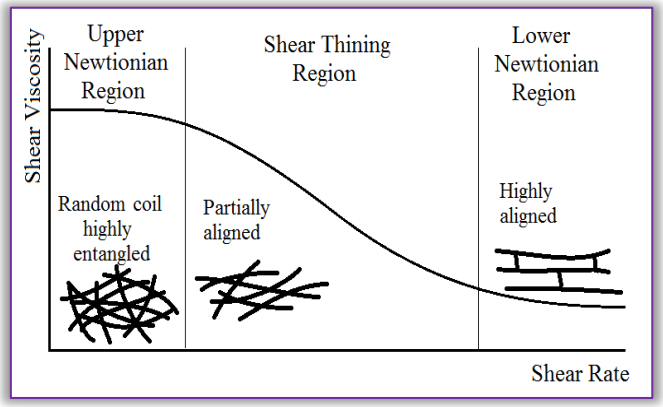

Figure 3. Characteristic viscosity curve of thermoplastics (log-log plot)

At low shear rates, the viscosity is almost constant. This is usually referred to as the upper Newtonian area. The polymer chains are evenly accordance with increasing shear rate so that the viscosity be reduced accordingly. This is called thixotropic region. When all the polymer chains fully with the shear viscosity becomes virtually insensitive to shear rate. This is called the Lower Newtonian region. The upper region and Newtonian shear thinning region is observed in the majority of polymers. The lower the Newton region is not completely clear in most thermoplastics, as shown in the molecular degradation of the ultra-high shear rates.

EXPERIMENTAL MATERIALS AND MEASUREMENT

In this case, the ratio of polypropylene with another fiber, and 0, was 10, 20, 30 and 40%. The thermoplastic is dried in an oven heraus T6 at 80°C for 4 hours. Measurement of the melt rheological properties of the model have been carried out LCR7001 Dynisco a capillary rheometer at a different speed of the piston from 0.9 up to 648 mm.min^{-1}. The diameter of the nozzle is 0.7 mm. The sample was placed inside the extrusion barrel assembly and forced into the nozzle, with the piston in a predetermined piston speed. Measuring conditions were maintained the same in all experiments, and the shear viscosity at various shear rates were obtained on a single charge of material. The measurements carried out at 230°C for each material.

The shear stress at different piston speeds are calculated using the formula:

$$\tau = \frac{F}{4A_P(l_c/d_c)} \quad (4)$$

RESULTS

Measured apparent viscosity vs. function of shear rate with varying proportions of glass fibers, at 230°C, shown in Figure 4. These curves are typical of pseudoplastic materials. They exhibit a decrease in viscosity with increasing shear rate. The behavior of measured curves can be described by the modified Cross equation:

$$\eta = \frac{\eta_0}{1+\left(\frac{\eta_0 \cdot \dot{\gamma}}{\tau^*}\right)^{1-n}} \quad (5)$$

where n is a power index and η_0 zero shear rate. This model is similar to cross. It also describes the dependence of the shear assessment across the top region of Newtonian and shear-thinning region. However, it is generally more suitable for thermoplastics with a broad molecular weight distribution (BMWD). Commercially available grade are usually made with BMWD, so this model is widely used in conventional databases simulation software. The model is exponential (EXP) and the temperature dependence is also known as a Cross-Exp model.

Inclusion of fibers increases the viscosity of polymer systems, and with an increasing fiber content. It is found that prevail at lower shear rates, where the fibers and the polymer molecules are not fully oriented increase in viscosity.

Results measured by capillary rheometer were obtained to discuss the rheological behavior of mixtures. The study showed that the viscosity of the glass fiber reinforced polypropylene, in the molten state, is dependent on the shear rate, and the different fiber content by weight. Chart analysis shows that raw PP is less viscous than reinforced polypropylene. The results in Figure 4 show that increasing the viscosity of the PP reinforced with a fiber material.

Effect of particular fillers on the viscosity is given in the following mathematical formula:

$$\eta = \eta_M + (C \cdot \psi + 1) \quad (6)$$

In Modified Cross model case:

$$\eta = \frac{\eta_0}{1+\left(\frac{\eta_0 \cdot \dot{\gamma}}{\tau^*}\right)^{1-n}} + (C \cdot \psi + 1) \qquad (7)$$

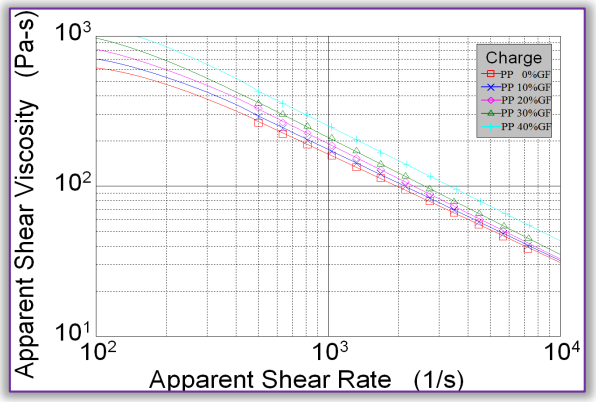

Figure 4. Graphical comparison of measured viscosity and regression viscosity curves at 230°C

In this case:

$$\eta = \frac{1875}{1+\left(\frac{1875 \cdot \dot{\gamma}}{89\,373}\right)^{1-0.232}} + (0.0132 \cdot \psi + 1) \qquad (8)$$

Values n and $\dot{\gamma}$ were calculated by the first and last points of unfilled material by Modified Cross equation. Variable ψ takes the values 0, 10, 20, 30 and 40 in our case.

Tables 1 to 5 show measured viscosity, calculated viscosity by equation 8 and ratio of these viscosities.

Table 1. Measured and calculated viscosity of composites at 0 % glass fibres

Point	Sh.rate (1/sec)	Apparent viscosity (Pa·s) Measured	Calculated	Difference of viscosities
1	500	265.33	264.81	-0.20%
2	637.5	224.82	225.15	+0.15%
3	812.8	190.06	190.72	+0.35%
4	1036.3	160.37	161.05	+0.42%
5	1321.3	135.2	135.62	+0.31%
6	1684.7	113.74	113.94	+0.17%
7	2147.9	95.44	95.54	+0.10%
8	2738.6	79.97	79.97	+0.00%
9	3491.7	66.87	66.84	-0.04%
10	4451.9	55.86	55.80	-0.10%
11	5676.2	46.51	46.54	+0.07%
12	7237.1	38.48	38.78	+0.78%

Table 2. Measured and calculated viscosity of composites at 10 % glass fibres

Point	Sh.rate (1/sec)	Apparent viscosity (Pa·s) Measured	Calculated	Difference of viscosities
1	500	291.96	299.76	+2.60%
2	637.5	245.46	254.87	+3.69%
3	812.8	204.42	215.90	+5.32%
4	1036.3	171.71	182.31	+5.81%
5	1321.3	143.03	153.52	+6.83%
6	1684.7	121.95	128.98	+5.45%
7	2147.9	100.88	108.15	+6.72%
8	2738.6	84.08	90.52	+7.12%
9	3491.7	69.94	75.66	+7.57%
10	4451.9	58.02	63.17	+8.15%
11	5676.2	48.25	52.68	+8.42%
12	7237.1	40.25	43.90	+8.32%

Table 3. Measured and calculated viscosity of composites at 20 % glass fibres

Point	Sh.rate (1/sec)	Apparent viscosity (Pa·s) Measured	Calculated	Difference of viscosities
1	500	333.17	334.72	+0.46%
2	637.5	267.7	284.59	+5.93%
3	812.8	226.78	241.08	+5.93%
4	1036.3	187.88	203.57	+7.71%
5	1321.3	154.32	171.42	+9.98%
6	1684.7	129.41	144.02	+10.14%
7	2147.9	107.57	120.76	+10.92%
8	2738.6	89.29	101.08	+11.66%
9	3491.7	74.26	84.49	+12.11%
10	4451.9	61.32	70.54	+13.06%
11	5676.2	50.63	58.83	+13.93%
12	7237.1	42.8	49.02	+12.69%

Table 4. Measured and calculated viscosity of composites at 30 % glass fibres

Point	Sh.rate (1/sec)	Apparent viscosity (Pa·s) Measured	Calculated	Difference of viscosities
1	500	355.18	369.67	+3.92%
2	637.5	301.19	314.31	+4.17%
3	812.8	250.78	266.25	+5.81%
4	1036.3	209.13	224.83	+6.98%
5	1321.3	171.99	189.33	+9.16%
6	1684.7	140.69	159.06	+11.55%
7	2147.9	117.27	133.37	+12.07%
8	2738.6	96.08	111.63	+13.93%
9	3491.7	78.92	93.31	+15.42%
10	4451.9	65.13	77.90	+16.39%
11	5676.2	54.45	64.97	+16.19%
12	7237.1	45.15	54.14	+16.61%

Table 5. Measured and calculated viscosity of composites at 40 % glass fibres

Point	Sh.rate (1/sec)	Apparent viscosity (Pa·s) Measured	Calculated	Difference of viscosities
1	500	405.8	404.63	-0.29%
2	637.5	342.72	344.02	+0.38%
3	812.8	287.18	291.43	+1.46%
4	1036.3	239.55	246.09	+2.66%
5	1321.3	198.14	207.23	+4.39%
6	1684.7	164.01	174.10	+5.79%
7	2147.9	135.47	145.98	+7.20%
8	2738.6	109.37	122.19	+10.49%
9	3491.7	89.9	102.13	+11.98%
10	4451.9	74.3	85.27	+12.86%
11	5676.2	60.4	71.11	+15.07%
12	7237.1	49.81	59.26	+15.95%

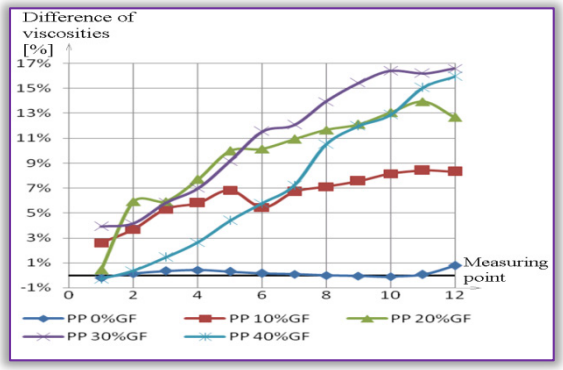

Figure 5. Comparison of measured and calculated viscosity ratio at different materials

CONCLUSION

In this paper, a rheological model for viscoelastic materials was modified in order to predict rheological properties and then compared with experimental results on polypropylene. The predictive results indicated that the developed model well supports the determination of rheological characteristics of the investigated material, such as viscosity and shear stress. All results were obtained from capillary rheometer.

Coefficients n and η_0 were calculated from unfilled material using the Modified Cross model. C was calculated from the filling material coefficient. This enabled to construct the function of the calculation using shear rate and fibre weight fraction.

The measured and calculated viscosities were compared for all materials. Their mutual ratio is shown in Figure 5. This implies that all the values differ by less than ±10%.Using the Power Law model, the values differed by less than ± 10% (different 20%) [5].

However using Modified Cross model the values differed by less than -0.29% and +16.61% (different 16.90%). This means that use of the Modified Cross model gives more accurate values (against Power Law model) comparable to the measured values.

Acknowledgment

This work was supported by the VEGA Grant No. 1/0122/16 of the Grant Agency of the Slovak Republic Ministry of Education.

References

[1] PEETU.P., A. J. NIRMAL, K. JUSTIN, K.E. GEORGE, A. B. Cherian, (2013), Development of Novel Polymer Composites, International Journal of Engineering and Innovative Technologies (IJET), vol. 3, Issue 2, August

[2] JAYAMOL., G., Melt rheological behaviour of short pineapple fibre reinforced low density polyethylene composites. Polymer [online]. 1996, vol. 37, issue 24, pp. 5421-5431

[3] ANTICH, P., VÁZQUEZ, A., MONDRAGON, I., BERNAL, C., Mechanical behaviour of high impact polystyrene reinforced with short sisal fibres. Composites. Part A, Applied science and manufacturing [online]. 2006, vol. 37, issue 1, pp. 139-150

[4] MALKIN, Al. Ya., ISAYEV I.A., Rheology: concepts, methods, and applications. Toronto: ChemTec Pub, 2005. ISBN 189519833x.

[5] LIKAVČAN, L. KOŠÍK, M. BÍLIK, J. MARTINKOVIČ, M., Determination of apparent viscosity as function of shear rate and fibres fraction in polypropylene. In International Journal of Engineering and Innovative Technology (IJEIT). Vol. 4, Č. 5 (2014), s. 23-26, online. ISSN 2277-3754. Projekt: 1/0615/12 113.

[6] Viscosity Model (Thermoplastic only). In: Online-Help [online]. Plastics U, 2013 [cit. 2015-04-04]. Available at: <http://help.plastics-u.com/online-help/molding-knowledge/reference/material/viscosity-model/>

[7] HERMAN, J., On rheology of cross-linked polymers: Some experiments on creep and stress relaxation. International journal of engineering science. 2015. ISSN 00207225.

ACTA Technica CORVINIENSIS
BULLETIN OF ENGINEERING

ISSN:2067-3809

ACTA TECHNICA CORVINIENSIS
– Bulletin of Engineering
Tome IX [2016], Fascicule 4 [October – December]
ISSN: 2067 – 3809

[1.]Marian MITROI, [2.]Anghel CHIRU

NEODYMIUM MAGNETS SUSPENSIONS FOR MECHANICAL SYSTEMS OF THE VEHICLE

1. "Transilvania" University of Brasov, ROMANIA
2. "Transilvania" University of Brasov, ROMANIA

Abstract: Mechanical vibration on the human body they represent a very dangerous factor, in fact they have been / and are considered by many researchers in the field, using various methods to reduce their dangerous values. In the field of automotive, mechanical vibration are induced by the tread and their functional mechanisms, it is transmitted to the human body mostly through the chassis and seats. Thus, in order to reduce dangerous values on while driving, as well as increasing the comfort were achieved various systems such as: magneto-rheological dampers to the vehicle structure and seat with air suspension, but can undertake research for development of new elements for amortization of shocks and vibrations at their level
Keywords: magnets, neodymium, damper

INTRODUCTION

The present paper, makes reference to the study of reduction values of shock and vibration to the vehicle medium, heavy, tractors and special vehicles, at the level of seats.

Current, for seats are encountered these systems: the springs and torsion bars, air suspension or hydro-pneumatic. These existing systems have each one limitations specific to the construction and usage, reason for which the values dangerous for the body are reduced under a certain level only.

The conditions to operating of vehicles or the special machinery, in the building site area, in the rough terrain,a impose permanent new technical solutions. Thus, the achievement of some researches on the development new types of dampers for vibration, lead to increasing the comfort and reducing occupational diseases.

In order to accomplish of these goals, the present approach contemplates the use permanent magnets with high power, for the development of new components for amortization of shocks and vibrations, at the level of vehicles and the human body.

Interaction between two permanent magnets of the same polarity (Figure 1) creates a magnetic field which acts from a distance by the dynamic effect of rejection, so that the trajectory travel of the magnets will change accordingly.

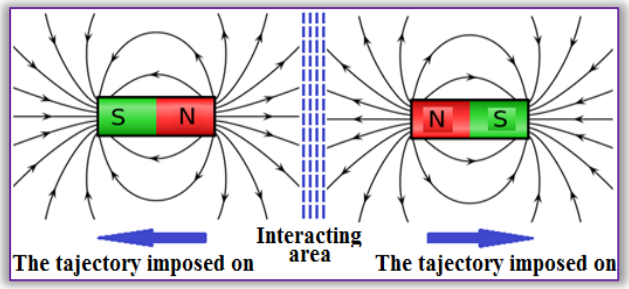

Figure 1. Interaction between two permanent magnets

In the mechanical applications, electromechanical are currently using various types of permanent magnets, composed of magnetic alloys with different properties, depending on the work requirements. Are encountered the magnets such as:

- Ferrite (ceramic) - strongest and breakable, has a intrinsic coercive force (Hci) high value, thing that creates a resistance to demagnetization fields.
- AlNiCo - have a high residual induction (Br), a high temperature stability, but have a low coercive force which causes them to be easily demagnetized.
- SmCo - are resistant to corrosion, have a high magnetism and an intrinsic coercive force (Hci) high, which makes them resistant to external demagnetization fields.
- NdFeB (neomagneţii) - the strongest type of magnets (rare earths) currently used.

The High Power magnets, constructed from rare earths (lanthanides) showed in the construction of trains with magnetic levitation(Maglev) it can give a surplus of comfort to people on while on the go, a major reduction ofmechanical stress and dynamic, and also a high durability thereof at the same times.
This paper aims at developing a system for vibration damping and shocks to seat level, usable for medium-large cars, tractors, but also for special purpose or military.

NEODYMIUM IRON BORON MAGNETS (NEO-MAGNETS) [1] [2] [5] [6]

Neo-magnets used are made most frequently by metallurgy technology of the powders. The powders of micron neodymium iron boron, into an atmosphere of inert gas are exposed to high temperatures close to the melting of the material, and then by pressure in the shapes rubber or steel is sintered. Under the influence of heat and pressure its forming a solid body with certain dimensions, with a much lower porosity.
Scheme of manufacturing process of these types of magnets is shown in the following figure (Figure 2).

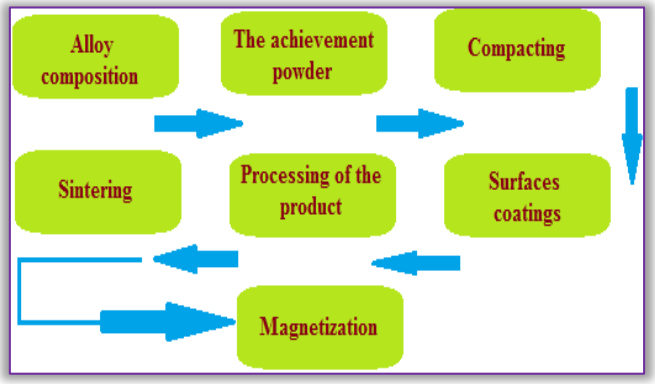

Figure 2. Scheme manufacturing process neodymium magnets

After pressing the alloy, alignment of anisotropic particles significantly favors the residual induction (Br).
The magnets obtained have high hardness (Rc58). Their processing can be done only in the state of non-magnetic, only with special equipment.
The chemical reaction that are frequently used in the manufacturing process, is given by:

$$57\ Fe + 8\ \underline{B} + 10\ Fe_2O_3 + 7.5\ Nd_2O_3 + 52.5\ Ca \rightarrow Nd_{15}Fe_{77}B_8 + 52.5\ CaO \quad (1)$$

The alloy obtained by technological processes may have a chemical composition richer in Nd or B. Geometry of The Magnets(shape) is a very important factor of its performance. Also, the performance of NdFeB alloy is optimized after pressing operation, following application to saturation of a very high magnetic field, which it creates a certain magnetic orientation.
The disadvantages of using these types of magnets are given by sensitivity to high temperatures, humid environment, corrosive, which accelerates the process of demagnetization, so the loss of properties.
Due to this, the magnets are subjected to the process of coating with different compounds having different thicknesses.
The applications of the Neodymium magnets are very broad and include various industrial fields.
Their use being performed primarily to machinery and equipment where is required the high power from a magnet as small as. Such magnets are used in:Energy = wind energy generators; transport =Maglev trains; Electrical = electric motors; Particle accelerators = CERN; Magnetic separators = recycling iron; for lifting very large tasks;Incinerators = extracting metal particles in the ash;
The following table (Table 1) shows the main types of coatings of neodymium of the magnets type and its properties.

Table 1: Type of coating of neodymium

Coverage	Thickness	Color	Resistance
Ni+Ni	10-20	Bright silver	Excellent against humidity
Ni+Cu+Ni			
Zn	8-20	Bright blue	Good against salt
Cu-Zn		Bright color	Excellent against salt
Ni+Cu+Sn	15-20	Silver	Good against humidity
Ni+Cu+Au	10-20	Golden	Good against humidity
Ni+Cu	10-20	Golden	Temporary protection
Epoxy	15-25	Black, red, gray	Excellent against humidity and salt
Ni+Cu+Epoxy			
Zn+Epoxy			

The following table (table 2) presents the main features and differences between neodymium-iron-boron magnet N48, chosen for the project and those of a magnet from Ferrite Y35.

Table 2: The diference of neodymium and iron magnets

Type	Remanence (Br)	Coercive Force (bHc)	Intrinsic coercive force (Hci)	Energy produced (BxH) max.	Maximum temperature (0C max.)
	N/Am (Tesla)	kA/m	kA/m	Kj/m3	0C
N48	1,37 – 1,42	10,8-12,5	> 12	358-382	< 80
Y35	0,40 - 0,41	2,20 - 2,45	2,26-2,51	30-32	< 250

In the project have been selected because of physical, properties the magnets N48, with the following specifications: N = maximum working temperature (80°C); 48 = coefficient of power.
The power of the magnet is determined by a number of factors including: the size, the shape, the ratio of its sizes (width / thickness), the combination of different materials.
Next image (Figure 4) shows the shape, size and magnetic orientation for - N48.

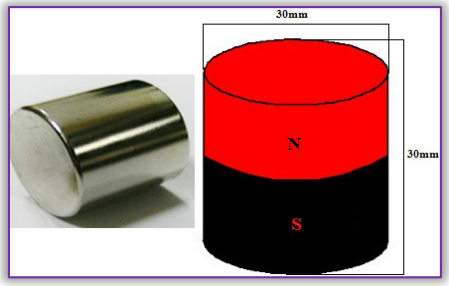

Figure 4. Magnet NdFeB - N48

The characteristics of this type of magnet are:- Shape: disc; size: 30mm x 30mm; weight: 159g; strength: approx. 60kg; coverage: Ni.
The magnetic flux density of the magnet cylinder used, can be calculated in an easy way, at a point located on the central axis of the poles, but a objective calculation must take into account the complexity of the three-dimensional field around the magnet.

NEODYMIUM PERMANENT MAGNET DAMPER

In the mechanical systems for vehicles, two components cand be found mainly for amortization of of mechanical oscillations with a particular importance: the suspension of vehicle and suspension of the seats.
The research foresees working towards a suspension system capable of being used in the construction of various types of vehicle seats. To achieving the damper have been taken into account specific conditions and factors that influence in a negative way desired results:

» The isolation of magnets of the external environment to reduce the influence of temperature or corrosive environment upon them.
» Isolating the magnetic field generated by magnets to not influence the equipment in the immediate area.
» Fixing a minimum distance between the working group of the two polarities magnets.
» a sufficient size for Inductors, to amplify the field created between the two groups of magnets.
» Manufacturing The electronic system which generate a variety of voltages and currents, so it can be seen as eloquent the values damping factor.

Damper cylinder (Figure 4) was built on five structures made of polypropylene (PP-R).

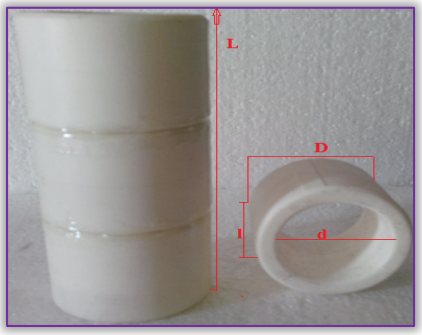

Figure 4. The dimensions of the cylindrical structure

The cylinder has the following dimensions:
- Outer diameter (D) = 66mm; Inner diameter (d) = 52mm;
- Length of section (I) = 50 mm; The total length of the cylinder (L) = 265mm.

Next image (Figure 5) shows the coil - N48 magnets inserted into the containment structures made of polypropylene (PP-R) this ensemble is subsequently inserted and fixed with an adhesive resin expohidic, inside the cylinder. The use of two different-sized structures, one for isolating and supporting the reel assembly - magnet, and the other to support in its entirety the the cylinder with the piston, performs a dual isolation of the magnetic field created by the external environment.

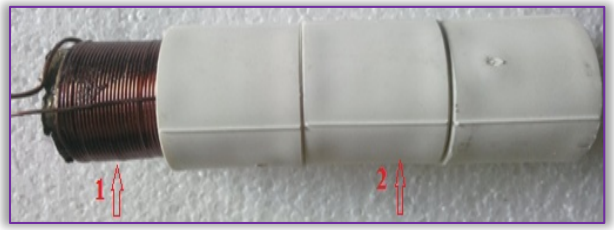

Figure 5. Assembly coil - magnets N48 and containment system PP-R

Composition:1 = inductor; 2 = fastening assembly and polypropylene isolation coil and magnet.
The dimensions of the containment structure (2) of the coil are:

» Outer diameter section (D) = 44mm; section inner diameter (d) = 36mm;
» Section length (l) = 43mm; The total length of the whole PP-R = 215mm.

The three magnets N48 are inserted inside the coil, with a total length of 90mm and representing 64.2% of
surface of the coils. The difference in area up to 100%, is useful for creating magnetic field concentrated in the presence of the other two magnets located on piston, under the influence of current / voltage witch circulating through the coil windings. The coil is achieved by a winding spiral after spiral, from CuEm wire of 0.7 mm in diameter, with a number of 200 windings, with a

total length of 140mm, with an inner diameter of 30mm.

The magnetic field strength generated by the coil to a point of the field is described by Biot-Savart law:

$$dH = \int \left(\frac{\mu_0}{4\pi} \times \frac{I \times dl \times r}{r^3} \right) [A/m] \quad (2)$$

where: r = distance of the point considered to conductor element; I = current intensity;

dl = length of the considered current browsing purposes; μ0 = permeability of the medium (4π x107).

The magnetic induction is influenced by the shape and geometry of the magnet and is calculated using the following equation:

$$B = \mu \times H \quad [T] \quad (3)$$

where: μ = permeability of the medium; H = intensity of the magnetic field.

The electromagnetic force occurring in the coil during the passage of the electric current is described by:

$$F = |B| \quad [N] \quad (4)$$

Where: I = current intensity; B = magnetic induction; l = length of the considered coil.

Repulsive force occurs between the two groups of magnets what interacting inside the coil is given by:

$$F = - \frac{\mu \times q_{m_1} \times q_{m_2}}{4\pi r^2} [N] \quad (5)$$

where: μ = permeability of the medium; q_{m_1}, q_{m_2} = amperage at the two poles; r = the distance between the poles.

The piston (Figure 6) is provided at the free end with two magnet N48 and passing through inside the coil, fixed in the same sense of polarity with the other three, from inside the coil, to achieve the rejection.

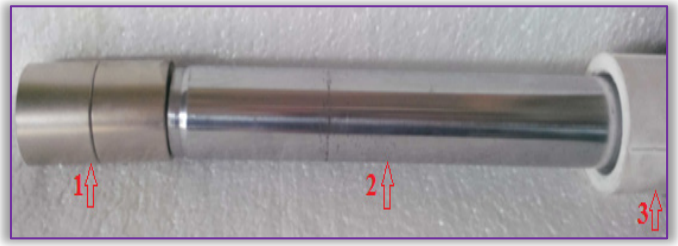

Figure 6. Piston with magnets N48 and limiter PP-R
Composition: 1 - magnets type N48; 2 -piston drive from steel; 3 - limiter PP-R

Composition of new system for research related of systems damping shocks and vibrations, is shown in the following figures (Figure 7 and Figure 8.

Functioning of the system is similar to a hydraulic shock absorber. The Piston, with two magnets mounted in the free end is moving through the inside coil crossed of electricity. The coil free space between the two magnetic structures creates a magnetic field is constant and variable intensity. In the event of an external force acting on the seat (vibrations caused by the road surface), the magnetic field created by the induction coil and the magnets, realize depreciation of shock created below a certain threshold,depending on the voltage and the current which circulating through the coil windings. The Electric coil supply system is equipped with a variable switch so that it can track and analyze way of operation to various voltages and currents: U = 0 - 24V; I = 0 - 5A.).

Figure 7. Assembly coil and insulation
1 = external insulation system and supportive of polypropylene (φint = 52mm); 2 = coil (140mm, d = 30mm, φ = 0.7 mm); 3 = insulator system and supportive coil and from polypropylene (φint = 32mm); 4 = base supportive and fixation outer cylinder from polypropylene; 5 = base star of support cylinder and assembly seat.

Figure 8. Assembly support of the magnetic cylinder
1 = grip and supportive seat system; 2 = limiter piston; 3 = spacer; 4 = cylinder with magnets N48; 5 = base star of support cylinder and assembly seat.

The control module (variator) to the experimental model is placed in the central area between the front seats and in the case serial fabrication of this type of seats suspension, it may be positioned as in the case others control commands, on the side of the seat support. Also, the electrical equipment to experimental module is provided with independent outputs for the voltmeter and ammeter, so they can

independently monitor the current and operating voltage.

CONCLUSIONS

By point of view, of physical properties of magnets neodymium iron-boron (NdFeB) they have the strongest in value, in relation to size and performance. Because of high intrinsic coercive force has a very high resistance to external demagnetization fields, so are indicated for use in electro-mechanical applications.

Magnetic field strength generated between the poles of two magnets, facilitate shock absorption and mechanical oscillations occurring in the seat, to a higher value compared to other existing systems (hydraulic, pneumatic).

The suspensions achieved for the mechanical systems for motor vehicles based on neo-magnets, have a great advantage in reducing vibration caused by the roads, by vehicle structure, and also on persons wich are inside.

The advantages created by this type of damper are related to: reduce shock and vibration values transmitted to the vehicle and its staff, achieving higher stability of vehicles on travel time on rough roads, reducing stress and diseases of the spine, substantial increase seating comfort.

Bibliography

[1.] Jane Paju, Neodymium processing experiences through different eras by Molycorp Silmet As, The Conference of Magnetic Materials in Electrical Machine Applications 2012, PORI;
[2.] V. Panchanathan, Processing of neodymium-iron-boron alloys by rapid solidification technology,Journal of Materials Engineering March 1989, Volume 11, Issue 1, pp 51-60;
[3.] Mitroi,M.,Experimental research, Cernavodă, România, Mai, 2016.
[4.] Mitroi,M.,Arama,C., The implications of random vibrations generated by rough trails and hardly accessible on military body, AFASES, Brasov, Romania, 2016
[5.] http://www.reehandbook.com/neodymium.html;
[6.] http://www.eamagnetics.com/info_sintered_neodymium_process01.asp
[7.] http://www.hobber.ro/index.php?main_page=page&id=3&chapter=100&zenid=1235dbd6bdbf3c9414cd1cbab176e460.

ACTA Technica CORVINIENSIS
BULLETIN OF ENGINEERING
ISSN:2067-3809

ACTA TECHNICA CORVINIENSIS
– Bulletin of Engineering
Tome IX [2016], Fascicule 4 [October – December]
ISSN: 2067 – 3809

ACTA TECHNICA CORVINIENSIS – BULLETIN OF ENGINEERING. Fascicule 1 [JANUARY–MARCH]

ACTA TECHNICA CORVINIENSIS – BULLETIN OF ENGINEERING. Fascicule 2 [APRIL–JUNE]

ACTA TECHNICA CORVINIENSIS – BULLETIN OF ENGINEERING. Fascicule 3 [JULY–SEPTEMBER]

ACTA TECHNICA CORVINIENSIS – BULLETIN OF ENGINEERING. Fascicule 4 [OCTOBER–DECEMBER]

ACTA Technica CORVINIENSIS
BULLETIN OF ENGINEERING

ISSN:2067-3809

ACTA TECHNICA CORVINIENSIS
– Bulletin of Engineering
Tome IX [2016], Fascicule 4 [October – December]
ISSN: 2067 – 3809

[1.]Horaţiu TEODORESCU-DRĂGHICESCU, [2.]Sorin VLASE,
[3.]Ioan SZÁVA, [4.]Imre KISS, [5.]Renata Ildikó SZÁVA

EXPERIMENTAL CHARACTERIZATION OF FIVE PLIES HELIOPOL/STRATIMAT 300 COMPOSITE LAMINATE

[1-3,5.] University Transylvania of Brasov, Brasov, ROMANIA
[2.] University Politehnica Timişoara, Faculty of Engineering Hunedoara, ROMANIA

Abstract: Five plies of Heliopol 9431ATYX_LSE/Stratimat300 glass fabric (300 g/m² specific weight), 6 mm thick laminate has been considered for experimental characterization using the three-point bend tests. Following distributions have been experimentally determined on five layers of Heliopol 9431ATYX_LSE/Stratimat300 glass fabric specimens using data recorded by the materials testing machine: Load (N)-deflection (mm), Stiffness (N/m) of each specimen, Young's Modulus of Bending (MPa) of each specimen, Flexural Rigidity (Nm²) according to each specimen, Maximum Bending Stress at Maximum Load (MPa)-Maximum Bending Strain at Maximum Load, Work to Maximum Load (Nmm) of each specimen, Load at Break (kN)-Deflection at Break (mm), Maximum Bending Stress at Break (MPa)- Maximum Bending Strain at Break and Work to Break (Nmm) of each specimen.
Keywords: Heliopol 9431ATYX_LSE, Stratimat300, Three-point bend tests, Composite laminate, Glass fibers

INTRODUCTION

There is a wide range of fiber formats that together with the process used, provide useful information of different classes of composite materials. The fibers lengths can vary from discontinuous fibers (milled, short and long) to continuous fibers in swirled mats, fabrics, non-crimped fabrics and so on. The major use of glass fibers is still represented by chopped strand mats (CSM). In general, a composite structure is manufactured of various plies of discontinuous or unidirectional fibers with different orientations, stacked together to form so called laminates [1],[6],[11],[16]. The E-glass fibers mat of 300 g/m² specific weight, also known as Stratimat by its trading name, represents the most common reinforcing material used in polyester, vinylester and epoxy based hand lay-up composite laminates. This mat can be used in a wide variety of composite laminates as well as to repair damaged polymer matrix composite structures such as spoilers, hubs, doors, subwoofer boxes and so on, mainly in the automotive industry. It is also recommended for gelcoat applications that require high quality surfaces even for complex shape structures. Various researches have been carried out in the Department of Mechanical Engineering within Transilvania University of Brasov including simulations and experiments of different composites. Some of these are presented in references [2]-[5], [7]-[10], [12]-[15] and [17]-[21].

MATERIALS AND EXPERIMENTAL PROCEDURE

Following polyester/glass fibers composite laminate has been manufactured at Compozite Ltd., Brasov and cured in specific dimensional panels from which specimens have been cut using a diamond mill and water as cooling agent to avoid introduce internal stresses in composite: five layers of Heliopol 9431ATYX_LSE/ Stratimat300 glass fabric (300 g/m² specific weight), 6 mm thick laminate. Specific compounds have been used to manufacture in the hand lay-up process the 6 mm thick laminate. These compounds are: Resin - Heliopol 9431ATYX_LSE; Hardener - Butanox M50; Glass fibers - Stratimat300 with 300 g/m² specific weight.

From cured plate, nine specimens have been cut using a diamond powder mill and a suitable cooling system to avoid introduce internal stresses in the composite laminate. The specimens have been subjected to three-point bend tests until break on a LR5K Plus Lloyd Instruments' materials testing machine using maximum 5kN load cell.

EXPERIMENTAL RESULTS

Following distributions have been experimentally determined on five layers of Heliopol 9431ATYX_LSE/ Stratimat300 glass fabric

specimens using data recorded by the materials testing machine:

- Load (N)-deflection (mm) plotted in Figure 1;
- Stiffness (N/m) of each specimen, presented in Figure 2;
- Young's Modulus of Bending (MPa) of each specimen, shown in Figure 3;
- Flexural Rigidity (Nm^2) according to each specimen, plotted in Figure 4;
- Maximum Bending Stress at Maximum Load (MPa)-Maximum Bending Strain at Maximum Load (Figure 5);
- Work to Maximum Load (Nmm) of each specimen, presented in Figure 6;

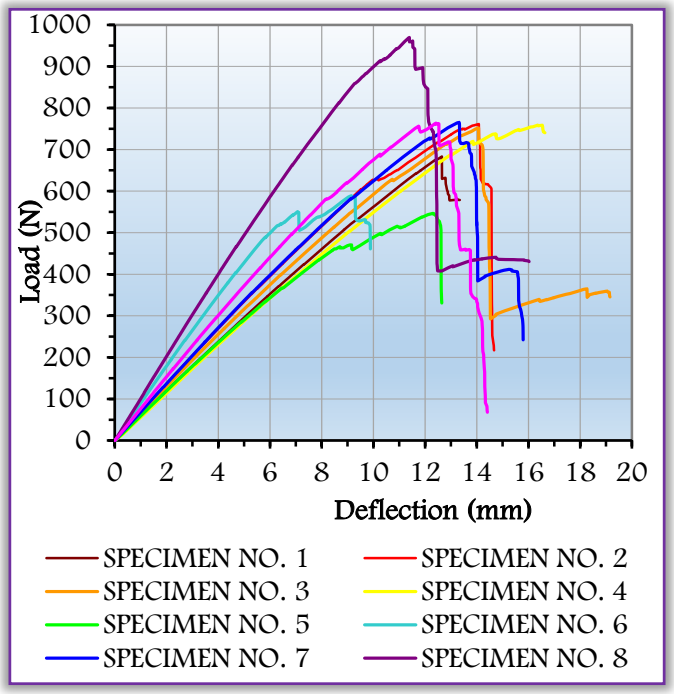

Figure 1: Load-Deflection distribution of five layers Heliopol/Stratimat300 composite laminate

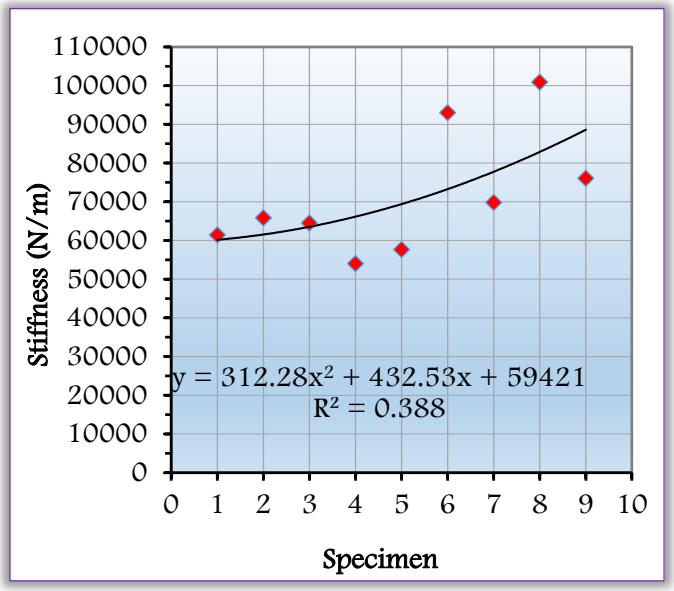

Figure 2: Stiffness distribution of five layers Heliopol/Stratimat300 composite laminate

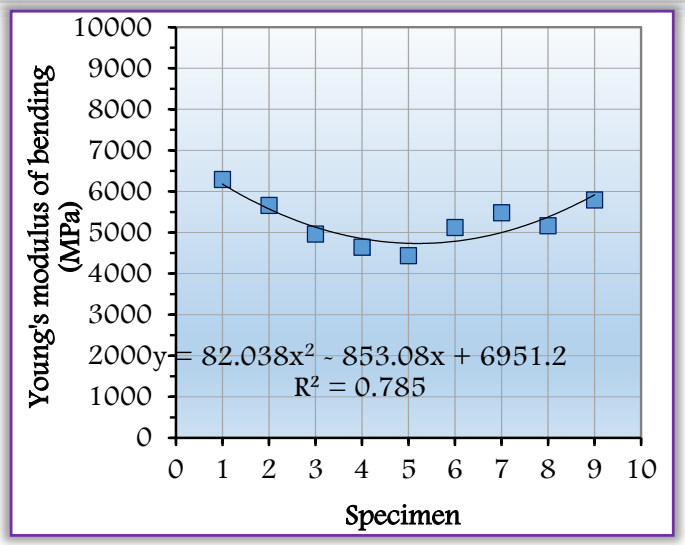

Figure 3: Young's modulus of bending distribution of five layers Heliopol/Stratimat300 composite laminate

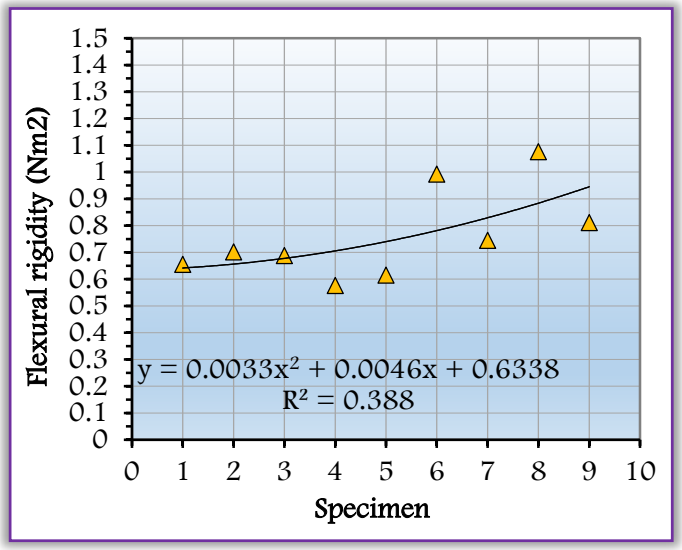

Figure 4: Flexural rigidity distribution of five layers Heliopol/Stratimat300 composite laminate

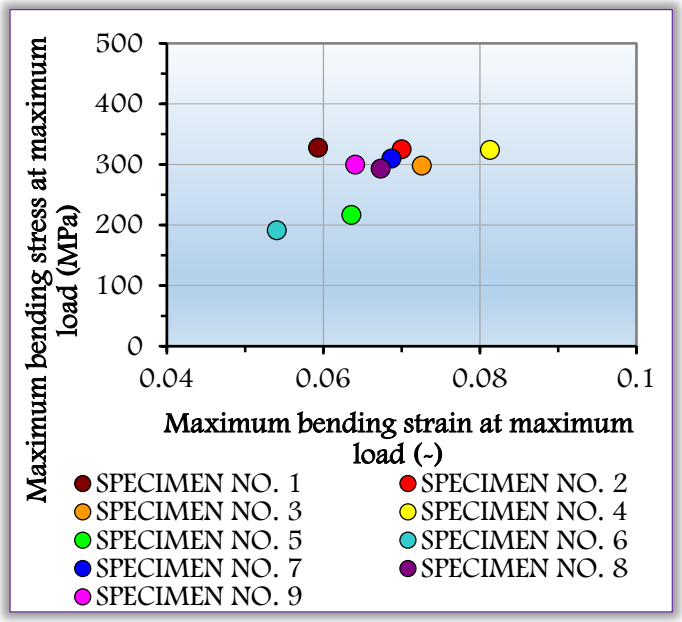

Figure 5: Maximum bending stress at maximum load distribution of five layers Heliopol/Stratimat300

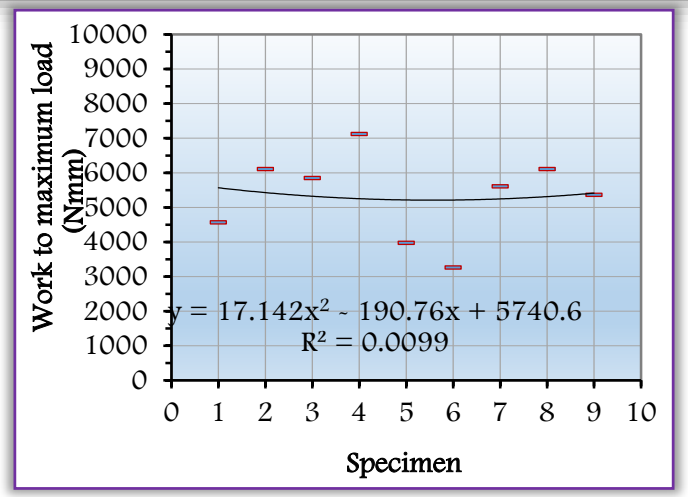

Figure 6: Work to maximum load distribution of five layers Heliopol/Stratimat300 composite laminate

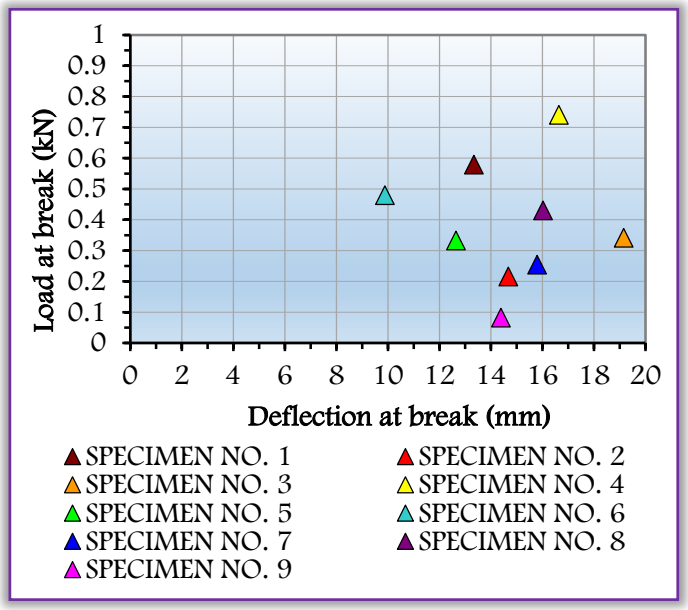

Figure 7: Load-deflection at break distribution of five layers Heliopol/Stratimat300 composite laminate

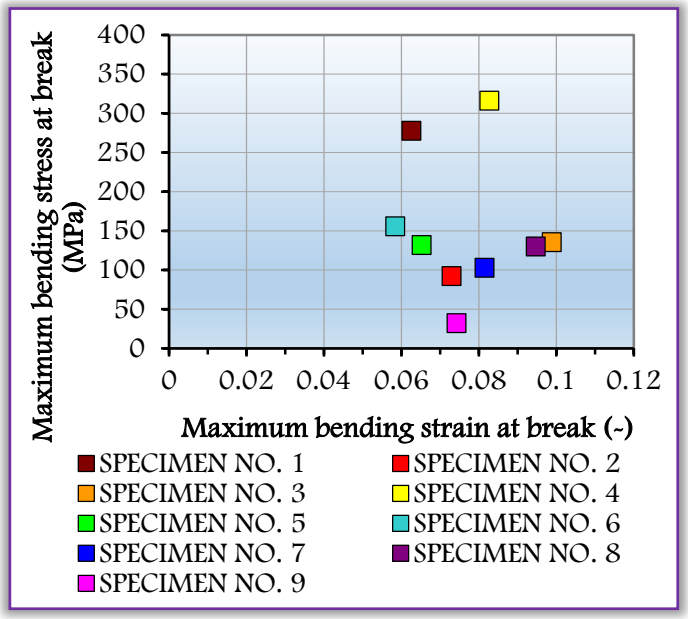

Figure 8: Maximum bending stress at break distribution of five layers Heliopol/Stratimat300

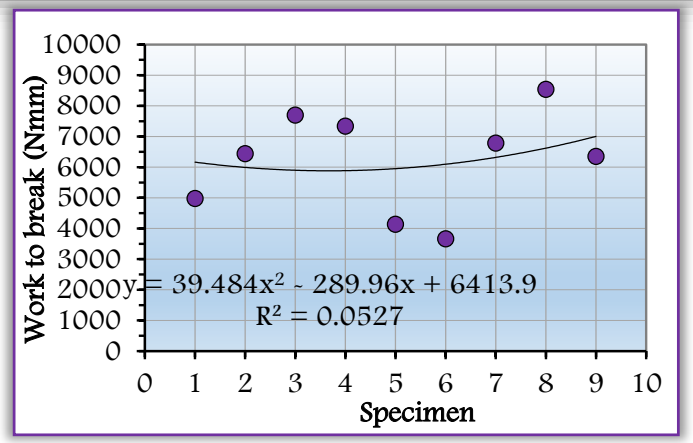

Figure 9: Work to break distribution of five layers Heliopol/Stratimat300 composite laminate

Also, the following distributions have been experimentally determined:

» Load at Break (kN)-Deflection at Break (mm), shown in Figure 7;
» Maximum Bending Stress at Break (MPa)-Maximum Bending Strain at Break (Figure 8);
» Work to Break (Nmm) of each specimen, presented in Figure 9.

CONCLUSION

Regarding the load-deflection distribution of nine Heliopol/Stratimat300 specimens subjected to three-point bend tests, maximum load of 942.12 N has been reached at specimen number eight and a maximum deflection of 18.8 mm presents specimens number three (Figure 1). Specimen number eight presents also maximum stiffness of 100911 N/m and specimens number four exhibits minimum stiffness of 54009.42 N/m (Figure 2).

Young's modulus of bending distribution is situated between a maximum value of 6.29 GPa at specimen number one and a minimum one of 4.43 GPa at specimen number five (Figure 3). The maximum value of Young's modulus of bending represents an outstanding value for this kind of composite laminate subjected to three-point bend tests. The flexural rigidity distribution follows the stiffness distribution and exhibits a maximum flexural rigidity of 1.07 Nm^2 in case of specimen number eight and a minimum value of 0.57 Nm^2 reached by specimen number four (Figure 4). Maximum bending stress at maximum load of 327.99 MPa has been obtained at specimen number one and maximum bending strain at maximum load of 0.08 presents specimen number four (Figure 5). Regarding the work to maximum load distribution of nine Heliopol/Stratimat300 specimens subjected to three-point bend tests, maximum value of 7121.64 Nmm exhibits specimen number four and a minimum value of 3264.84 Nmm has been experimentally determined at specimen number six (Figure 6). Specimen number four exhibits the greatest load at break of 0.74 kN and the greatest

deflection at break of 19.15 mm has been reached by specimen number three (Figure 7). Maximum bending stress at break follows the same distribution as the load at break distribution, the maximum value of 316.27 MPa being noted at specimen number four and the maximum bending strain at break of 0.098 exhibits specimen number three (Figure 8). The work to break distribution of nine Heliopol/Stratimat300 specimens subjected to three-point bend tests present a maximum value of 8541.08 Nmm in case of specimen number eight and a minimum value of 3660.39 Nmm has been reached by specimen number six (Figure 9).

References

[1.] Cristescu ND, Craciun EM, Soos E., Mechanics of elastic composites, Chapman & Hall/CRC; 2003.

[2.] Modrea A, Vlase S, Teodorescu-Draghicescu H, Calin MR, Astalos C., Properties of advanced new materials used in automotive engineering. Optoelectronics and Advanced Materials – Rapid Communications, 7, 5-6, 2013, p. 452–455.

[3.] Niculita C, Vlase S, Bencze A, Mihalcica M, Calin MR, Serbina L., Optimum stacking in a multi-ply laminate used for the skin of adaptive wings. Optoelectronics and Advanced Materials – Rapid Communications (OAM-RC), 5, 11, 2011.

[4.] Teodorescu-Draghicescu H, Scutaru ML, Rosu D, Calin MR, Grigore P., New Advanced Sandwich Composite with twill weave carbon and EPS. Journal of Optoelectronics and Advanced Materials (JOAM), 15, No.3-4, 2013, p.199–203.

[5.] Teodorescu-Draghicescu H, Vlase S, Chiru A, Purcarea R, Munteanu V., Theoretical and Experimental Approaches Regarding the Stiffness Increase of Fibre-Reinforced Composite Structures. Proc. of the 1st Int. Conf. on Manufacturing Engineering, Quality and Production Systems (MEQAPS'09), Transilvania University of Brasov, Romania, WSEAS Press, 2009, p. 449–452.

[6.] Teodorescu-Draghicescu H, Vlase S., Homogenization and Averaging Methods to Predict Elastic Properties of Pre-Impregnated Composite Materials. Computational Materials Science, 50, 4, 2011, p. 1310–1314.

[7.] Vlase S, Teodorescu-Draghicescu H, Motoc DL, Scutaru ML, Serbina L, Calin MR., Behavior of Multiphase Fiber-Reinforced Polymers Under Short Time Cyclic Loading. Optoelectronics and Advanced Materials – Rapid Communications (OAM-RC), 5, 4, 2011.

[8.] Vlase S, Purcarea R, Teodorescu-Draghicescu H, Calin MR, Szava I, Mihalcica M., Behavior of a new Heliopol/Stratimat300 composite laminate. Optoelectronics and Advanced Materials – Rapid Communications, 7, 7-8, 2013, p. 569–572.

[9.] Teodorescu-Draghicescu H, Vlase S, Goia I, Scutaru ML, Stanciu A, Vasii M., Tensile Behaviour of Composite Specimens Made From Chopped Strand Mat Reinforced Polyester Resin. 24th Danubia – Adria Symposium on Developments in Experimental Mechanics, 19-22 September, 2007, Sibiu, Editura Universităţii Lucian Blaga Sibiu, p. 255–256.

[10.] Vlase S, Teodorescu-Draghicescu H, Calin MR, Serbina L., Simulation of the Elastic Properties of Some Fibre-Reinforced Composite Laminates Under Off-Axis Loading System. Optoelectronics and Advanced Materials – Rapid Communications, 5 (3–4), 2011, p. 424–429.

[11.] Naughton BP, Panhuizen F, Vermeulen VC., The Elastic Properties of Chopped Strand Mat and Woven Roving in G.R. Laminae. Journal of Reinforced Plastics and Composites, 4 (2), 1985, p. 195–204.

[12.] Modrea A, Vlase S, Teodorescu-Draghicescu H, Calin MR, Astalos C., Properties of advanced new materials used in automotive engineering. Optoelectronics and Advanced Materials – Rapid Communications, 7 (5–6), 2013, p. 452–455.

[13.] Teodorescu-Draghicescu H, Vlase S, Chiru A, Purcarea R, Munteanu V., Theoretical and Experimental Approaches Regarding the Stiffness Increase of Fibre-Reinforced Composite Structures. Proc. of the 1st Int. Conf. on Manufacturing Engineering, Quality and Production Systems (MEQAPS'09), Transilvania University of Brasov, Romania, WSEAS Press, 2009, p. 449–452.

[14.] Purcarea, R. Motoc, DL, Scutaru, ML., Mechanical behavior of a thin nonwoven polyester mat subjected to three-point bend tests, Optoelectronics and Advanced Materials – Rapid Communications, 6 (1-2), 2012, p. 214 – 217.

[15.] Vlase S, Teodorescu-Draghicescu H, Calin MR, et al., Advanced Polylite composite laminate material behavior to tensile stress on weft direction. Journal of Optoelectronics and Advanced Materials (JOAM), 14, (7-8), 2012, p. 658–663.

[16.] Modrea A, Vlase S, Calin MR, et al., The influence of dimensional and structural shifts of the elastic constant values in cylinder fiber composites. Journal of Optoelectronics and Advanced Materials (JOAM), 15, (3-4), 2013, p. 278–283.

[17.] Niculita C, Gabor A, Gheorghe V, Calin MR, Scutaru ML., A new epoxy glass roving fabric material with a nonwoven PES fibers structure used in a composite laminates, Journal of Optoelectronics and Advanced Materials (JOAM), 15, (3-4), 2013, p. 176-181.

[18.] Scutaru ML, Baritz M, Galfi BP., Radiation influence on micro-structural mechanics of an advanced hemp carbon hybrid composite, Optoelectronics and Advanced Materials – Rapid Communications, 8, 11-12, 2014, p. 1145-1149.

[19.] Scutaru ML., Toward the use of irradiation for the composite materials properties improvement, Journal of Optoelectronics and Advanced Materials, 16, (9-10), 2014, p. 1165-1169.

[20.] Scutaru ML, Baba M, Baritz MI., Irradiation influence on a new hybrid hemp bio-composite, Journal of Optoelectronics and Advanced Materials (JOAM), 16, (7-8), 2014, p. 887-891.

[21.] Scutaru ML, Baba M., Investigation of the Mechanical Properties of Hybrid Carbon-Hemp Laminated Composites Used as Thermal Insulation for Different Industrial Applications, Advances in Mechanical Engineering, Article Number: 829426, 2014.

ACTA TECHNICA CORVINIENSIS
– Bulletin of Engineering
Tome IX [2016], Fascicule 4 [October – December]
ISSN: 2067 – 3809

[1.]József SÁROSI, [2.]Bence GYÜRKY

DESIGN AND CONSTRUCTION OF A HUMANOID ARM DRIVEN BY PNEUMATIC MUSCLE ACTUATOR

[1-2.] University of Szeged, Faculty of Engineering, Szeged, HUNGARY

Abstract: Electrics, hydraulics and pneumatics can be the main motion power of industrial robots. Pneumatic cylinders, pneumatic motors, pneumatic stepper motors and pneumatic bellows are widely used in industrial environment due to their power/weight ratio, power/volume ratio, strength, compactness, simplicity, reliability and cost. Disadvantages of pneumatic actuators can be summarized as follows: difficult to control accurately, air compressibility, compliance and noisiness. Relatively new type of the pneumatic actuators is the pneumatic artificial muscle (PAM) or pneumatic muscle actuator (PMA). Fluidic Muscle made by Festo Company is one of the most investigated commercially available PMA. Pneumatic muscle actuators can be used in industrial environment as well as in prosthesis or rehabilitation devices. In this paper a humanoid arm actuated by Fluidic Muscle is developed and presented.
Keywords: pneumatics, pneumatic muscle actuator, Fluidic Muscle, humanoid arm

INTRODUCTION

Automation and robotics have become well-grounded in the industry. Modern manufacturers and companies could hardly operate without robots and automated processes [1], [2]. In this study pneumatic muscle actuator as one of the least investigated type of actuators but an important driver element is applied.

History of PMAs dates back to 1930s. Unfortunately, due to lacks in technology the production was limited. In 1950s, Joseph L. McKibben was the first who designed an artificial muscle for practical use in medicine. McKibben is often mentioned as the pioneer in PMA. In 1980s, engineers in Birdgestone Company in Japan produced the so called Rubbertuator PMA. Recently, the most often applied is the Fluidic Muscle and also the Shadow Air Muscle (SAM) produced by the Shadow Robot Company.

The structure of the most PMAs can be divided into two main parts: a flexible membrane (e.g. latex, silicone rubber or chloroprene) and a load carrying element (e.g. nylon, fiberglass or aramid). On the basis of their connection, Daerden in [3] discriminates braided muscles, netted muscles and embedded muscles (Figure 1).

The difference between netted and braided muscles is in the density of the threads in the braided mesh shell (network of load carrying element) surrounding the membrane: it is higher for the braided muscles. In embedded muscles the loaded threads are settled into the elastic tube. In the paper this type of muscles is considered [4].

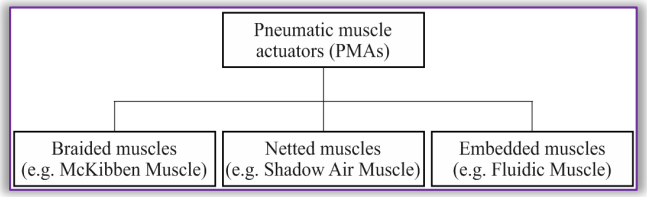

Figure 1. Classification of PMAs

Working principle of PMAs is simple: when a PMA is pressurized, the flexible membrane tends to increase its volume against the braided mesh shell which is non-extensible, therefore the actuator will be shortened and a pulling force will be produced if the muscle is connected to a load [5-7].

This flexible actuator shows similarity to human muscle, because the force and motion generated by PMA are linear and unidirectional. For two-direction motion an antagonistic pair of PMAs or a spring returned PMA has to be used [8]. Typically, one muscle moves the load, while the other serves as a brake. During the motion in opposite direction the mechanisms commute their action. These serially connected muscles are named antagonistic pair: the muscle for motion is a flexor while the braking muscle is named an extensor or antagonist [9].

PMAs differ from general pneumatic cylinders as they have no inner moved parts and there is no

sliding on the surfaces. The main disadvantages are nonlinear and time variable behaviour, existence of hysteresis and step-jump pressure. This is why number of control schemes and static and dynamic models can be found in the literatures [10-19].

This paper is organized in 5 sections. After Introduction, in Section 2 the design process and the 3D printing are described. A key moment of the design and construction (choosing PMA) is presented in Section 3. Section 4 shows the assembling and testing the arm. The paper ends with Conclusions (Section 5).

For this study DMSP-10-250N-RM-RM (with inner diameter of 10 mm and initial length of 250 mm) type Fluidic Muscle is selected.

DESIGN AND 3D PRINTING

The humanoid hand was designed with the help of the Autodesk Inventor software (Figure 2). As a first step, the digits of the fingers were made. For reasons of practicality each finger was designed to be the same length and instead of three degrees of freedom they were provided with two ones meaning that the upper digit was designed to be bent at a 45° angle.

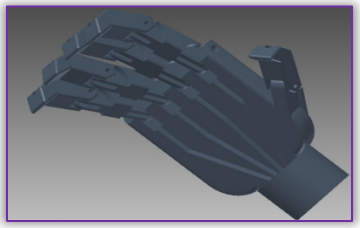

Figure 2. 3D plan of the hand

PLA (polyactic acid) was used as the base material for 3D printing which is a biodegradable and thermoplastic polymer. It is produced from high-starch grains (Figure 3).

The printing of the fingers took a total of 6 hours and 10 minutes at a speed of 40 mm/s with a layer resolution of 300 microns and a printer nozzle of 0,4 mm diameter. During this time the printer used up 32,85 m of 1,75 PLA fiber filament (total mass: 98 g). During printing the temperature of the platen was 60°C and the temperature of the nozzle was 222°C.

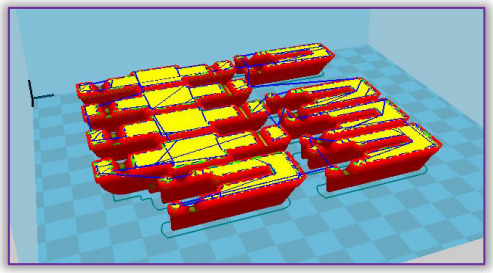

Figure 3. Fingers in the 3D printer's slicing program

The printing of the hand (Figure 4) with the same parameters as the ones used for the fingers took altogether 7 hours and 30 minutes. This required a total of 46,83 m of 1,75 PLA fiber filament (total mass: 140 g).

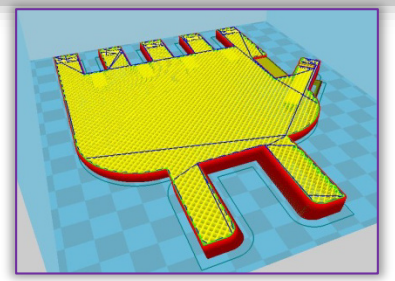

Figure 4. Hand in the 3D printer's slicing program

Figure 3 and Figure 4 show the slicing program of the 3D printer. The parts in red represent the outer layer of the body, which the printer builds at a slow speed. The green and yellow parts refer to the filling of the body where the head works at a higher speed. Blue shows the lines where the head is inactive.

CHOOSING PNEUMATIC ARTIFICIAL MUSCLE

Moving the fingers of the humanoid arm requires one or more PMAs. The first step in sizing the Fluidic Muscles was determining the correct diameter [20]. The diameters and corresponding maximum forces of the muscles are the followings:

- 5 mm - 140 N,
- 10 mm - 640 N,
- 20 mm - 1500 N,
- 40 mm - 6000 N.

Since the 10 mm PMA's maximum force is the closest to the force developed by a human hand this diameter was chosen (Figure 5).

After deciding on the diameter the length of the muscle had to be determined. It is clearly visible in Figure 5 that at 800 kPa (8 bar) of maximum pressure the extent of the greatest contraction is 25%, and that the exerted force is 0 N. In that case, the maximum contraction of a 250 mm long muscle is 62,5 mm. Since the required range was 45-50 mm, a muscle of 250 mm length and 10 mm in diameter was chosen.

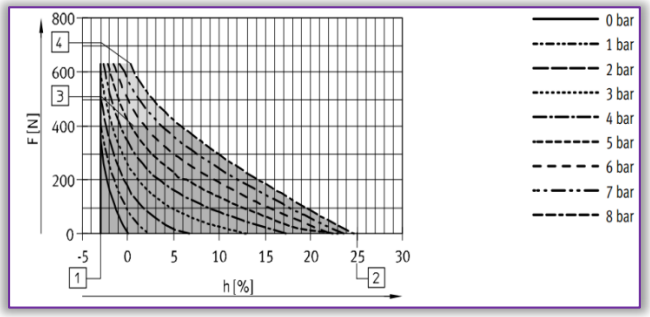

Figure 5. DMSP-10 muscle's force-contraction (relative displacement) diagram [21]

ASSEMBLING AND TESTING THE ARM

The humanoid arm consists of 3 main parts. One of them is the forearm. Since 3D printing is still a relatively expensive technology these days, the forearm was made from a 480 mm long and 63 mm diameter PVC tube. Another part is the muscle and the device holding it. The device consists of 2

shackles and a rail. The back shackle was fixed to the arm and the front shackle to the rail which made it possible for the muscle to move linearly. The third and final part is the hand. The humanoid arm is visible in its assembled form in Figure 6.

Figure 6. Assembled form of the arm

The last step was testing the arm. The first test was carried out without PMA. By pulling the shackle back the fingers closed, while letting go of the shackle caused the rubbers to pull them back into their original (straight) position.

As the next step, the arm was tested with pressurized air. It was made to hold a filled and cylinder-shaped 250 ml volume plastic bottle. The pressure was continuously increased in the muscle. At a pressure of 600 kPa the arm was able to hold the bottle. Following this success, it held several other common household objects. Figure 7 illustrates a few examples of them.

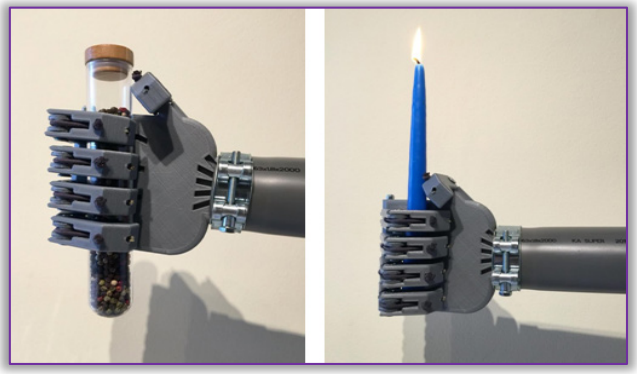

Figure 7. Holding some common household objects

CONCLUSION

The main aim of this work was to design and produce a humanoid arm that can be moved at the fingers by a pneumatic artificial muscle. Based on the results it can be concluded that the humanoid arm meets the objectives as it performs the expected task (moving the fingers).

Since pneumatic muscles were available only in limited numbers it is only possible to move the fingers together, but by using more muscles it can be used as the hand of a humanoid robot as well.

References

[1.] Mester Gy.: Improving the Mobile Robot Control in Unknown Environments, Proceedings of the Conference YUINFO' 2007, Kopaonik, Serbia, 11-14 March, 2007, pp. 1-5

[2.] Mester Gy.: Distance Learning in Robotics, Proceedings of The Third International Conference on Informatics, Educational Technology and New Media in Education, Sombor, Serbia and Montenegro, 1-2 April, 2006, pp. 239-245

[3.] Daerden, F., Lefeber, D.: Pneumatic Artificial Muscles: Actuator for Robotics and Automation, European Journal of Mechanical and Enviromental Engineering, 2002, Vol. 47, No. 1, pp. 11-21

[4.] Sárosi J., György L.: Comparison of Static Force Exerted by Fluidic Muscle and Shadow Air Muscle, Analecta (Review of Faculty of Engineering, Analecta Technica Szegedinensia), 2015, Vol. 9, No. 2, pp. 15-19

[5.] Toman P., Gyeviki J., Endrődy T., Sárosi J., Véha A.: Design and Fabrication of a Test-bed Aimed for Experiment with Pneumatic Artificial Muscle, International Journal of Engineering, Annals of Faculty of Engineering Hunedoara, 2009, Vol. 7, No. 4, pp. 91-94

[6.] Sárosi J., Gyeviki J., Szabó G., Szendrő P.: Laboratory Investigations of Fluid Muscles, International Journal of Engineering, Annals of Faculty of Engineering Hunedoara, 2010, Vol. 8, No. 1, pp. 137-142

[7.] Sárosi J., Szabó G., Gyeviki J.: Investigation and Application of Pneumatic Artificial Muscles, Biomechanica Hungarica, 2010, Vol. 3, No. 1, pp. 208-214

[8.] Sárosi J., Csikós S., Asztalos I., Gyeviki J., Véha A.: Accurate Positioning of Spring Returned Pneumatic Artificial Muscle Using Sliding-mode Control, 1st Regional Conference - Mechatronics in Practice and Education (MECH-CONF 2011), Subotica, Serbia, 8-10 December, 2011, pp. 350-356

[9.] Enoka, R. M.: Neuromechanics of Human Movement, Human Kinetics Publishers, Champaign, United States, 2008

[10.] Gyeviki J., Sárosi J., Csikós S.: Position Control of Pneumatic Actuators with PLC, 2011 IEEE/ASME International Conference on Advanced Intelligent Mechatronics (AIM 2011), Budapest, Hungary, 3-7 July, 2011, pp. 742-747

[11.] Sárosi J., Fabulya Z.: New Function Approximation for the Force Generated by Fluidic Muscle, International Journal of Engineering, Annals of Faculty of Engineering Hunedoara, 2012, Vol. 10, No. 2, pp. 105-110

[12.] Sárosi J.: Accurate Positioning of Pneumatic Artificial Muscle at Different Temperatures Using LabVIEW Based Sliding Mode Controller, 9th IEEE International Symposium on Applied Computational Intelligence and Informatics (SACI 2014), Timisoara, Romania, 15-17 May, 2014, pp. 85-89

[13.] Tothova M., Pitel J., Hosovsky A., Sárosi J.: Numerical Approximation of Static Characteristics of McKibben Pneumatic Artificial Muscle, International Journal of Mathematics and Computers in Simulation, 2015, Vol. 9, pp. 228-233
[14.] Sárosi J., Bíró I., Németh J. Cveticanin L.: Dynamic Modelling of a Pneumatic Muscle Actuator with Two-direction Motion, Mechanism and Machine Theory, 2015, Vol. 85, pp. 25-34
[15.] Sárosi J.: Dynamic Investigation of a PAM Actuated Vibrating Pendulum, International Journal of Engineering, Annals of Faculty of Engineering Hunedoara, 2015, Vol. 13, No. 1, pp. 141-144
[16.] Sárosi J., Pitel J., Seminsky J.: Static Force Model-Based Stiffness Model for Pneumatic Muscle Actuators, International Journal of Engineering Research in Africa, 2015, Vol. 18, pp. 207-214
[17.] Sárosi J.: Elimination of the Hysteresis Effect of PAM Actuator: Modelling and Experimental Studies, Technical Gazette, 2015, Vol. 22, No. 6, pp. 1489-1494
[18.] Hosovsky A., Pitel J., Zidek K., Tothova M., Sárosi J., Cveticanin L.: Dynamic Characterization and Simulation of Two-link Soft Robot Arm with Pneumatic Muscles, Mechanism and Machine Theory, 2016, Vol. 103, pp. 98-116
[19.] Mukhtar, M., Akyürek, E., Kalganova, T., Lesne, N.: Implementation of PID, Bang-bang and Backstep-ping Controllers on 3D Printed Ambidextrous Robot Hand, In Studies in Computational Intelligence, Springer, 2016, 21 p.
[20.] Sárosi J., Gergely A., Tölgyi F.: Student Project on Pneumatically Driven Muscle-like Actuators, 3rd International Conference and Workshop Mechatronics in Practice and Education - MECHEDU 2015, Subotica, Serbia, 14-15 May, 2015, pp. 153-157
[21.] Festo: Fluidic muscle DMSP/MAS datasheet: https://www.festo.com/cat/en_us/data/doc_enus/PDF/US/DMSP-MAS_ENUS.PDF

ACTA Technica CORVINIENSIS
BULLETIN OF ENGINEERING
ISSN:2067-3809

ACTA TECHNICA CORVINIENSIS
– Bulletin of Engineering
Tome IX [2016], Fascicule 4 [October – December]
ISSN: 2067 – 3809

[1.]Z. KRIAUCIŪNIENĖ, [1, 2.]R. VELICKA, [1.]S. CEKANAUSKAS, [1, 2.]L.M.BUTKEVICIENĖ, [3.]L. MASILIONYTĖ, [4.]E. ŠARAUSKIS, [5.]D. KARAYEL, [2.]P. LAZAUSKAS

EVALUATION OF SOIL TILLAGE PROCESS TO IMPROVE SEEDBED PREPARATION AND CROP DENSITY

[1.]Experimental Station, Aleksandras Stulginskis University, LITHUANIA
[2.]Institute of Agroecosystems and Soil Science, Aleksandras Stulginskis University, LITHUANIA
[3.]Joniškėlis Experimental Station, Lithuanian Centre for Agriculture and Forestry, LITHUANIA
[4.]Institute of Agricultural Engineering and Safety, Aleksandras Stulginskis University, LITHUANIA
[5.]Akdeniz University, TURKEY

Abstract: The humidity of the soil and the quality of seedbed preparation is an important factor influencing crop density and early establishment. It largely depends on weather conditions, but partly it can be controlled by soil management system. Field experiments of different soil tillage methods were carried out at Experimental Station of Aleksandras Stulginskis University in 2009. Treatments involved: 1) direct drilling, 2) shallow ploughing (10 cm depth), and 3) deep ploughing (20 cm depth). In the experiment spring barley (Hordeum vulgare L.) variety 'Simba' was cultivated. The soil of experimental site – Calc(ar)i-Endohypogleyic Luvisol (Drainic). The aim of the research was to estimate the influence of soil management system on seedbed parameters and crop density. It was estimated, that the highest roughness of the soil surface (31.8 mm) was, when the soil was ploughed at 20 cm depth, but contrarily the seedbed roughness was the lowest (15.2 mm). Estimated direct drilling depth was 15.6 mm and in ploughed soil it was 51.7–57.4 mm. In ploughed soil at 20 cm depth the seeds were sown too deep – 88.4 % of them were below sowing depth. When direct drilling was used – too shallow – 57.8 % of seeds were above sowing depth. The highest accuracy was estimated in shallow ploughed soil – 43.8 % of the seeds were at sowing depth. Nevertheless in the dry weather conditions spring barley germinated faster when direct drilling was used, later on, experimental results showed, that spring barley crop density was significantly thinner (180 plants per m²) compared to deep or shallow ploughing, whereas depth of the ploughing did not influence thickness of crop stand: it was 431–445 plants per m².
Keywords:deep and shallow ploughing, direct drilling, seedbed, crop stand density

INTRODUCTION

Seedbed preparation is crucial for the growth of seedlings, plant establishment and the final yield of crops. A great consideration is needed to determine the most suitable conditions for crop growth. An important aspect of this is the physical characteristics of the seedbed such as soil strength, bulk density, water content, water retention, aggregate size and distribution, aggregate stability, temperature, oxygen and nutrient availability [2,8]. Experimental evidence suggests that different soil tillage and sowing methods has a significant effect on soil structure, soil bulk density, total and air-filled porosity, soil moisture and crop yield [5,14,12,9,6].

A seedbed is defined as a loose shallow surface layer, tilled during seedbed preparation with a basal layer underneath which is untilled and usually firm [3]. A seedbed is required to provide a medium for germination, root growth, emergence and establishment [1], as such this covers a wide range of determinate factors. Seedbed preparation and sowing, often referred to as secondary tillage, aim primarily to create suitable soil conditions for germination, plant emergence and subsequent crop growth: the seed should be placed at a desired depth; the soil at sowing depth should contain enough water and suitable temperature and aeration conditions for germination; the seedbed should act as an evaporative barrier; the soil should not be over-compacted; tillage operations should also control weeds [1]. Seedbed practices are therefore key as cultivation implements impose varying degrees of alterations to both the surface soil and sub-soil. As such it is crucial to determine the best practice for seedbed preparation to maximise crop establishment and yield. The aim of our experiment was to estimate the influence of soil

management system on seedbed parameters and crop density.

MATERIALS AND METHODS

» **Experimental site and soil.** Field experiments were carried out at the Experimental Station of the Aleksandras Stulginskis University (former Lithuanian University of Agriculture) (54°53′ N, 23°50′ E) in 2009. The soil of the experimental site is Calc(ar)i-Endohypogleyic Luvisol (Drainic) according to the WRB 2014 [4]. The main soil properties were: soil pH_{KCl} 6.7–7.2, arable layer 25 cm, humus content in the arable layer 2.2–3.0%, total N 1.47 g kg^{-1}, available phosphorus (P_2O_5) 119–242 mg kg^{-1}, and available potassium (K_2O) 100–124 mg kg^{-1}.

» **Experimental design.** The experiment had a one-factor design. It was performed in four replications. Spring barley (Hordeum vulgare L.) variety 'Simba' was cultivated using different soil management practices: 1) direct drilling, 2) minimum tillage (10 cm depth), 3) deep tillage (20 cm depth).

» **Method to characterize the quality of a seedbed.** Immediately after sowing the mean depth is determined by transferring all loose soil within a 40x40 cm^2 steel frame to a measuring cylinder. Before this, the difference in elevation between the highest and the lowest points of the soil surface within the frame is measured to give a simple characterization of the roughness of the surface, and afterwards, the roughness of the base of the seedbed is determined in the same way. The seedbed in the open frame at the side is separated into two or three sub-layers using a scoop and simple hand tools. The soil from each sub-layer is transferred to a hand sieve set to determine the aggregate size distribution and the number of seeds.

» **Crop density.** Density of spring barley crop was evaluated by counting method (with 20 x 30 cm frame) in 16 places of each plot.

» **Meteorological conditions.** April 2009 was 2.8 times warmer compared to the annual average and extremely dry. Rainfall was 4.5 times less than usual and all it dropped out during the first ten days, the hydrothermal coefficient of the April was 3.8 (very wet). During the sowing time of spring crops, the hydrothermal coefficient of the second and third ten days was 0; there were no rainfall at all. At May, the average temperature was 2°C below the annual average. At the end of the first ten days started to rain, but moisture, however, was too low, because during the second ten days was too little rainfall. A little more rainfall was only at the end of May. This month's average hydrothermal coefficient was 1.3 (sufficient moisture). June was nearly 1°C cooler and precipitation was 1.7 times more than the usual, hydrothermal coefficient 2.6 (very wet). The air temperature and precipitation in July was a close to the annual average estimate hydrothermal coefficient 1 (sufficient moisture). August was wet (hydrothermal coefficient 1.7), although the average air temperature and precipitation was close to the annual average. However, the first ten days was favourable for harvesting, there were no rainfall.

» **Statistics.** Statistical significance of differences between treatments was evaluated by Fisher's protected least significant difference test at $P_{(level)} < 0.05$ was performed using package of statistical programmes SELEKCIJA [15].

RESULTS

The roughness of the soil surface shows the difference in elevation between the lowest and highest points of the surface. In our experiment the influence of soil management practices on soil surface roughness was significant (Figure 1). The highest unevenness of soil surface after barley sowing was when the soil was deep ploughed in autumn, compared with shallow ploughing (8.5 %) and direct drilling (18.6 %). The lowest soil surface roughness was in direct sowing plots. A. Kairyte (2005) found that all methods of minimised soil tillage and direct drilling significantly reduced the soil surface roughness in comparison with deep ploughing in autumn [7]. In our experiment the highest roughness of the base of the seedbed was in shallow ploughed soil – 39.9 % higher compared to direct drilling, and 49.0% if compared with deep ploughing in the autumn.

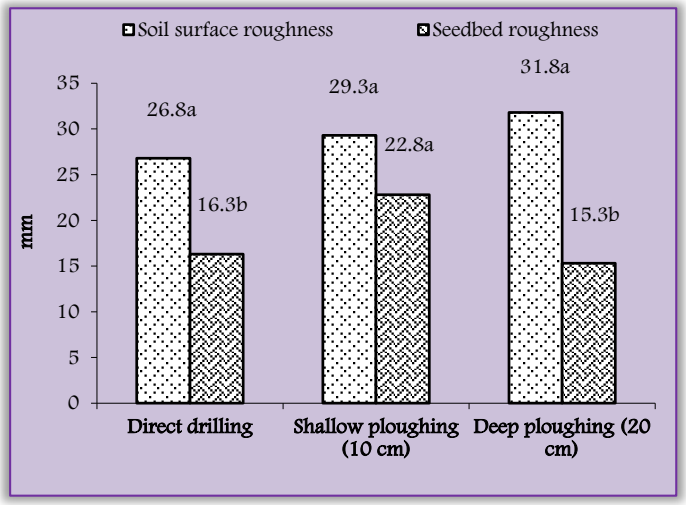

Figure 1 – The roughness of the soil surface (LSD_{05} = 6.40) and the roughness of the base of the seedbed (LSD_{05} =4.34) using different soil management practices

Seedbed quality/conditions determine plant uniformity and growth intensity in the beginning of the vegetation. Fast and uniformly emerged crops have capability to smoother weeds and are the basis

for a good harvest. The quality of seedbed depends on tillage and quantity of organic matter [16,11].
According to I. Hakansson et al. (2002), A. Velykis and A. Satkus (2005) the optimal depth for sowing in heavy soils is 3–5 cm [3,16]. In our experiment sowing depth closest to the optimal was in the shallow and deep ploughed soil (51.7–57.4 mm) (Figure 2). In direct drilling sowing depth was on average 3.4 times shallower than in autumn ploughed soil. This difference was significant.

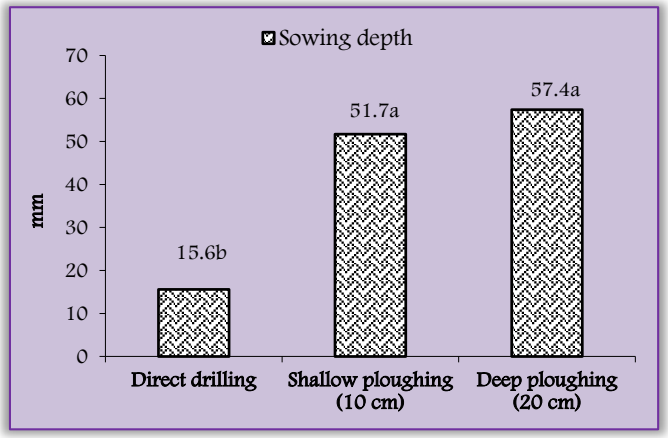

Figure 2 –Sowing depth using different soil management practices (LSD_{05} = 13.45)

Table 1. The effect of primary soil tillage on the seed distribution in seedbed layers

Soil management practices	Spring barley seed distribution %		
	Soil surface (L1)	Sowing depth (L2)	Under sowing depth (L3)
Direct drilling	57.8	37.0	5.2
Shallow ploughing (10 cm)	10.7	43.8	45.5
Deep ploughing (20 cm)	0	11.6	88.4
	LSD_{05} = 10.44	LSD_{05} = 13.39	LSD_{05} = 25.43

The highest quantity of seeds (57.8%) in the top seedbed layer (L1) were distributed when direct drilling was used, that was significantly higher (5.8 times more) compared to shallow ploughing plot (Table 1). In this layer no seeds were found when deep ploughing in the autumn was used. In the sowing depth (L2) the most quantity of seeds (43.8%) were when soil was shallow ploughed in the autumn: that was 1.2 times and 3.8 times more compared with direct drilling and deep ploughing, accordingly. When soil was shallowly ploughed in the autumn, almost half of seeds (45.5%) were distributed deeper than the optimum sowing depth (4–5 cm), and when the soil was ploughed deeply, most of the seeds (88.4%) were incorporated too deep. It could be stated that sowing depth of spring crops in direct drilling largely depends on soil compaction. Autumn and pre-sowing tillage allows more even seed distribution in soil and less seeds remains on soil surface. Experiments made by other authors showed that even seed introduction was also reduced when the intensity of soil tillage was minimized, because the soil surface became harder, the greater part of the plant residues remained in the soil surface or was introduced into the upper soil layers, preventing seed introduction [11].

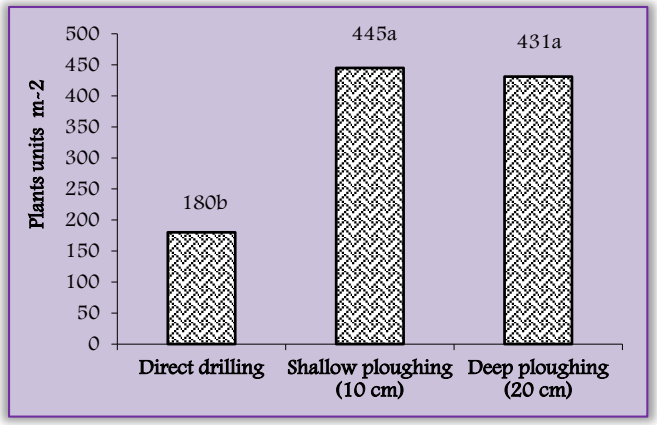

Figure 3 – Spring barley germination using different soil management practices (LSD_{05} = 87.14)

The quality of soil preparation for sowing, soil physical mechanical properties, and moisture content has a great influence on the field seeds germination. Proper seedbed preparation significantly increases seeds contact with the soil. Our experiment showed that a soil management practice has a significant effect on the germination of spring barley (Figure 3).
When the soil in the autumn was deeply or shallowly ploughed the germination of barely was on average 2.4 times higher than in direct drilling. Nevertheless the moisture content in the no tilled soil was sufficient, but during winter soil was compacted therefore the seed was sown too shallow and that had significant influence on poor germination of barley. Minimum soil tillage according to seedbed quality in heavy soils is more suitable for the winter crops than for spring crops [16,10]. Reduced primary soil tillage can be applied in cereal cultivation on Central Lithuania's cultivated sandy light loamy soils: instead of conventional soil tillage (stubble breaking at a depth of 10–12 cm and deep ploughing at a depth of 22–25 cm) it is feasible to apply direct drilling or minimal soil tillage at a depth of 10–12 cm. Replacement of conventional soil tillage by direct drilling into non-tilled and into minimally tilled soil suits best for oats and winter wheat grown after good preceding crops [14]. Application of shallow ploughing for the pea provided the worst germination [17].Spring barley and peas were more susceptible to the simplification of autumn soil tillage: when barley and peas were sown into minimally tilled soil or direct-drilled into non-tilled soil spray-applied with Roundup (4 l ha^{-1}), a significantly lower yield was obtained [14].

CONCLUSIONS

Experiments of different soil tillage methods showed, that the highest roughness of the soil surface (31.8 mm) was when the soil was ploughed in the autumn at 20 cm depth, but contrarily the seedbed roughness was the lowest (15.2 mm).

Sowing depth of spring crops in direct drilling largely depended on soil compaction. Deep or shallow soil ploughing allowed more even seed distribution in soil and less seeds remained on soil surface. The highest accuracy was estimated in shallow ploughed soil – 43.8 % of the seeds were at sowing depth.

When the soil in the autumn was deeply or shallowly ploughed the germination of barely was on average 2.4 times higher than in direct drilling. Nevertheless in the dry weather conditions spring barley germinated faster when direct drilling was used. Later on, spring barley crop density was significantly thinner (180 plants per m^2) compared to deep or shallow ploughing, whereas depth of the ploughing did not influence thickness of crop stand: it was 431–445 plants per m^2.

References

[1.] Arvidsson J., Rydberg T., Feiza V. (2000) - Seedbed preparation in Sweden. Soil and Tillage Research, 53: 145–155.

[2.] Atkinson B. S. (2008) - Identification of optimum seedbed preparation and establishment using soil structural visualisation: doctoral thesis, the University of Nottingham, UK.

[3.] Håkansson I., Myrbeck Å., Etana A. (2002) - A review of research on seedbed preparation for small grains in Sweden. Soil and Tillage Research, 64: 23–40.

[4.] IUSS Working Group WRB (2014) - World reference base for soil resources 2014. International soil classification system for naming soils and creating legends for soil maps. World soil resources reports No. 106. FAO, Rome

[5.] Jodaugienė D. (2002) - The influence of long term ploughing and loosening on soil and crops in the system of reduced soil tillage: Doctoral Dissertation, LŽŪU, Akademija.

[6.] Juchnevičienė A., Raudonius S., Avižienytė D., Romaneckas K., Bogužas V. (2012) - Effect of long-term reduced soil tillage and direct seeding on winter wheat crop. Agricultural Sciences, 3: 139–150.

[7.] Kairytė A. (2005). Tillage intensity and straw incorporation effect on barley agrocenosis: Doctoral Dissertation:, LŽŪU, Akademija.

[8.] Romaneckas K., Pilipavičius V., Šarauskis E. (2010) - Impact of seedbed density on sugar beet (Beta vulgaris L.) seed germination, yield and quality of roots. Journal of Food, Agriculture & Environment, 8: 599–601.

[9.] Romaneckas K., Šarauskis E., Pilipavičius V., Sakalauskas A. (2011) - Impact of short-term ploughless tillage on soil physical properties, winter oilseed rape seedbed formation and productivity parameters. Journal of Food, Agriculture & Environment, 9(2): 295–299.

[10.] Satkus A., Velykis A. (2008) - Modelling of seedbed creation for spring cereals in clayey soils. Agronomy Research, 6: 329–339.

[11.] Šarauskis E., Vaiciukevičius E., Sakalauskas A., Romaneckas K., Jasinskas A., Lillak R. (2008) - Impact of sowing speed on the introduction of winter wheat seeds in differently-tilled soils. Agronomy Research, 6: 315–327.

[12.] Šarauskis E., Romaneckas K., Buragienė S. (2009) - Impact of conventional and sustainable soil tillage and sowing technologies on physical-mechanical soil properties. Environmental Research, Engineering and Management, 3(49): 36–43.

[13.] Šimanskaitė D. (2002) - Effect of different soil tillage and sowing methods on soil and yield. Žemdirbystė-Agriculture. T. 79. P. 131–138.

[14.] Šimanskaitė D. (2007) - The effect of ploughing and ploughless soil tillage on soil physical properties and crop productivity. Agricultural Sciences, 14(1): 9–19.

[15.] Tarakanovas P., Raudonius S. (2003) – Statistical data analysis in agronomic research using computer programs ANOVA, STAT, SPLIT-PLOT from the packages SELEKCIJA and IRRISTAT. Akademija.

[16.] Velykis A., Satkus A. 2005. Factors of seedbed quality on heavy soils. Žemdirbystė=Agriculture, 1(89): 53–66.

[17.] Velykis A., Satkus A. 2012. Response of field pea (Pisum sativum L.) growth to reduced tillage of clayey soil. Žemdirbystė=Agriculture, 99(1): 61–70.

ACTA Technica CORVINIENSIS
BULLETIN OF ENGINEERING

ISSN:2067-3809

ACTA TECHNICA CORVINIENSIS
– Bulletin of Engineering
Tome IX [2016], Fascicule 4 [October – December]
ISSN: 2067 – 3809

[1.]Adrian-Catalin VOICU, [2.]Gheorghe I. GHEORGHE

3D DIGITIZATION TECHNOLOGY - A NEW MECHATRONIC METHOD OF INTELLIGENT INTEGRATED DIMENSIONAL CONTROL OF COMPLEX COMPONENTS FROM AUTO INDUSTRY

[1-2.]National Institute of Research & Development in Mechatronics & Measurement Technique, Bucharest, ROMANIA

Abstract: The progressive replacement of traditional methods with high-tech (complex) intelligent mechatronic systems, technologies and equipment is one of the most important aspects of the production processes evolution in all industrial fields. Due to accelerated progress of technology transferred in multiple technological innovations, extremely favorable conditions have been created for the development of production and thus of the manufacturing technologies and intelligent control on the automatization way of all subsystems constituting technological processes. New intelligent mechatronic technologies of 3D integrated control offer an integrated portfolio of software solutions and measurable difference for an enhanced quality by accelerating the time needed to produce the components, while the costs of new products are considerably reduced, but also for product development, fundamentally oriented towards ensuring a high level of efficiency in manufacturing and integrated control by increasing the profitability and satisfaction of product delivery requirements.
Keywords: auto industry, mechatronics, 3D integrated control, laser scanning, digitization

INTRODUCTION

The invention of the automobile revolutionized the transportation of goods and people starting with the XX and XXI centuries, changing forever the way people live and conduct business, providing jobs for millions of people and generating a basis for a variety of related services. This represents at the moment 4% of European GDP and over 9% of employment in the manufacturing sector and establish itself as a key sector of the European and world economy.

Progressive replacement of traditional tools with intelligent technological equipment more complex and automated constitutes one of the most important aspects of development processes and production systems in all industrial fields [1]. New technologies for processing and assembly, coupled with the continued growth performance of computing systems and their integration in all industrial activities constituted the foundations for the development of automatic type flexible production system (FMS - Flexible Manufacturing System), or integrated production systems served by a global system of control or management (CIM - Computer Integrated Manufacturing).

Technological and economic developments due to the introduction of mass production have led to the concept of automation of production, everything starting with the introduction in 1920 by Henry Ford, the „transfer line" and „robot man" that serve with the imposed rhythm the automobile manufacturing process lines existing on the model Ford T.

a) Individual assembly of Ford automobiles (1903)

b) production lines Model Ford T (1925)

Figure 1: Comparison of automated assembly lines

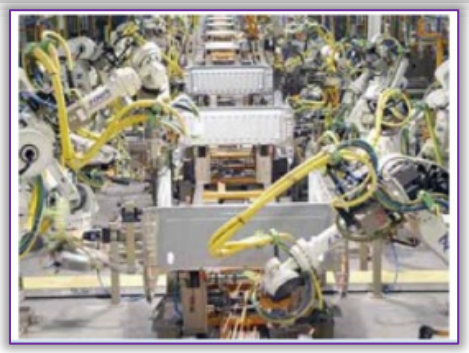

c) robotized assembly Michigan (2000)
Figure 1: Comparison of automated assembly lines

DIMENSIONAL CONTROL IN AUTO INDUSTRY

The first systematic technical and scientific preoccupations for quality have emerged with the increasing production of parts in the second half of the nineteenth century, developments taking place in several stages, with specific characteristics: the stage of inspection quality, quality control stage through various statistical methods, step by step quality assurance and total quality control stage. The control systems implemented in the automotive industry operates in compliance with requirements continuously updated on product quality, which they control [2]. For machinery construction, as in other industries, quality control is organized under four forms: before processing, after processing (passive), during processing (active) or integrated.

- Passive control consists of verify the accuracy of parts after the whole batch was processed, in which case it is excluded the prevention of defective goods (hence the term „passive") and may take place by universal or special means who can be automated and non-automated.
- Active control is conducted during the batch processing of parts and his aim is the conducting of technological process to avoid defective goods. Control can be performed during processing itself (without the removing of piece from work device) or immediately after processing, information about measurement being used in this case to regulate the technological system for the next batch of pieces.

The most important factor in dimensional controlling is the precision of measuring equipment, the method and means of measuring, their choice being made according to two categories of indicators (factors): metrology indicators (graduated scale, the limits of measurement, power measurement) and economic indicators (cost control means), and the time for checking and adjusting device, instrument or machine measurement / control.

With the development of society, it was passed into a wider characterization of the quality through a growing number of operations that are part of the following categories [5]: obtain measurements and calibrations, recognition and identification of specific features, reading character or information code, detecting the presence of an object or a mark, comparing an object with a model or guide whit a machine or a robot.

The modern methods for 3D measuring, checking or dimensional control for quality products can be: „with contact" (coordinate measuring machines - CMM), many of which are currently controlled by computer or CN); „without contact", divided into two categories: optical and non-optical. The methods that are most commonly used for 3D dimensional control are with contact which in practice is generally used for lengths and diameters, the most representative equipment being the coordinate measuring machines (CMM). Optical systems are the most commonly used inspection methods without contact for product quality and relies on the technology use of microelectronics and computer processing of signals from sensors or transducers (computerized view, laser scanning, and photometry)[6].

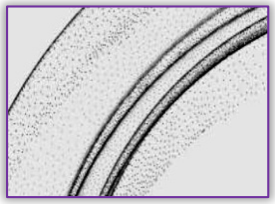

a) 3D point cloud

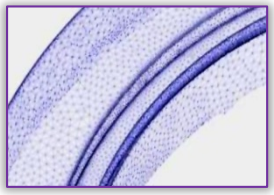

b) 3D polygonal network (mesh)

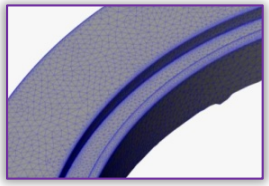

c) resulting surface
Figure 2: 3D digitize process

3D scanning is the process of copying the digital information of a physical object (solid), his geometry, so it is known as digitization. „Digitizing" or „3D digitize" is a process that uses a digitizer probe with contact or without contact to capture the shape of objects and recreate them in a virtual workspace through a very dense network of points (xyz) as a 3D graphical representation. Dates that are collected under the form of points and the resulting file is called „point cloud" (Fig. 1). That „point cloud" type of information is then usually post-processed in a network of small polygons,

which are called 3D polygonal network. The technologies used to build 3D scanning devices are multiple and each technology has its own limitations, costs, advantages and disadvantages [3]. The architectures of laser and video sensors used in the dimensional control without contact were developed as an alternative to replace the sensors (probes) with contact, where physical contact is not generally possible, in the super finished areas, rough high or where sharp edges are present. Total accuracy of a 3D acquisition system depends above all on the precision of the system probe used (contact or without contact) and the features of acquisition device for acquisition with contact or the structure of acquisition system for the ones without contact. This accuracy may vary from one micron to one millimetre depending on the system used and the acquisition speed may vary from several thousands to several points per second [7].

3D DIGITIZING TECHNOLOGY

The current stage of development of configurable intelligent systems is represented mainly by two functional solutions [9]:

- software solution;
- hardware solution.

Design and implementation of some intelligent mechatronic systems for installation and control of manufacturing lines in the automotive industry is a complex process that involves several steps.

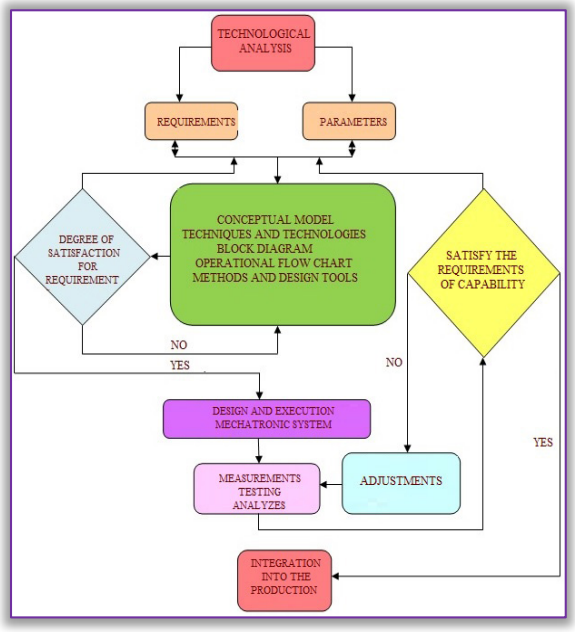

Figure 3: Design and implementation of mechatronic systems

Because intelligent mechatronic systems for 3D integrated control are used both on the production lines and in metrological laboratories and because the parts can have different shapes and complex surfaces an adaptive intelligent mechatronic system generally has the following configuration as in figure 4 [9].

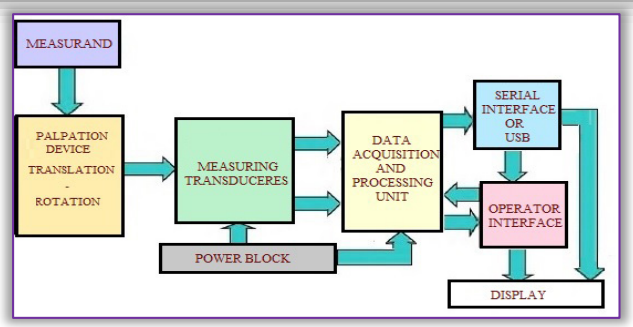

Figure 4: Schematic diagram of a measurement intelligent mechatronic system

Based on this design methodology and general configuration was developed an intelligent mechatronic system for bimodal dimensional control by laser scanning for parts and complex families of parts in automotive industry. It is composed of:

- Laser scanning device (scanner laser probe): acquisition system, hardware and software library with acquisition and primary processing functions (image improvement, alignment, excess points elimination, colour combination). Chosen scanning system is a Class II laser scanner type of short distance (because we want the highest possible accuracy - required for complex parts), with triangulation, having two CMOS acquisition sensors [8]. The optimal scanning distances are between 51 mm and 251 mm, the width of the scanning line may vary between 30 and 100 mm, this being of the cross type. Average accuracy of control at point level is 1-2 μm. This acquisition rate is between 50 and 500 frames per second and the number of points read on a scanning line is equal to 500. This laser acquisition system interfaces with the PC using a standard USB port and has a digital signal RS485 that can be used to synchronize with the robot controller.
- Articulated vertical robotic arm or measurement arm (anthropomorphic) with 6 degrees of freedom – mechanical system, multitasking controller, guidance by visual feedback from the control room (GVR), learning module, driving software for moving robot with GVR extension. The robot system used for scanning the laser is a vertical articulated robot with six degrees of freedom [4]. Repeatability of the robot arm movement is about 0.01 mm. Areas of movement (6 axes, 6 rotation joints) of the robot system are: axis (joint) 1: ± 170°, axis (joint) 2: -170°, + 45°, axis (joint) 3: -29°, +256°, axis (joint) 4: ± 190°, axis (joint) 5: ± 120°, axis (joint) 6: ± 360°. Maximum speed composed at peak is 4400 mm.
- Rotary table with precise positioning in regulation loop of the displacement and rotation

speed. The rotary table is driven as external motion axis by the controller of the robot arm and table motion is synchronized with the movement of the robot, in other words, the robot has added an additional degree of freedom (the 7th). The use of the rotary table is necessary because the robot arm cannot reach behind the object without causing a collision or without changing its position.

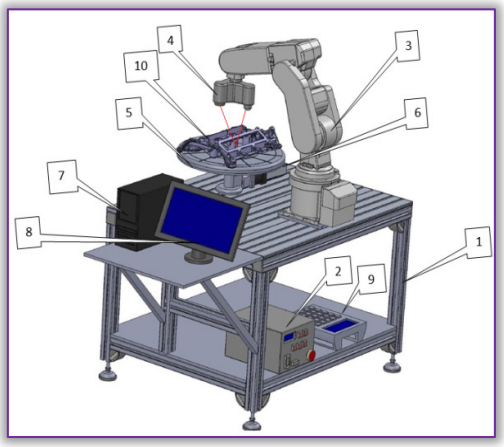

Figure 5: Hardware and software structure of the laser scanning system
1 - table; 2 - controller; 3 - robotic arm (6 degrees of freedom); 4 - laser scanning system; 5 - table positioning piece (rotary); 6 - control axis for the table; 7 - PC; 8 - Display; 9 - manual control and teaching device (teaching pendant); 10 - measured piece.

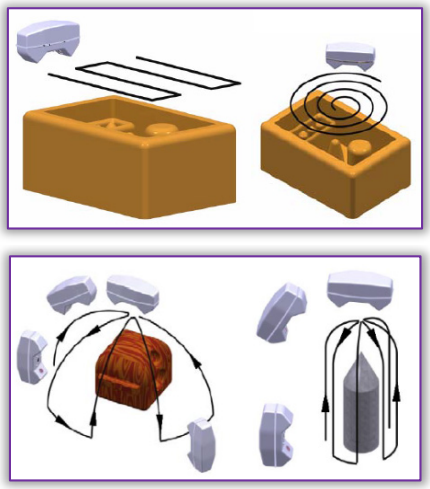

Figure 6: Scanning models

Synchronizing the three components of the scanning system - robotic arm, rotary table and laser scanning device - is essential for the operation at high-speed operation without sacrificing the scanning accuracy. Control of complex parts can be achieved both by the 2D artificial vision system (optical camera) that can provide an accuracy of the measurement up to 0.017 mm and, if the quality requirements are of high precision or require complex measurements (conical features, profiles or other critical dimensions) by the 3D laser scanning system composed of the vertical articulated robotic arm, the scanning tool and the rotary table. This solution provides the flexibility and adaptability of the system to a variety of parts and complex family parts in the automotive industry.

The scanning time estimated for a simple surface will vary according to the chosen control devices:

a) Quick scan, with a resolution of 0.7-0.9 µm, 2500 mm²/s, with a forward speed of 50 mm/s and an acquisition rate of 50 frames/second, a 50 x 50 mm² surface will be scanned in 1-5 seconds.
b) Accurate scanning, with a resolution of 0.3-0.5 µm, 375 mm²/s, with a forward speed of 7.5 mm/s and an acquisition rate of 150 frames/second, a 50 x 50 mm² surface will be scanned in 10-20 seconds.
c) Ultra-accurate scanning, with a resolution of 0.1-0.2 µm, 175 mm²/s, with a forward speed of 2.5 mm/s and an acquisition rate of 350 frames/second, a 50 x 50 mm² surface will be scanned in 1-5 min.

Scanning and digitizing software is the solution for transforming the 3D scanning data into parametric CAD models. Generally, it enables the transformation of 'point cloud' obtained from scanning the piece and its transformation into the CAD model by the mesh NURBS (Non-Uniform Rational B-spline) process that allows the creation of smooth surfaces and curves.

After the tests conducted in laboratory on the developed prototype resulted that the 3D integrated control technology is effectively realized in two stages:

» proper scanning and digitization step;
» transfer and dimensional control step.

Scanning and digitizing stage comprises the following sub-stages:

» stage of preparation and positioning piece;
» stage of providing scanning trajectories;
» stage of scanning and digitization in real time;
» stage of finishing the information obtained (removing isolated areas);
» stage of effective realization of the 3D model.

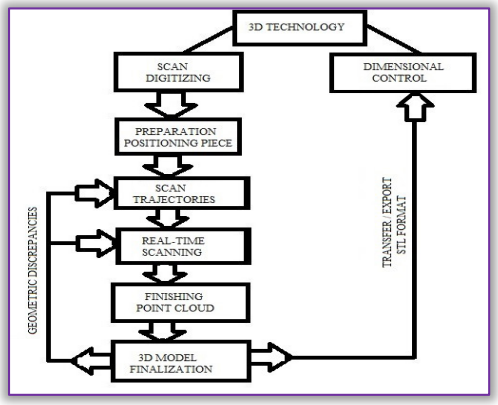

Figure 7: Block diagram of the 3D integrated control technology stages

With the help of the dimensional control software used, respectively VX Model and Solid Works [10] (AutoCAD, Catia V5 or other special measurement software) was developed integrated control itself for the scanned part for a range of geometric dimensions. The obtained results were compared with the original dimensions or those of the other measuring devices.

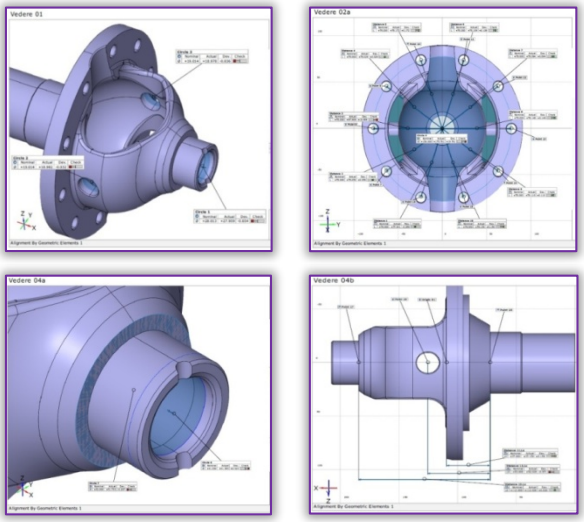

Figure 8: Different types of measurements realized with the 3D integrated control system.

After carrying out the 3D scanning operation, data resulting from all scanning devices are inserted into digitization software and, using markers localization tools and by combining them, it can be realized a single image with a much improved quality. The whole quality control process of the 3D parts can be automated. Specification of minimum and maximum tolerances accepted, in which the set points of the inspected surface must be, and of the threshold value, allows the display of points with different colours depending on the results of measurements, points with a lower tolerance than the threshold value being displayed with a different colour dots with a higher value.

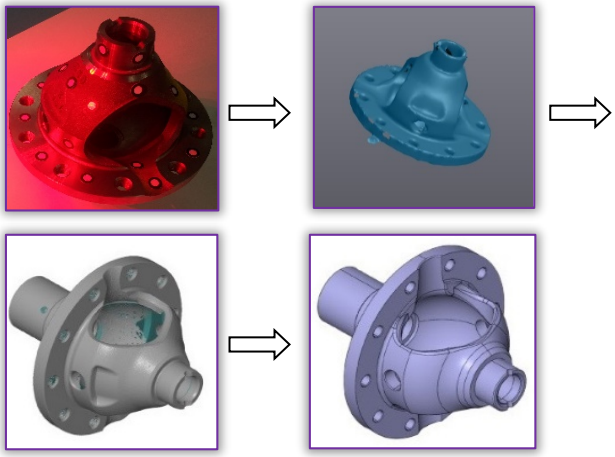

a) real piece, b) digitized piece (intermediate stage) c) digitized piece (final stage), d) 3D model.

Figure 9: Stages of 3D scanning

CONCLUSIONS

The importance which 3D scanning technology has it and its accuracy is dictated by the tracked application type in such that typically applications do not require a very high tolerance (± 0.3mm), can be use a variety of control techniques without contact to achieving their results, but because the auto industry requires a high degree of accuracy, we can only use certain types of mechatronic systems for integrated 3D control with laser being required a fairly high level of data quality (number of points and space control), the permissible tolerances in most cases is between ± 0.01mm ± and 0.001mm.

3D scanning and rapid prototyping techniques plays an important role in reverse engineering techniques in the automotive industry, even if such a procedure does not necessarily mean physical realization of the prototype. Using this type of 3D integrated mechatronic system for dimensional control presented, a prototype piece can be realized, controlled and approved very easily and quickly, all in one day. The resulting data can be accessible to a large number of equipment or prototyping, production or quality control.

Once a product has been produced in its physical form, it can be scanned and the resulting data compared with the geometry models and the deviations (errors) from the initial geometric model can be determined precisely if it does not have a virtual model. Another advantage that is not so obvious is that once the object is in electronic format, complex ideas can be applied easily and accurately, the manufacturing processes can take place in several branches of the same company in different locations around the world, the contribution of design and manufacture compartments can be carried out on the same pattern and at the same time.

After taking some tests on the prototype achieved based on the virtual model presented, on a number of complex parts and families of complex parts in the automotive industry, revealed that the dimensional inspection error depends on the scan resolution used and the type of scan used (trajectories, forward speed, complexity, method of preparation part, etc.), the inaccuracy of measurement being approximate in calculations equal to ± 0.7 + L / 300.

References

[1] Gheorghe Gh. I., Vocurek M., Beca P., Stadiul actual și de perspectivă al controlului automat integrat în procesele tehnologice inteligente în complementaritate cu tendințele pe plan European, CEFIN Publishing House, Bucharest, Romania, 2010.

[2] Bradley D., Seward D., Dawson D., Bruge S., Mechatronics and the design of intelligent machines and systems, CRC Press Taylor & Francis, 2000.
[3] Lkeuchi K., Modeling from Reality. 3rd International Conference on 3-D Digital Imaging and Modeling: proceedings, Quebec City, Canada. Los Alamitos, CA: IEEE Computer Society. pp. 117–124, 2001.
[4] Larsson S, Kjellander J.A.P., Motion control and data capturing for laser scanning with an industrial robot, Robotics and Autonomous Systems, Volume 54, Issue 6, pp. 453-460, 2006.
[5] Curless B., From Range Scans to 3D Models, ACM SIGGRAPH Computer Graphics 33 (4), pp. 38–41, 2000.
[6] Song Z., Peisen H., High-resolution, real-time 3-D shape measurement, Optical Engineering 45(12), 2006.
[7] Soloman S., Sensors and Control Systems in Manufacturing. New York: McGraw-Hill, 2010.
[8] Peng T., Algorithms and models for 3-D shape measurement using digital fringe projections, Ph.D. Dissertation, University of Maryland, USA. 2007.
[9] Gheorghe Gh. I., Beca P., Vocurek M., Sisteme și echipamente inteligente mecatronice de control integrat pentru optimizarea proceselor tehnologice și dezvoltarea capacității de monitorizare multiparametrică a variabilelor proceselor industriale, CEFIN Publishing House, Bucharest, 2010.
[10] Filip V., Marin C., Gruionu L., Negrea A., Proiectarea, modelarea, simularea sistemelor mecanice, utilizând Solidworks, CosmosMotion şi CosmosWorks, Valahia University Press, Targoviste, 2008.

ACTA Technica CORVINIENSIS
BULLETIN OF ENGINEERING
ISSN:2067-3809

ACTA TECHNICA CORVINIENSIS
– Bulletin of Engineering
Tome IX [2016], Fascicule 4 [October – December]
ISSN: 2067 – 3809

[1.]Ioan ENESCU

NUMERICAL METHODS FOR DETERMINATION THE ELASTIC STRESS AND DEFORMATIONS IN ROLLINGS BEARINGS

[1.] „Transilvania" University, Braşov, ROMÂNIA

Abstract: The modern methods of mathematical theory of mathematical theory of elasticity permit to solve a large series of the problematic of bearings. In this study is presented the results of the use of plane theory of elasticity for study of the state of tensions in intern inner.The projection of the bearings elements, special the rolling bearings and the roller way is very important. It was studied the aspect of stresses in rolling with half-space method, finite elements (contact element), MathCad programmes. The compression of a cylinder in contact "nonconformist" with two surfaces, who are in opposition at the extremity of roles, can be analyses.
Keywords: numerical methods, finite elements, half-space, mathcad, bearings

INTRODUCTION

One of the best methods to determinate the stresses are the numerical methods. In this application we use same different numerical methods for determination the state of bearings stresses, very important for your projections.

The modern methods of mathematical theory of mathematical theory of elasticity permit to solve a large series of the problematic of bearings. In this study is presented the results of the use of plane theory of elasticity for study of the state of tensions in intern inner. The system is compound by the intern inner and the motor shaft acting by concentrated force applied on rolling way.

Classical elastic contact stress theory concerns bodies whose temperature is uniform. Variation in temperature within the bodies may, of itself, give rise to thermal stresses but may also change the contact conditions through thermal distortion of their surface profile.

The skill of machines tools is based in very large measure on the reliability of the bearings.

HALF-SPACE METHOD - Uniform pressure applied to a polygonal region

We shall consider in this section a uniform pressure p applied to a region of the surface consisting of a straight-sided polygon, as shown in fig (1.a). It is required to find the depression at a general point B (x, y) on the surface and the stress components at a subsurface point A(x, y) ,BH_1, BH_2, etc, are perpendiculars of lengths h_1,h_2, etc. onto the side of polygon DE,EF respectively. The loaded polygonal is then made up of the algebraic addition of eight right angle triangles:

$$EFG = [BEH_1+BEH_2+BFH_2+BFH_3] - [BDH_1+BDH_4+BGH_3+BGH_4] \quad (1)$$

A similar breakdown into rectangular triangles would have been possible if B had lain, inside the polygon a typical triangular area is shown in fig (1.b)

$$(\bar{u}_y)_B = \frac{1-\nu^2}{\pi E} p \int_0^{\phi_1} d\phi \int_0^{s_1} ds = \frac{1-\nu^2}{\pi E} p \int_0^{\phi_1} h \sec\phi d\phi = \frac{1-\nu^2}{\pi E} p \frac{h}{2} \ln\left(\frac{1+\sin\phi_1}{1-\sin\phi_1}\right) \quad (2)$$

The total displacement at B due to a uniform pressure on the polygonal region DEFG can then be found by combining the results of equations (2) for the eight constitutive triangles. The stress components at an interior point A(x, y, z) below B can be found by integration of the stress components due to a point force given by known equation but the procedure is tedious [2]

The effect of a uniform pressure acting on rectangular area 2a*2b has been analysis in detail by Lowe (1929). The deflection of a general point (x, y) on the surface is given by:

$$D = \frac{\pi E}{1-\nu^2}\frac{\bar{u}_z}{p} = (x+a)\ln\left[\frac{(y+b)+\left((x+a)+(x+a)^2\right)^{1/2}}{(y-b)+\left((y-b)+(x+a)^2\right)^{1/2}}\right] + (y+b)\ln\left[\frac{(x+a)+\left((y+b)^2+(x+a)^2\right)^{1/2}}{(x-a)+\left((y+b)^2+(x-a)^2\right)^{1/2}}\right] + (x-a)\ln\left[\frac{(y-b)+\left((y-b)^2+(x-a)^2\right)^{1/2}}{(y+b)+\left((y+b)^2+(x-a)^2\right)^{1/2}}\right] + (y-b)\ln\left[\frac{(x-a)+\left((y-b)^2+(x-a)^2\right)^{1/2}}{(x+a)+\left((y-b)^2+(x+a)^2\right)^{1/2}}\right] \quad (3)$$

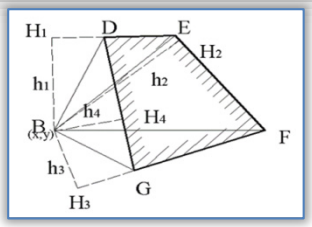

a)

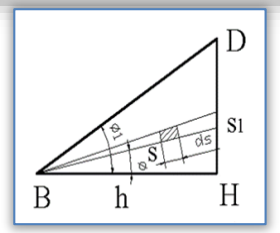

b)

Figure 1: a) Uniform pressure;
b) A typical triangular area

Expressions have been found by Lowe (1929) from which the stress components at a general point in the solid can be found. Lowe comments on the fact that the component of shear stress
theoretically infinite value at the corner of the rectangle. Elsewhere all stress components are finite. On the surface at the centre of the rectangle:

$$[\sigma_x]_0 = -p\{2\nu + (2/\pi)(1-2\nu)\tan^{-1}(b/a)\}$$
$$[\sigma_y]_0 = -p\{2\nu + (2/\pi)(1-2\nu)\tan^{-1}(a/b)\} \quad (4)$$
$$[\sigma_z]_0 = -p$$

These results are useful when a uniform loaded rectangle is used as a 'boundary elements' in the numerical solution of more general contact problems.

The elastic deformation in a point (x, y) make by the uniform distribute pressure from the rectangular surface (2a*2b) will be Figure 2.

$$\delta' = \frac{p}{\pi E}\int_{-a}^{a}\int_{-b}^{b}\frac{dxdy}{\left[(y-y_1)^2+(x-x_1)^2\right]^{1/2}} \quad (5)$$

By integrations the equation effect:

$$\delta = \frac{pD}{\pi E'} \quad (6)$$

where: - the displacement D, is calculated by the formula (2)

The expression δ represent the elastic deformation in the point (x, y) make by the uniform pressure p, distribute from the rectangular surface (2a*2b). If the contact surface is divided in a number of rectangular equal surface, the total deformation in point (x, y) make by contribution of the diverse uniform rectangular surface load, in the contact surface made by numerical evaluated.

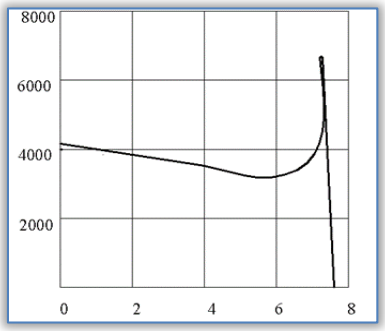

Figure 2: Uniform distribute pressure from the rectangular surface

The total deformation make by the uniform load from the rectangular surface in the inside of the con

$$\delta_i = \frac{1}{\pi E}\sum_{j=1}^{n} p_j D_{i,j} \quad (7)$$

The results obtained by this method using for the contact of cylindrical bearings N2256 is giving in application [2].

FINITE ELEMENT METHOD

The compression of a cylinder in contact "nonconformist" with two surfaces, who are in opposition at the extremity of roles, can be analyses satisfactory (Figure 3).

A compression force on the unity of length we give a hertz distribution of pressure in O_1 equal with:

□xy has a

$$p = \frac{2P}{\pi a_1}\left(1-\frac{x^2}{a^2}\right)^{\frac{1}{2}} \quad (8)$$

$$a_1^2 = 4PR/\pi E_1^* \quad (9)$$

E_1^* - Young modulus

The tensions in A are given by the contribution:

» the tensions given by the hertz distribution in O_1
» the tension given by the pressure in O_2, may be considered as for a concentrate force P
» the biaxial tension given by the equation

$$\sigma_1 - \sigma_2 = P/\pi R \quad (10)$$

Assembly the three contributions, we obtain:

$$\sigma_x = \frac{P}{\pi}\left[\frac{1}{R} - \frac{2(a_1^2+2z^2)}{a_1^{2(}(a_1^2+z^2)^{\frac{1}{2}}} + \frac{4z}{a_1^2}\right]$$
$$\sigma_z = \frac{P}{\pi}\left[\frac{1}{R} - \frac{2}{2R-z} - \frac{2}{(a_1^2+z^2)^{\frac{1}{2}}}\right] \quad (11)$$

The real cylinders are finite length and the important deviations at the Hertz theory appear to their end.

» The description of the construction solution

With the finite element program ANSYS use plane elements (triangular, rectangular and contact elements 48 we realized in the case of a cylindrical roles one other profile, a Lundberg modified profile.

» The advantage of the proposed solution

The programmer utilized the contact elements and has on view the relative positions of the two surfaces.

The finite elements are triangular, rectangular and contact elements, where the base is make by the nodes of the twice surfaces target and by the last contact with the first surface-contact.

These elements of contact are finite elements that utilize one pseudo-element as the techniques of establish of the two surface of contact.

Also they equalize the forces who existing in the contact nodes between two surfaces (in reality this perfect contact is not real).

The compatibility of the contact is one combination at a penalization functions and a Lagrange multipliers used in program.

In the fig (4) is presented the discretisation and the deformation of the case of the contact of the roles with right generator and in fig (3) is presented the discretisation and deformation in cylindrical right roles

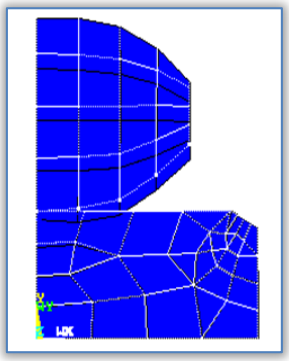

Figure 3: Discretisation and deformation in cylindrical right roles

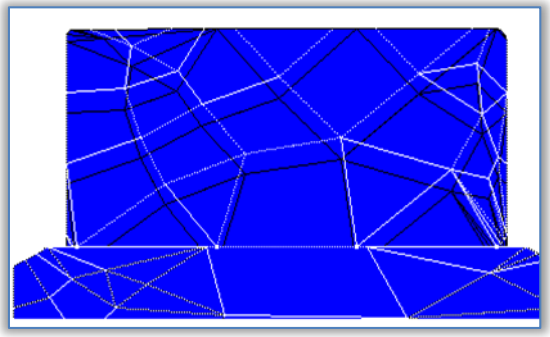

Figure 4: Discretisation and deformation in cylindrical roles with Lundberg modified profile

In (Figure 5) and (Figure 6) we can observe the distribution of stresses in two type of roles – cylindrical right roles (fig 5) and cylindrical roles with Lundberg modified profile propose by author (Figure 6).We can also observe that the stresses at the end of the roles are large small in the second case [4].

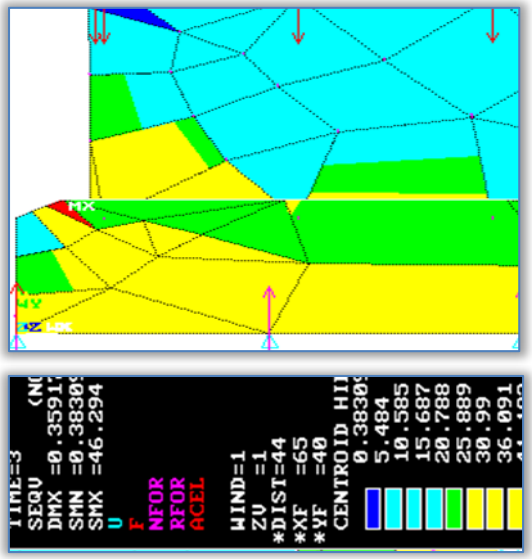

Figure 5: Distribution of tensions in cylindrical right role

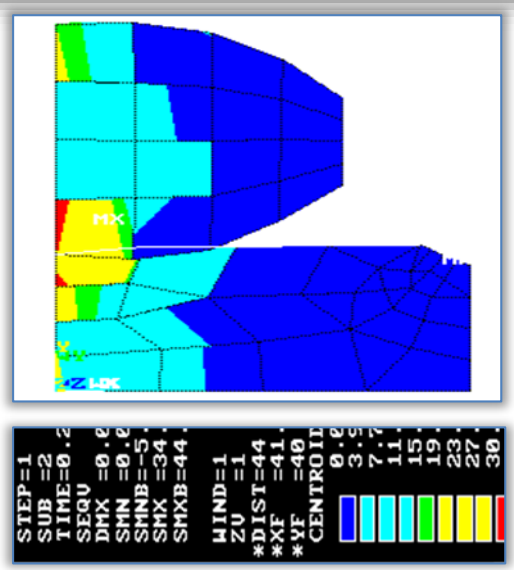

Figure 6: Distribution of stresses in cylindrical roles with Lundberg modified profile

HERTZIAN CONSTANTS COMPUTER ASSISTED PROCESS DESIGN USIGN MATHCAD

For the understanding the hertzian models, it was study first the constituent equations for the vertical displacement u_z.

The hypothesis I is associate to establishment the path in a median elastic plane dependent by the curves of the conjugated surface and the elastics contacts of the two surface cylinders the account of contact verifying the consigns equations (Figure 7).

$$(z_0 + u_0) + (z_1 + u_1) = h,\ h = h_0 + h_1 \qquad (12)$$

The external point of the contact, verifiable the non-equation

$$(z_0 + u_0) + (z_1 + u_1) < h \qquad (13)$$

Take by P_z (x, y), the distribution of the contact pressure we have:

$$u_i' \frac{1}{\pi E_i^*} \iint \frac{P_z(\xi,\eta)}{r} d\xi d\eta,$$

$$E^*_i = \frac{E}{1-\nu^2} \quad I=0...n \qquad (14)$$

where: E_i, ν_I - is the Young and Poisson coefficients of this two materials

The description of the construction solutionE_i, ν_I - is the Young and Poisson coefficients of this two materials.

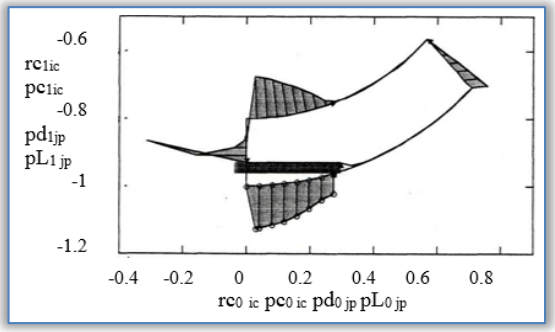

Figure 7: Pressure of contact distribution

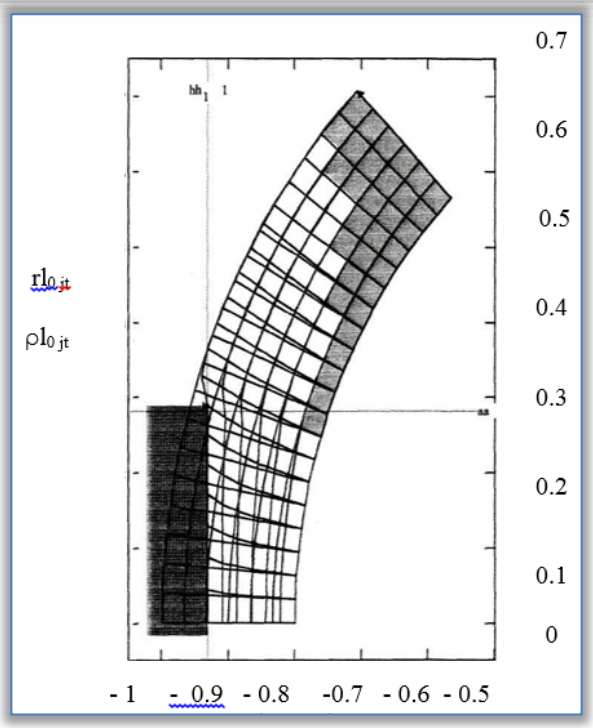

Figure 8: Flatten in the profile plane

For construct an imagine of the sliding in the hertz plain I am stimulated one of two sphere by the plane structural complex by beam elements, for 7 radial level and twenty one angular (266 elements, 21*7=147 nodes).

To fix to structure embed for the contour 0… 20, 41, 62, 146 radial sliding for the 21, 42…126 nodes.

It rested that the slides for the contact plane and at the same time is making be determinates the pressure of contact distribution (Figure 7).

The impose reshuffle of force is corresponding of flatten in the profile plane (Figure 8) [3].

CONCLUSIONS

The numerical methods are one of the best methods to determinations the stress in the roles and rolling ways. It is very important the projects of the profile of roles for determinations of the state of stress.

The numerical methods are one of the best methods to determinations the tensions in the rolls and rolling ways. It is very important to now, because the project of the profile of roll is very outstanding for determinations of the state of tensions. It results that the static model Lundberg modified had to be performed carefully, from the upper mentioned details.

Our work proposed also a model of analysis of the tensions and contact situation at the roller bearings And an analysis of the contact situation, created on the ANSYS program structure.

References

[1.] Enescu I., Aspecte ale mecanicii contactului la rulmenţi, Editura Lux Libris Braşov, 1999
[2.] Johnson K. L., Contacts mechanics, Cambrige University Press, 1985
[3.] Tofan M.C., Ulea M., Enescu I., O aproximată sugestivă a alunecării în contactul Hertzian, Buletinul celei de-a XXII-a Conferinţei Naţionale de Mecanica Solidelor, Braşov, 1998.
[4.] Enescu I., Ceptureanu G., Enescu D., Rulmenti Editura Universitatatea „Transilvania” Brasov, 2005.
[5.] Gafiteanu M. Rulmenti, vol. I, Proiectare si tehnologie, Ed. Tehnica Bucuresti 1985
[6.] Marciuk G.I., Metode de analiza numerica, Ed. Academiei R.S.R., Bucuresti , 1983
[7.] Rao S. S., The Finite Element Method, Pergamon Press, 1982
[8.] Gafiteanu M., Rulmenti, Vol II., Ed. Tehnica, Bucuresti, 1985

ACTA Technica CORVINIENSIS
BULLETIN OF ENGINEERING
ISSN:2067-3809

ACTA TECHNICA CORVINIENSIS
– Bulletin of Engineering
Tome IX [2016], Fascicule 4 [October – December]
ISSN: 2067 – 3809

[1.]Penka ZLATEVA, [2.]Siyka DEMIROVA

LOGISTICS CHAIN OF NATURAL GAS IN BULGARIA

[1.] Technical University of Varna, Department of Thermal Engineering, BULGARIA
[2.] Technical University of Varna, Department of Industrial Management, BULGARIA

Abstract: The purpose of this publication is to trace the supply chain of natural gas in Bulgaria. Is described his way - from the extraction in deposits of natural gas to distribution to the end user. Detail elucidated transmission of gas to Bulgaria from its neighboring countries. Is made overview of the types and storage facilities proposed are terms used for gas storage.
Keywords: natural gas, supply chain, gas distribution

INTRODUCTION

One of the causes the growing popularity of natural gas lies in the advantages which he offers in terms of environmental protection. In the composition of the natural gas used in Bulgaria main component is methane (CH4) - about 98% for 1m^3. The methane releases energy when burned around - 8000 (kkal). For thirty years, natural gas has changed the role of co-product to a power source that is used worldwide. The annual consumption of natural gas Bulgaria is about 3 billion cubic meters.

EXPLANATORY

The Logistics chain of gas goes through the following stages:

Yield

In the drilling in gas fields gas pressure reaches 300-500 bar (30-50 MPa), depending on the depth of the productive horizon. After processing, which involves separation of the liquid and the other undesirable components, the pressure was reduced to about 55 bar. With this pressure gas is transported via the gas transmission network in the Republic of Bulgaria [6].

The gas fields can be classified depending on the composition of the gas, condensed gas and clean gas, and depending on where the yield - on land and underwater. Natural gas from gas condensed fields except methane contains a significant amount of higher hydrocarbons - mostly propane and butane (in some cases above 150 g/m^3). These hydrocarbons condense easily upon the increase of pressure and gas cooling [11], [15]. The natural gas from "clean" gas field is composed mainly of methane and content of higher hydrocarbons is below 50 g/m^3 [9]. In Bulgaria, natural gas is extracted in deposits Bhutan, Dolni Lukovit, Balgarevo and Galata.

Transportation

To be productive and efficient transportation of natural gas from production to consumption regions require a complex transmission system. In most cases the natural gas produced from a source must travel a great distance to reach the point of its use. The conventional system for land supply is composed of gas pipelines designed for quickly and efficiently transport from original source to areas with high consumption of natural gas. The present methods for gas transport in the majority limited to pipeline transport, occupying 75% of the trade. Gas pipelines on the territory of Bulgaria are classified as transmission - transporting the natural gas in various regions and the border of the Republic of Bulgaria; and distribution - provide delivery to the end users [5].

Choice and features of the route of the highway gas pipelines

The route of the main gas pipelines should be chosen with maximum rectilinearity, possibly open area with calm relief. It is necessary to avoid crossings deposits of minerals, landslides, marshes, irrigated arable land, real estate with valuable farm crops, saline soils, ravines and other natural obstacles.

The passage of gas through natural or artificial obstacles is performed by one or several sections. Upon crossing the railway lines and highways first and second category the distance between parallel gas pipelines is taken not less than 30m, in water barriers - from 30m to 50m. Not permitted the laying of gas pipelines on the territory of villages, industrial areas them through railway and automobile tunnels, together with electric cables and other pipelines in automotive and railway bridges.

Between the route of the pipeline and gas regulation lines of settlements and urban-industrial agglomerations, construction sites and facilities is necessary to have a distances from 25m to 250m depending on the diameter and pressure of the gas pipeline and the type of facilities.

Than those identified linear closing armatures such as providing for more deviations from the route of the the gas pipeline to the gas distribution station as well as on both sides of the intersections of natural and artificial obstacles in special purpose shafts. All major facilities, compressor stations and regulating stations along the route of the gas pipelines have encircling sections (bypass) with off (shut off) armatures. With purpose release of the gas and blowing him from damaged areas in repair and restoration works between two consecutive switchgear are mounted flush candles (nozzles) with shut-off armatures. To remove condensation moisture in the gas pipeline at the lowest point along the route in special chambers are mounted and water accumulation devices.

The passage of the gas pipeline under the tracks of railways and roads going through the protective casing (steel pipe) with a diameter of over 100 to 200 mm diameter of the gas pipeline. The space between the two pipes are mounted centering dielectric suffixes for protection against Cohesion (deformation) and stray currents. The ends of this space are sealed with a stuffing box, as to one side (left or right depending on the relative density of the gas) is arranged ventilation pipe.

When crossing water obstacles trunk pipelines are laid under the bottom of the river, lake, canal. Such underwater transition is known as "siphons". The width of the water barrier over 50m, siphons be implemented in two, while navigable rivers - in three parallel branches. Depending on the diameter of the gas pipeline and the width of the water obstacle the distance between branches of siphons accepted by 30m to 50m. To ensure the sustainable position the branches of siphons, apart from supporting blocks in bends additionally on their path are placed weights. Such load against emergence is made in flooded areas with high groundwater.

If necessary, an additional connection to the main gas pipeline of relatively small users of gas (50 to 100 m^3/h) are developed not big gas regulation stations delivered along the route in prefabricated form [7].

Transmission of gas from neighboring countries of Bulgaria

After the gas crisis in the winter of 2009, with EU assistance, it was decided to build local networks for transfer of gas with Romania, Turkey, Greece and Serbia [12].

The gas pipeline with Romania - IBR, will be only 24 kilometers and will connect Rousse and Giurgiu will pass 1.2 kilometers beneath the Danube. 15 kilometers will be on the territory of Bulgaria. Will have a capacity 1.5 bcm. The project is about 27 million euros and is expected to be completed in 2018.

In 2012. Romania has acquired 10.9 bcm, in their own consumption from 13.5 bcm. In the Black Sea drillings have already proven reserves to 80 bcm, and its possible reserves of shale gas are estimated now to 1,400bcm - rank third after those of France and Poland.

From January 2014. gas connection between Kulata and Valovishta in Greece is reversible, with a capacity of 3,000,000 m^3 per day. Does Greece backup gas to Bulgaria? In 2012 the state has spent 4.4 bcm gas as 3.0 bcm (a little more than annual consumption of Bulgaria) is used to generate electricity. Question of Bulgaria's agreement to swap electricity, whose production it has plenty of capacity for natural gas. Separately, Greece is now the second country in the EU after Italy's share of production of electricity from photovoltaics, which reduces the proportion of its electricity produced from gas naturally.

The other link with Greece - IGB is long stagnation due to unclear reasons. The gas pipeline has a capacity of 3-5 bcm per year, reversible and will be 168.5 km long, 28.5 km of which 140 km in Greece and in Bulgaria. Will start from Komotini, will pass through Haskovo and reached to Stara Zagora. Its price is estimated at € 200 million, with about 25 percent will be covered free of charge from the EU. The last start of construction is delayed to the autumn of 2016. The project is particularly important because it will provide to Bulgaria indirect connection to all providers in the world liquefied gas. In 2011 Greece specially upgraded its LNG terminal in Revythousa, 45km west of Athens for capacity from 5.2 bcm a year in order to facilitate the supply of liquefied gas for Bulgaria and Turkey. The reconstruction involves the construction of a third tank that increase capacity by 40% to 225,000 m^3 LNG. It is also considering the construction of a new LNG terminal in northern Greece, a large share of incoming liquefied gas there could be directed to Bulgaria at IGB. In northern Greece will pass and TAP pipeline with an initial capacity of 10 bcm per year, which will be increased with additional compressor stations then to 20 bcm per year. In this pipeline will be completely reversible and will allow transfer of gas from Italy to Greece and Bulgaria. Construction is expected to start in his 2016-2017 and end in 2019-2010, and will provide Caspian gas from

Greece to Bulgaria through its local connection in Komotini with IGB.

The gas pipeline with Turkey - ITB can provide gas to the country from Azerbaijan and indirectly connected to the terminal with LNG. It is envisaged that its capacity is 1-3 bcm with the possibility to increase to 5 bcm. The project provides gas to go through back in 2017.

The gas pipeline to Serbia - Sofia - Dimitrovgrad - Nish will be reversible, with a capacity of 1.8 bcm and the ability to rise to 5 bcm per year. It will be 150 km long as 50 km will be in Bulgaria. The link will also extremely important as it would give the state access to large gas transmission and trading center in Baumgarten, Lower Austria.

In implementing the these links will be possible to organize a free competitive market in the Balkans, similar to those existing in Western Europe and the US [8], [13] [14].

Storage

The storage of natural gas is an important step in the process of gas supply. The gas as energy can be stored for an unlimited period of time. The Storage applied to meet the needs at times of peak consumption or difference in seasonal needs. Another positive effect of storage of natural gas is the balance between consumption and flow received from gas companies. In the absence of storage facilities each peak and decline in gas supply would lead to sanctions for the supplier. Market speculation is not excluded by the storage of gas purchased at a lower price and spreading at increasing the market value.

Terms used in the storage of natural gas:

- full capacity of gas storage - represents the maximum amount of gas that can be stored in the facility. It depends on the volume of the tank and methods of processing gas.
- buffer gas - the volume of gas that is permanently available to maintain adequate pressure and constant flow rates in seasonal withdrawal from the tank.
- Working amount of gas - formed like a full capacity subtracting the buffer gas. This is the amount of gas that can be delivered to market within the specified time.
- losses of gas - gas penetrated into cracks and pores of the gas pocket that can not be recovered.
- extraction rate - measuring the amount of gas that can be provided by gas storage for 24 hours.
- degree of filling - measuring the amount of gas that can be injected into the storage.

The most common types gas storage are underground tanks. They are divided into 3 types:

- depleted gas fields - this type stores are the most important and common. The use of this reservoir has a big advantage because of the relatively easy conversion of already built facilities for the extraction of gas in such storage, which significantly reduces the initial investment and project costs. Another positive factor is their location - geographical and physical characteristics they are now widely studied by geologists and petroleum engineers, which defines them as the cheapest and easy for developing, operation and maintenance of the three types of underground gas storage facilities.

For proper operation of depleted fields have 50% of the natural gas to be stored as a buffer. Usually these facilities are used based on annual consumption will be filled during the summer months and emptied during the winter.

- Aquifers - underground formations with a porous structure, which are essentially water tanks, but in some cases can be used as storage facilities. In developing such a storage facility is necessary to be done geological analysis, construction of new facilities such as wells and equipment for loading and unloading of the tank, dehydrators and compressor stations, which significantly raises the cost of investment for this type of storage.
- Salt formations - the underground salt pans are a good reservoir for gas storage due to the strong and solid walls, which prevents of the gas to penetrate into them, as with other types of underground gas storage facilities. Once open subterranean formation from salt creation of gas storage is done by injecting water under high pressure in place by dissolution of the salt forms a cavity which is used for storage. Water soluble salt may be used for other purposes. This type of storage facilities need to 33% buffer gas, which makes them highly effective. The disadvantage is their small size compared with the depleted fields, but that can be filled and emptied several times a year makes them competitive.
- Artificial repositories - containers for liquefied natural gas supply offer gas at any time no matter the season can build up in key positions close to consumers store large quantities, there is no need to provide for a buffer gas and provide access to world markets. The disadvantage is their high operational and structural value.
- Pipe capacity - the gas can be temporarily stored in pipelines through a process of sealing the line. A larger amount of gas can be sealed only if the pressure in the pipeline system. This method can be used at times of low load in anticipation of short-term peak. Not enough resources for long-term high consumption [1].

Gas distribution

The gas distribution is the last step of the way of the natural gas to consumers. Although some large

industrial users receive gas directly from the main gas pipelines, the average user is supplied by local distribution companies. The function of these companies is to transport gas from the main gas pipelines to households and the business sector through thousands of miles of gas pipelines with a small diameter [10]. The placein which connects the distribution company to gas pipelines is called the "urban bias" and is an important hub for charging of the natural gas for cities. Before the settlements, for lowering the pressure to permissible distribution networks (16 bar), build automatic gas regulating stations / AGRS / after which the gas fed into urban distribution networks. By these were powered consumer of natural gas. It is used in the chemical industry and as fuel in industrial, residential and public administration sectors [2], [3], [4]. Due to the need for distribution of gas in many directions at relatively large area, approximately half of the costs of accession of households are intended for distribution. The supply of natural gas to the end user like transportation. The differences consist in that in the distribution move smaller amounts of gas at lower pressures, shorter distances, a larger number of consumers. After the "urban bias" the gas is odoration with substances such as mercaptans that underlie the familiar scent. This is done because the natural gas is essentially colorless and odorless. In the odoration aims to detect a leak before it has reached 5 times lower concentration of explosive in the air. The distribution of the natural gas takes place mainly through: closed (ring) and branched (antenna) networks. The most effective is the use of a combination of the two types of networks. Depending on the maximum working pressure urban gas distribution gas pipelines are divided into 4 categories:

- up to 0,01 MPa;
- from 0.01 to 0,2 MPa;
- from 0.2 to 0,5 MPa;
- do1,6 of 0.5 MPa;

Depending on the number of degrees of pressure control gas distribution networks are single-stage, two-stage, three-stage and multi-stage.

CONCLUSIONS AND ANALYSIS

Based on the above-described, may be made the following findings and analysis:

1. The logistics chain of natural gas in Bulgaria is extremely expensive, as only one terminal would cost billions of levs, and the state is not ready to put large investments in building gas distribution infrastructure.
2. The logistic chain of liquefied gas costs about 100 Levs to 1000m^3 as the price varies depending on the distance of its transport. It is necessary to take measures for more efficient management of the entire logistics chain, which would lead to optimization of transmission costs.
3. The market for natural gas in Bulgaria at the beginning of 2016 has monopolized and the company - monopolist in the period 2006-2041 has exclusive rights to conclude deals: with extraction companies and traders of natural gas for the purchase of natural gas for the sale of natural gas with customers; for transmission of natural gas transmission and distribution companies; for storing of natural gas with storage operators and others.
4. Lowering the price of natural gas on the London Stock Exchange at the end of 2015 automatically lead to reduced the price of Bulgarian market. Proof of this is consumer attitudes towards the use of "blue fuel" for domestic and industrial needs.

CONCLUSION

The study of the logistics chain of natural gas in Bulgaria is of particular importance because the gas distribution network in Bulgaria is facing a number of challenges. It is necessary the logistics chain to larger scale studies because one of the most important indicators of its effectiveness that it should be shortened. This would lead to flexibility of the chain, lowering the price of natural gas and increased consumption.

References

[1.] APICS Dictionary. The Industry Standarts for More than 3500 Terms and Definitions, 11 th edition, The Association for Operation Management, 2005
[2.] Bowersox Donald J., David J. Closs, M. Bixby Cooper, "Supply Chain Logistics Management", International edition, McGraw – Hill, 2002
[3.] Chopra, S., P. Meindl, "Supply Chain Management - Strategy, Planning, and Operation", 3-rd Edition, Pearson Prentice Hall, 2007
[4.] Coyle, J., E. Bardi and C. John Langley Jr., "The management of Business Logistics", 6-th Edition, West Publishing Company, 1996
[5.] Dimitrov D., Atanasov B., Transport and storage of compressed / liquefied natural gas, National Review for Young Explorers "Energy, Economics and Mathematical Modeling 2015
[6.] Energy Strategy of Bulgaria until 2020
[7.] Journal. Energy Review - Issue 3, May 2013
[8.] IGU World LNG Report – 2013 Edition", International Gas Union
[9.] Nikolov, D. "Distribution and use of natural gas," Uconomics C, 2007
[10.] Vitasek, K., "Supply Chain Management. Terms and Glossary", CSCMP, Updated: August 2013
[11.] www.bgenh.com
[12.] www.capital.bg www.gas.bghot.com
[13.] www.gas.bghot.com www.gie.eu
[14.] www.gie.eu
[15.] www.naturalgas.org

ACTA TECHNICA CORVINIENSIS
– Bulletin of Engineering
Tome IX [2016], Fascicule 4 [October – December]
ISSN: 2067 – 3809

[1.]Dominika PALAŠČÁKOVÁ

INSIGHT INTO THE PROGRAMMING OF MACHINE TOOLS

[1.] Department of Production Technology, Faculty of Mechanical Engineering TUKE, Košice, SLOVAKIA

Abstract: The article deals with the development of NC machines up to the most modern CNC machines. Automation in the production process provides a number of advantages. Great progress in the production process can deliver both quality products as well as saving time, which is nowadays one of the important aspects of production.
Keywords: geometric axis, synchronous axis, asynchronous axis

INTRODUCTION

During the twentieth century there was a massive substitution of human labor work machines. At the beginning of the fifties were in the United States developed the first NC machine. Since 1966 began gradually all global manufacturers to pass on a third-generation CNC system, figure 1.

The long-term direction of development has become a production process automation across all manufacturing industries therefore also in engineering. Automation brings a number of advantages, in particular, increased productivity, which is associated with the reduction of the cost of production.

Numerically controlled machines are machines with a high degree of automation flexibly adaptable to changes in production. Data necessary to manage the machine are pre-prepared in the form of a control program recorded on carriers or information stored directly on the computer. These machines are now the backbone of flexible automation of machining processes in medium and small batch production. Statistics show the number of hours of downtime when the machine farmed. Most of them compromises the dissipation time in establishing the workpiece, tool setting and inspection of the first piece. Using measuring probes eliminates the need for an ambitious adjustment devices, clamps expensive and time-consuming alignment of the workpiece using a numerical example gauge. Software measurement cycles automatically compensates current length and diameter of tools to calculate the position and rotation angle of the workpiece size and distribution of allowances for machining, dimensional inaccuracies and the like. The result of the use of measuring probes is to reduce lost time and optimum distribution of chips.

Figure 1. The first NC machine from 1951 and the most modern CNC technology

ORIENTATION AXIS IN SPACE ON MACHINE TOOLS

To unify movements CNC was chosen following placement rules coordinate system, figure 2:

- starting from the stationary workpiece,
- always be defined by axis X,
- the x-axis workpiece clamping plane or is parallel to it,
- Z axis is identical or parallel to the axis of the work spindle, which carries the main cutting motion,
- axis is a positive meaning from the workpiece to the tool in the direction of expanding the workpiece,

» if the machine other additional movements in X, Y, Z, are designated U, V, W,
» when the workpiece is moved against the tools are referred to such axis X', Y'and Z'.

In keeping with these basic rules is for the programmer to create a simple program to various types of CNC machines. The position of the machine axes is still the same and made the program can be used on more than machines with minimum modification.

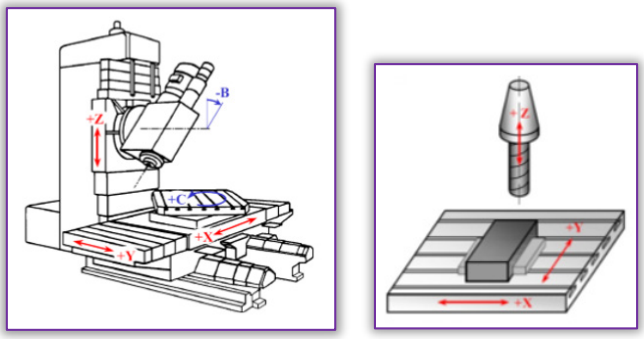

Figure 2. 5-axis vertical machining center and milling machine

Before describing types of movements and interpolation it is necessary to define the concepts of geometric axes, synchronized axes, internal axes and NC axes. From the perspective of a programmer are important mainly geometric and synchronous axes:

» **Geometrical axis** - geometric axis are three and at a given time defining a space - clockwise coordinate system X-Y-Z. Only in these axes, the system performs interpolation in these axes is defined speed. If you have interpolated axes that are not geometry, which can be considered for more complex machines should be switched (eg. From partprogram) as the geometrical axis (see function SetGAx (XNO, Yno, ZnO) in chapter 3). Simple machines have a fixed allocation axes configuration.
» **Synchronous axis** - If programmed together with the geometric axes, this means that basically only that their movement will begin simultaneously with the geometric axes and ends also move together with the geometric axes. If they are programmed separately, traveling speed that enters the system parameter, i.e. not operate the speed programmed address or system parameter F Feed! Unless the system parameter specified speed, traveling at a preset configuration files, type * .ChannelConfig.
» **Asynchronous axis** - generally are fully controlled by the PLC program, mostly various auxiliary axes, often only M-programmed functions. Their use must be in the instructions for a specific machine. Movement is started at the beginning of the block, going "its" speed that is they can end movement earlier or later than possibly simultaneously programmed geometric axis.
» **Internal axis** - used in the preparation part program, is an array of values that can be set and read from part program. Internal axes can be programmed to 9 and AXI0 - AXI8. For normal programming mostly this record is not used. Use is mainly in general programs (macrocycle fixed cycles) which are written, regardless of what axes are actually on the machine. Three of the internal axis are always identified as geometric - either configuration, or switching from part program.
» **NC axis** - the axis with which the module works in real time. They may be connected to internal axes - are derived from this behavior (geometric / synchronous / asynchronous axis). They can be controlled from the PLC.

PROGRAMMING OF NUMERICALLY CONTROLLED MACHINE TOOLS

Automation is a higher form of modern mechanical engineering, in which the number of manufacturing techniques and in the final stage and the race it is automatically controlled according to an established program through monitoring, measuring and control devices. This is a new development path Machinery substitutes not only the physical activity of the worker but also his mental activity. The first steps were machining process automation through a mechanical system to control the timing shaft and Curve drum where all the movements and actions are derived from the control discs. A typical representative of the Line and turret machines. The electrical and hydraulic system is realized duty cycle control successively switching control circuit in accordance with the data control program. The servomotor is controlled by the real position of the tool, which is difficult especially as the tool feed speed and the trajectory along which the tool is moving, depend on the load of the actuator of the components of cutting forces.
On the principle of management by the actual position are comprised all methods of automatic control machine tools, and according to the method of deriving the actual position of the tool is divided into:

a) Control by limit switches, where the dimensions of the workpiece respectively path lengths in different directions, are designed shocks for limit switches for switching servo feed.
b) Copy control, where the locus of tool is template driven.
c) Digital metering track where the tool path relative to the workpiece given electrical signal showing how the digital information about the track, the direction and sense of movement.

Digital metering track where the tool path relative to the workpiece given electrical signal showing how the digital information about the track, the direction and sense of movement:

a) Program management, cross driver. It is essentially a system of two perpendicular to each other Stripping of which is a horizontal sections of the working operations (the steps) and then a vertical machine functions (turn and traverse levels, start and stop, cooling etc.). Inserting a conductive pin to link the respective horizontal and vertical wires which provide gradually switching functionality required in this step. The exclusion of mistakes when setting up the machine at the conductor cross attached card, in which the respective node points of the punched holes. The process was conducted as. the program-controlled lathes and copying program-controlled milling machines with a rectangular cycle, management cues. Currently, this kind of control no longer produced.
b) Analog control enables implementation also significantly more complex machining cycles. On magnetic tapes when making the initial unit records the electrical phase of Synchro, who served as a metering device. Records corresponding to motion phases of the machine and vice versa. The control signal controls the machine tool in a closed control loop and a systematic comparison phase, recorded on a cassette tape with electrical phase of the metering selsyn.
c) Management software used to enter the control program information medium in the shape of the wearer's portable information most often perforated paper tape and innuendo.
d) Numerical control, which is the culmination of a program-controlled machine tools, allows for the fastest entering the control program and machine settings. Its hallmark is the application of digital metering tracks.

Economic program-controlled deployment of these types of machines and better adaptability settings defined area of production for medium size batches and for numerically controlled machines for small-lot and piece production. Since the mass production characteristic inflexible (hard) automation differs mainly by its flexibility and allows settings to automate the area of piece, from medium-sized and small-lot production.

METHODS OF PROGRAMMING OF NUMERICALLY CONTROLLED MACHINES

NC Programming is a challenging and highly skilled work, which is the inclusion in the technical preparation of production. This is a relatively new field of activity, created the deployment of NC machines into production. It requires not only practical knowledge of machining technology especially in the field of the technique, and the sequence of operations in individual operations, but also select the optimum cutting tools, designing cutting parameters etc. The quality control program is influenced knowledgeable programmer functions NC programming and control systems. With increasing levels of technical complexity and technology are increasing demands on adequate skills and knowledge programmer. High intensity and complexity of managing programs for the continuous control systems, where at NC machines must be assumed even more simultaneously controlled axes increasingly requires recollection of programmer's work, with a significant risk of error. Therefore, it focused attention on the possibility of creating control programs, particularly for CNC machine tools in the environment of CAD/CAM, which is characterized by the full possibility of continued creation of CNC programs from basic drawing components.

Then the creation of the program comprises two steps:

a) CAD part, which is defined by the closed contour machined workpiece based on downloaded information from the drawing or CAD system solid modeling,
b) CAM part, which is generally the application of appropriate programs created automatically by the control program for the CNC machine or dialog To create your own CNC program with the possibility of being completed and amended (Tolerances, normalized undercuts etc.).

CNC machines programming is done in two ways:

» system online, directly on the CNC machine shop programming (SAP Shop Floor Programing),
» offline programming, outside the part of the program control system, most often by means of the CAM system, but can be manually.

Reasons for the introduction of offline programming with a focus on CAD / CAM are:

a) NC Programming is a challenging and highly skilled services in TPV,
b) requires a practical knowledge of machining technology, particularly in the technique,
c) with increasing technical complexity and the complexity of the technology increases the demands on the skills and knowledge programmer associated with significant risk of error,
d) focus on the possibility of creating control programs, particularly for CNC machine tools in the environment of CAD / CAM, which is characterized by fully traceable creation of CNC programs from specified parts of the drawing or CAD solid modelers.

This procedure can solve the problems of formation control program in the form of a computer modeling approach for complex shapes and then generate control programs for machine tools, figure 3.

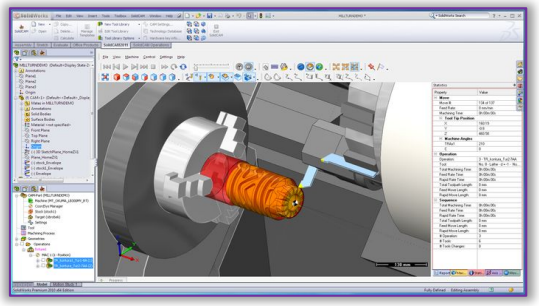

Figure 3. Preview with CAD system

The control panel is used for communication between the operator and the machine control system, fig. 4. With it inserts the operator in the control system commands control program and special machine parameters. The control panel has a display, keyboard, buttons for special functions and knobs. Manual control programmatically controlled machines (NC and CNC machines) is performed using a variety of control surfaces that are different for control systems. The control panel is used for communication between the operator and the machine control system. Manual control of NC and CNC machines is performed by each special buttons on the control panel. Use the buttons can be triggered manually all machine functions. Panel buttons are provided with graphical symbols to indicate control functions numerically controlled machines. Key designations are determined by standards (eg. To DIN 55003) and consist of the basic signs and additional functions. Signs are divided into tags for machine control and construction program. Used symbolic signs facilitate orientation and allow to overcome the problem of the language barrier.

Figure 4. The control panel - Sample dashboards

CONCLUSION

This article shows a rapid development of manufacturing technology over the last few decades. This development obviously affects the whole range of industries, including NC machining. Programs to create 3D applications (CAD) enables very fast and efficient design of components and the whole assembly. Thus created 3D models can then be used in the CAM programs for the creation of control program for CNC machines. Team falls off time-consuming manual programming.

Acknowledgement

This article was created within the grant project VEGA 1/0124/15 Research and development of advanced methods for virtual prototyping manufacturing equipment.

Reference

[1.] http://www.newtechsolutions.pl/produkty/systemy-cam/solidcam/
[2.] KOCMAN, Karel. Speciální technologie obrábění . Brno: CERM, ISBN 80-214-25628
[3.] NESLUŠAN, M. Experimentálne metódy v trieskovom obrábaní . Žilina : EDIS, 2007.
[4.] http://www.sjf.tuke.sk/vitralab/upload/CNC%20prirucka_CZ.pdf
[5.] Virtual machining on horizontal machining centre with rotary table / Peter Demeč - 2012. In: International Scientific Herald. Vol. 3, no. 2 (2012), ISSN 2218-5348

ACTA Technica CORVINIENSIS
BULLETIN OF ENGINEERING

ISSN:2067-3809

ACTA TECHNICA CORVINIENSIS
– Bulletin of Engineering
Tome IX [2016], Fascicule 4 [October – December]
ISSN: 2067 – 3809

[1.]Ana JOSAN

IMPROVING THE QUALITY OF CASTINGS BY OPTIMIZATION OF THE MOULDING-CASTING TECHNOLOGY

[1.]University Politehnica Timisoara, Faculty of Engineering Hunedoara, Hunedoara, ROMANIA

Abstract: One of the main stage of obtainig of castings is the pouring of the liquid alloy. Durring this process may occur a series of defects in the matherial structure or the configuration of the casting. According to the specialty literature the casting defects represent any deviation from the shape, dimensions, weight, the external aspect, macro and/or micro-structure and mechanical or chemical properties of the piece required by standards, norms or contractual technical conditions. The occurrence of these defects in castings can lead to increased the percentage registered with direct effects on company costs. For castings to obtain without defects Romanian foundries places great importances on the liquid alloy elaborating technology, moulding-cating technology and the materials used to achievement the moulds and cores. Thus, the development of the foundry department leads to a decrease in operations performed in the cutting processing department (by increasing the casting precision the allowances are smaller and share of the further processing will decrease). The paper presents the possibility of improving the quality of grey cast iron castings by moulding-casting technology optimization in order to decrease the percentage of rejects registered in industrial practice. Thus, the casting Supporting Roll-type is analyzed because it was registered a high percentage of defects (adherences, burrs and misalignment of the castings). These types of defects that lead to rejection of castings could be eliminated by changing the moulding technology, respectively by changing the way location of the plan of separation of the pattern and the mould and application of technological measures for the use of two types of cores (a vertical central core for obtaining the hollow from inside the casting and a lateral cores for obtaining the external configuration of the casting). The optimization of the moulding-casting technology for castings analyzed lead to a decrease percentaje of rejects and decrease the company costs.
Keywords: grey cast iron, castings, quality, mould, core

INTRODUCTION

After the industrial revolution the problem of quality have imposed increasingly more. Besides the fact that the concept of quality is a characteristic that accompanies any product the concept of quality structure becomes more complex. Besides the basic characteristics of a product the quality issues begin to target some elements related to exploitation behavior of products: reliability, maintenance and availability.

Structurally the quality issues are targeting the following processes: research and design, production, sales, corrective and preventive maintenance activities, issues of internal and external logistics and quality issues the users of the manufactured products [1].

Depending on the alloy that is poured is necessary to take into account certain technological aspects related to mould and casting. Thus, [2,3]:

» The mould must:
  - withstand all the mechanical, thermal and chemical stresses to which is subject by the liquid alloy;
  - to reproduce as accurately (shape and size) both exterior and interior of the casting

» The casting:
  - must be appropriate to technical specifications;
  - must have commercial aspect;
  - must be appropriate in terms of quality;
  - must be advantageous in point of view price/quality ratio.

PRESENTATION THE TECHNOLOGY FOR OBTAINING THE CASTING (SUPPORTING ROLL TYPE)

In the industrial practice of the foundry the diversity of castings imposes the analysis of the technologies used so that the castings to results no defects. For this is analyzed the moulding-cating technology for the piece Supporting Roll. This

casting is a component of the hoist gearing of an industrial furnace door. This cating was chosen for study because they registered a high percentage of defects of this type of castings (adherences, burrs, misalignment).

The piece Supporting Roll is poured of unalloyed grey cast iron with lamellar graphite EN-GJL-350 and the elaboration of the cast iron was made in normal conditions [2,4,5]. The moulding technology starts from the finished part drawing (figure 1) and includes two main stages: the manufacture of pattern and achievement of mould [3,6,7,8].

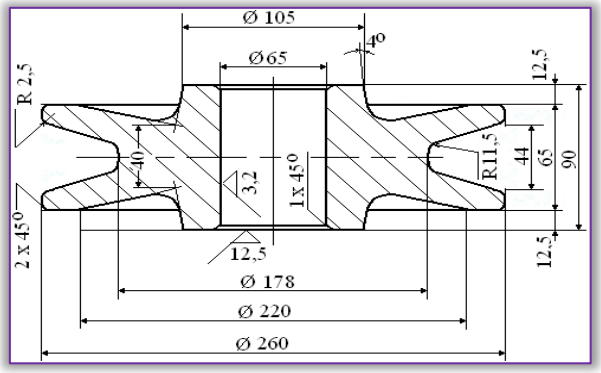

Figure 1. The finished part drawing (Supporting Roll)

For realization of the pattern it is necessary to establish the mould separation plan and pattern separation plan. Thus, for casting analyzed the symmetry plane is the same with sectioning plan of the pattern and also the same with the mould separation plan. The separation surface is plane and the castin position is horizontal. According to the technology used the sectioning plane of the pattern divides the pattern into two symmetrical parts (figure 2).

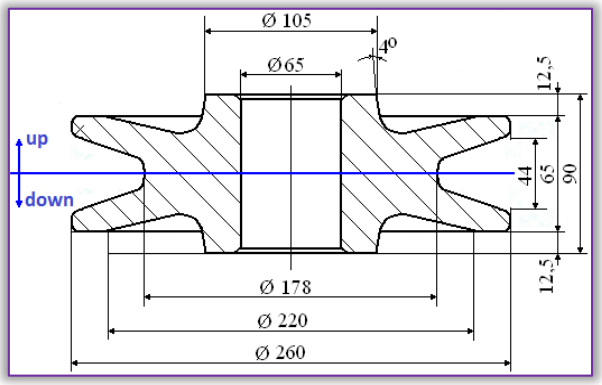

Figure 2. Choosing separation plan

To obtain the pattern dimensions is taken into account the contraction coefficient α. For the piece analyzed is chosen α = 1% [6,8]. After establishing the size of allowances of contraction, the constructive inclinations and the dimensions of the core marks are determined the configuration and the dimensions of the pattern. The pattern is made of wood and is presented in figure 3. This pattern is made up of two assembled halves (M1 şi M2).

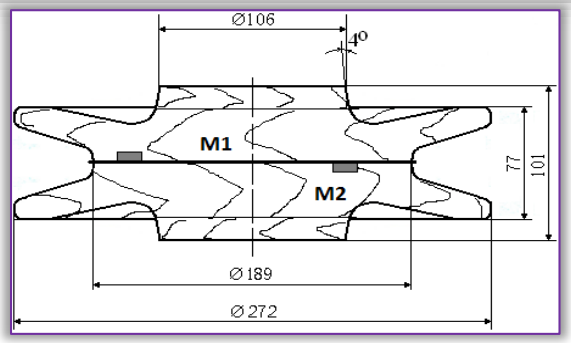

Figure 3. The wooden pattern

For removal the shrinkage cavity the moulding technology requires the use of a central riser (figure 4). On the technological drawing (figure 5) are presented the dimensions of the central core marks. Thus, the height of the upper mark is 106 mm and the heigh of the lower mark is 20 mm (figure 5).

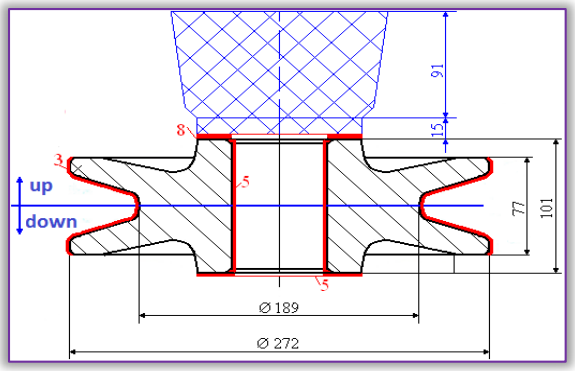

Figure 4. The location of the riser and the presentation of the allowances

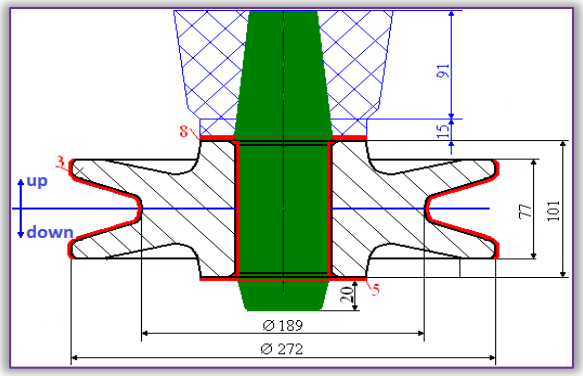

Figure 5. The dimensions of the vertical cylindrical core marks

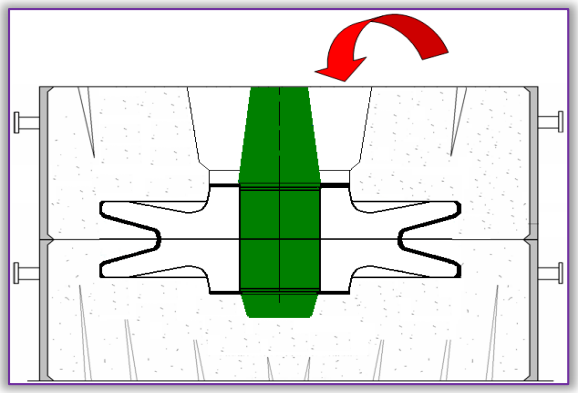

Figure 6. The mould assembled for casting

After making the wooden pattern and determining the location of the riser is achieved the mould parts and their assembly in order to casting the liquid alloy (figure 6).

OPTIMIZATION OF MOULDING – CASTING TECHNOLOGY OF THE CASTING STUDIED

The quality control carried out on a batch of castings *Supporting Roll* type shows that were registered mainly three types of defects: adherences, misalignments and burrs [2,11,12]. Removal these types of defects requires critical analysis of moulding-casting technology used and its optimization. Thus, for the removal of adherences is necessary to use the antiadherence paints and the use of the appropriate moulding sand [2,12,14].

Performed the analysis of actual moulding-casting technology for the casting *Supporting Roll* is noted that it is wrong taken on the problem of establishing the separation plane of both the pattern and mould. This is due to the fact that the location of the separation plane (for actual technology) lead to appearance of defects such as:

» Misalignment is a defect of the type F221 and occurs when the mould is submitted to a shearing action in a separation plane [13]. This defect is manifested by displacement a part of the casting in relation to other part that leads to deformation of outlines or sections of the casting (the halves of the casting are displaced relative to the longitudinal axis).

» Burr is a defect of the type A111 which appears as a surplus of mettalic material that adheres to casting in the plane of the separation surface [13].

To avoid occurrence of such defects is necessary to change the positioning of the separation plane (both the pattern and mould) and the optimal solution is considered as shown in figure 7 and the position of pouring is also horizontal.

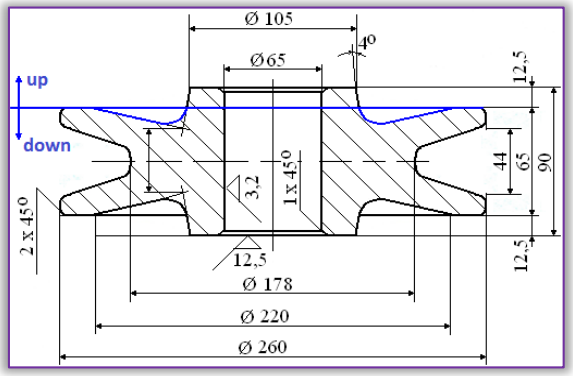

Figure 7. Sectioning of the patterns and the moulds

After establishing the separation plane (for pattern and mould) on the finished part drawing are added the allowances. Location of allowances is similar to current technology (as well as dimensioning the pattern).

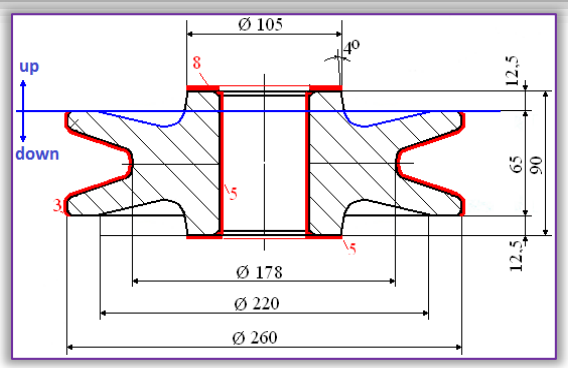

Figure 8. The presentation of the allowances

In the case of improved technology the pattern has the same dimensions, the gluing mode of components parts is the same but the pattern is no longer made of two symmetrical parts placed in two mould-parts. Thus, the pattern M1 (representing 2/3 of the pattern of the casting) will be located in the lower mould-part and the pattern M2 will be located in the upper mould-part (figure 9).

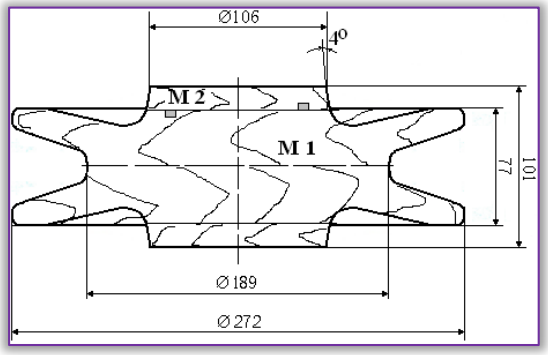

Figure 9. The wooden pattern in the case of improved technology

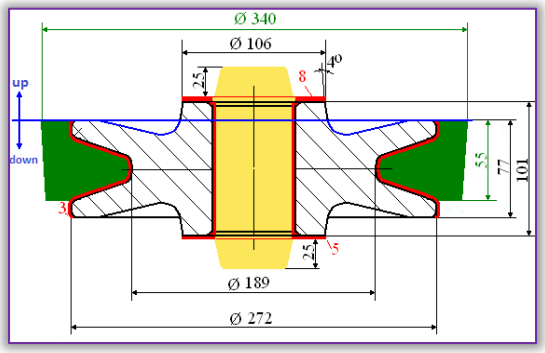

Figure10. Establishing the manner of location of cores

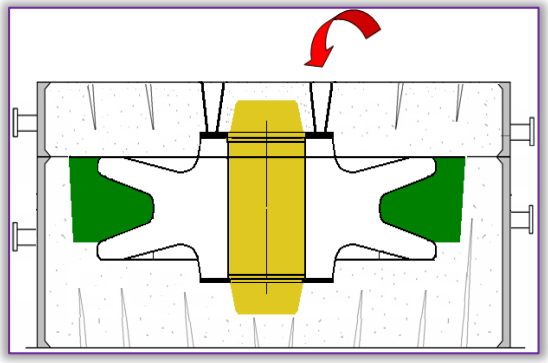

Figure11. The mould assembled for casting

For casting analyzed in technological point of view can choose the moulding technology with two cores (figure 10):

- a central core in order to obtain the hollow from inside the casting
- a lateral core in order to obtain the lateral configuration of the casting.

CONCLUSIONS

Generally, the quality of a product represents all the characteristics of the product which expresses the degree to which it satisfies the social needs based on technical and economic parameters, aesthetics, the usefulness and efficiency in exploitation [11]. Thus, the founfries is intended to achieve at least two of the objectives of the quality assurance system (7 *Zero*) namely *zero defects* şi *zero rejects*. In accordance with these all defects are detected before delivery products on the market and also put special emphasis on the preventive side so after each stage of the production process should result components that meet all requirements [11].

Thus, after performing the critical analysis of moulding-casting technology for casting *Supporting Roll* (this piece is cast of grey cast iron with lamellar graphite) are required few changes of current technology in order to decrease the percentage of registered rejects in industrial practice:

» Changing the positioning of the separation plane prevents the occurrence of casting defects (burrs, misalignments) and lowering labor processing of casting for their removal with direct effect on the price of casting;
» The use of two types of cores for casting has beneficial effects on quality of the castings and on their cost price ;
» The adoption of these technological measures lead on the one hand to reducing of the central core dimensions (of the upper core mark) and therefore to manufacturing of a simple core box and secondly to improve the quality of casting on the concave side due to application of lateral core;
» Changing the central core dimensions respectively of an upper mark of the central core and removing from moulding-casting technology of the riser involves the changing the dimensions of the upper mould jacket (which is reduced by half).
» In conclusion, there is a considerable drop (by approx. 50%) of the moulding sand for upper mould-part.

References

[1.] Dumitrescu C, Implementarea sistemului de mangement al calităţii, condiţie necesară pentru integrare în Europa, Buletinul AGIR, Anul VIII, nr.4-oct-dec 2003, pg.2
[2.] Josan A, Pinca Bretotean C - Using the antiadherence paints to manufacturing of the moulds intended for iron castings, International Conference on Applied Sciences 2016, ICAS 2016, Hunedoara, Romania
[3.] Josan A., Casting and moulding technologies of metal parts – the project guide-book, Publishing Polytechnic, Timişoara, Romania, 2012
[4.] SR EN 1561- 2011- Grey cast iron
[5.] A. Josan, V. Puţan, S. Raţiu - Analysis of the technology of steel elaboration T35Mn14 intended for casting the pieces, Annals of the Faculty of Engineering Hunedoara - Journal of Engineering, Tome VIII, Fascicule 3, pp. 59-61, (2010)
[6.] Ştefănescu, Cl. ş.a. – The designer of technology guide-book in foundries, Technical Publishing, Bucharest, Romania, 1985
[7.] A. Josan, Technology moulding and casting alloys, Publishing Polytechnic, Timişoara (2002).
[8.] Ştefănescu, Cl, Cazacu, I.- Tehnologii de executare a pieselor prin turnare, Technical Publishing, Bucharest, Romania, 1981
[9.] Josan A, Using the refractory cast irons at casting parts for heat treatment furnaces, Annals of the Faculty of Engineering Hunedoara - Journal of Engineering, Tome XI, Fascicule 4, pp. 103-106, (2013)
[10.] Josan A., Pinca Bretotean C., Păucă A. – The use of regenerated mold mixtures in manganese steel piece casting, Proceedings of the 3rd International Conference on Energy, Environment, Devices, Systems, Comunications, computers (INEEE 12), Mathematical Modelling and Simulation in Applied Sciences, pg. 162-164, Rovaniemi, Finland, 2012
[11.] Josan A, Managementul calităţii, Ed. CERMI, Iaşi, 2008
[12.] Josan A 2010 The analysis of casting defects recorded in the metallurgical enterprises, International Symposium on Advanced Engineering & Applied Management - 40th Anniversary in Higher Education (1970-2010), Hunedoara, 7pg, CD
[13.] International Atlas of casting defects Technical Publishing, Bucureşti, Romania
[14.] Davidov N.I. 2004 Refractory daies for moulds and cores, Romanian Foundry Journal, no. 3/4, 17 (translation Phd.Eng. Constantin Cosneanu)
[15.] Josan A, Pinca Bretotean C, Ardelean E and Ardelean M 2015 Using lateral cores to casting of carbon steel parts, of drive wheel tyle in a metallurgical enterprise, International Conference on Applied Sciences 2014 (ICAS 2014), Hunedoara, Romania, IOP Conf. Series: Materials Science and Engineering 85(2015) 012016, ISI Proceedings

ACTA TECHNICA CORVINIENSIS
– Bulletin of Engineering
Tome IX [2016], Fascicule 4 [October – December]
ISSN: 2067 – 3809

[1.]Aseel A. KAREEM, [2.]Zaina RAHEEM

MICROHARDNESS AND ADHESION STRENGTH OF PMC'S COATINGS BY NiCr ALLOY

[1-2.]Department of Physics, College of Science, University of Baghdad, IRAQ

Abstract: The use of polymer matrix composites (PMC's) in the gas flow path of advanced turbine engines offers significant benefits for aircraft engine performance but their useful lifetime is limited by their poor environmental resistance. Flame sprayed NiCr graded coatings are being investigated as a method to address this technology gap by providing high temperature and environmental protection to polymer matrix composites. In this research coating was spread with two configuration, coating with bound coat and coating without bound coat. In general the coating with bound coat and coating without bound coat showed increase in micro hardness and adhesion temperature with increase curing temperature; this is due to the microstructural changes the physical splat structure of the coating also changes with heat treatment. All coating failed at the interface between the composites and the coating, failure occurs along the weakest plane within the system, some of the coating systems that have presented fracture at the bond coat/top coat interface. The surface topography of NiCr films was further examined by using AFM atomic force microscopy as a function of curing temperature at 100,200 and 300°C for 1 hour each, it can be clearly seen that the island structure was observed and the R_{max} increase, the surface became rougher with increasing curing temperature. The surface morphology and microstructure of the coating were examined using SEM.
Keywords: protective polymer fiber composites; polymer matrix composites in aerospace applications; high temperature flame spray coating; hard coating

INTRODUCTION

Coating and surface modification technologies allow the engineer to improve the performance, extend component. Surface engineering is defined as the design of a composites system of a surface and a substrate together to give a performance which cannot be achieved breather the surface or the substrate alone [1]. The primary benefit in replacing metals with lower density, higher specific strength PMC's is the weight savings. Additional advantages are the lower processing and fabrication costs [2]. Polymer matrix composites can be successfully deposited by with Thermal spray coating. Successful deposition of a wide array of materials shows that thermal spray coating is available technology for the polymer composites surface protection [3]. A graded coating composition or structure improves the load coatings is astright forwoard process and not as defecult as metallographic preparetion. The system can consist of a coating with or without an interface [4]. Since polyimides are thermally stable at high temperature they are a popular choice for structural parts in aerospace applications, where metal replacement is required with lightweight materials. Polyimide adhesives are used for joining metals and high temperature composites because their coefficient of thermal expansion is comparable to that of metals [5].

Applications of these coatings are widespread and can be found in aerospace, petrochemical [6]. The material selection for turbine engines is a balance between the cost and efficiency, high-strength NiCr alloys are often used in the aero-engine applications for weight reduction [7].

The microindentation indentation technique has been used to characterize the material properties and of coating materials because it is simple and can be performed on small specimens [8].

EXPERIMENTAL

A woven Carbon fiber epoxy composite was selected as substrate; the hand lay-up technique was used to prepare these composites with volume fraction 30%. The composites specimen was cleaned with acetone to remove moisture, dirt oil and other foreign particle. The coating that improves the adherence of the subsequent deposited is called bond coat. Polyimide are used as bond coat, In this

work, pyromelliticdianhydride (PMDA) and p-phenylenediamine (PDA), which are commercially available from Sigma-Aldrich are used to prepare polyimide by thermal evaporation technique. These two monomers, 2 gm each, were evaporated from two separated boats to form a poly(amic acid) (PAA) thin film on substrate. The deposition process began at vacuum of 2 X 10^{-5} mbar. The resultant polyamic acid PAA film was then soft baked to remove nH_2O from the substrate followed by a thermal treatment at 250°C for 1 hour each in an air circulating oven, and deposited polyimide film into the composites substrate .The final thickness of films is $5\pm0.1\mu m$

On the other hand NiCr is used as atop coat .The elemental composition of NiCr alloy samples used in this work was made by using X-ray fluorescence (XRF) analysis technique as shown in Table 1.

Table 1. Elemental composition of the powder used for deposition of coatings.

Powder	Elemental composition (%)					
	Ni	Cr	Si	C	Fe	other
NiCr	43.4	52.6	0.13	0.62	0.17	0.08

Spray Gun (rototec 80), it's used for thermal spraying by flame which was made in Germany by (Castolin+Eutectic) Company. In this process oxygen-acetylene mixture is passed through a nozzle and ignited to form a combustion flame. Ni-Cr Coating powder with particle sizes ranging from 50 to 90 μm were used is fed into the flame, accelerated and projected onto the substrate to form a top coating with thickness about 70 ± 2 μm calculated by magnetic induction measurement methods. The flame temperature is limited to around 1400°C, particle velocities are relatively slow.

Operating parameters during coating deposition process are listed in Table 2.

Table 2. Operating parameters during coating deposition process

Operating Parameters	Values
Oxygen pressure	4 bar
Acetylene pressure	0.7 bar
Standoff distance	200 mm

Before coating the samples are cured at (100,200 and 300)°C.

Hardness type Vickers was conducted for all samples by using (Hensddt-Wetzlar). Vickers hardness values were calculated according to the following equation:

$$HV = 1.8544\frac{F}{d^2}\ (kgf/mm^2) \qquad (1)$$

where F is applied load (kgf) and d is the main diagonal of indentation (mm).

The controlled electronic universal testing machine used for pull off adhesion tests, and it is type is (WDW-200E). The bond strength is found from the simple relation:

$$UTS = L / A \qquad (2)$$

where: UTS = cohesive or adhesive strength - force per unit of surface area, L = load to failure (force), A = cross sectional area of specimen.

RESULTS AND DISCUSSIONS

Hardness is described as resistance to surface indentation of the material.

It can clearly see in the Figure1. At room temperature PMCs with NiCr coatings had enhanced high hardness this is due to the hardness of NiCr. The increase in the hardness in the composites coating with polyimide bound coat is the indication of good polyimide bonding between the composites and the NiCr top coating [9,10].

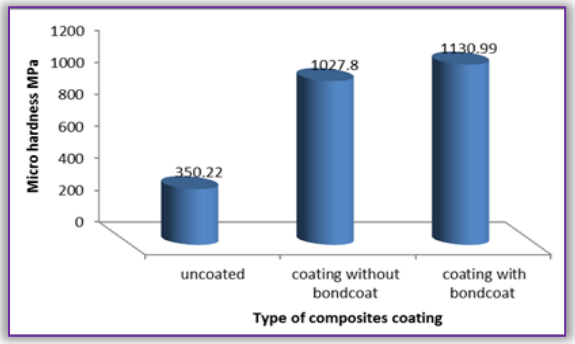

Figure1. Microhardness of coated and uncoated PMCs at room temperature

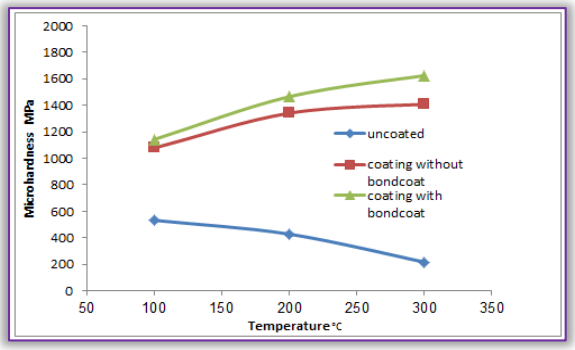

Figure 2. Microhardness of coated and uncoated PMCs as a function of temperature

In Figure 2, in general, the response of the uncoated composites to heat treatment induced softening of the microstructure and account for the reduction in hardness. Heat treatment in air generated higher average hardness values in coating systems, the coating with bound coat and coating without bound coat showed increase in micro hardness with increase temperature; this is due to the microstructural changes the physical splat structure of the coating also changes with heat treatment [11]. It is found that the degree of fusion of the particles and the presence of an oxide phase have effect on the microhardness of the coatings [7,12].

The results of pull off tests are shown in Figure3 adhesion strength for the PMCs coating with polyimide bound coat is higher than PMCs coating without bound coat. The adhesive strength between the polyimide and metal was affected by the

chemical state of bonding on the surface in polyimide films; the hydrophilic bonding such as C-O bonding is believed to be suitable for enhanced adhesion between polyimide thin films and NiCr [13]. During the spray process, there is some partial formation of intermetallic phases. Subsequent fusing of the coating causes a complete transformation of the materials [14].

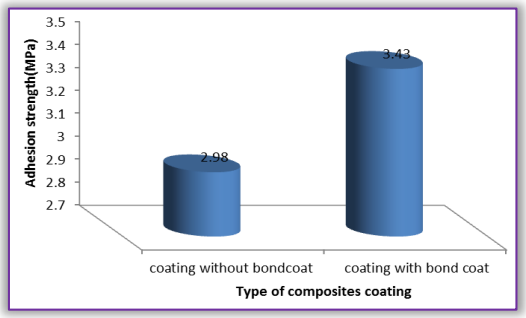

Figure 3. Adhesion strength of coated and uncoated PMCs at room temperature

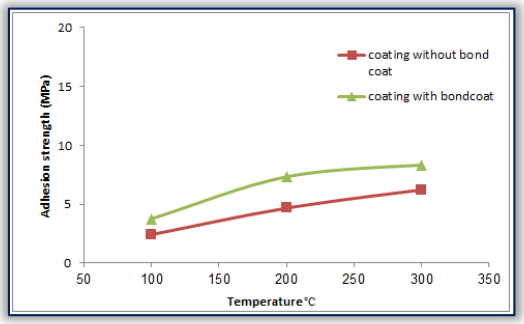

Figure 4. Adhesion strength of coated and uncoated PMCs as a function of the temperature

We can see from Figure 4. When curing temperature increase the interlocking (and then adhesion) increase because of diffusion into the substrate also occurs, improving bonding. Porosity is nearly eliminated, with no interconnecting porosity and the formation of hard oxide phases leads to increases the roughness of substrate surface [10,15].

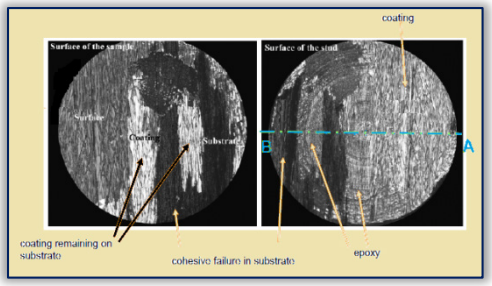

Figure 5. Microscope pictures of failed specimens showing types of failure

Figure 5 shows that all coating failed at the interface between the composites and the coating failure occurs along the weakest plane within the system, some of the coating systems that have presented fracture at the bond coat/top coat interface. In most cases there is a cohesive failure occur of the substrate [15].

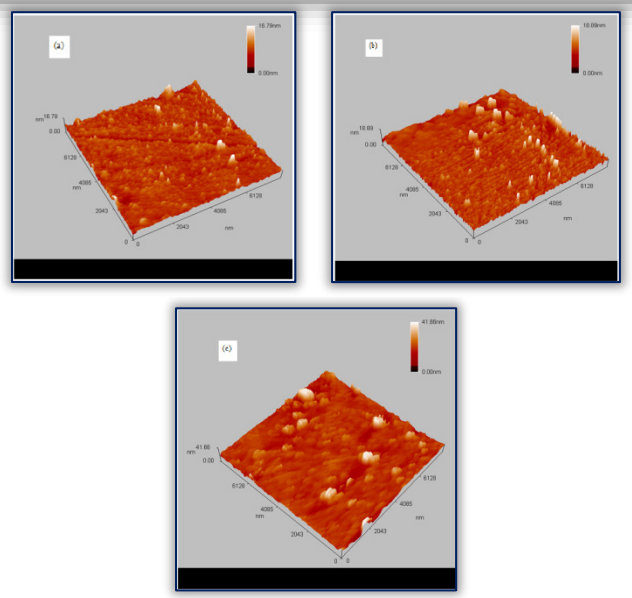

Figure 6. 3D AFM images of NiCr films with different curing temperature from (a) to (c) are 100,200 and 300°C.

Figure 6 gives 3D topography of films. For film surface, R_{max} is explained as maximum height of peak to valley for the depicted surface. Σ is the root mean square roughness. With curing temperature ranging from 100°C to 300°C, it can see the R_{max} is equal (0.8, 0.9 and 2.28) nm and σ is equal (1.16, 1.47 and 3.54) nm. When the film is cured at100°C, islands with small size are observed. However, when the film is cured at 300°C, the islands have agglomerated or coalesced to form bigger structure. The phenomenon can be explained by film growth process: during deposition process, particles are deposited and form nucleus first and then islands on substrate. This is mostly caused by atomic shadowing effects, which makes R_{max} reach 2.28 nm and σ 3.54 nm, and the film surface turns rough correspondingly as shown in Figure 6.(c).

However, when surface diffusion dominates the growing process, the coalescence of neighboring islands makes the valleys become higher and the peak become lower, consequently the surface becomes flat and R_{max} is decrease as known in Figure 6.(a). The film growth is finished by coalescence of neighboring islands. Surface morphology not only relates to film thickness but also to substrate type, works pressure, annealing and so on [14,16].

When the temperature reaches 100°C, the substrate was covered completely by spherical grains with similar radius. With an increase of temperature, the lateral grain size tends to increase. As seen from Figure 7, the lateral grain size changes from about 14.8 nm to 36.7nm when temperature ranges from 100°C to 300°C. The increase of lateral grain size with temperature is common for films [16].

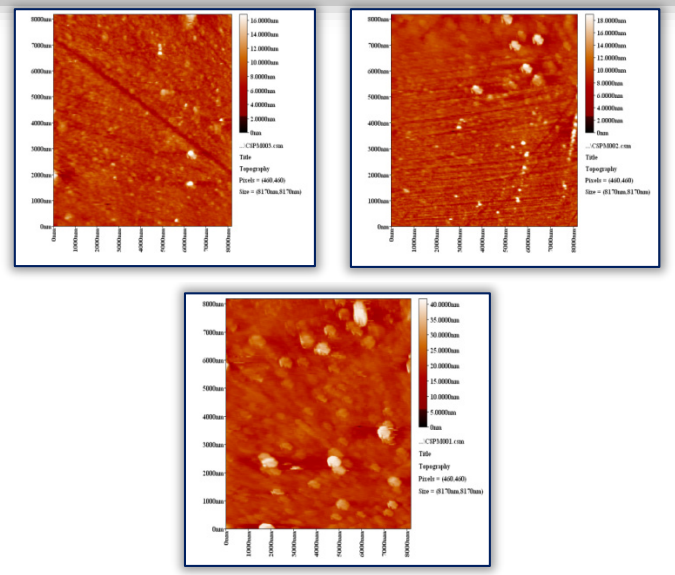

Figure 7. 2D AFM images of NiCr films with different curing temperature from (a) to (c) are 100, 200 and 300°C.

In Figure 8 an abrupt transition from the bond coating to the top coating that leads to their top coating in intimate contact with bond coating [2].

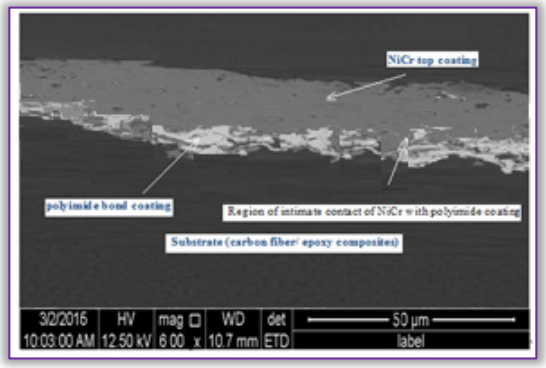

Figure 8. Microstructure of cross-section of carbon-epoxy CMPs with polyimide bond layer and NiCr top coating layer

CONCLUSIONS

This paper presents an experimental process to protect polymer matrix composite (PMCs) by metallic flame spray coating.

The results of the investigations provide useful information for applying the NiCr coating for the improvement of the hardness of PMCs. According to the results of this study, In general the coating with bound coat and coating without bound coat showed increase in micro hardness and adhesion strength with increase temperature. The adhesion strength for the PMCs coating with polyimide bound coat is higher than PMCs coating without bound coat.

The AFM analysis also provides information on the changes in the surface morphology and roughness introduced by the heat treatment. When a temperature change from 100°C to 300°C, the island structure was observed and the R_{max} increase from (0.8 to 2.28)nm, and σ increase (1.16 to 3.54)nm.

References

[1.] Muktinutalapati, N., (2011), Materials for Gas Turbines – An Overview, in: Ernesto Benini (Ed.), Advances in Gas Turbine Technology, Croatia: InTech.

[2.] Miyoshia, K., Suttera, J., Horanb, R., Naikb, S. and Cupp, R.(2004). Assessment of erosion resistance of coated polymer matrix composites for propulsion applications.Tribol.Lett., 17(3),377-387.

[3.] Amado, J., Montero, J., Tobar, M. and Yáñez, A.(2012). Ni-based metal matrix composite functionally graded coatings.Phys.Proced., 39, 362 – 367.

[4.] Hetmańczyk, M., Swadźba, L. and Mendala, B. (2007). Advanced materials and application, protective coatings in aero-engines.J.Achiev. Mater.Manufact. Eng., 24(1), 372-381.

[5.] Ivosevic, M. Knight, R. Kalidindi, S., Palmese G. and Sutter, J. (2005). Adhesive /cohesive properties of thermally sprayed functionally graded coating for polymer matrix composites. J. therm.spray technol., 14(1), 45-51.

[6.] Picas, J., Forna, A. and Matth¨aus, G.(2006). HVOF coatings as an alternative to hard chrome for pistons and valves.Wear, 261, 477–484.

[7.] Hadad, M., Marot, G., De´mare´caux, P., Chicot, D., Lesage,J., Rohr, L. and Siegmann, S.(2007). Adhesion tests for thermal spray coatings: correlation of bond strength and interfacialToughness.Surf. Eng., 23(4), 279-283.

[8.] Sidhu, H., Sidhu, B.and Prakash, S.(2006). Comparative Characteristic and Erosion Behavior of NiCr Coatings Deposited by various High-Velocity Oxyfuel Spray Processes.J. Mater. Eng. Perform., 15(6), 699-704.

[9.] Brossard, S., Munroe, P., Tran, A. and Hyland,M.(2010). Study of the Splat-Substrate Interface for a NiCr Coating Plasma Sprayed onto Polished Aluminum and Stainless Steel Substrates.J. Therm. Spray Technol., 19(1-2), 24-30.

[10.] Richert, M. and Leszczyńska-Madejj, B. (2011). Effect of the annealing on themicrostructure of HVOF deposited coatings. Achiev.Mater.Manufact.Eng., 46(1), 95-102.

[11.] Sidhu, B. and Prakash, S.(2006). Nickel-Chromium Plasma Spray Coatings: A Way to Enhance Degradation Resistance of Boiler Tube Steels in Boiler Environment.J. Therm. Spray Technol., 15(1), 131-140.

[12.] Harsha, S., Dwivedi, D. and Grawal, A.(2007). Influence of WC addition in Co–Cr–W–Ni–C flame sprayed coatings on microstructure, microhardness and wear behavior. Surf. Coat. Technol., 201, 5766–5775.

[13.] Nakamura, Y., Suzuki, Y. and Watanabe Y.(1996). Effect of oxygen plasma etching on adhesion between polyimide films and metal. Thin Solid Films, 290-291, 367-369.

[14.] Jicheng, Z., Li, T. and Jianwu, Y.(2008). Surface and Electrical Properties of NiCr Thin Films Prepared by DC Magnetron Sputtering.J. Wuhan Univer. Technol. Mater. Sci. Ed., 23(2), 159-162.

[15.] Lesagea, J., Staiab, M., Chicota, D., Godoyc,C. and De Miranda, P.(2000). Effect of thermal treatments on adhesive properties of a NiCr thermal sprayed coating. Thin Solid Films, 377-378, 681-686.

[16.] Patil, A., Patil, V., Choi, J., Kim, H., Cho, B. and Yoon, S. (2009). Structural and electrochemical properties of Nichrome anode thin films for lithium battery. J. Electroceram., 23, 230–235.

ACTA TECHNICA CORVINIENSIS
– Bulletin of Engineering
Tome IX [2016], Fascicule 4 [October – December]
ISSN: 2067 – 3809

[1.]Ana-Maria AVRAMESCU

THE SMART DESIGN OF AN ELECTRICAL HOUSEHOLD APPLIANCES – IRON

[1.] University Polytechnic Bucharest, Faculty of Aerospace Engineering, ROMANIA

Abstract: Through designing standards and technolgical development, electrical household appliances are manufactured by respecting well defined and regulated parameters. In order to fit into our courrent environment these appliances should be manufactured using efficient technologies that imply lower costs and lower amounts of energy. The performance of the appliances is targeted through continuous development and transformation. The quality of all electrical appliances is a decisive factor in creating the features that aim to make our life better. In this article, we present the intelligent appliance named – iron.
Keywords: Design, home appliances, iron, innovation, project

INTRODUCTION

This article aims to present the designing process of an electrical appliance. This project was proposed during the „Electrolux Design Lab" contest for the year 2013. Looking into the recent past, soon after the year 1989 some poor quality appliances were sold on the Romanian market. This situation was caused from carelessness but also because of the manufacturer's failure to consider highest quality standards.

If we follow the idea of continuous development in the process of designing and building appliances, we have to determine producers to be aware of the necessity for using an adequate quality standard. This way, our environment is also protected.

In order to increase the performance of appliances, producers should use modern and effcient materials and production systems [1], [2]. Nowadays, the market offers a wide range of appliances, for example the modern iron. This machine is a tool used for smoothing out clothing or fabrics by hot pressing. This ironing operation loosens the links between the long molecules of the fabric. Also, taking into account the weight of the machine, the fabric shall be smooth and cooled in the desired shape. Some fabrics like those made of cotton need some added water in the process so that the molecules can be loosened.

In the current business environment, consumers are increasingly fastidious and competitors are fiercely fighting to harness new ideas, innovative products and services [3]-[7]. Hence, this article is presenting a new product design for household iron series.

HISTORY

In China, starting with the first century, metal pots filled with charcoal were used for ironing. In Europe, triangular cast iron plates were used starting with the seventeenth century. Afterwards, charcoal filled cast iron flatiron appeared. The electrical iron was presumably inivented in 1882 by Henry W. Seeley. The first iron with thermoregulator was launched in 1920. Later, Thomas Sears invented the steam iron and these products were continuously developing.

The steam iron also helped for smoothing and finishing rippled fabrics. Although the steam iron was invented somehow early, it only became popular in the 1940' [8], [9].

PRODUCT PRESENTATION – CONCEPT

The underlying concept of this iron represents a rechargeable iron that identifies the fabric structure (using a sensor) and automatically sets the ironing temperature for the specific fabric. Aside of these features, this iron has all the functions of a modern one; images 1-a) and 1-b).

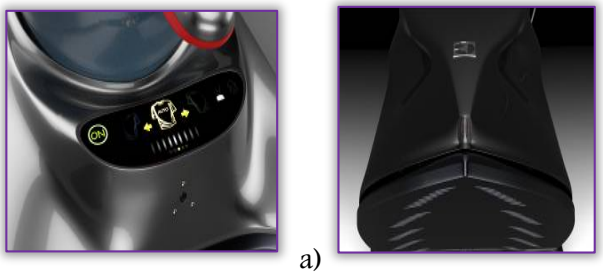

a) b)

Figure 1 – a) The LCD screen;
b) The thermoregulatory sensor

MATERIAL AND METHOD

The 3-D Model was performed using the 3-D Studio Max sofware; image 2. In the next sequence we present the steps of the modeling process.

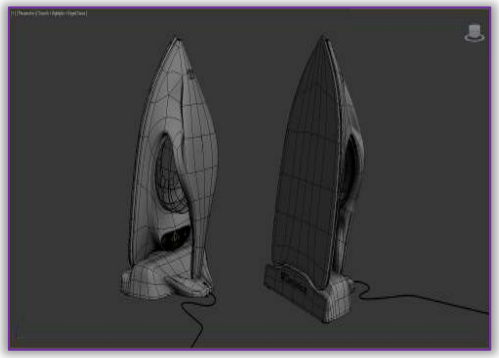

Figure 2 – Product modeling

In order to create the model, basic geometrical forms were shaped in order to accomplish the desired result. In the image of figure 3, we can see how the soleplate was modeled starting from a box (1) and then adding parts using the ‚connect' function. In the second step, the vertex (3) is modeled alongside with other added parts. In the third step, the ‚turbo smooth' function was added (4). In the final step the ‚symmetry' function was used to complete the other half of the model and finish the entire element (5); images 3-a) and 3-b).

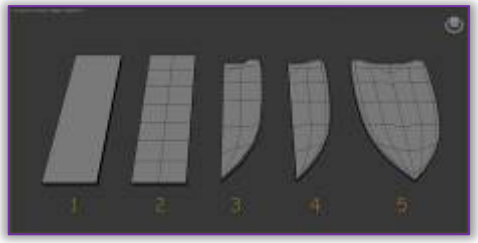

a)

b)

Figure 3 – a/b) Modeling steps - 1

The next image presents the steps of creating the body structure. This element was created starting from the upper part of the soleplate that was shaped on one side of the model. Moving forward, the inner side was erased in order to start the modeling process (3)-(5). Also, turbo smooth and symmetry functions were applied; image 4-a).

The water tank was created starting from the basic geometrical form which is a sphere that was manipulated on the X and Y axes, (3). In the next phase, the inner quarter was cut in order to obtain a flat surface (4). Here, the turbo smooth function was added once more; image 4-b).

a)

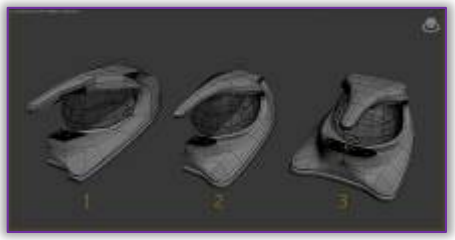

b)

Figure 4 – a/b) Modeling steps - 2

As specified earlier, the symmetrical elements have been modeled only on one half. In the image below, the three phase model is presented as following: (1) raw model (unchanged); (2) turbo smooth added; (3) symmetry added (on elements that support the function).

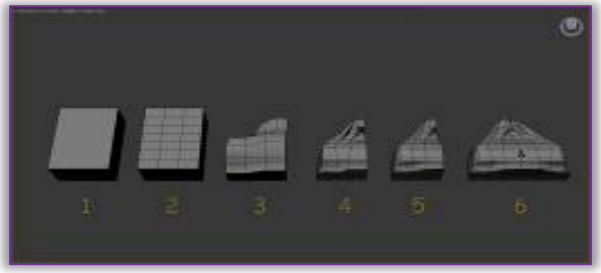

Figure 5 – Modeling steps - 3

In the image above we can see the steps for modeling the iron charging station. This was created starting from a box form that was divided for better modeling purposes. This process is presented in the steps (3),(4). The turbo smooth and symmetry functions are added in steps (5), (6); Image 5.

TURBO SMOOTH

In this section, the turbo smooth function is explained. In the image below, two perpendicular planes are presented in three phases:

- In the upper side we have the two perpendicular planes with the turbo smooth function disabled and in the lower side we have the two perpendicular planes with the turbo smooth function enabled. When this function is enabled we can observe how the right angle becomes a curve. This curve is defined by the distance between the edge and the closest line.
- In order to better demonstrate this effect and obtain a smaller curve, a line on each plane was added between the two planes and close to the edge.
- In this phase, the lines are very close to the edge and a very small edge was obtained. Here, the

curve is perceived as a sharp edge and the deformation of the two planes is much smaller.

To conclude, various phases can be used in modeling in order to obtain the desired shapes, from very sharp edges to very smooth curves, all without the deformation of the initial geometrical form.

Figure 6 - Modeling – Turbo Smooth

RESULTS

The chosen iron design is futuristic and has aerodynamic shapes, smooth curves and a quality finish that exposes the structure and features. The ultimate model was obtained by creating elements around the water tank which is the starting point of this design project. The materials used comprise glossy surface plastic and rubber for a better grip on the handle. In the rear side, a touch screen display was added for accessing and utilizing the iron functions. The following images represent 3-D rendering created in 3-D studio Max Software; Image 7.

Figure 7 - Presentation of design product

Launching new products is extremely costly and, for this reason, careful planning is essential. When a new product is released on the market, it already has a history behind it. The process starts from identifying a need or demand which should be analyzed prior to developing the product and creating packaging. Afterwards, the role of marketing and communication strategies sets the future course of development.

Considering that innovation is not an option but a prerequisite, creating new products is a very difficult task and that's why only a few ideas prove to be good enough to attain success in the market. In this case, the proposed item offers remarkable solutions, image 8.

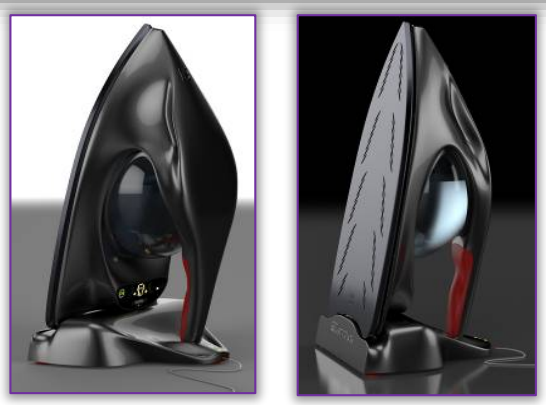

Figure 8 - Presentation of design product – front / back

In the present time, the customers' demands for increased comfort are manifold so, to offer maximum satisfaction, the new irons are elegant in both design and functional features. The body and structure of the iron emphasizes the differentiation and makes it stand out among similar products, image 9.

Figure 9 - Presentation of design product – front / back

CONCLUSIONS

The process of designing an iron is a complex activity that comprises multiple steps before accomplishing a state-of-the-art product, like the iron presented above. Knowing that design can be represented at various levels, this iron fits the Product Design category meaning the process was created with regard to both design standards and technical standards. The end product is the result of common efforts from mechanical engineers, designers and marketing specialists.

The product is part of durable goods that are bought infrequently and the buying decision is decisively influenced by the following ratio: price-quality-brand. This specific product is an exceptional electrical appliance that has innovative functional attributes, a state of the art iron in terms of ergonomics, quality and authenticity.

Acknowledgement

The work has been funded by the Sectoral Operational Programme Human Resources Development 2007-2013 of the Romanian Ministry of Labour, Family and Social Protection through the Financial Agreement POSDRU/107/1.5/S.76813.

References

[1.] Wang S, Kaufman A, (1995), Volume sculpting, In: Proceedings of the symposium on interactive 3D graphics, Pages 151–56;
[2.] Armaş I., Mechatronics and Robotics Design, Editure A.G.I.R., 2011;
[3.] Guangping Wang, C. Fred Miao (2015), Effects of sales force market orientation on creativity, innovation implementation, and sales performance, Journal of Business Research, Volume 68, Issue 11, November 2015, Pages 2374-2382;
[4.] Balin S., Giard V., (2007), La qualité des services et leurs processus deproduction, 7th International Congress of Industrial Engineering, Trois-Rivières, Québec;
[5.] Saïd Echchakoui, (2016), Relationship between sales force reputation and customer behavior: Role of experiential value added by sales force, Journal of Retailing and Consumer Services, Volume 28, January 2016, Pages 54-66;
[6.] Annie Chen, Norman Peng, Kuang-Peng Hung, (2015), Managing salespeople strategically when promoting new products—Incorporating market orientation into a sales management control framework, Industrial Marketing Management, Volume 47, May 2015, Pages 147-155;
[7.] Lena Hohenschwert, Susi Geiger, Interpersonal influence strategies in complex B2B sales and the socio-cognitive construction of relationship value, Industrial Marketing Management, Volume 49, August 2015, Pages 139-150;
[8.] Irfan Shah, Rohana Adnan, Wan Saime Wan Ngah, Norita Mohamed, Iron impregnated carbon materials with improved physicochemical characteristics, Materials Science and Engineering: B, Volume 201, November 2015, Pages 1-12;
[9.] Stefano Bracco, Carlo Cravero, Dynamic simulation of a steam generator for ironing machines, Energy Conversion and Management, Volume 84, August 2014, Pages 13-19.

ACTA Technica CORVINIENSIS
BULLETIN OF ENGINEERING

ISSN:2067-3809

ACTA TECHNICA CORVINIENSIS
– Bulletin of Engineering
Tome IX [2016], Fascicule 4 [October – December]
ISSN: 2067 – 3809

[1.]Miruna MAGAON, [2.]Teodor HEPUȚ

RESEARCH ON THE DISPOSAL OF HYDROGEN CONTENT FROM THE STEEL DESIGNED FOR MANUFACTURING STEEL PIPES

[1-2.] University Politehnica Timisoara, Faculty of Engineering Hunedoara, Hunedoara, ROMANIA

Abstract: The paper presents the results of the research conducted in order to reduce the hydrogen content from the steel designed for manufacturing pipes used to transport oil. The steel was produced in an electric arc furnace, type E.B.T. (Eccentric Bottom Tapping) 100t capacity, treated in L.F. (Ladle - Furnace) plants and V.D. (Vacuum -Degassing). In L.F. plants takes place a process of desulfurization and deoxidation with synthetic slag and steel heating plant for processing in vacuum without heat input (V.D.). This research was particularly aimed at explaining the influence of vacuuming parameters (during vacuuming, pressure vacuum system, and temperature of steel) over the hydrogen removal efficiency and hydrogen final content. The obtained data was processed in Excel program, the obtained correlations were analyzed from a technological standpoint and consequently the vacuum optimum parameters were established.
Keywords: Steel pipes, hydrogen content, electric arc furnace, E.B.T. (Eccentric Bottom Tapping), L.F. (Ladle-Furnace), V.D. (Vacuum-Degassing)

INTRODUCTION

Hydrogen and nitrogen are impurities for steel products, but their negative influence is manifested especially in steel.

The negative influence of the hydrogen is manifested by the fact that:

- is one of the causes of sulphides in ingots and calmed steel castings;
- contribute to the occurrence of the defect called "flakes" (very small cracks) in steels alloyed with chromium and nickel, which substantially reduces fatigue strength of steel parts;
- decreases the elasticity and toughness of the steel;
- affects the electrical and magnetic properties of steels.

The primary sources of hydrogen are air and moisture.

In steel making processes, hydrogen comes from:

- metallic and nonmetallic cargo (iron cargo, scrap iron cargo, mining cargo, limestone cargo, chalkstone cargo etc.);
- the aggregate development atmosphere (air, fuel combustion products, oxygen blew in steel etc);
- ferroalloys used for the deoxidation and alloyage of steel.

To prevent the ingress of hydrogen in the steel is indicated to be taken a number of technological measures from raw and auxiliary materials, such as:

- to not be used in the cargo scrap iron with oil remnants or rust;
- the burned limestone should be as fresh as possible, and, unless has its own limestone factory, the limestone transport has to be carried out in closed containers;
- the iron ore has to be calcinated;
- calcinated ferroalloys used for deoxidation and alloying.

During the decarburization of the metal bath, a part of the hydrogen is eliminated by the carbon monoxide bubbles. Decarburization speed compliance provided in the technological instructions reduces the hydrogen absorbtion in the steel bath. Currently, in most steel mills, to intensify the elimination of hydrogen, bubbling with argon method is used in L.F. facilities and when prompted very low hydrogen contents it is used the treatment of steel under vacuum (desirable for at least 15 min. under high vacuum).The processing parameters in the casting ladle shows a particular importance in order to reduce the gas content in the steel.

THE STUDY PROBLEM

Oil industry requests high quality steel for manufacturing the steel pipes that carries oil, resistant to corrosive oil components, the external environment acting on pipelines, the temperature variations, etc.

In what concerns the quality of the steel, one of the factors influencing the behavior of steel in use is the hydrogen content that exists in the steel, respectively in the finished product (rolled pipe).
For this research we watched the process of steel making in an electric arc furnace, type E.B.T. (Eccentric Bottom Tapping) 100t capacity, treated in L.F. (Ladle - Furnace) and V.D. (Vacuum -Degassing) facilities. In the L.F. facility a process of desulfurization and deoxidation takes place with synthetic slag as well as heating the steel in order to be processed in the vacuum plants without heat input (V.D.).
This research was particularly aimed at explaining the influence of the vacuuming parameters (during vacuuming, pressure vacuum system, and temperature of steel) over the hydrogen removal efficiency and hydrogen final content. 35 charges of were followed and after analyzing the parameters values due to technological deviations, 30 charges was selected. All the obtained data was processed in Excel program.

DATA INTERPRETATION

After processing the data, correlations between vacuuming parameters were obtained, considered independent parameters and dependent parameters, hydrogen removal efficiency and final hydrogen content. The correlations are expressed by polynomial functions of grade II and III, exponential and logarithmic, analyzed from a technological point of view and based on those data the optimal vacuum parameters were established.

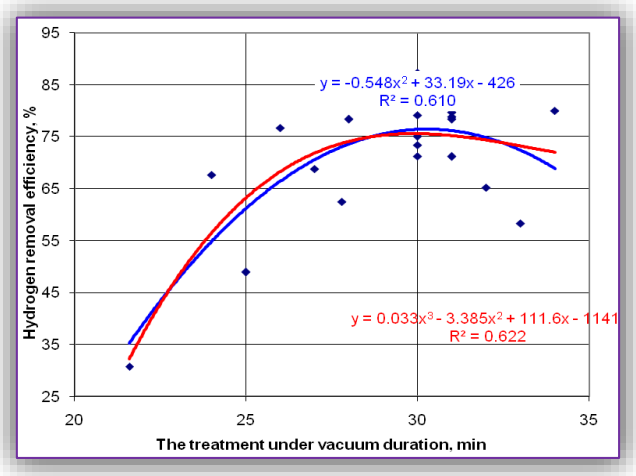

Figure 1. Hydrogen removal efficiency depending on the treatment under vacuum duration

From the graphical representation shown in Figure 1 it appears that with increasing duration of vacuum, hydrogen removal efficiency increases. Once the duration of the vacuum switch 30 min, the hydrogen removal efficiency begins to decrease slightly. Technologically this increase is explained by the fact that in these circumstances there is appropriate time for the hydrogen diffusion from the steel bath in an argon bubbles and thus to the vacuum atmosphere. Within 30-34 minutes there is a slight decrease in the hydrogen removal efficiency, due to lower rate of hydrogen diffusion caused by lowering the temperature. It can be considered that treatment durations of 30-34 minutes are great.

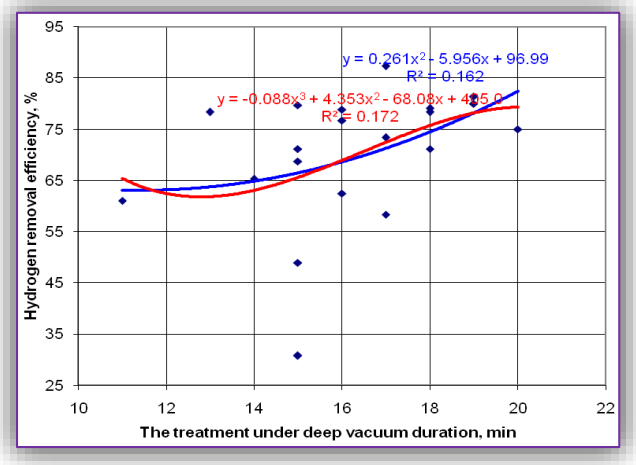

Figure 2. Hydrogen removal efficiency depending on the treatment under deep vacuum duration

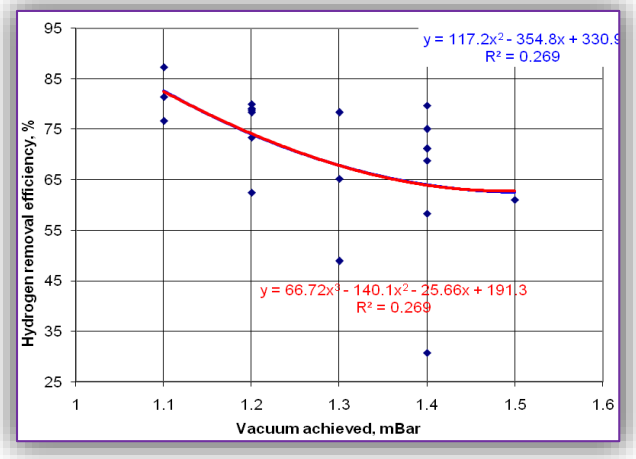

Figure 3. Hydrogen removal efficiency based upon the vacuum achieved

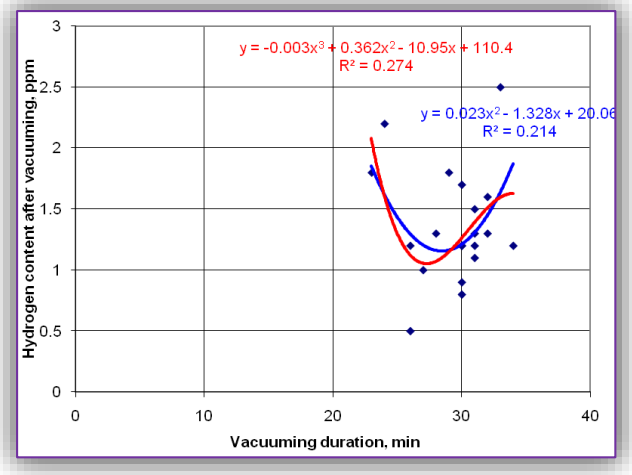

Figure 4. Hydrogen content after vacuuming depending on the vacuuming duration

Figure 2 notes that increasing duration of treatment under deep vacuum (advanced) leads to increased hydrogen removal efficiency. Technologically this is explained by the fact that there is an increase of the hydrogen diffusion speed, dependent on the hydrogen partial pressure from the system. Decreasing the total pressure above the metal bath (from vacuum space) clearly decreases the hydrogen partial pressure. At a vacuum of 30-34 minutes duration, treatment duration under deep vacuum of 18-20 minutes is representative.

Analyzing the graphical representation in Figure 3, it can be noted the treatment under high vacuum efficiency, resulting in increasing the efficiency of hydrogen removal. Therefore, under a vacuum of 1.1-1.2 mbar are obtained, for the efficiency of hydrogen removal, values within the range of 75-85%. Decreasing the pressure over the metal bath (in the vacuum system) also causes the decrease in the partial pressure of hydrogen, so it creates favorable conditions for reactivating the diffusion of hydrogen.

The technological analysis of the graph shown in Figure 4 shows that an increase in the duration of the treatment under vacuum, up to 26-30 minutes, leads to a reduction of hydrogen content from the liquid steel as a result of the favorable conditions (temperature, time) of degassing. If achieving high values for the treatment under vacuum duration, then the hydrogen content no longer decreases, on the contrary, it increases slightly due to lower bath temperature and the ingress of hydrogen from slag (the diffusion speed from slag in the bath is higher than the diffusion speed from bath to slag). The results shown are correlated very well with those shown in Figure 1.

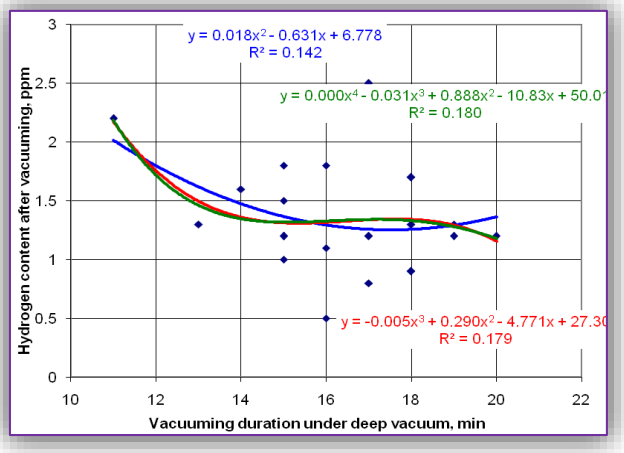

Figure 5. Hydrogen content after vacuuming based upon the vacuuming duration under deep vacuum

The results shown in Figure 5 confirm that the treatment under high vacuum leads to the reduction of hydrogen content from the metal bath. The treatment duration was up to 20 minutes, the decrease being intense until duration of 16 minutes, after which remains steady. The obtained results are correlated very well with those shown in Figure 2.

Analyzing the results shown in Figure 6 it can be noted an advanced reduction of hydrogen content from the metal bath to less than 1ppm. The results are correlated very well with those shown in Figure 3.

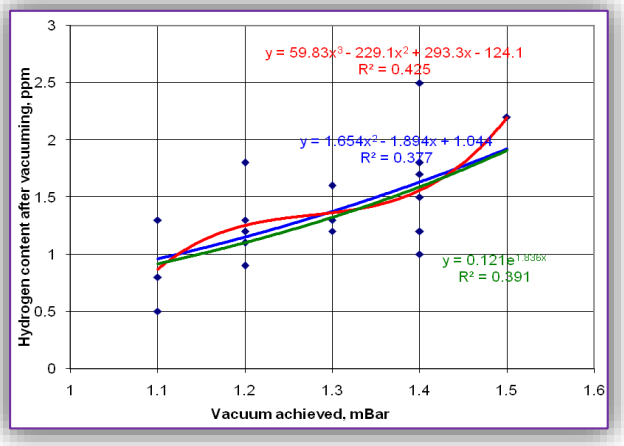

Figure 6. Hydrogen content after vacuuming based upon the vacuum achieved

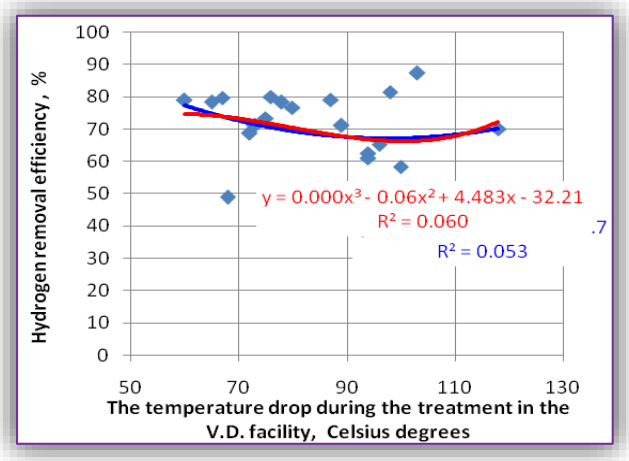

Figure 7. Hydrogen removal efficiency depending on the temperature drop during the treatment in the V.D. facility

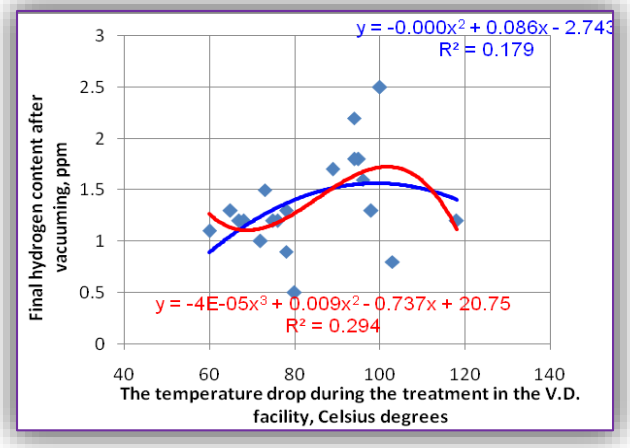

Figure 8. Final hydrogen content after vacuuming depending on the temperature drop during the treatment in the V.D. facility

Referring to Figure 7 and Figure 8 it is found that the values for steel temperature in the vacuum facility are suitable for quality standards imposed on steel pipes.

CONCLUSIONS

From the research made in the industrial phase one can conclude the following:

- The main parameters of vacuuming, the total duration, the duration under high vacuum and the vacuum pressure in the system, they all influence both the hydrogen removal efficiency, and the final hydrogen content;
- In the technological sense there is a very good correlation between the correlations obtained in EXCEL program relating to the hydrogen removal efficiency and the hydrogen content at the end of vacuuming;
- Through the treatment of liquid steel in the LF facility it is ensured a reduction of the sulfur and oxygen contents through the means of synthetic slags, and through vacuum treatment a reduction of the gas content, in particular less than 2.5 ppm hydrogen;
- The steel processing in L.F. facility ensures a good overheating of the steel so that the duration of vacuum treatment reaches 30-35 minutes and the high vacuum treatment reaches up to 20 minutes, thereby ensuring the appropriate time for the oxygen diffusion from the liquid steel in the argon bubbles under suitable conditions of heat;
- Significant influence over the content of hydrogen at the end of the treatment has a very low pressure achieved in the vacuum facility (1,1mBar);
- Due to steel overheating in L.F. facility the treatment duration under vacuum can be increased up to 30 -34 minutes, compared to 18 -20 minutes without the L.F. facility.

References

[1.] Dragomir, I., Theory of Metals, Didactic and Pedagogic Publishing, Bucharest 1985.
[2.] Geantă, V., Stefănoiu, R., The Engineering of Steel Production, BREN Publishing House, Bucharest 2008..
[3.] Putan, A., Research on steel refining elaborated on the flow: electric arc furnace-ladle furnace-continuous casting, PhD Thesis, University Politehnica Timisoara, 2013.
[4.] Drăgoi, F., Research on reducing the gas content of the drafted steel treated on the technological flow EBT-TC, PhD Thesis, University Politehnica Timisoara, 2012.
[5.] Lăscutoni, A., Research on mathematical modeling of thermal aggregates in liquid steel at the ladle - distributor -cristalizorlevel, PhD Thesis, University Politehnica Timisoara, 2015.

ACTA Technica CORVINIENSIS
BULLETIN OF ENGINEERING
ISSN:2067-3809

ACTA TECHNICA CORVINIENSIS
– Bulletin of Engineering
Tome IX [2016], Fascicule 4 [October – December]
ISSN: 2067 – 3809

[1.]Ştefan S.BIRIŞ, [1.]Edmond MAICAN, [2.]Eugen MARIN, [3.]Sorin BUNGESCU,
[2.]Valentin VLĂDUŢ, [1.] Nicoleta UNGUREANU, [1.]Daniel IonVLĂDUŢ, [4.]Atanas ATANASOV

STRUCTURAL STATICAL ANALYSIS OF WORKING BODIES OF AGRICULTURAL CULTIVATORS

[1.]University "POLITEHNICA" Bucharest, Faculty of Biotechnical Systems Engineering, ROMANIA
[2.]INMA Bucharest, ROMANIA
[3.]USAMVB Timişoara, ROMANIA
[4.]University of Russe, BULGARIA

Abstract: In this paper is presented an advanced methodology for the analysis of stress and strain distribution (statical structural analysis using the finite element method) in the working bodies of agricultural cultivators for seedbed preparation in order to optimize them. The geometrical model of soil working body was develoepd in SolidWorks format before being taken and transferred to the program of analysis with finite elenets (ANSYS), in order to perform the necessary resistance calculations made in linear static domain. The obtained results provide valuable information on proper geometric dimensioning of the working bodies of agricultural cultivators.
Keywords: finite element method, structural statical analysis, working body, agricultural cultivator

INTRODUCTION

Following the expansion of soil degradation processes due to conventional agriculture and technological mistakes, over the years, the so-called conservative agricultural technologies have been studied and implemented in practice. These technologies have contributed substantially to the improvement of soil fertility and productivity and, thus, of other environmental resources. The most important component of conservation technological systems, as in the case of conventional ones, is soil tillage – loosening and processing – and the introduction of seed into the soil. Switching from conventional tillage systems to the conservative ones was not easy and generated a lot of questions that needed relevant answers, scientifically based, some of them being obtained through fundamental and applied research carried out under local specific conditions. Conservative systems are based on the less intense loosening of soil, made by different methods, without furrow return and only while maintaining a given amount of crop residues on soil surface, being considered for this reason as environmental protection strategies.

Agriultural cultivators are equipment with an increasingly widespread for seedbed preparation in order to establish crops, especially in the current conservative cultivation technologies. Besides the fact that these equipment must achieve a soil processing with superior qualitative and energy indices, their weight must be as small as possible and their reliability must be as good as possible. Currently, it is possible to shorten spectacularly the cycle of conception-design-testing-production of such equipment by using the finite element method for the analysis of stress and strain distribution of their resistance elements (frames, tool holders, working tools, etc.).

MATERIAL AND METHOD

The experimental model of technical equipment for conservative processing of soil is semi-mounted and works in aggregate with tractors in range of 330-550 HP.

Theequipment (Figure 1) consists of: drawbar with towing ring (1); working bodies type knifechisel with extension (2); preceding disks (3); double bearingsupport (4); identification tablet (5); central frame (6); transport train (7); rearroller (8); lights kit (9); hydraulic installation for folding of lateral frames (10);); hydraulic installation for working depth adjustment of the discs (12); disc levening bar (13).

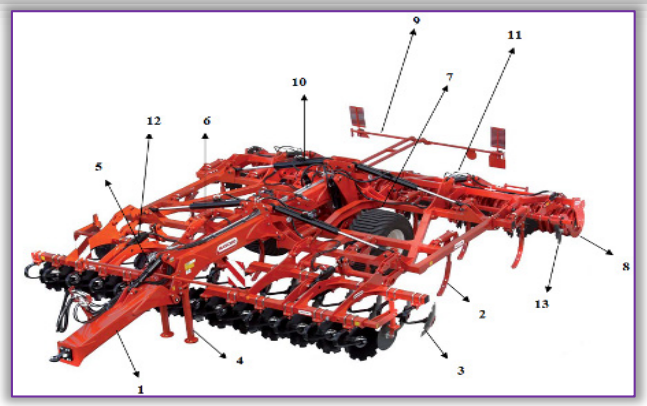

Figure 1 – Technical equipment for conservative soil processing – three-dimensional view

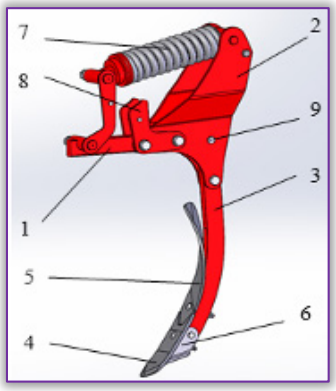

Figure 2 – Main working body of the cultivator

Soil working body (Figure 2) is designed to dislodge the soil to a depth of up to 25 cm, to raise, stir and turn crop residues, is mounted on the frame of technical equipment for conservative soil processing. Soil working body consists of a support (1) on which are mounted two support plates (2) on one hand, for assembling a rigid support (3) provided with a chisel (4) for soil decompaction, an extension (5) for slight twisting of crop residues and a cutting knife (6) of the bottom of the furrow and on the other hand, for assembling a pretensioned spring (7) which allows absorbing most part of the towing tension and of the plates (8) for the limitation of the spring stroke.

The geometric model of soil processing in conservative system was developed in SolidWorks format and transferred to the analysis program with finite elements (ANSYS), in order to perform the required resistance calculations, which were made in linear static domani. In figure 4 is presented the meshed model of the working body. Given that the investigated structure was modeled geometrical three-dimensional, it was chosen that in the meshing process to use a 3D finite element, of Solid type. His is a three-dimensional element, of rectangular shape, with 20 nodes (on each corner and at each mid side) with three degrees of freedom on each node: nodal translations in the directions of OX, OY and OZ axis. The element supports the theory of plasticity, hiperplasticity, large specific displacements and strains; the material used S355OL52.

In figure 5 is presented dthe geometrical shape of the finite element, used in the meshing process. The rectangular shape of the finite element represents the native shape, whereas the other shapes, found in the right side of the figure, represent degenerated forms, that may arise in the case of complex geometries as shapes (in areas in which are found junction radius, thickness variations etc.).

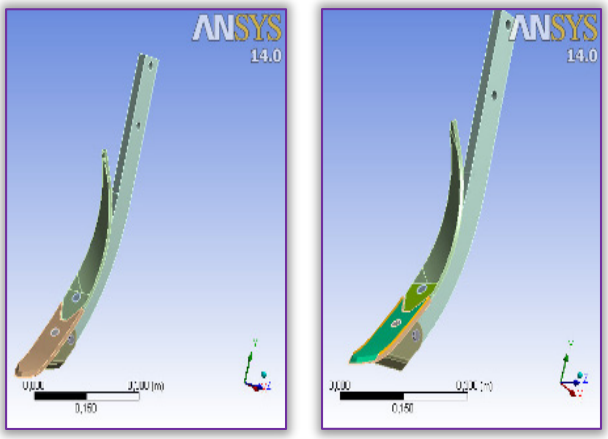

Figure 3 – Geometric model of working body taken in ANSYS

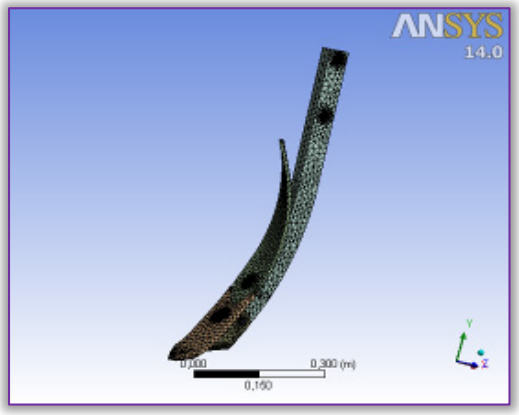

Figure 4 – Meshed model of the working body

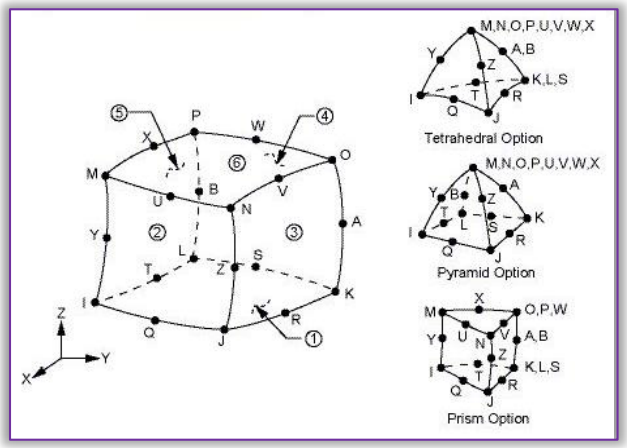

Figure 5 – Geometry of the finite element

RESULTS

The results of the static analysis of the working of the cultivator are presented in the following figures. These consist of: distribution of total deformation,

distribution of normal pressures on the coulter of the working body, distribution of equivalent stress by the Von Mises criterion in both the coulter and the wing of the working body, but also in support of the working body.

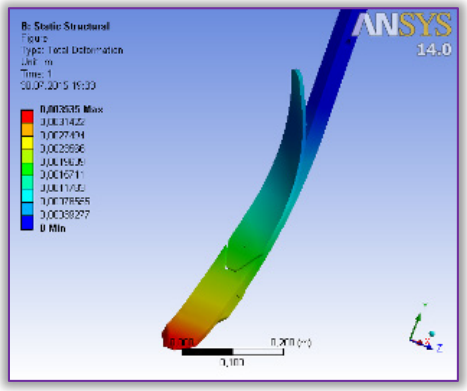

Figure 6 – Distribution of total deformation

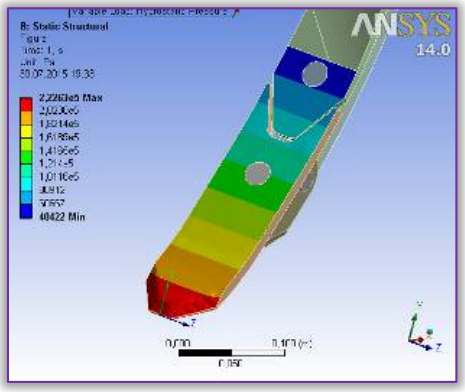

Figure 7 – Distribution of normal pressures on the working body

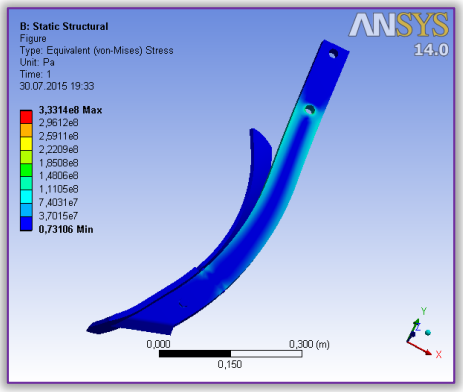

Figure 8 – Distribution of equivalent stress

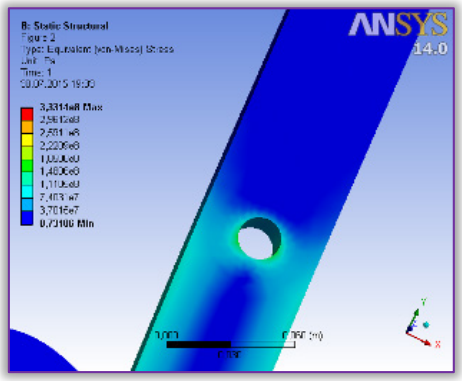

Figure 9 – Detail of the distribution of equivalent stress

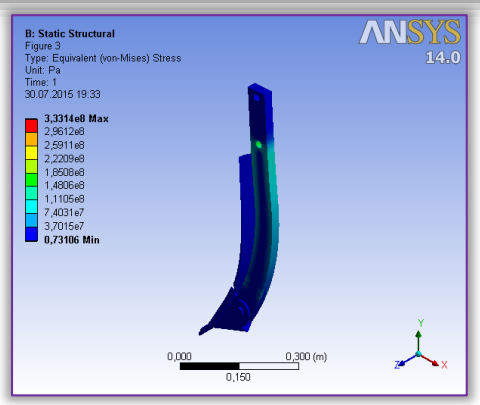

Figure 10 – Distribution of equivalent stress in the support of the working body

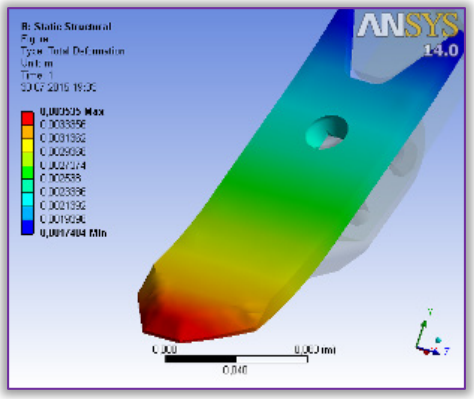

Figure 11 –Distribution of deformation on the coulter of the working body

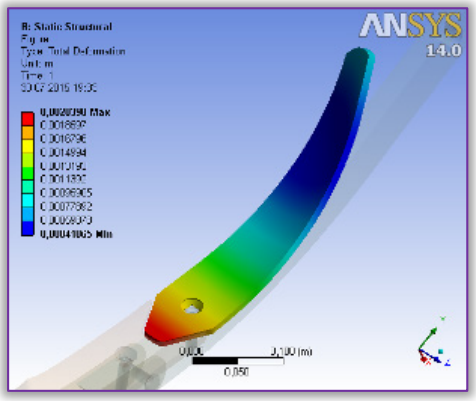

Figure 12 – Distribution of deformation on the working body wing

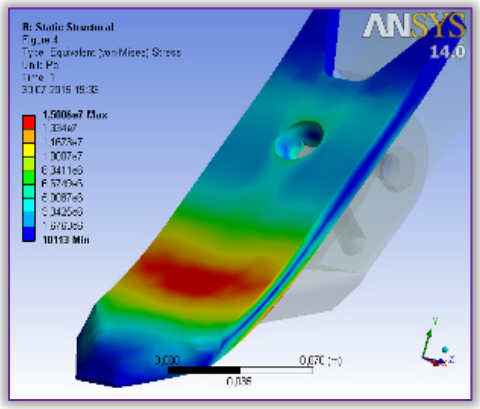

Figure 13 – Distribution of stress on the coulter of the working body

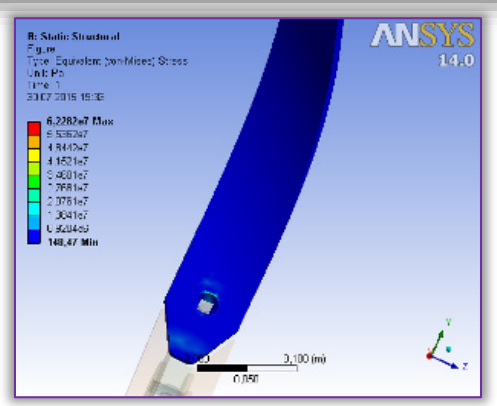

Figure 14 – Distribution of stress on the working body wing

CONCLUSIONS

- Theoretical structural static analysis of the working body can be used to determine deformations in plastic field;
- This analysis can be used as a tool for determining the mechanical strength and hence the reliability of the working;
- To obtain a conclusive result on the active organ deformation resistance, static structural analysis is completed with tests under real working: the stand - Hidropuls or in expoitation).

ACKNOWLEDGEMENTS

This work was supported by UEFISCDI based on 181/2014 financing program.

REFERENCES

[1.] Benites J. (2000) - Manual on integrated soil management and conservation practices The Challenge of Agricultural Sustainability for Asia and Europe, FAO Land and Water Bulletin, No. 8, pp. 1-4.
[2.] Bhatti M.A. (2003) - Finite Element Analysis. Theory and Applications, Zephyr Copier, Iowa State University;
[3.] BirişS.Şt. (2005) - Finite Element Method. Fundamental Concept, Publishing House PRINTECH, Bucharest;
[4.] Chen Y, Munkholm L.J., Nyord T. (2013) - A discrete element model for soil–sweep interaction in three different soils.Soil& Tillage Research 126, pp. 34–41;
[5.] De Miranda S., Ubertini F. (2002) - Recovery of consistent stresses for compatible finite elements, Computer Methods in Applied Mechanics and Engineering, vol. 191 (15–16), pp. 1595-1609;
[6.] Duarte C.A., Hamzeh O.N., Liszka T.J., Tworzydlo W.W. (2001) - A generalized finite element method for the simulation of three-dimensional dynamic crack propagation, Computer Methods in Applied Mechanics and Engineering, vol. 190 (15–17), pp. 2227-2262;
[7.] Javadi A., Hajiahmad A. (2006) - Effect of a New Combined Implement for Reducing Secondary Tillage Operation, Int. J. of Agr. & Biol., Vol. 8, No. 6, pp. 724-727;
[8.] Pisante M., Corsi S., Kassam A. (2010) - The Challengeof Agricultural Sustainability for Asia and Europe, Transist. Stud. Rev., Springer, Vol. 17, No. 4, pp. 662-667;
[9.] Plouffe, C., Richard M.J., Tessier S., Lague C. (1999) - Validations of mold board plow simulations with FEM on a clay soil, Transactions of the ASAE, vol. 42(6): 1523-1529;
[10.] Quaranta G. (2011) - Finite element analysis with uncertain probabilities, Computer Methods in Applied Mechanics and Engineering, vol. 200 (1–4), pp. 114-129;
[11.] Shmulevich I. (2010) - State of the art modeling of soil–tillage interaction using discrete element method, Soil & Tillage Research, vol. 111, pp. 41–53;
[12.] Tamas K., Jori J.I., Mouazen A.M. (2013) - Modelling soil–sweep interaction with discrete element method, Soil & Tillage Research, vol. 134, pp. 223–231.

ACTA Technica CORVINIENSIS
BULLETIN OF ENGINEERING

ISSN:2067-3809

ACTA TECHNICA CORVINIENSIS
– Bulletin of Engineering
Tome IX [2016], Fascicule 4 [October – December]
ISSN: 2067 – 3809

[1.]Elżbieta KARAŚ, [2.]Roman ŚMIETAŃSKI, [3.]Teodor Florin CILAN

EMPLOYEES' ASSESSMENT OF KAIZEN IMPLEMENTATION IN INDUSTRIAL ENTERPRISE – RESULTS OF EMPIRICAL RESEARCH

[1-2.]Opole University of Technology, Faculty of Economics and Management, POLAND
[3.]"Aurel Vlaicu" University of Arad, Faculty of Economic Sciences, ROMANIA

Abstract: The aim of this article is to present the philosophy of kaizen, which may support the strategy for implementation of innovative changes, and thereby increase the innovativeness of Polish enterprises. The paper developed a theoretical and an empirical parts. The first part generally describes the core philosophy of kaizen and the second part shows the results of empirical studies conducted in the Polish enterprise which concern the state of employees' readiness and commitment to the implementation of kaizen.
Keywords:innovation, kaizen, employees, process of changes, polish enterprise

INTRODUCTION

Contemporary there are many concepts and management methods which allow the search for new and better direction for the development of enterprises and contribute to improve their competitiveness and innovation. The system solutions in the field of innovation become an important point, they are implemented in order to improve the functioning of the enterprise and its better adaptation to rapidly changing environmental conditions. The source of these changes are usually the natural human desire to improve the status quo and are the essence of streamlining the organization [12, 6]. This principle is the main message for Japanese management concepts such as Total Quality Management, Lean Management and kaizen. As part of these there are a number of methods and instruments to improve, used with varying results by enterprises around the world, including Poland.

This article describes the philosophy of kaizen in theory, and presents the results of empirical studies conducted in the Polish enterprise on the state of readiness of employees to the implementation of kaizen.

MATERIAL AND METHOD

The theoretical part of article was developed on a base of polish and foreign literature and Internet sites. The empirical part was developed from performed research. The study was conducted in 2014 in the Polish manufacturing plant operating in the metal industry in Lower Silesia. The study used a questionnaire, the fulfillment of which was supervised by a competent person dealing with the issues of implementation of kaizen. The questionnaires were addressed to the production employees working on the assembly line. The results of research were analyzed and graphically presented in the second part of paper.

THEORETICAL APPROACH OF KAIZEN VS INNOVATIONS

The term "kaizen" is a combination of two Japanese words: kai - "change" and zen - "good." The literal translation means "change for the better." In the literature there are many definitions of the term. In the Polish publication: "Handbook of Quality" kaizen is interpreted as "gradual, ordered and continuous improvement, increasing the value, perfecting, advancement" [17]. According to another definition it is: "The concept of management based on the constant search for and application of even the smallest improvements in all areas of activity at each workplace. Its aim is to achieve significant success through small steps" [2]. However, the most important interpretation of this concept refers to the human factor and it is: "the desire of all employees and executive-level to the continuous improvement of all aspects of enterprise" [13]. Such an approach is consistent with the original meaning of the concept, which was promoted by Japanese scientists: "Kaizen means improvement. In addition, means continuous improvement in your personal life, your home, in social and work. In the enterprise kaizen is continuous improvement of all - managers and employees" [5, 6].

For the development of this philosophy the great importance have the extension of the concept of

TQM, which was originally part of kaizen improvement of Japanese quality management techniques, such as: zero defects, E. Deming cycle, quality circles, prevention system, just-in-time. This approach meant that you can do all better than before, that small steps can achieve the desired results. Perfecting everything, and the advancement should be done every day, by everyone, from small incremental improvements to major strategic changes [10, 12, 15]. Kaizen in its assumption should encourage employees to improve workplace, contribute to greater self-reliance and self-control. The basic objectives of kaizen is to improve the three parameters: quality, costs and delivery time. This means improving the quality of products and services, processes, striving to reduce costs at every stage of the business organization and shortening delivery times.

Table 1. Characteristics of kaizen and innovation [6]

Criteria	Kaizen	Innovation
Effect	The long-term effect, but not breakthrough	Short-term, breakthrough
Steps	Small steps	Big steps
Time frame	Continuous operation of gradually increasing effects	Action incidental effect of a sudden
Change	The gradual and continuous	Sudden and disposable
Involvement	Everybody	Selected leaders
Approach	Team effort, a systematic approach	Individual ideas and action
Method of work	Maintenance and improvement	"Fire fighting" and reconstruction
Ideas	Conventional know-how and traditional technology	The use of technological breakthroughs, new theories
Practical requirements	Requires a small investment, but a huge effort to maintain	Requires large investments, but little effort to maintain
Orientation	On the people	On technology
Criteria	Processes and commitment to achieving better results	Results directly affecting the profits
Utilization	Works well in a stable growing economy	Works better in a rapidly growing economy

In the world of business innovations are regarded as one of the key factors of the development of each enterprise [3, 19]. In the literature, innovation generally is interpreted as: "the first use of certain ideas or inventions with adequate economic criteria in order to profit" [1]. Some authors refer innovation to all areas of enterprise's activities whilst others have in mind something new that works on the market [1, 4]. Thus, innovation is a significant improvement on the existing situation especially in the field of technology and management (this applies to: tools, techniques and processes). All these activities are expected to bring the enterprise changes in the form of improvements, which in turn are translated into concrete benefits [18].General comparison of innovation and kaizen are presented in Table 1.

The classic approach to innovation differs from kaizen in many aspects: the pace and scope of change, working methods and the essential - in the philosophy of kaizen human factor plays a key role in the improvement. Kaizen is a kind of innovation, in which improvement "is a state of mind inherently connected to maintaining and improving standards" [5, 6]. Important elements of the concept of kaizen are: ensuring standardization and creating system maintain the level of change. In practice, defining standards means their continuous raising, only that way you can aim to improve the status quo, as a result of continuous kaizen activities. However, should be aware that the application of this philosophy does not exclude the introduction of radical improvements, they can be supported and fixed by using kaizen. Such actions affect both the measurable economic effects, as well as the behavior of employees, their knowledge, skills and attitude of openness and commitment. Therefore, an additional value of the implementation of kaizen is increasing awareness of workers for further improvement of the organization [7, 8]. In this context, the combining of kaizen and innovation can be very rational, as: "kaizen is understood as maintaining and improving standards by means of small, incremental steps, and innovation is regarded as a radical change related to major investments in technology and/or equipment" [6].

The result of kaizen activities is usually new organizational culture, focused on process improvements, resulting primarily with a positive message among employees. They should take the initiative in submitting new ideas. Acquiring even the slightest improvement suggestions from employees becomes essential. The new approach requires the development of a motivation system that takes into account the training and evaluation of employees, the verification of improvements, the definition of rules for employee teams responsible for each task. New motivation system must be adequate to the changes associated with the implementation of kaizen. It becomes essential to evaluate employees not only because of the results obtained, but you should appreciate their attitude and effort they put in to achieve results. Regardless of the stage of implementation of kaizen the main aim should be to ensure for employees the share in the benefits of their better work and more efficiently, using appropriate incentives that encourage employees to become more involved in the process of permanent change. A major role is played by the motivation of the material through the proper and fair remuneration of workers and immaterial motivation, which in many cases may be even more effective. Immaterial instruments may

be to increase self-esteem and belonging, satisfaction with the work itself or participation in the success of the organization [4, 11]. The additional result of such activities in the area of management may be an increase of the knowledge and skills of employees, awareness of the requirement for improvement and problem solving using new techniques and methods. Those methods in consequence, not only allow for recognition and elimination of negative elements in the enterprise, but also develop the ability to learn from mistakes and creating favorable conditions for the implementation of innovations, exploring new opportunities. Appropriate use of these capabilities give the enterprise "the ability to dynamically integrate, build and reconfigure internal and external competencies to be able to adapt to a rapidly changing surrounding" [20]. Regardless of the state of preparation of participants and the conditions which induce the enterprise to make changes, kaizen is generally considered to be very cost effective and efficient.

EMPIRICAL APPROACH - THE RESULTS OF RESEARCH ON THE STATE OF READINESS OF EMPLOYEES FOR THE IMPLEMENTATION OF KAIZEN IN POLISH MANUFACTURING ENTERPRISE

In this part of the article are presented the results of research on the assessment of the attitudes of employees in the Polish enterprise, which is in the process of implementation of organizational changes. The key element is to implement kaizen program in order to minimize manufacturing costs while improving productivity. The study was conducted in 2014 in the Polish manufacturing plant operating in the metal industry in Lower Silesia. The study used a questionnaire, the fulfillment of which was supervised by a competent person dealing with the issues of implementation of kaizen. The questionnaires were addressed to the production employees working on the assembly line. The enterprise selected for testing has undergone restructuring in recent years and has some experience in implementing modern management methods and tools. Changes to improve the functioning of the enterprise concerned are currently applying to Lean Management with improvement based on the philosophy of kaizen. As part of the recovery program general principles of kaizen are used, and one of the recently implemented measures is employee suggestion system named as "I have an idea." The aim of the study was to analyze the level of awareness and involvement of employees in the implementation of "I have an idea" kaizen program. Survey was anonymous and conducted on a group of 22 people (2 women and 20 men) working at various positions in the enterprise, they were: electricians, locksmiths, logisticians, warehouse, fitters, machine operators, and one quality controller. Characteristics of the study group are presented in Table 2.

Table 2. Characteristics of the study group

Age	No. of people	Seniority in the enterprise	No. of people	Education	No. of people
20-29	2	1-9	14	Vocational	6
30-39	12	10-19	4	Secondary	13
40-49	4	20-29	0	Higher	3
50+	4	30+	4		

RESULTS AND DISCUSSION

The study was conducted in 2014 in the Polish manufacturing enterprise. The results represent the opinion of employees on kaizen program implemented at the plant. In the opinion of the workers for the main objectives of the kaizen program were considered elements such as (Fig. 1):

- Improving performance.
- Improvement of the quality.
- Improvement of working conditions.
- Creation of a structured management system.
- Reducing costs.
- Improving employee motivation.

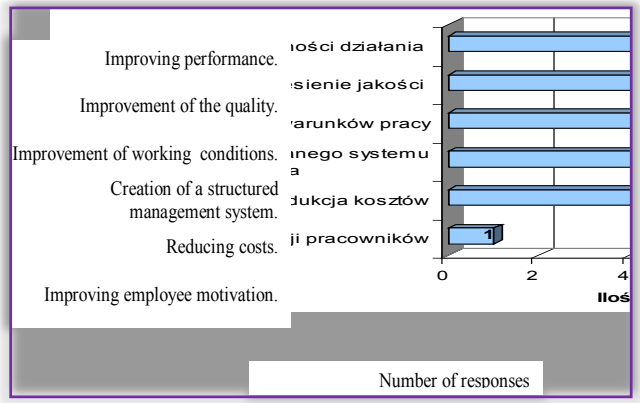

Figure 1 - The objectives of the program's implementation in the opinion of kaizen plant employees

Improving performance of the plant is the main goal resulting from the need to implement a new philosophy; it is a characteristic to the most of Polish companies. However, not all employees are properly motivated to implement process of kaizen activities. Generally, all employees are aware of the presence of organizational changes; however, only 8 respondents (36%) believe that the "I have an idea" program has significant impact on the functioning of the enterprise. Only 13 workers (60%) know the applicable rules and regulations of "I have an idea" program.

Most of workers report its improvements at least once a year, which are ideas involving not only the work they perform, but the overall operation of the enterprise. The structure of the responses is shown in Table 3.

Table 3. Number of reported improvements during the year by the employees of the plant

Number of reported improvements in the year	None	1	2-5	6-10	More than 10
In the operation of the plant	3	15	3	0	1
In terms of work	7	9	5	0	1

Workers report their improvements because they have the opportunity to win a prize or they expect to facility in their work. Unfortunately, most employees thinks that the reward system does not meet their expectations (55% of negative responses), and waiting for a response to proposed improvements is too long, in 70% of cases it ranges from 1 to 3 months. About the implementation of the proposed improvements workers are usually informed from their supervisor or at a meeting of the staff.

In the opinion of workers implementation of the kaizen program should be transferred into specific benefits. A list and order of priority of the benefits to be achieved following the introduction of kaizen as indicated by the workers is presented in Tab. 4.

The structure of Table 4 shows that in the opinion of workers the most important benefits of the implemented program were: better organization of work, improving quality, reducing losses and wastage, saving the enterprise's financial resources; as the second in the order important benefits were indicated: the involvement of the entire staff in problem solving, improving and maintaining new standards of work, the opportunity to ask questions about new ways to solve problems.

Table 4. The validity of the various benefits of kaizen program implemented by the number of employees indicated.

Advantage:	Very important	Important	Not important
Reduce losses and waste	11	11	0
Better organization of work	12	8	2
The involvement of the whole staff in troubleshooting	3	18	1
Changing the awareness of employees	6	12	4
Opportunity to ask questions	1	18	3
Better communication among workers	7	13	2
Improvingof the quality	12	10	0
Improvement and maintenance of the new labor standards	4	18	0
Saving the enterprise's financial resources	10	10	2
Shorter lead-times	9	13	0

The survey also asked to identify the barriers that exist in the implementation of kaizen program. The responses received in the form of a hierarchy of importance for individual barriers shows Table 5.

Table 5. The importance of different barriers that exist in the implementation of the program by the number of indications kaizen employees

Barrier:	Very important	Important	Less important	Not important	No opinion
Too high expectations of employees	1	7	2	11	1
Strained relations between employees	1	7	0	10	2
Competition for ideas	1	2	2	15	2
Inadequate reward for ideas submitted	2	5	1	12	2
Mutual criticism of ideas	3	12	4	2	1
General reluctance of workers to change	4	15	1	0	2
Fear of difficulties and additional responsibilities	3	8	2	8	1
Bureaucracy	11	3	3	2	3
Lack of time on implementation	10	8	2	0	2
The high cost of new system requirements	2	9	3	4	4

The employees recognized bureaucracy and lack of time for implementation for very important barriers, for the second in order of importance were listed barriers of: the general reluctance of workers to change and concerns about the mutual criticism of ideas.

In order to reduce barriers, resistance and reluctance towards the implementation of the "I have an idea" employees detailed the activities that they believe could assist in the process of innovative change in the plant (the order is given by the number of responses), they are:

- Regular rewarding of employees for reporting ideas (64%).
- Systematic training for employees (33%).
- Support from the kaizen team advisors (1%).
- Support from top management (1%).
- Support from co-workers (1%).

The worst assessed by the employees area was training, half of surveyed workers do not understand the reason for change and do not have complete

information on the planned kaizen activities. Among the respondents there were only 7 employees trained (31%), although workers themselves recognize the systematic training of employees as a very important factor facilitating the implementation of the kaizen (was listed as the second most important factor to minimize resistance and a reluctance of employees).

It is worrying that in surveyed enterprise none of the respondents were involved in the work of the kaizen team. For the question: "Are you a member of the »I have an idea« kaizen team?" nobody gave affirmative answer. Unfortunately, in the enterprise direct production workers are not involved in team. This is a serious fault of the management. Numerous publications emphasize that teamwork and group problem solving have great importance for achieving positive results in the implementation of any organizational changes. Teams of employees increased ease in the implementation of innovation through the creating the opportunity to learn new solutions, the use of integrated knowledge or information exchange. Unfortunately, this has not been taken into account by the enterprise and created a real threat that in the long term kaizen would not fulfill its role.

The final evaluation of workers indicates that the "I have an idea" kaizen program has been assessed generally positive, the results are presented in Fig. 2.

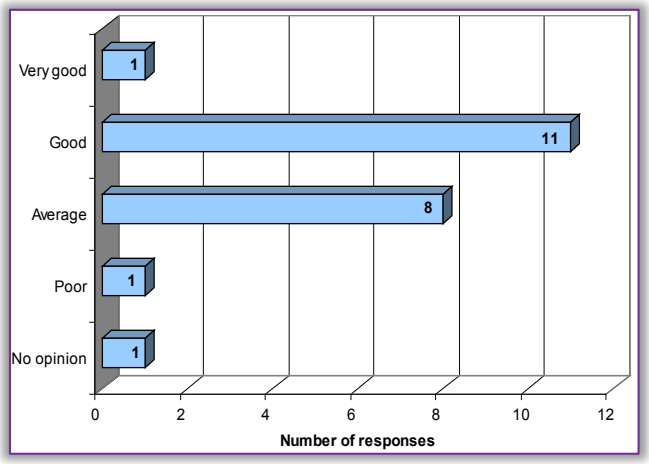

Figure 2 - Evaluation of the implementation of the kaizen program in the opinion of employees

The results, however, are not a complete success, in the study appeared a number of negative opinions, and this means that the enterprise's management has yet to work out a strategy of change. There are basic faults in the implementation of the kaizen philosophy and not all employees understand the essence of the new approach and are not prepared to create improvements for the needs of the surveyed enterprise.

CONCULSIONS

Based on the survey some basic irregularities and faults which may occur in the process of implementing the philosophy of kaizen in Polish enterprises can be pointed out. Among them the most common causes of failures include: lack of training, ignorance and wrong approach of employees, lack of commitment, lack of teamwork in delivering results, too high or too poorly defined expectations of management. Improvement actions require a fundamental change in the functioning of the entire enterprise, especially for training in order to improve the skills and knowledge among employees and for appropriate communication. Effective implementation should be combined with an indication of the best ideas (publicizing and rewarding), and measurable results will be the basis for further action here. The employees are specifically required to have a broad knowledge of the variety of tasks and functions in enterprise and were able at any time to meet the demands of the changing situation.

Generally, the faster the enterprise has reached a sufficient level of employee involvement in the process of continuous improvement, the more effectively employees would realize it. The philosophy of kaizen is an appropriate way to increase innovation of enterprises and achieve their long-term competitiveness.

References

[1.] Baruk, J. (2006). Zarządzanie wiedzą i innowacjami, Adam Marszałek Publishing. Toruń, p. 94

[2.] Bernais, J., Ingram J., Kraśnicka T. (2010). ABC współczesnych koncepcji i metod zarządzania, Akademia Ekon. im. K. Adamieckiego Publishing. Katowice, p. 164

[3.] Chodyński A. (2002). Zarządzanie rozwojem firmy jako realizacja strategii doskonalenia jakości organizacji. Przegląd Organizacji. No. 2.

[4.] Cholewicka–Goździk K. (2001). Metoda LEAN – doskonalenie procesów i produktów. Problemy Jakości, No.1.

[5.] Imai M. (2006). Gemba kaizen. MTBiznes Sp. z o. o. Publishing. Warsaw, p. 36-37

[6.] Imai M. (2007). Kaizen. The Key to Japan's Competitive Success. MTBiznes Sp. z o.o. Publishing. Warsaw, p. 18-54

[7.] Farris J., Van Aken E., Doolen T., Worley J. (2009). Critical success factors for human resource in kaizen events: an empirical study. International Journal of Production Economics. Vol.117, No. 1, p. 46

[8.] Grudzewski W. M., Hejduk I. K. [ed.] (2000). Company of the Future. Difin Publishing, p. 141

[9.] Hamrol A. (2011). Quality Management. PWN Publishing. Warsaw.

[10.] Karaś E. (2013). Lean i kaizen jako metody doskonalenia procesów logistycznych przedsiębiorstwie. [in:] Kulińska E. [ed.]. Logistyka w zarysie – wybrane problemy badawcze. Politechnika Opolska Publishing. Opole, p. 89

[11.] Karaszewski R. (2006). Nowoczesne koncepcje zarządzania jakością. Dom Organizatora Publishing. Toruń, p. 226-228
[12.] Machaczka J. (1998). Zarządzanie rozwojem organizacji. Czynniki, modele, strategia, diagnoza. PWN Publishing. Warsaw, p. 27
[13.] Mikuła B., Pirtruszka-Ortyl A., Potocki A. [ed.] (2007). Podstawy zarządzania przedsiębiorstwami w gospodarce opartej na wiedzy. Difin Publishing. Warsaw, p. 217
[14.] Olszewski L. (2007). Kaizen Management System, Quality Management. No. 3.
[15.] Piasecka–Głuszak A. (2009). Kaizen – rozwój japońskiej ewolucyjnej metody zarządzania zmianą. [in:] Integracja Azji Wschodniej. Mit czy rzeczywistość?. Publishing House of Wrocław University of Economics. Reasearch Papers, 67. Wrocław, p. 372
[16.] Piasecka–Głuszak A. (2011). The main problems in the implementation of Japanese kaizen/lean tools in companies in the Polish market in accordance with the kaizen Management System – the analysis of research. [in]: Faces of Competitiveness in Asia Pacific. Skulska B., Jankowiak A.H. [ed.], Publishing House of Wrocław University of Economics. Reasearch Papers 191. Wrocław, p. 196
[17.] Pieczonka A., Tabor A. (2003). Vademecum jakości, Cent. Szkolenia i Organizacji Systemów Jakości Politechniki Krakowskiej im. T. Kościuszki Publishing. Cracov, p. 86
[18.] Szewczyk M., Łobos K. (2012). Wybrane aspekty aktywności innowacyjnej podmiotów z branży chemicznej w województwie opolskim w świetle wyników badań pilotażowych. [in:] KNOW HOW – efektywna komunikacja w regionalnym transferze wiedzy. Diagnoza i wprowadzenie do badań. Malik K., Dymek L. [ed.]. Instytut Trwałego Rozwoju Publishing. Opole, p. 53-71
[19.] Szewczyk M., Widera K. (2011). Innowacyjność przedsiębiorstw warunkiem rozwoju. Ekonomika i Organizacja Przedsiębiorstwa, 12 (743), p. 41-48.
[20.] Szuster M. (2011). Kaizen in Manufacturing Companies, [in:] The Culture of Kaizen, Wróbel G. [ed.]. WSIiZ Publishing. Rzeszów, p. 183

ACTA Technica CORVINIENSIS
BULLETIN OF ENGINEERING

ISSN:2067-3809

ACTA TECHNICA CORVINIENSIS
– Bulletin of Engineering
Tome IX [2016], Fascicule 4 [October – December]
ISSN: 2067 – 3809

[1.]Gheorghe NEGRU

RESEARCH ON NUMERICAL SIMULATION APLICABLE TO THE PRESSURE RELIEF VALVE ON THE BORE GAS EVACUATION DEVICE

[1.] Military Equipment and Technologies Research Agency, Bucharest, ROMANIA

Abstract: The paper presents the research approach on the numerical simulation applicable to pressure relief valve on the bore gas evacuation device embedded on the high pressure barrels with special destinations. The numerical simulations were conducted in order to asses the behavior of the components elements of the pressure relief valve belonging to bore gas evacuation device. Consequently the present research could contribute at the problem of solving of an increased number of requirements with reduced resources in terms of functioning assessment of high pressure barrels with special destinations.
Keywords: High pressure barrels, bore gas evacuation and pressure relief valve

INTRODUCTION

The bore gas evacuation device enables the evacuation of the gas from the high pressure barrel channel in the bore gas reservoir. After a short period of time the gas stocked in the reservoir will be ejected in the atmosphere in the direction of the muzzle barrel. [6]

Consequently the quantity of the burned gas from the interior of the special destination vehicles will be decreased.

The interior of the bore gas evacuation communicate with the high pressure barrel channel through different dedicated holes drilled in the barrel. [7].

A salient factor in the bore gas evacuation device functioning is represented by the pressure relief valve. The pressure relief valve controls the gas admission from the barrel channel within the bore gas reservoir.

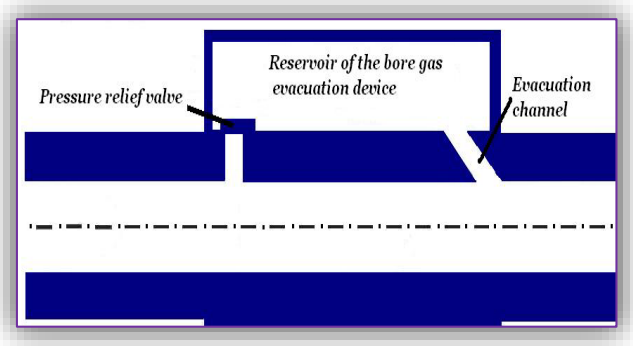

Figure 1. A schematic view of an bore gas evacuation device

EXPERIMENTAL AND NUMERICAL MODEL

The functioning of the bore gas evacuator depends on the proper functioning of the pressure relief valve. The pressure relief valve could have different technical constructive solutions.

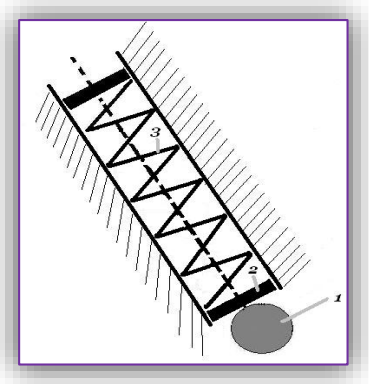

Figure 2. A schematic view of the pressure relief valve

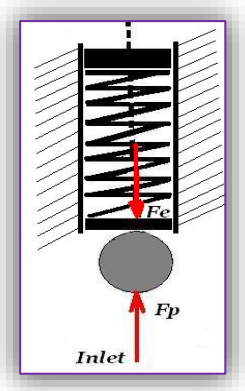

Figure 3. A schematic view of the pressure relief valve dynamic

For the current research the main components of the pressure relief valve, taken into consideration, are presented in Figure 2. Thus was taken into consideration a pressure relief valve which consists in 1-ball, 2-plunger rod, 3-elastic damping elements.

The equation of the motion of the pressure relief valve mobile mass according to the D'Alambert principle is:

$$F_p = F_e + m\ddot{y} + F_d + mg \quad (1)$$

The mobile mass of the pressure relief valve include the mass of the ball, plunger rod and of the elastic damping elements.

The force induced by the gas pressure at the admission of the gas inside the reservoir of the bore gas evacuation device is computed with

$$F_p = Ap(t) \quad (2)$$

where *A* represent the area of the admission gas hole and p(t) represent the variation of the pressure inside of the channel barrel. The variation of the pressure p(t) is computed according to the provisions of the dedicated technical literature books. [3]

The force which is opposed at the movement depends on the velocity the plunger rod and is computed with

$$F_p = k_d \dot{y} \quad (3)$$

The critical damping coefficient [4] is computed with

$$k_{dc} = \sqrt{4mk_e} \quad (4)$$

The damping ratio [4] is computed with

$$\delta = \frac{k_d}{k_{dc}} \quad (5)$$

The restoring force of the elastic damping elements is computed with

$$F_p = k_e y \quad (6)$$

In order to asses the functioning of the pressure relif valve of the bore gas evacuation device was computed a dynamic simulation within the SYMULINK dedicated software.

CASE STUDY

Input data

The integration scheme of the functioning ecuation of the pressure relief valve according to the SYMULINK notations is presented in Figure 4.

The simulation of the functioning of the pressure relief valve was conducted with the inlet force depicted in Figure 5. The signal of the inlet force is applied for a extermely short period of time up to 0.1 seconds. In this manner is emphasised the particular behavior of the gazodinamic phenomenon in the admission area of the gas within the bore gas evacuation device. Input data are: inlet force, mass of the ball, plunger rod and of the elastic damping elements, elastic coefficient k_e.

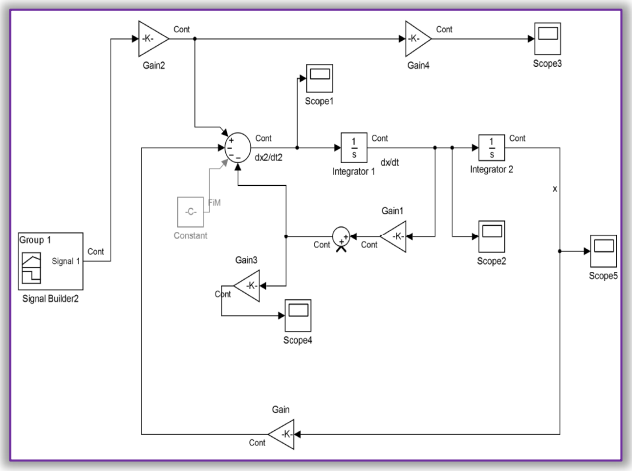

Figure 4. SYMULINK diagram

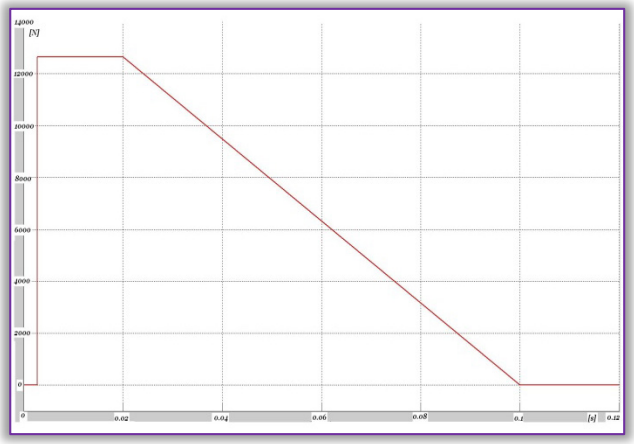

Figure 5. The force applied on the ball of the bore gas evacuation device

Output data

Based on the input data was computed the critical damping coefficient k_{dc} and where plotted the diagrams of movement, velocity and acceleration of the ball-plunger rod assembly. (Figure 6, Figure 7 and Figure 8)

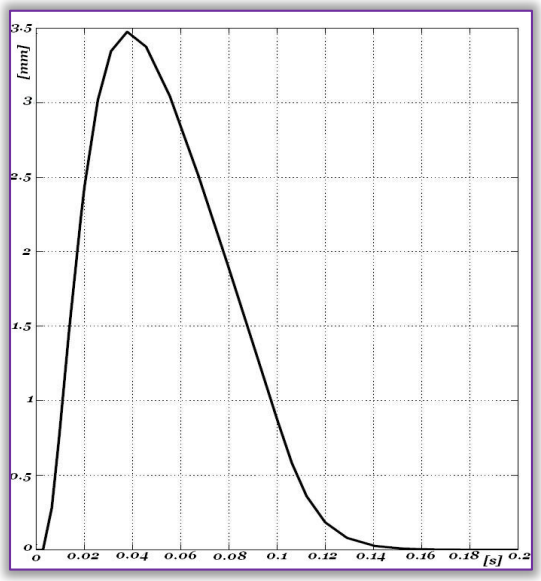

Figure 6. Ball-Plunger rod movement

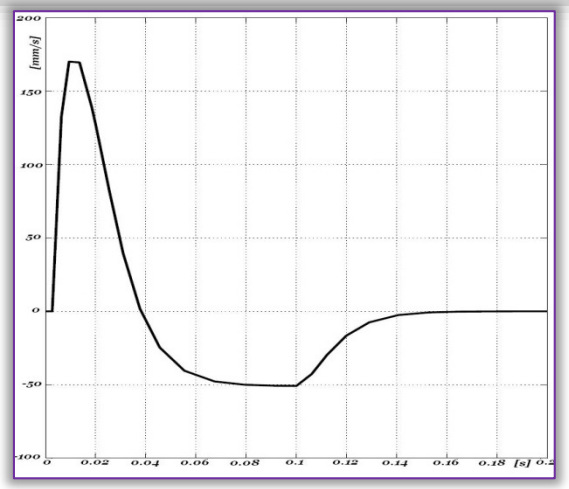

Figure 7. Ball-Plunger rod-velocity

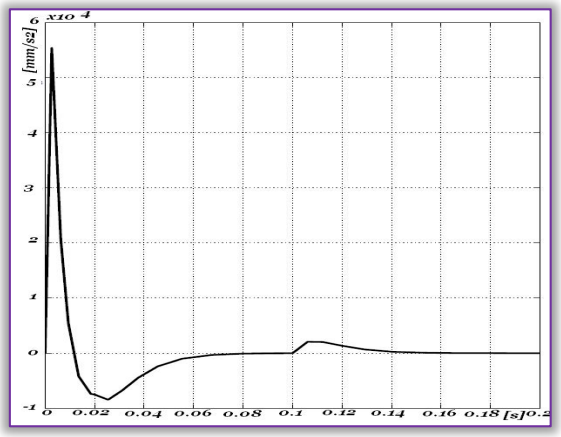

Figure 8. Ball-Plunger rod acceleration

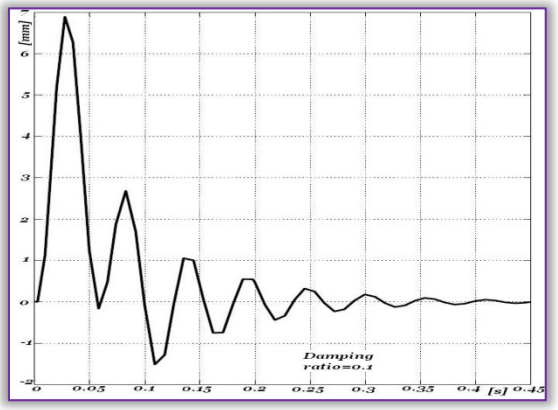

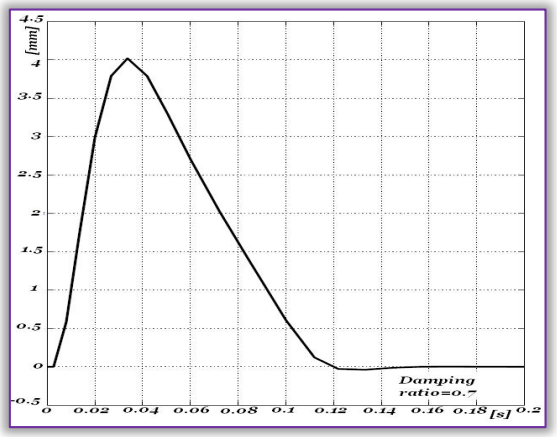

Figure 9. Ball-Plunger rod movement

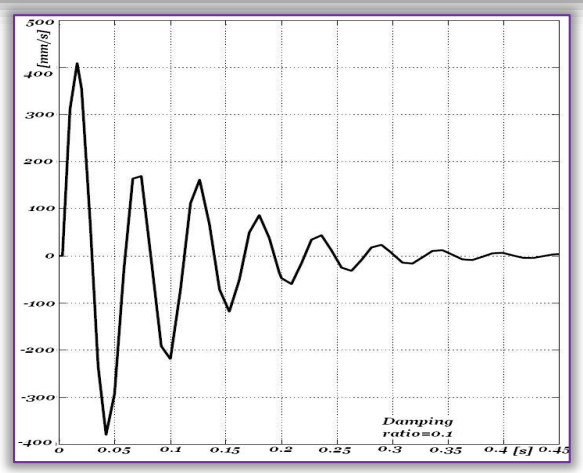

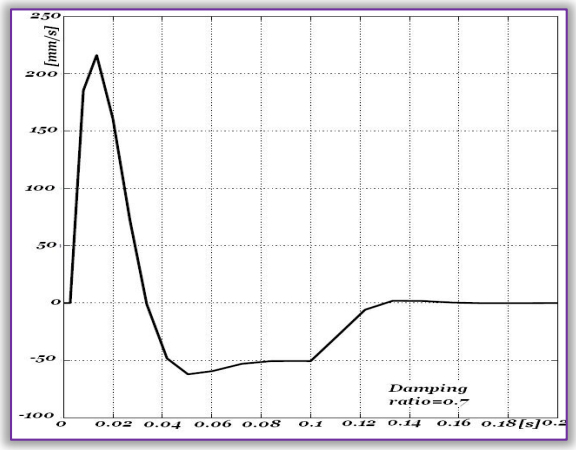

Figure 10. Ball-Plunger rod-velocity

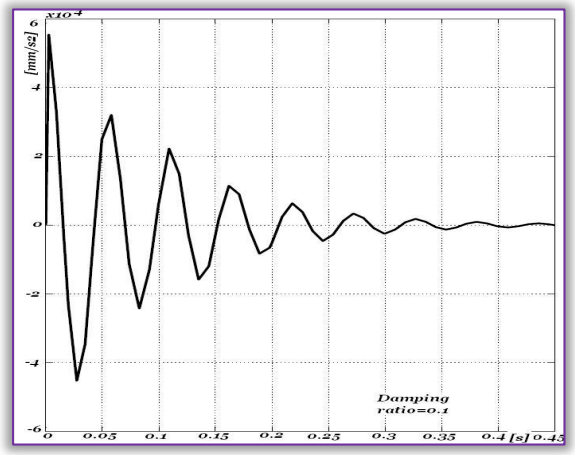

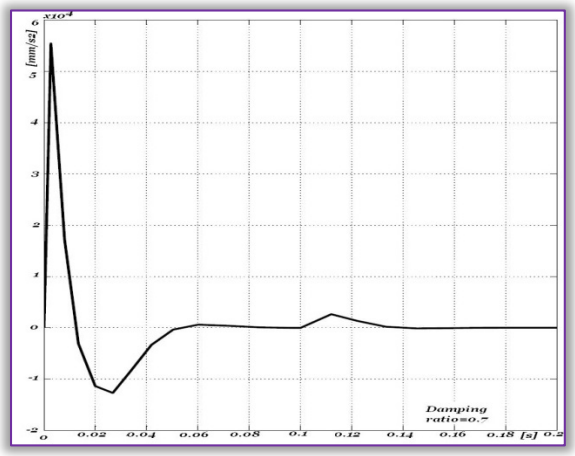

Figure 11. Ball-Plunger rod acceleration

To assess the behavior of the ball-plunger rod assembly where conducted numerical simulations in the variants with damping ratio values 0.1 and 0.7. For the before mentioned values of the damping ratio where computed the corresponding values of the actual damping coefficient. With these values as input data for the SYMULINK calculus where plotted the diagrams of the movement, velocity and acceleration (Figure 9, Figure 10, Figure 11).

The obtained diagrams present the possible options for the functioning of the components elements of the pressure relief valve. Thus in principle could be defined the followings approaches:

» mechanical elements with damped movement in a period of time up to 0.45 seconds
» mechanical elements with fast damped movement in a period of time up to 0.14 seconds
» In the context of the high pressure barrels with special destination the numerical dynamic simulation has a couple of advantages:
» the costs to identify a proper technical solution for the pressure relief valve are decreased. In this context is to emphasize that a real test for a bore gas evacuation device is expensive.
» the behavior of the components elements of the pressure relief valve is assessed also in the case with a high value of the friction coefficient. This is equivalent with the dissipation of enhanced quantity of heat due the functioning of the pressure relief valve. At this phenomenon is added also the heat induced by the intense thermodynamic regime within the inlet zone of the bore evacuation device.
» assessment of the behavior of the components of the pressure relief valve enable the establishment of their optimal technical solution.
» the value of the ball-plunger rod movement enable the design of the pressure relief valve in term of its size.

CONCLUSIONS

The proposed model can contribute at the assessment of the functioning behavior of the bore gas evacuation device embedded on the high pressure barrels.

The results of the numerical simulation emphasizes the achievements of the presented method as follows:

» the depiction, through the mechanical theory equations, of the behavior of the pressure relief valve belonging to the bore gas evacuation device is a genuine approach in the field of the high pressure barrels with special destination;
» the method enable to be established a data base in terms of assessment of the dynamic behavior of the elements components belonging to the bore gas evacuation device;
» the method contribute to a proper design of the bore gas evacuation device through parameters like movement, velocity or acceleration of the ball-plunger rod assembly;
» the future research work can be focused on a thorough evaluation of the thermal effect on the reliability and dynamic behavior of the pressure relief valve.

References

[1.] Control valve handbook, Fourth Edition, Fisher Controls International LLC, 2005
[2.] Crosby Pressure Relief Valve Engineering Handbook, Technical Document No. TP-V300 Effective: May 1997
[3.] Petrisor E, Titica V, Interior ballistic, Military Publishing House, Bucuresti, 1975
[4.] Graham s. K, PhD, Schaum's outline of Theory and problems of Mechanical vibrations, McGraw Hill, ISBN 0-07-034041-2, 1996
[5.] Xue G. S., Ji H. J., Hyeong S. L., Dong K.K., Young C. P., 2 D Dynamic analysis of a pressure relief valve by CFD, Proceedings of the 9th WSEAS International Conference on Applied Computer and Applied Computational Science
[6.] SMT 40035/1991, Specialised standard
[7.] Carlucci D.E, Jacobson S., Ballistics: Theory and Design of Guns and Ammunition, Second Edition, CRC Press, August 26, 2013
[8.] Stefanski F., Nowak A., Minorowicz B., Pneumatic single flapper nozzle valve driven by piezoelectric tube, Poznan University of Technology, Division of mechatronics devices, 2015
[9.] Adadande A.S, Naniwadekar A.M, Patil R.B, Reliability Analysis of Pressure Relief Valve Manufacturing System, International Journal of Emerging Engineering Research and Technology Volume. 2, Issue 2, PP 64-70, May 2014
[10.] Saha B.K, Numerical Simulation of a Pressure Regulated Valve to Find Out the Characteristics of Passive Control Circuit, International Journal of Mechanical, Aerospace, Industrial, Mechatronic and Manufacturing Engineering Vol:7, No:5, 2013

ACTA Technica CORVINIENSIS
BULLETIN OF ENGINEERING
ISSN:2067-3809

ACTA TECHNICA CORVINIENSIS
– Bulletin of Engineering
Tome IX [2016], Fascicule 4 [October – December]
ISSN: 2067 – 3809

[1.]Marius LOLEA, [2.]Simona DZIŢAC

ABOUT THE URBAN ELECTROMAGNETIC POLLUTION

[1-2.]Department of Energy Engineering, University of Oradea, ROMANIA

Abstract: This paper presents a brief statement of electromagnetic pollution generated by public sources of electromagnetic field, wich are distributed on the territory of City of Oradea, Bihor County, Romania. The Beginning of the paperwork is related to define and a general description of electromagnetic pollution. Followed by the description of the characteristics of public sources of electromagnetic field and finally the values of the electric field and magnetic induction in the vicinity of sources. These values were obtained by direct measurements made by the authors. With their help authors mapped and statistical analysis to prioritize city neighborhoods depending on the density of electromagnetic field sources and amplitude values for the electric and magnetic field.
Keywords: electromagnetic pollution, electric field strength, magnetic field density, electromagnetic map, electromagnetic field effects

INTRODUCTION

At present, due to the development of devices that operate on electricity, ambient electromagnetic field intensity has increased greatly. Thus appeared the concept of electromagnetic pollution. It occurs when the electric and magnetic fields through the characteristic parameters, become negative factors on technical and biological systems. These negative effects by impacts are called electromagnetic disturbances and ways of transmission from source to receiver are multiple [4],[5],[10]. Fears about the negative effects related to the use of electromagnetic devices have not ceased to occur in times [9], while the accusations relating to these issues occurring several decades [6], [8]. Among the most common electromagnetic devices are the mobile telephones. A further study on the internet, leads to the idea that the number of mobile telephones in use equates, to the population of the planet. Of course, there are countries where because poverty , their number is reduced but in developed countries almost everyone owns such a device. Although buying a mobile phone is optional, allowing the rapid transmission of information at distance it becomes a necessity.

A large spread have also the household electrical appliances that help facilitate the work of the house and increases the comfort in homes or at working places. Industrial and telecommunications equipment generates electromagnetic fields that cover the entire spectrum.

SOME OF THE ELECTROMAGNETIC FIELD EFFECTS ON THE HUMAN BODY

There is great interest from specialists on the effects of electromagnetic field exposure on the human body and its impact on different anthropogenic technical systems. Electromagnetic pollution, given by electromagnetic field parameters can be determined by calculation and simulation using digital techniques, or by measurement. The two-way results should be compared for appreciation the deviations between methods. The Multiple case studies available at worldwide, that shown the results of measurements on the electromagnetic field parameters for different sectors, can be compared as means for general guidance. [14]. Because of the specific of electromagnetic devices and also their physico-chemical characteristics degradation in time, electromagnetic compatibility tests that determine electromagnetic pollution, should be repeated periodically. As a general effects of electromagnetic field impact with the human body are cataloged thermal and non-thermal [8]. Depending on affections on the human body may be direct or indirect effects [16].

Among the direct effects is include [16]:

- vertigo and nausea caused by static magnetic fields;
- effects on the sensory organs, muscles and nerves caused by low frequency fields (up to 100 kHz) - shivering;
- heating the whole body or parts of it due to high frequency fields (10 MHz and above); above a

few GHz warming increasingly limited over the body surface;
» Effects on the nerves and muscles and heating as a result of exposure to intermediate frequencies (100 kHz-10 MHz).

That indirect effects are [16]:
» interference with medical electronic equipment and devices;
» interference with medical devices or active implanted devices such as pacemakers or defibrillators;
» interference with medical devices worn on the body, such as insulin pumps;
» interference with passive implants (artificial joints, rods, wires or metal plates);
» shrapnel effects, piercings, tattoos and body designs;
» design the risk of ferromagnetic objects in a static magnetic field
» unintentional ignition of detonators;
» fires or explosions caused by ignition of flammable or explosive materials;
» electric shocks or burns caused by contact currents.

Restrictions on exposure to electric fields, magnetic and electromagnetic variable over time which are based directly on established effects on human health and biological considerations are defined as basic restrictions [17]. Depending on the frequency of the field, the physical quantities used to describe these restrictions are the magnetic flux density (B), the current density (J), Specific Absorption Rate (SAR) and power density of electromagnetic waves (S) [17]. In [6]-[9] mentioned some possible long-term effects of exposure. Among these include visual disturbances, heart rhythm and blood pressure disturbances, various cancers, Alzheimer's disease, impaired humanitarian system, infertility, changing calcium metabolism in the brain, diminishing skin resistance, reduced cerebral blood flow, etc.Some people are more affected by the momentarily presence of electromagnetic field generating devices, effects which are generic called Electrosensitivity [6]. Even these, effects are uncertain or not, because of the precautionary principle, measures must be taken to protect against them. Regularly informing the population on those possible effects beyond the scope of the various relevant international fora, including the European Commission. This issue directives in this regard, they have access to all EU citizens. [14][16].

The European Directive 35/2013, issued by the European Commission to electromagnetic fields do not address suggested long-term exposure whereas it is considered that there is no scientific evidence establishing a well established relationship clearly influence health, possibly the future if they appear clearer scientific evidence, to consider the most appropriate methods to protect humans by such effects [16].For evaluating the interest of specialists in the effects of high frequency electromagnetic fields and their impact on biological environment, investigations may be carried within the international scientific databases, that manage articles of interest to this paper. The results of personal research, statistically processed using IEEE Xplore Database - Digital Library are shown in Figure 1.

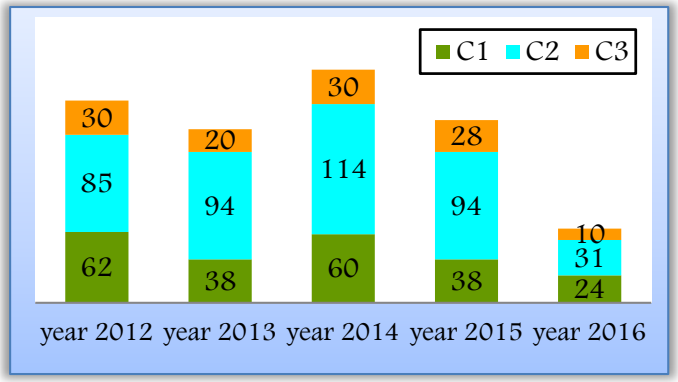

Figure 1. The statistic processing of the number of items identified on the criteria C1-C3
Explanation: C1- electromagnetic field of mobile phones, C2 - electromagnetic field of base station, C3 - electromagnetic field effects on human body

Figure 1 shows a breakdown by years of appearance of articles in the database accessed for three search criteria chosen by the authors, for the period of 2012-2016. The search criteria were formed by the juxtaposition of words that highlights the effects of electromagnetic field exposure (figure 1).

Thus, the results at the criterion by search called „Electromagnetic pollution" were generated 1056 results; at the criterion „Biological effects of electromagnetic fields" were generated 2082 results and for the criterion „Electromagnetic field of mobile telephones", the search results were 460 in number. At the time of the search in this database had recorded a total of 3,997,943 references. For the period under review, the first criterion C1, have generated a total of 222 titles. For criterion C2, they were generated a total of 418 titles. Criterion C3, 118 results are recorded for the same period.

Analyzing public opinion polling tools like the Eurobarometers, initiated by the European Commission, it can be deduced for example, what are the opinions of european citizens related to the various hazards that affect their lives. The Eurobarometer no. 347/2010, contain the answers and their statistical analyzes on health damage due to exposure to electromagnetic field of various electrical and electronic equipment [15].

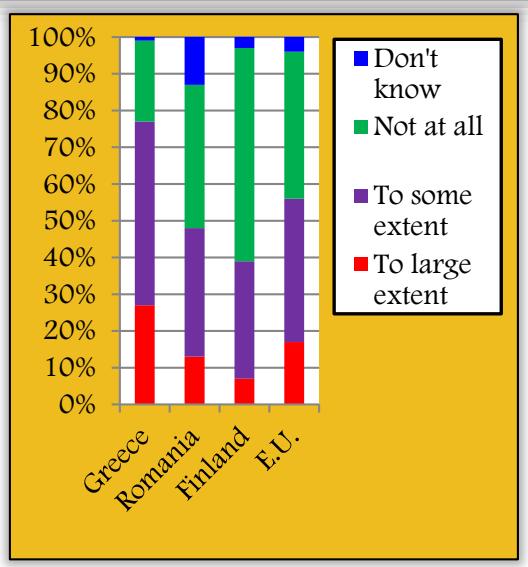

Figure 2. Types of sources: household electrical equipment (adapted by[15])

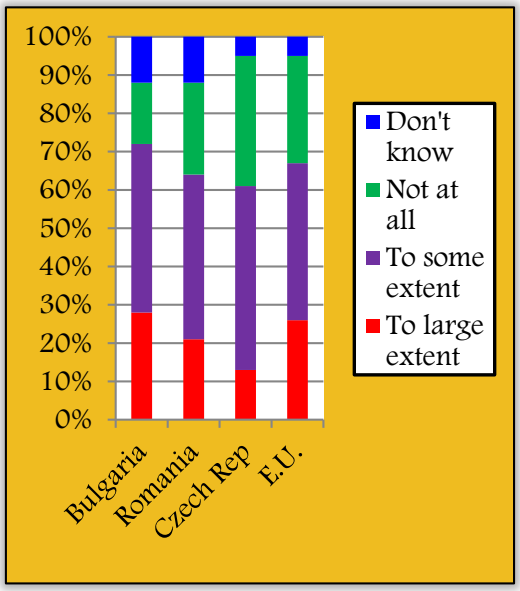

Figure 3. Types of sources: mobile telephones (adapted by[15])

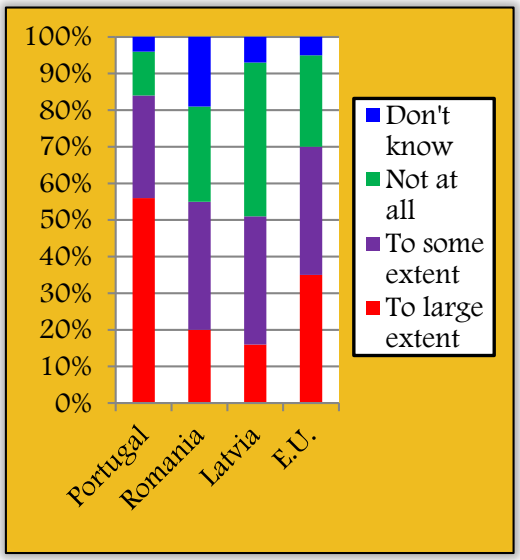

Figure 4. Types of sources: hight voltages power lines (adapted by[15])

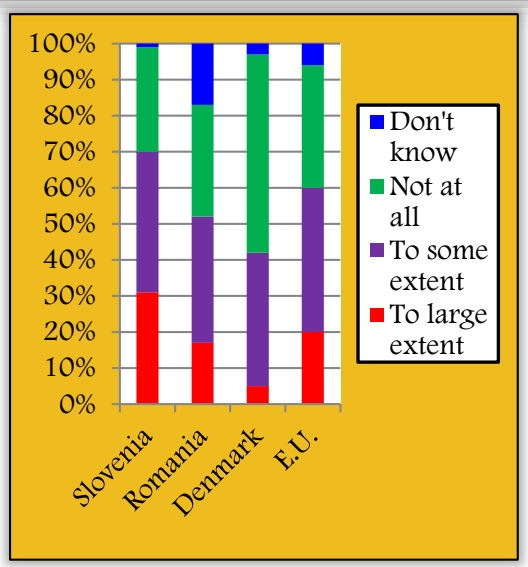

Figure 5. Types of sources: computers (adapted by[15])

Even if there is not a global consensus against risks caused by electromagnetic field exposure, the European population has some worries about the health effects generated by the operation of electrical devices, as can be seen from the responses investigations presented in [15]. By source of electromagnetic field, the answers of europeans citisens are presented in four situations in Figures 2-5.

Analyzing the same sources [15], it appears that fears highest against the negative influence of power lines high tensiunese recorded in Italy (78%), as exposure to the electromagnetic field of mobile phones (69%), personal computers (60%) and household appliances (53%). Lowest fears at european level were recorded by the answers given by dutch citizens who accounted for 13% to the influence of high voltage power lines, 7% to 5% of mobile phones and computers connected influence. Danish citizens stated at a rate of just 3% that appliances have large negative influences on health.

PUBLIC SOURCES OF ELECTROMAGNETIC FIELD

A public source of electromagnetic field is that installation or device accessible to anyone and is located on the public domain or direct border with the public area. Thus,the humans or any other type of receiver will be affected by electromagnetic radiation emitted outside the domain of location of the source. A private or occupational of electromagnetic field source is accessible to only one person, a group or a family property which is or included in the area of property and in a particular workspace where access of unauthorized persons it is prohibited or restricted. Within public sources are included in the context of the work the following: telecommunication installations with mobile base stations (BS) transceivers antennas, and additional electrical installations, recovery stations (RS) for urban electric traction and contact

wires with injection points, electrical distribution stations(power substation - PS) and transformer substations (TS) and high-voltage (HV) overhead power lines (PL). Since this paperwork refers to electromagnetic pollution will interest only urban sources which are located in the city.

To assess the electromagnetic pollution produced by these public domain have the following steps: identifying the sources of electromagnetic field and analyze their technical characteristics, design schemes extent and choice of the measuring points, setting measurement equipment and determining how to use in land, assessment practical quantities that characterize electric and magnetic field, noting obtained data, statistical data processing, statistical analysis, comparing the values obtained with the permitted limit of normative and determining the level of electromagnetic pollution. The Sizes of electromagnetic field of low frequency networks easily measurable are the electric field strenght E[V/m] and magnetic induction B[μT].

ELECTROMAGNETIC POLLUTION SITUATION IN CITY OF ORADEA. METHODOLOGY AND RESULTS

The current paragraph is meant to answer the question, what are the benefits of a study on the level of electromagnetic pollution of a city. There are many preoccupations about electromagnetic pollution assessment urban and natural environment in general. [1]-[3][11]-[13].

Usually, empirical research based on measurements of electromagnetic field around public sources and comparing the values obtained with those considered dangerous to humans, utilities and electronic or digital devices. In case of human exposure on long term, the limits for sizes of electromagnetic field for the general population provided the normative[17], are: electric field strength E_{lim} = 5000 V/m, magnetic induction B_{lim} = 100 μT, S.A.R. = 2 W/kg, power density at high frequency of electromagnetic waves, S = 1 mW/m^2.

Following similar directions but with personal contributions, in the current paragraph we present the results of investigations to identify public sources of electromagnetic field and electromagnetic pollution levels generated by them in the territory of city of Oradea, from Bihor County, Romania. The original elements consists of designing measure schemes, statistical processing of data, applications created and case studies initiated and presented.

On the date conduct of the study, the type and number of public sources of electromagnetic field located in the city of Oradea, was: 8 power substations (PS1 Oradea center, PS2 Oradea east PS3 Mecanica, PS4 Sinteza, PS5 CET II, PS6 ERA park, SE7 Industrial park Eurobussines Borsului, SE8 Crişuri), 744 transformer substations (TS), 43 GSM sites comprising base stations (BS) and antennas, 5 recovery stations (RS), 13 high-voltage power lines (HVPL) single and double circuit on the 110 kV level, 19.21 km tram lines with 14 injection points. In figures 6 and 7 is presented two types of this installations.

Measurements were made at the height of 1 m and 1, 7 m from the ground (the average height of people in Romania is 1.61 m for women and 1.74 m for men) at the level of two sensitive body areas corresponding to head and the confluence to under abdominal and above inguinal areas

Figure 6. P.S. Oradea Center

Figure 7. GSM Antennas on living block in civic center

For P.S. and T.S. as well as the RS for urban electric traction urban, the measure routes correspond of sides where the public has access. The model of the measure routes for P.S. Sinteza situated in the neighborhood Ioşia, is shown în Figure 8.

For telecommunications antennas and BS, measurements were performed at the door of access to the site and in living places or similar from immediate vicinity thereof. For tramlines, the measurements were carried out at a height of 1 m above the ground in the middle of the track rails, at the level of the injection point. The following model is shown in Figure 9.

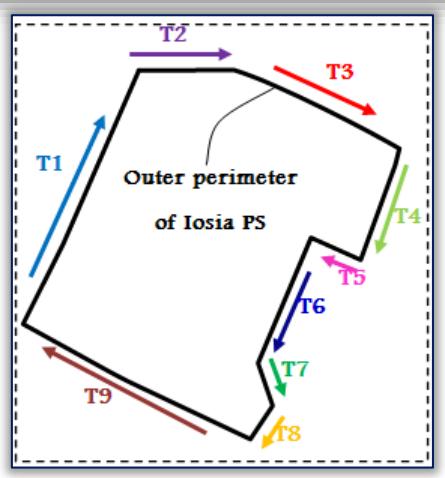

Figure 8. Measurement scheme for a P.S.

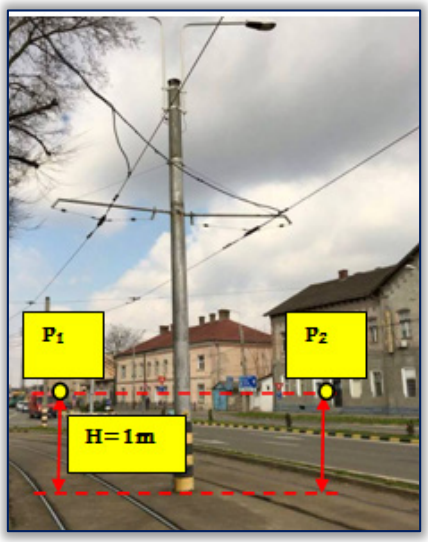

Figure 9. Measuring points for tramways

In case of PL, the routes extent correspond to the longitudinal axis thereof. For measuring routes from the PS, RS and PL, measuring step(distance between two consecutive points) as noted Δp is equal to 3 m. In case of TS, measuring step is Δp = 0,5 m(at the same height from the ground as in the case of PS). At injection points for electric traction and BS or transceiver antennas, was considered just a point in central position where values were identified maximum values of electromagnetic field quantities. Measure distance to hedge or the external wall of installations analyzed, is d = 1 m. Measuring devices used were: for the magnetic field of low frequency electric and magnetic - CA 42 Meter; the electric field and magnetic high frequency – the device SPECTRAN 5035 and for the height of the suspending wires or their gauge their, the device SupaRule 600 E. Images of the measuring devices used is shown in the Figure 10.

In addition, for measurement were also used the electromagnetic field meter Tenmars TM-196 for high frequency, triaxial isotropic type, to evaluate the electromagnetic field in the vicinity of mobile telecommunications installations and laser rangefinder Bosch PLR 50 for measuring distances from the source in the horizontal direction or obliquely.

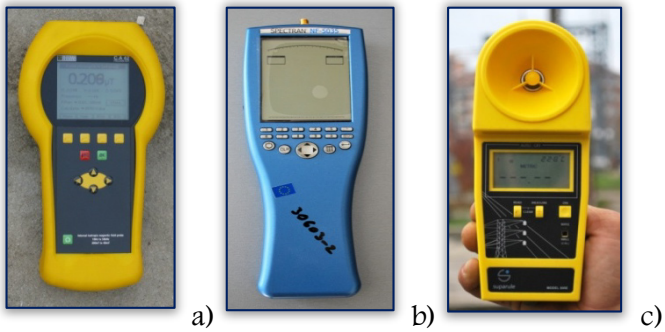

a) b) c)

Figure 10. Measuring devices used: a- CA42; SPECTRAN 5035; c- SupaRule 600 E

With the results of investigating the sources and values of the measurements revealed the following applications: the map of territorial distribution on neighborhoods and streets of the sources of electromagnetic field, the map of the most polluted neighborhoods depending on the value of electric field strength, the map of electromagnetic pollution of neighborhoods depending on the value of magnetic induction and pollution map on the neighborhoods depending by the power density of high frequency electromagnetic waves generated by telecommunications systems. For example, the figure below shows the density map of public sources of electromagnetic field in the city of Oradea.

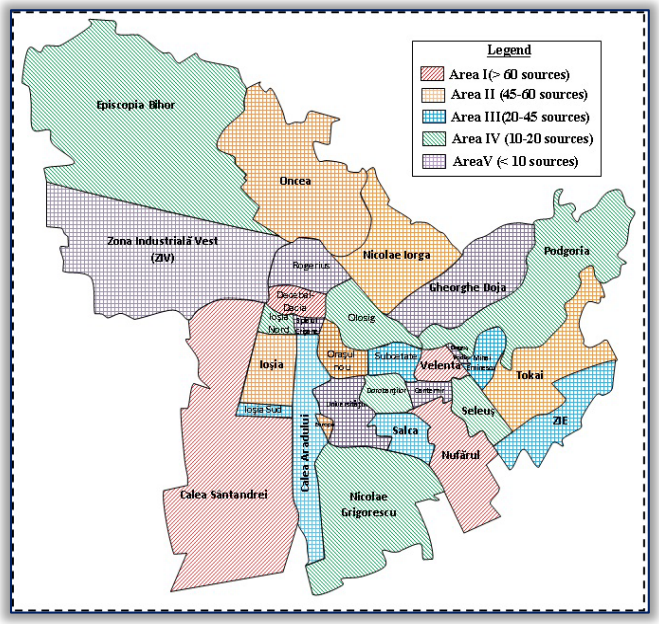

Figure 11. The density map of Electromagnetic field poublic sources on City of Oradea territory

The results of measurements fall into the following intervals:

» for RS, B = 0.016-0.082 μT and E = 60-120 V/m;
» for tram lines, B = 2.37-6.15 μT and E = 240-360 V/m;

» for BS and GSM antennas, B = 0.212-0.325 μT, E = 2.5-6.5 V/m and S = 0.256-0.885 mW/m².

Based on processing and statistical analysis of the values obtained by measurement was performed and a hierarchy on the neighborhoods according to criteria mentioned above. Thus, the figures 12 and 13 show two of statements obtained.

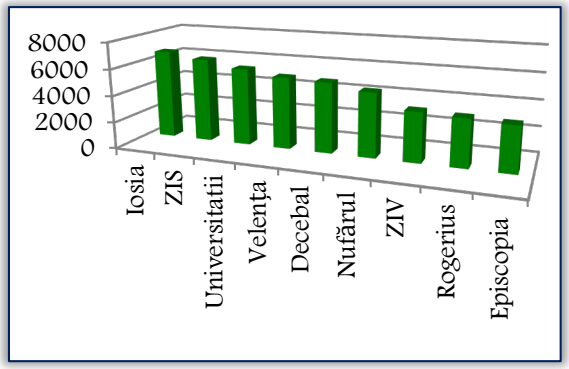

Figure 12. Hierarchy of neighborhoods by values of E [V/m]

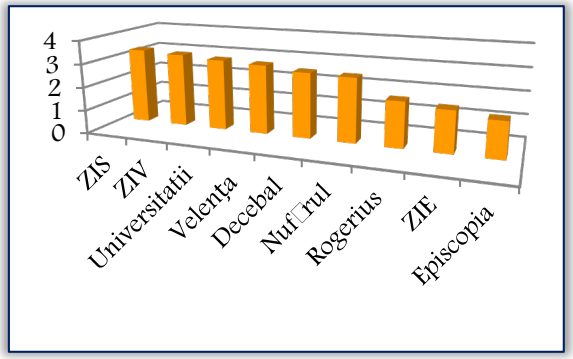

Figure 13. Hierarchy of neighborhoods by values of B[μT]

Also, with all the data, including the location on the streets of sources of electromagnetic field, their technical characteristics and the values of the field around them, was compiled a Database using Excel software from the Office suite.Figures 14 and 15, indicates the maximum and average values of the electric field intensity and magnetic induction, for common portions of the power lines crossing in the city. These lines have a nominal voltage of 110 kV and are the type of double circuit.

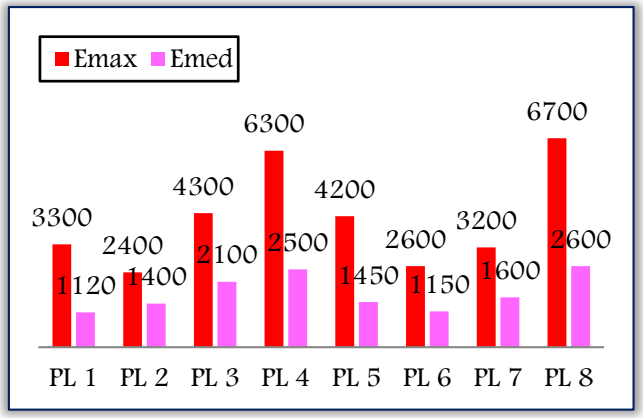

Figure 14. The Values of E[V/m] for HVPL

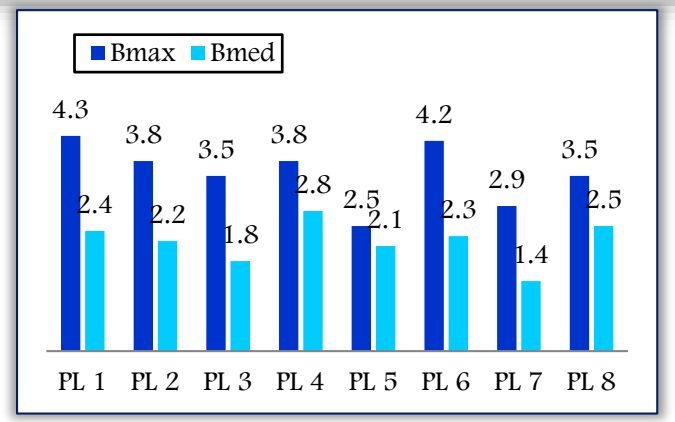

Figure 15. The Values of B[μT] for HVPL

The maximum and average values of the electric field intensity and magnetic induction, for PS are prezented in figures 16 and 17.

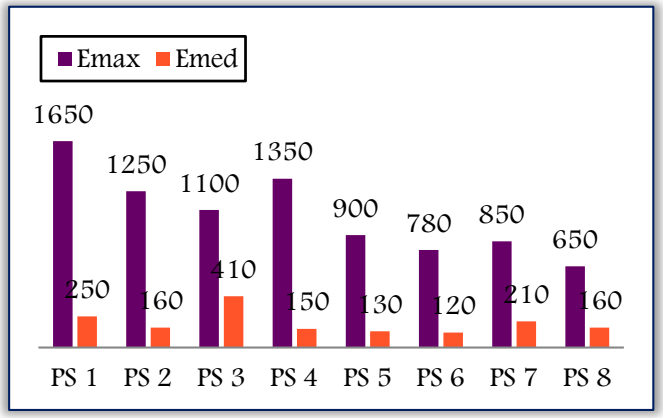

Figure 16. The Values of E[V/m] for P.S.

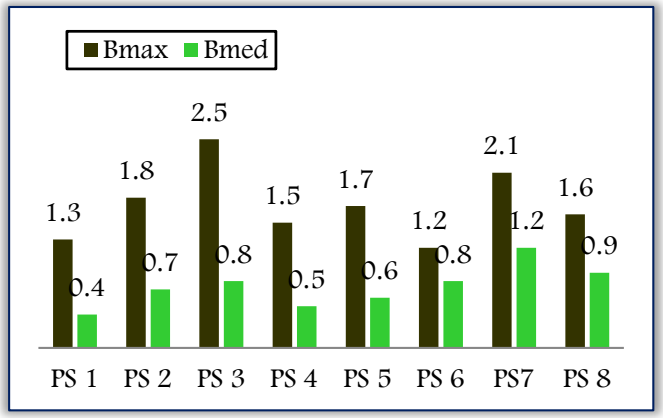

Figure 17. The Values of B[μT] for P.S.

The significances of overhead power lines from Figures 14 and 15 are: PL1 Oradea South - Sudrigiu, PL2 Mecanica - Săcueni, PL 3 Oradea South - Velenţa, PL4 Oradea West - Ioşia, PL 5 Oradea South - Alesd, PL 6 Oradea West - Mecanica, PL7 Oradea South - Nufărul and PL 8 Oradea Oradea South - Oradea West.

DISCUSSIONS

The instantaneous values of the electromagnetic field quantities depend on the operational status of installations from power substations, recovery stations and power lines, more accurate by voltages and currents values existent during measurement.

For tram lines, sags and currents absorbed depend on the number of trams in traffic and loading them with people. In each case measured values are highly variable, with a strong dynamic. In case of power lines, the fluctuations of values of field characteristics, largery depend on the land configuration and the type of road crossings and installation of utility that influences suspension height of the conductors and the choice of optimal pillar. Multiple cases are reported in the literature in which individuals or organizations have initiated legal proceedings to prove the harmfulness of mobile phones on humans [6]. And in Romania are few conclusive cases. Thus, in Oradea, a notable case is that of the university professor Ph.D. Mudura Pavel, who proved that cerebral diseases they contacted due to antennae mounted on the block where he lived, obtaining as a result of his actions, a judicial sentence that obliged the mobile operators concerned to change their location. Is the case of telecommunication facilities from the Figure 8. In the experimental researches conducted, were initiated and measurements at different distances from energy objectives advised, but since sizes field envisaged are inversely proportional to distance, to varying degrees, these have resulted lower than in areas reference and thus were not considered for this paper. They will be subject to an analytical study in the future.

CONCLUSIONS

In terms of the number of sources of electromagnetic fields and their territorial spread, Oradea is a polluted town. In few places normalized values of electric and magnetic field strengths were exceeded. This is due to low height suspension of conductors or proximity to roads and utilities in residential areas or commercial places, where expanded after the construction of high voltage power lines or electricity distribution stations. For High voltege power lines, these points with exceedances are more numerous. In cases of power stations the points with higher values coincide with the areas of power lines input, on the high-voltage for electric field intensity or where equipment or power transformers are closer to the fence and connections are above the heights of the outside fence.

If global trends are maintained to reduce the allowable values for the parameters of the electromagnetic field considered dangerous it is possible that and other locations in Oradea, to transform into some with high electromagnetic pollution generated by exceeding the new threshold values in the environment. The companies in the domain of mobile telecommunications services after installing antennas and related equipment of base stations are required to take measurements for determining values for the electromagnetic field in and around places of assembly. If these quantities are not below the permissible limit should not receive authorization to operate. But, given the degradation in time of functional characteristics and structure of material equipment used, the need arises more frequent repetition periods of such measurements. Same happens with mobile stations or cell phones. Most times the interest for periodic checks of antennas and base stations is dropped from specialized companies.Lodgers or residents of the buildings that are mounted telecommunication installations are the ones who must insist on these periodical checks.

References

[1.] Aliyu, O., Maina I, Ali H., 2011, Analysis of Electric Field Pollution due to 330 kV and 132 kV Transmission lines, Inovations in Science and Engineering, Vol. 1, No.4, pp.69-73;

[2.] Aliyu, O., Maina I, Ali H., 2011, Analysis of Magnetic Field Pollution due to 330 kV and 132 kV Transmission lines, Abubakar Tafawa University Bauchi, Nigeria, Journal of Technology and Educational Research, Vol. 4, No.2, pp.87-93;

[3.] Aliyu, O., Maina I, Ali H., 2012, Analysis of Electromagnetic Field Pollution due to High Voltage Transmission lines, Journal of Energy Technologies and Policy ,Vol. 2, No.7, pp.1-10;

[4.] Cepişcă, C ş.a. , 2002, Poluarea electromagnetică, vol I. , Ed. Electra ICPE, Bucureşti;

[5.] Cepişcă, C ş.a. , 2005, Poluarea electromagnetică, vol. II , Ed. Electra ICPE, Bucureşti;

[6.] Drăgulinescu A - Idolii fără fir. Telefonia mobilă şi poluarea electromagnetică, Editura Christiana, Bucureşti, 2010;

[7.] Milham S., 2012, Dirty Electricity, Electrification and the Diseases of Civilization, Publisher: Universe Star, New York, U.S.A.;

[8.] Morega Mihaela - Bioelectromagnetism, Editura Matrix Rom ,Bucureşti, 1999;

[9.] Păunescu Gabriela, 2010, Câmpul electromagnetic. Studii asupra posibilelor efecte ale câmpului electromagnetic asupra sănătăţii, www.infoscola.webgarden.ro;

[10.] Schwab A., Kurner W, 2013, Compatibilitate Electromagnetică, Editura AGIR, Bucureşti;

[11.] Vasilescu G, Popenţiu F, 2009, Renewable energy generators and electromagnetic pollution:a case study on residential solar energy, Analele Universităţii din Oradea Fascicula de Energetică, Vol. 15, pg. 311-316;

[12.] Vătău D., Şurianu F.D., Bianu A.E., Olariu A.F.,2011, Considerations on the Electromagnetic Pollution Produced by High Voltage Power Plants, Proceedings of European Computing Conference ECC'11, Paris, France, April 28-30, pp. 182- 187;

[13.] Vătău D., Şurianu F.D., Muşuroi S., Frigură Iliasa F.M., Proştean O.,2011, 220 kV and 400 kV Power Plant Electromagnetic Pollution Analysis,

Proceedings of IEEEEUROCON 2011, the International Conference on Computer as a Tool, Lisbon, Portugal, April 27-29, 2011, www.eurocon2011.it.pt, pp. 569-572;

[14.] *** Comisia Europeană, Serviciul Europe Direct, Ghid facultativ de bune practici, pentru punerea în practică a Directivei 2013/35/UE privind câmpurile electromagnetice, Studii de caz,Vol.II.

[15.] *** European Commission, Special Eurobarometer 347, 2010, Electromagnetic Fields Report, Eurobarometer code 73.3, Conducted by TNS Opinion & Social at the request of Directorate General for Health and Consumer Affairs Survey, co-ordinated by Directorate General Communication, Avenue Herrmann Debroux, 40-1160 Bruxelles, Belgique, internet source: http://ec.europa.eu/public_opinion/archives/ebs/ebs_347_en.pdf;

[16.] *** Comisia Europeană, Serviciul Europe Direct, Ghid facultativ de bune practici, pentru punerea în practică a Directivei 2013/35/UE privind câmpurile electromagnetice, Ghid practic,Vol.I.

[17.] *** Hotărârea Guvernului României Nr. 1193 din 29.09.2006 privind limitarea expunerii populaţiei generale la câmpuri electromagnetice de la 0 la 300 GHz;

ACTA Technica CORVINIENSIS
BULLETIN OF ENGINEERING

ISSN:2067-3809

ACTA TECHNICA CORVINIENSIS
– Bulletin of Engineering
Tome IX [2016], Fascicule 4 [October – December]
ISSN: 2067 – 3809

[1.]Viktor J. VOJNICH

BIOMASS AND LOBELINE PRODUCTION OF IN VITRO PROPAGATED INDIAN TOBACCO

[1.] Pallasz Athéné University, Faculty of Horticulture and Rural Development, Kecskemét, HUNGARY

Abstract: *Lobelia inflata* L. is a medicinally important species of the *Lobeliaceae* family. It is native to North America, it contains numerous piperidine alkaloids. The main alkaloid lobeline has been used as a respiratory stimulant. Recently, it has been come into the limelight due to research on CNS, drug abuse and multidrug resistance. It has been found that the plant can be successfully introduced (cultivated) and due to its favourable active principle production it can qualify for utilization. The outlined experiments have verified that N- and Mg-fertilization exerts a positive effect on plant production. The aim of this project was to examine the effect of magnesium and nitrogen fertilisation on the biomass and on the lobeline production of *in vitro* propagated *Lobelia inflata* in Hungary.
Keywords: *Lobelia inflata* (Indian tobacco), lobeline, biomass production, in vitro

INTRODUCTION

Indian tobacco (*Lobelia inflata*) is a native North American species (Canada and US. east countries) [1]. It is mainly an annual plant [2], but biennial populations can be found, too. Lobelia is named after Flemish Botanist Matthias de L'Obel (1538-1616) [3].

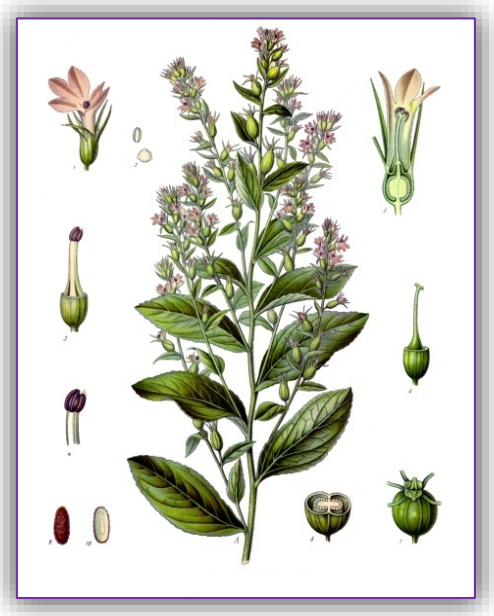

Figure 1. Indian tobacco (*Lobelia inflata*)

The *Lobelia inflata* synthesize important medicinal materials. The herb contains several piperidine skeleton alkaloids [4]. Its main alkaloid is the lobeline that due to its stimulating effect on the respiratory centre is used in cases of gas- and narcotic poisoning [5]. Recently, it has been come into the limelight due to research on CNS, drug abuse and multidrug resistance [6,7].

Figure 2. Indian tobacco (*Lobelia inflata*) habitus

Another important active agent in the plant is an antidepressant known β-amirin-palmitate. To satisfy the market needs, it is important to increase the content values and the biomass of the plant [8,9], for which a great opportunity arises through the nutrient supply of the plant.

It is important to increase the biomass and lobeline content of the plant by nitrogen and magnesium treatments in vitro [8,9,10] and in vivo in open field [11,12,13,14]. There was a favourable effect of NH_4^+ and NO_3^- on the biomass formation of in vitro cultures [15,16,17], of in vivo in open field [18,19] and aquatic cultures [20,21]. Britto and

Kronzucker [22] described the inhibitory effect of ammonia on growth in open field conditions.
Several previous experiments examined the influence of macroelements on growth and alkaloid production of hairy roots [23,24].
The aim of this project was to examine the effect of magnesium and nitrogen fertilisation on the biomass and on the lobeline production of *in vitro* propagated *Lobelia inflata* in Hungary.

MATERIAL AND METHODS

The open field trials were carried out in 2011 in Mosonmagyaróvár, University of West-Hungary (Széchenyi István University). Nitrogen and Magnesium were applied in the form of ground fertilizers. The nutrients were applied in the following methods and quantities in 2011: untreated (control), 50 kg/ha N-, 100 kg/ha Nitrogen ground fertilizer, 50 kg/ha Magnesium- and 100 Mg ground fertilizers. Soil analytical values in 2011: pH 7.12; humus 3.08 m/m%; Mg 310 mg/kg; NO2-NO3-N 20.1 mg/kg, K2O 518 mg/kg, P2O5 358 mg/kg.
An extended soil analysis was carried out according to standard methods of UIS Ungarn laboratory (Hungary, Mosonmagyaróvár).
In the open field trials, Mg (2%) - and N (34%) fertilizers were spread onto the soil surface, one day prior to transplanting. Transplanting of in vitro Lobelia inflata plants into open field soil was carried out on 26th May 2011. The number of plants per plot was 40. The experimental design was randomized blocks with 4 repetitions. During cultivation, mechanical weed control was applied. Plant heights (cm) were measured three times (22nd July, 29th July and 7th August) in 2011. In each treatment group 8 plants were measured both in 2011 (dry biomass production, g/plant of L. inflata herb).
The first harvesting was on 9-10th August 2011. During harvesting, the plants were flowering and the biomasses were recorded. After harvesting, the plants were dried in a shaded and well-ventilated glasshouse. The dry weight determination was carried out in early September. The flowering phenophase was observed in the period of July to September [25]. The total alkaloid content was determined by a spectrophotometric method elaborated by Mahmoud and El-Masry [26] and modified by Krajewska [27]. The statistical analysis was preformed with SPSS v19 software [28].
Alkaloid Extraction: Lobelia inflata L. (1 g), dried and powdered, was extracted with 1x20 ml, and 2x15 ml of 0.1 N HCl-methanol (1:1, v/v) by sonication for 3x10 minute. After centrifugation and filtration the methanol was evaporated off and the remaining aqueous phase was made up to a stock solution with 0.1 N HCl. Samples of this solution were purified by solid-phase extraction (SPE) for the quantitative HPLC (High Performance Liquid Chromatography) determinations.

RESULTS

References in the literature on the mineral nutrition of *L. inflata* are scarce, although it is one of the basic factors for the successful production of this species. The analysis of dry biomass production (g/plant) also underlined the favourable effect of Magnesium.
Dry biomass production was highest of the 100 kg/ha Mg-treatment of above-ground plant parts, as compared to the untreated control and N-application (Figure 3). The lobeline content was the highest *in vitro* culture (Figure 4) of the 100 kg/ha Mg-treatment (635 µg/g).

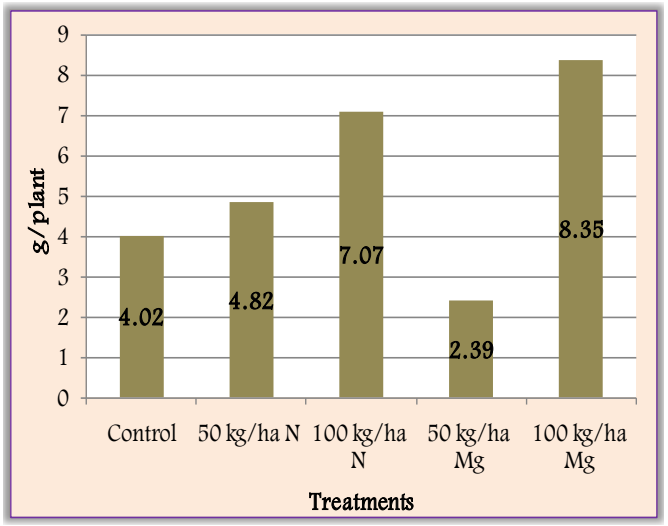

Figure 3. Dry biomass (g/plant) production of *in vitro Lobelia inflata* herb (2011)

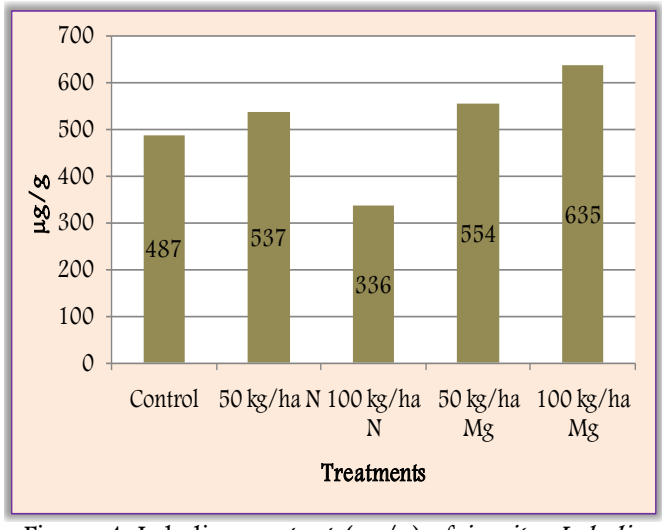

Figure 4. Lobeline content (µg/g) of *in vitro Lobelia inflata* herb (2011)

There were several economy experiments on lobeline content in the 1970s in the United States. 1% of the dry matter content was lobeline. In the 1970s, selling prices ranged from $0.25 to $0.80 per pound (1 pound = 453 g), which means that a

yield of 1,700 pounds (770 kg) of dried plant material would gross $425.00 to $1,360.00 per acre (1 acre = 4,047 m²) [29].

CONCLUSIONS AND RECOMMENDATIONS

The results indicate the favourable effect of Mg-fertilization and are in harmony with our previous *in vitro* experiments. Lobeline content (µg/g) determination by HPLC.

With respect to the lobeline content determined by HPLC it can be stated that values of plants treated with Magnesium (dry biomass production) and Mg 100 kg/ha treatments (lobeline content) were the highest.

References

[1.] Gottfried, Y. (2001): Lobelias-Beautiful components of our Fall Flora. The plant press. Vol. V, No. 4

[2.] Felpin, F.-X. - Lebreton, J. (2004): History, chemistry and biology of alkaloids from Lobelia inflata. Tetrahedron (60) 10127–10153.

[3.] Mottram, R. (2002): Charles Plumier, the King's Botanist - his life and work. With a facsimile of the original cactus plates and text from Botanicon Americanum (1689-1697). Bradleya 20, pp. 79-120.

[4.] Kursinszki, L. - Ludányi, K. - Szőke, É. (2008): LC-DAD and LC-MS-MS Analysis of Piperidine Alkaloids of Lobelia inflata L. (In Vitro and In Vivo). Chromatographia. (68) 27– 33.

[5.] Glover, E.D. - Rath, J.M. - Sharma, E. - Glover, P.N. - Laflin, M. - Tonnesen, P. - Repsher, L. - Quiring, J. (2010): A Multicenter Phase 3 Trial of Lobeline Sulfate for Smoking Cessation. Am J Health Behav 34:101-109.

[6.] Beckmann, J.S. - Siripurapu, K.B. - Nickell, J.R. - Horton, D.B. - Denehy, E.D. - Vartak, A. - Crooks, P.A. - Dwoskin, L.P. - Bardo, M.T. (2010): The novel pyrrolidine Nor-Lobelane analog UKCP-110 [cis-2,5-di-(2-phenetyl)-pyrrolidine hydrochloride] inhibits VMAT2 function, methamphetamine-evoked dopamine release, and methamphetamine self- administration in rats. J Pharmacol Exp Ther 335:841–851.

[7.] Szőke, É. - Lemberkovics, É. - Kursinszki, L. (2013): Alkaloids derived from lysine: Piperidine alkaloids. In: Ramawat KG, Mérillon JM (eds) Natural Products, Springer, Berlin/Heidelberg, pp 303-341.

[8.] Bálványos, I. (2002): Lobelia inflata L. hairy root kultúrák növekedésének és speciális anyagcseréjének vizsgálata. Doktori értekezés, Budapest.

[9.] Takács- Hájos, M. - Szabó, L. - Rácz, I.-né - Máthé, Á. - Szőke, É. (2007): The effect of Mg-leaf fertilization on Quality parameters of some horticultural species. Cereal Research Communications. 35, (2) 1181-1184.

[10.] Szőke É.–Máthé Á.: 2007. GVOP 3.1.1.-2004-05-0309/3.0 report of research. NKTH, Budapest

[11.] Vojnich V. J. – Máthé Á. – Szőke É.: 2012a. Comparison of the production of Indian tobacco (Lobelia inflata L.) propagated in vitro and in vivo. 34th Óvári Science Day, Mosonmagyaróvár, 537-542.

[12.] Vojnich V. J. – Máthé Á. – Szőke É. – Gaál R.: 2012b. Effect of Mg treatment on the production of Indian tobacco (Lobelia inflata L.). Acta Hort. 955. 125-128.

[13.] Vojnich V. J. – Máthé Á. – Szőke É. – Bányai P. – Kajdi F. – Gaál R.: 2013. Effect of nitrogen and magnesium nutrition on Indian tobacco (Lobelia inflata L.). J Cent Eur Agric. 14. 77-85.

[14.] Vojnich V. J.: 2014. Study of the Indian tobacco (Lobelia inflata L.) productions, specifically the plant grows in Hungary. PhD theses, University of West-Hungary, Mosonmagyaróvár

[15.] Breteler H.–Siegerist M.: 1984. Effect of ammonium on nitrate utilization by roots of dwarf bean. Plant Physiol. 75. 1099-1103.

[16.] Taya M. – Kino-Oka M. – Tone,S. – Kobayashi T.: 1989. A kinetic model of branching growth of plant hairy roots. J Chem Eng Jpn. 22. 698-700.

[17.] Kino-Oka M. – Taya M. – Tone S.: 1993. Evaluation of inhibitory effect of ammonium ion on cultures of plant hairy roots. J Chem Eng Jpn. 26. 578-580.

[18.] Cserni I. - Bné Pető J. - Hüvely A. - Németh T.:2008. Nitrogen, phosphorus, potassium, acid, sugar and vitamin C content in tomato grown in different soil types and under different nitogen doses, VII. Alps-Adria Scientific Workshop, Stara Lesna, Slovakia, 2008. Cereal Research Communications 1415-1418.

[19.] Hüvely A. - Hoyk E. - Pető J. - Cserni I.:2013 The effects of different NPK nutrients doses of red pepper's yield and vegetative parts in pots. Review on Agriculture and Rural Development 2 (2): pp. 583-586. ISSN: 2063-4803

[20.] Murray L. – Dennison W. C. – Kemp W. M.: 1992. Nitrogen versus phosphorus limitation for growth of an estuarine population of eelgrass (Zostera marina L.). Aquat Bot. 44. 83-100.

[21.] van der Eerden L. J. M.: 1982. Toxicity of ammonia to plants. Agric Environ. 7. 223-235.

[22.] Britto D. T.–Kronzucker H. J.: 2002. NH_4^+ toxicity in higher plants: a critical review. J Plant Physiol. 159. 567-584.

[23.] Bálványos I. – Szőke É. – Kursinszki L.: 1998. Effect of magnesium on the growth and alkaloid production of Lobelia inflata L. hairy root cultures. In: Kiss SA (ed)Magnesium and interaction of magnesium with trace elements. Hung Chem Soc, Budapest, 358–361.

[24.] Bálványos I. – Szőke É. – Kursinszki L.: 2003. Effect of macroelements on the growth and lobeline production of Lobelia inflata L. hairy root cultures. Acta Horticult. 597. 245–251.

[25.] Krochmal A. – Wilken L. – Chien M.: 1970. Lobeline Content of Lobelia inflata: Structural, Environmental and Developmental Effects.

U.S.D.A. Forest Service Research Paper NE- 178. Northeastern Forest Experiment Station, Upper Darby, PA. Forest Service, U.S.Department of Agriculture.
[26.] Mahmoud Z. F. – El-Masry S.: 1980. Colorimetric determination of lobeline and total alkaloids in Lobelia and its preparations. Sci Pharm. 48. 365-369.
[27.] Krajewska A.: 1986. The effect of new type of growth regulators on the Lobelia inflata L. tissue cultures (in Hungarian). PhD theses, Semmelweis University, Budapest
[28.] Huzsvai, L.: Biometriai módszerek az SPSS-ben. SPSS alkalmazások. Debreceni Egyetem, Mezőgazdaságtudományi Kar, Debrecen. 2004
[29.] Krochmal A. – Wilken L. – Chien M.: 1971. Plant and Lobeline harvest of Lobelia inflata L. Respectively Principal Economic Botanist, Southeastern Forest Experimental Station, Forest Service, U.S.D.A., Auburn University, Auburn, Alabama, 216-220.

ACTA Technica CORVINIENSIS
BULLETIN OF ENGINEERING

ISSN:2067-3809

ACTA TECHNICA CORVINIENSIS
– Bulletin of Engineering
Tome IX [2016], Fascicule 4 [October – December]
ISSN: 2067 – 3809

[1.]Akinlabi OYETUNJI, [2.]Henry Kayode TALABI

EFFECTS OF HEAT TREATMENT PROCESS ON MECHANICAL AND MICROSTRUCTURAL PROPERTIES OF GRAY CAST IRON

[1-2.]Department of Metallurgical and Materials Engineering, School of Engineering,
Federal University of Technology, Akure, Ondo State, NIGERIA

Abstract: This study investigated the effects of heat treatment process on mechanical and microstructural properties of gray cast iron. The charged materials used were graphite, cast iron scraps and ferrosilicon which were subjected to chemical analysis using spectrometric analyzer, the charge calculation to determine the amount needed to be charged into the furnace was properly worked out and charged into the rotary furnace from which the as-cast was obtained. The as-cast was subjected to various degree of normalized heat treatment at different operating temperatures of 885°C, 893°C, 901°C, 909°C, 917°C and after which the mechanical properties of the gray cast iron produced were assessed by hardness, wear, tensile strength and microstructure tests. It was observed that hardness properties continued to increase as operating temperature increases and graphite flakes break the continuity of ferrite matrix results into an increase in hardness and tensile strength of the gray cast iron.
Keywords: Gray cast iron, Normalized, Hardness, Tensile strength, Wear, Temperature

INTRODUCTION

Gray iron is one of the oldest cast ferrous products. Gray cast iron is a very unique engineering material. It is known to be the most versatile of all foundry metals. This makes them particularly suitable for the manufacture of engineering components [1]. Possessing quite high carbon content which is responsible for the ease of melting, casting of this metal in the foundry and for ease of machining in subsequent manufacturing,

Gray iron offers a unique versatility at lower cost that can be obtained through microstructure control [2-3]. In spite of competition from newer materials and their energetic promotion, gray iron is still used for those applications where its properties have proved it to be the most suitable material available. Next to wrought steel, gray iron is the most widely used metallic material for engineering purposes.

The automobile engine is the single most important without it, the car simply will not move. Hence it is important that the engine block is built to withstand the high temperatures and pressures that are put into it and it is equally important that the engine block is built to last. Over the years, materials used for making engine blocks have changed and materials sciences have matured enough to find the best possible materials to build engine blocks. Common materials used for engine blocks include Grey Cast Iron, aluminum and compacted graphite iron (CGI) [4].

There are several reasons for its popularity and widespread use. It has a number of desirable characteristics not possessed by any other metal and yet is among the cheapest of ferrous materials available to the Engineer. Gray iron castings are readily available in nearly all industrial areas and can be produced in foundries representing comparatively modest investments. Gray iron is one of the most easily cast of all metals in the foundry, It has the lowest pouring temperature out of the ferrous metals, which is reflected in its high fluidity and its ability to be cast into intricate shapes. As a result of a peculiarity during final stages of solidification, it has very low and, in some cases, no liquid to solid shrinkage this enables sound castings to be achievable. For the majority of applications, gray iron is used in its as-cast condition, thus simplifying production.

Gray iron has excellent machining qualities producing easily disposed off chips and yielding a surface with excellent wear characteristics. The resistance of gray iron to scoring and galling with proper matrix and graphite structure is universally recognized. Gray iron castings can be produced by virtually any well-known foundry process. Surprisingly enough, in spite of gray iron being an

old material and widely used in engineering construction, the metallurgy of the material has not been clearly understood until recent times. Mechanical properties of gray iron are not only determined by composition but also greatly influenced by foundry practice, particularly cooling rate in the casting.

All of the carbon in gray iron, other than that combined with iron to form pearlite in the matrix, is present as graphite in the form of flakes of varying size and shape. It is the presence of these flakes formed on solidification which characterize gray iron, the presence of these flakes also imparts most of the desirable properties to gray iron. Its versatility arises from the wide range of physical properties which are possible due to the addition of alloying elements and various heat treatment procedures [5]. This research therefore is aimed to determine the effects of heat treatment process on mechanical and microstructural properties of gray cast iron.

MATERIALS AND METHOD

Materials

White silica sand (SiO_2) obtained from Igbokoda, its geographical coordinates are 6° 21' 0" North, 4° 48' 0" East of Ondo State, Nigeria, bentonite, coal dust and small proportion of water were used to prepare the mould. The charged materials include; graphite, cast iron scraps, and ferro-silicon. The ferro-silicon and graphite were obtained from Engineering Materials Development Institute (EMDI), Akure, Ondo State, Nigeria.

Mould Preparation

A woodworking lathe machine model MCF3020 was used to machine the wooden pattern materials obtained from hard wood that produced the pattern, sprue and risers with adequate taper. The patterns were dimensioned 300 mm long and of different diameters; 15 mm, 20 mm, 30 mm, 35 mm. The size of the patterns was made 2% oversize than the specified dimension to compensate metal contraction during solidification. The down sprue of diameter 50 mm, was tapered to diameter 40 mm and 30 mm long was also made [6].

The mould is prepared with green sand being the main material used which comprises of the mixture of bentonite, recycled silica sand and water. The green sand has good permeability, good grain size, accurate moisture content and with a very good refractoriness which can withstand heat at very high temperature. Bentonite is added to the green sand to increase its bonding strength. Suitable moulding boxes is first selected, large enough to accommodate the pattern of its varying sizes and then rammed slowly but with good force. Facing sand was mixed into the drag and the content was well rammed. The drag was turned upside down on the mould board, the pattern as well as its accessories were placed on the board inside the flask in such a position that space is left for gate cutting. The excess sand will be cut off to bring it in line with the edge of the cope, a parting sand was properly applied for the easy removal of the mould from the pattern.

The gating system was properly designed for smooth channeling of the molten metal into the mould cavities through the sprue, runner, in-gates and riser that were perfectly placed in position [7]. The cope was placed over the drag and top parts of the pattern assembled in position.

Melting, Casting and Cleaning Operation

Rotary furnace of 100 Kg capacity was used to melt the cast iron scraps, graphite and ferrosilicon were charged and heated to a temperature of 1300°C. The rotary furnace was tilted to allow the melt flow out through the ladle and then poured into the already prepared mould of various diameters where it was allowed to cool freely in air then solidify. The solidified castings were subsequently shaken out of the mould 24 hours later after cooling [8].

Stainless wire brush was used to remove sand that adhered to the castings and fettling was done by abrasive wheel-cutting machine to remove gates and risers. Afterwards Dong Jin heavy hydraulic power hacksaw was used to cut the samples and universal lathe machine type C80 was used to machine the cast samples into standard test samples for mechanical and microstructural analysis [8].

Determination of Chemical Composition

The chemical composition of the as-cast samples of the gray cast iron was determined using spectrometric analyzer

Chemical Equivalent Value

The carbon equivalent (CE) is a simplified method of evaluating the effect of composition on cast iron. One of the most common equations used is

$$CE = Tc + \frac{\%Si+\%P}{3} \quad (1)$$

where T_C is the total carbon, and %Si and %P are the silicon and phosphorus contents [9]

The value is important because it can be compared with the eutectic composition (4.3%) to indicate whether the cast iron will behave as a hypoeutectic iron or hypereutectic iron during solidification [9]

MECHANICAL TEST

Hardness Measurement

LECO Micro hardness tester LM700AT at E.M.D.I, Akure was used to determine the hardness of the samples. The surfaces of the test samples were dimensioned to 10mm length and 8mm thickness and were properly grounded to give flat and stable surfaces. Test load 490.3 MN and dwell time of 10 seconds was applied on the test samples before taking the readings [10].

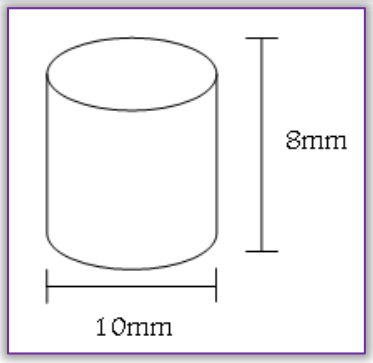

Figure 1. Hardness Test Sample

Tensile Strength Test

The samples were machined with universal Lathe Machine TYPE C80 to produce standard test samples [11]. Instron universal tensile testing machine of model 3369 at the speed of 0.02m/s was used to carry out the tensile test by subjecting it to 10KN load.

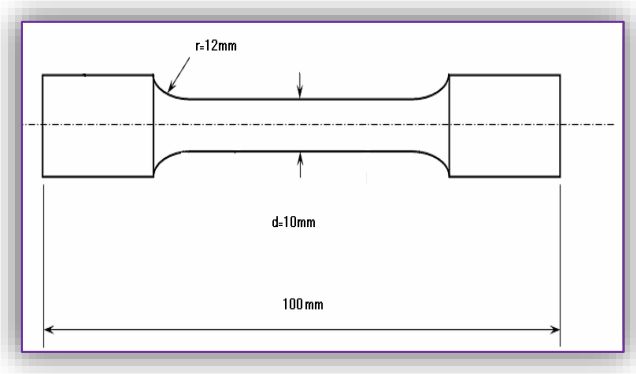

Figure 2. Tensile Test sample

Wear resistance

The wear resistance was carried out with Taber Abrasers. Model ISE-AO16. Taber tests involve mounting a flat round specimen approximately 100 mm^2 to a turntable platform that rotates on a vertical axis at a fixed speed. The volume of the loss material is taken with the force applied, velocity of the revolution and the time taken for the wear is recorded.

$$W = K \times F \times V \times T \quad (1)$$

whereW is wear volume (mm^3); F is force (N); K is wear factor (mm^3/Nm) 10^{-8}; V is velocity (m/s)and T is time (s)

Heat Treatment

The 25 as- cast samples were subjected to heat treatment by heating the samples in a muffle furnace after which they could be examined mechanically by hardness, wear and tensile tests and microscopically.

Normalizing temperatures, which were used for the samples were 885°C, 893°C, 901°C, 909°C and 917°C respectively and cooled in air to room temperature [12].

Metallographic Test

The specimens are prepared for metallographic test, using the following procedures. The as-cast and heat treatment already cut with power hack saw into specimens were subjected to grinding process. The microstructural examination was performed using Optical Metallurgical Microscope model AXIA. The specimen for the optical microscopy were polished using series of emery paper of grit sizes ranging from 60-1200, while fine polishing was performed using polycrystalline diamond suspension of particle sizes ranging from 10 - 0.5µ. The specimens were etched using 2% nitric to 98% alcohol (Nital).

RESULTS AND DISCUSSIONS

All the mechanical and micro structural analysis were carried out at room temperature and the following results were obtained. The spark analysis of the produced grey cast iron were carried out with the aid of spectrometer analyzer and the results are shown in Table 1.

Table 1: Chemical composition of the produced grey cast iron

%C	%Si	%S	%C	%P	%Mn
2.92	2.75	0.06	0.18	0.17	0.11
%Cr	%Mo	%V	%Cu	%W	%Ti
0.1576	0.0206	0.0113	0.1517	0.00027	0.0082
%Sn	%Co	%Al	%Nb	%Mg	%Fe
0.0215	0.0085	0.0031	0.00001	0.0026	93.4092

Effects of Normalizing on the Mechanical Properties

There were variations in the hardness property of the various samples as a result of different normalizing temperature. Sample with normalizing temperature 885°C had hardness value of 54.6 HRC, sample with normalizing temperature 901°C had hardness value of 49.5 HRC, sample with normalizing temperature 909°C had hardness value of 37.6 HRC and sample with normalizing temperature 917°C had hardness value of 34.7 HRC.

From the figure 8, as the normalizing temperature increases, the hardness values decreases, the microhardness value of the cast iron decreases as a result of decrease in pearlite. Also the lower the normalizing temperature, the faster the cooling rate which aid the refinement of the grain structure. When cast iron cooled at a faster rate, the resulting pearlite is fine [12].

There were also variation in the tensile strength values, at normalizing temperature 885°C, the tensile strength value was 1952 N/mm^2 and at normalizing temperature 893°C, the tensile strength value was 1644 N/mm^2, it was then observed from figure 9 that as the normalizing temperature increases, the tensile strength value decreases.

It was observed from figure 10, that as the normalizing temperature increases, the wear rate increases.

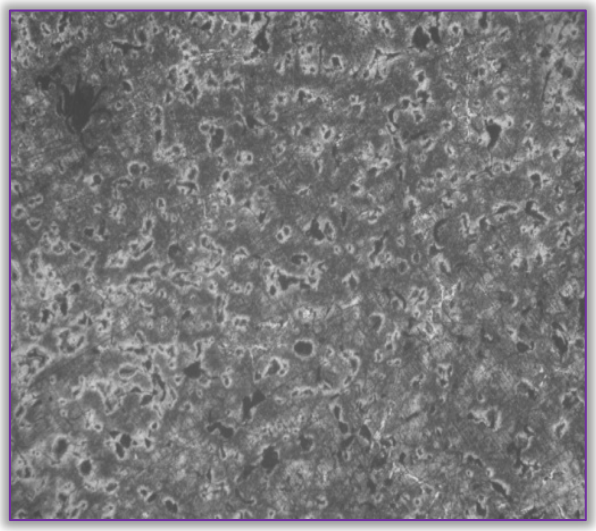

Figure 3: Microstructure
of Normalized sample at 885°C

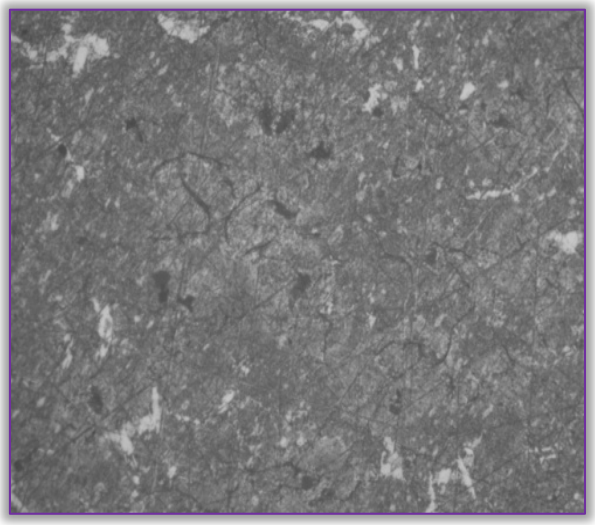

Figure 4: Microstructure
of Normalized sample at 893°C

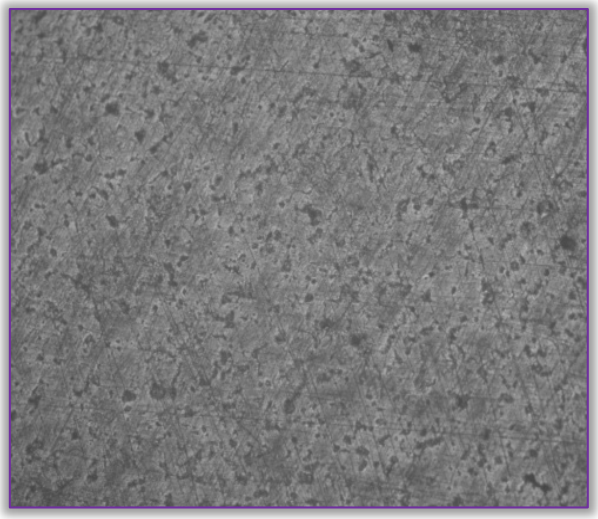

Figure 5: Microstructure
of Normalized sample at 901°C

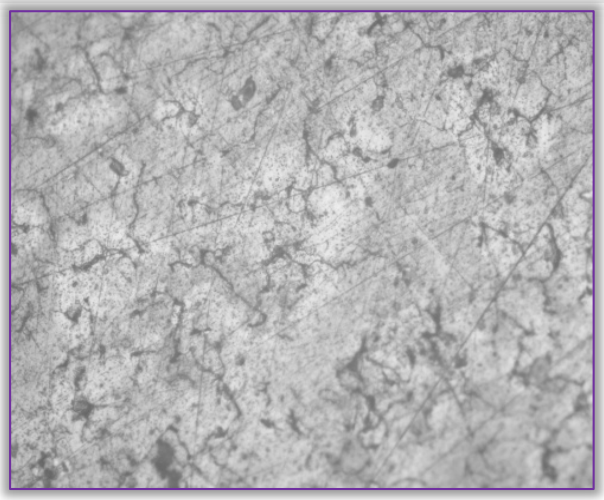

Figure 6: Microstructure
of Normalized sample at 909°C

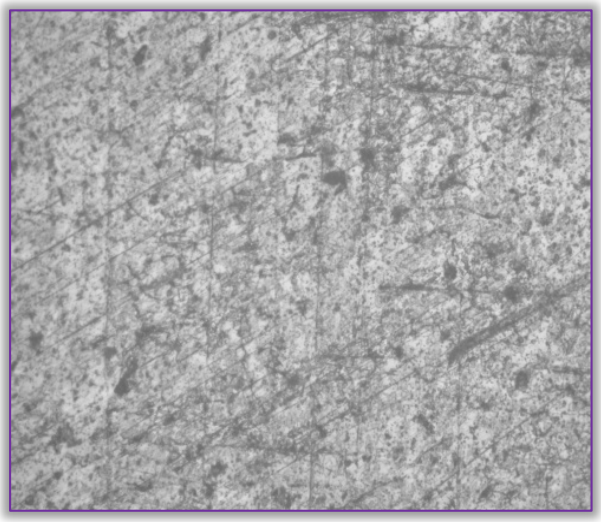

Figure 7: Microstructure
of Normalized sample at 917°C

Microstructure

Usingthemetallurgicalmicroscope,the micrographs of each sample were shown in such a way that the graphite flakes morphologies could be easily analyzed. The figures 3-7 show an important view of the distribution of the graphite flakes and also the effects of the different normalizing heat treatment temperatures on the mechanical properties of gray cast iron.

Effects of Normalizing on the Microstructure

Microstructure of the normalized specimen with tiny flakes graphite of type A which are uniformly and completely distributed in cementite-rich pearlitic matrix as shown in figure 3, may have resulted from air cooling. Coarser carbide were observed in the normalized samples because of the higher normalizing temperatures [13].

However the area adjacent to the graphite flake experienced carbon decomposition and ferrite will result around the flakes. It is clear from the microstructures in figures 3-7, that the normalizing process will give more pearlite which is stronger

than ferrite because of cementite layers inhibited in it [13].

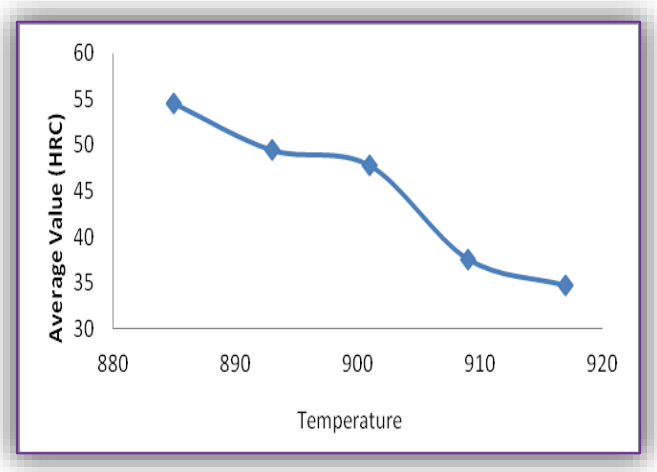

Figure 8: Variation of hardness with normalizing temperature

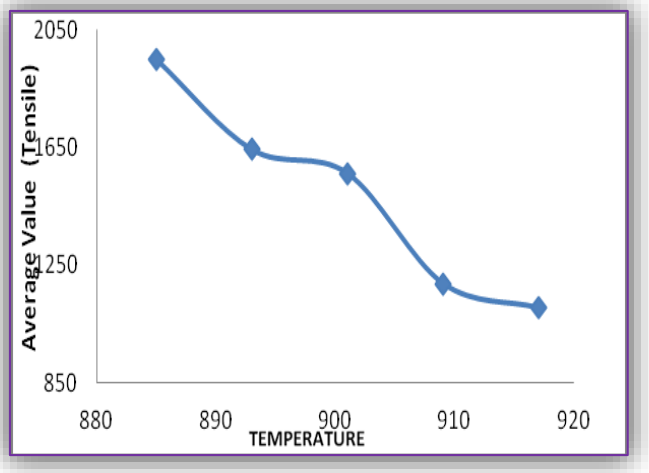

Figure 9: Variation of tensile with normalizing temperature

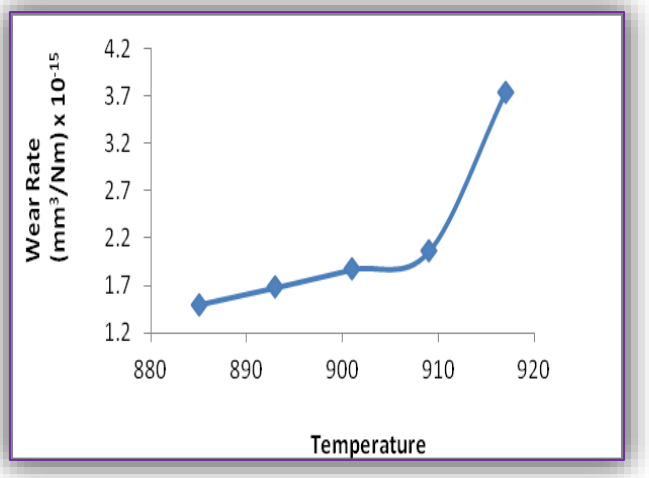

Figure 10: Variation of wear resistance with normalizing temperature

CONCLUSIONS

From the results of this work, normalizing heat treatment process was found to produce noticeable effects on the material's micro structural characteristics and mechanical properties. Hence the following conclusions were drawn;

i. The mechanical properties such as hardness and tensile showed appreciable decrease corresponding with increased normalizing temperatures of the grey cast iron.
ii. Tensile properties of the grey cast iron also increased with decrease in the heat treatment temperatures.
iii. Normalized samples showed higher hardness properties which continued to increase as operating the temperatures increased.
iv. Graphite flakes breaking the continuity of ferrite matrix results into an increase in hardness and tensile strength of the grey cast iron.

References

[1.] Bocus S. and Zaldarys G.: "Production of Ductile Iron Casting with Different Matrix Structure", Materials Science (Medziagotyra) 11(4), 307-310, 2010.
[2.] Zhou W., Zhu H., Zhang D, Zheng H., Hua Q. and Zhai Q. Niobium Alloying Effect in High Carbon Equivalent Grey Cast iron China Foundry, 8(1), 36-40, 2012.
[3.] Agbu S. "The Iron and Steel industry and Nigeria's Industrialization" Exploring Cooperation with Japan, 418, 1-146, 2007.
[4.] Whitney B., Sessler, and Peter C.: Ultimate American V-8 Engine Data Book. MBI Publishing, ISBN 978-0-7603-3681-6, 2010.
[5.] Jezerki J. and Bartocha D. Properties of Cast Iron Modifying with Inoculants, Journal of Achieving in Materials and Manufacturing Engineering, 22 (1), 25-28, 2007.
[6.] Ibhadode, A. O. Introduction to Manufacturing Technology, Ambik Press: Nig, 2001.
[7.] Talabi H.K., Adewuyi B.O., Oyetunji A. and Daramola O.O. Effects of Selected Casting Methods on Mechanical Behaviour of Al-Mg-Si Alloy- Leonardo Electronic Journal of Practices and Technology (LEJPT) 25, 109-117, 2014.
[8.] Oyetunji, A. Effect of Foundary Cast-size Distribution on the Mechanical and Structural properties of Grey Cast Iron. Nigerian Journal of Engineering Research, 1 (3), 1-18, 2010.
[9.] Ajayi J.A. and Adeleke O.A. Failure Analysis of Railway Brake Blocks, Engineering Failure Analysis, Vol. 4,(3), 205-213, 1997.
[10.] Oaikhinan, E.P. Introduction to Materials testing part 1, 45-47, 2005.
[11.] Pavlina, E. J., and Van-Tyne, C. J. Correlation of Yield Strength, Journal of Materials

Engineering and performance, 17(6) 123-126, 2008.
[12.] Krause, D. E. Gray iron-A Unique Engineering Material. PWS publishing, Boston, 3-28, 1969.
[13.] Atanda, P., Fatudimu, A., Oluwole, O. Sensitization Study of Normalized 316L Stainless Steel,Journal of Minerals & Materials Characterization & Engineering, 9,(1) 13-23, 2010.

ACTA Technica CORVINIENSIS
BULLETIN OF ENGINEERING

ISSN:2067-3809

ACTA TECHNICA CORVINIENSIS
– Bulletin of Engineering
Tome IX [2016], Fascicule 4 [October – December]
ISSN: 2067 – 3809

[1.]Csaba Attila GHEORGHIU, [2.]Teodor HEPUȚ

RESEARCH CONCERNING THE INFLUENCE OF THE COOLING PARAMETERS ON THE SPEED OF THE CASTING IN CONTINUOUS CASTING OF STEEL

[1-2.]University Politehnica Timisoara, Faculty of Engineering Hunedoara, Hunedoara, ROMANIA

Abstract: The paper presents the results of research conducted in the form of semi-finished steel casting for the manufacture of pipes that are intended to transport hydrocarbons. The research was aimed at determining the influence of the parameters that affect the process of cooling (hardening) on the liquid steel casting speed. Were included in the study the temperature of the steel at the entry into the cristalizor, steel overheating and cooling water flow in different areas, considered independent parameters and casting speed dependent parameter. The data obtained was processed in MATLAB, multiple correlations were obtained and are presented in both graphical and analytic form. The analysis conducted shows a comparison between the results obtained by three types of equations for each correlation which were analyzed from a technological point of view.
Keywords:steel casting, matlab, casting speed, steel cooling, pipes, EBT

INTRODUCTION

Since the six decade of the last century, in the practice of steel casting was imposed the continuous casting, whose share increased gradually replacing the conventional casting or ingot form. Continuous casting steel industry in developed countries, the share of continuous casting is at least 95% of the total number of cast steel. The difference up to 100% is represented by cast steel ingots intended for processing by forging.

Continuous casting was introduced quickly in practice because of the advantages they represent, namely: metal production is over 99% in sequential casting, investments, labor price is lower, significant reduction of thermal power and electricity, high degree of mechanization and automation etc. . Particular attention should be paid toof the speeds of molding, drag and solidification point.

STUDY OF THE PROBLEM

The research conducted was aimed to establish the correlation equations between parameters characterizing the continuous casting of steel, temperature at the entrance to the crystallizer, steel overheating, cooling water flow in the crystallizer and different areas of the secondary cooling. Along with these parameters were followed the values of casting speed, on the casting of round blanks ϕ270mm.

The steel was produced in an electric arc furnace EBT type, capacity 100t treated in installations L.F. (Ladle - Furnace), and VD (vacuum-degassing) and then poured in a continuous casting plant with five threads.

MATHEMATICAL DATA MODELING

The data processing was made in the computing program MATLAB, using three types of correlation equations. The results are presented both analytical and graphical form, each correlation being analyzed technologically indicating optimal values for the independent parameters.

The analysis conducted shows a comparison between the results obtained by three types of equations for each correlation.

» Equation 1:

$$z_1 = a_{(1)}\, x^2 + a_{(2)}\, y^2 + a_{(3)}\, xy + a_{(4)}\, x + a_{(5)}\, y + a_{(6)}$$

» Equation 2:

$$z_2 = a_{(1)} + a_{(2)}\, x + a_{(3)}\, x^2 + a_{(4)}\, x^3 + a_{(5)}\, y + a_{(6)}\, y^2 + a_{(7)}\, y^3 + a_{(8)}\, y^4 + a_{(9)}\, y^5$$

» Equation 3:

$$z_3 = a_{(1)} + a_{(2)}\, \log(x) + a_{(3)}\, \log(x)^2 + a_{(4)}\, \log(x)^3 + a_{(5)}/y + a_{(6)}/(y^2) + a_{(7)}/(y^3) + a_{(8)}/(y^4) + a_{(9)}/(y^5)$$

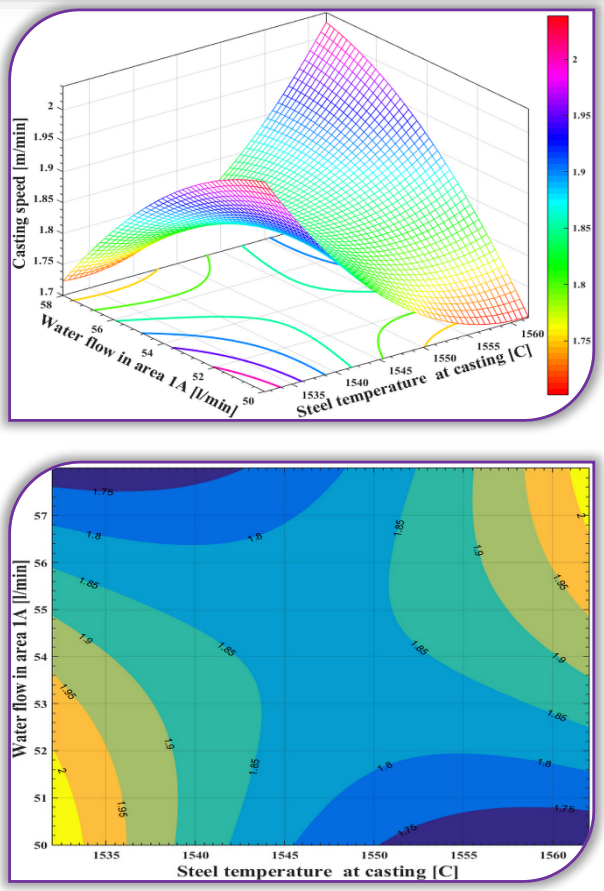

Figure 1. Casting speed= f (Steel temperature at casting, Water flow in area 1A, equation 1);

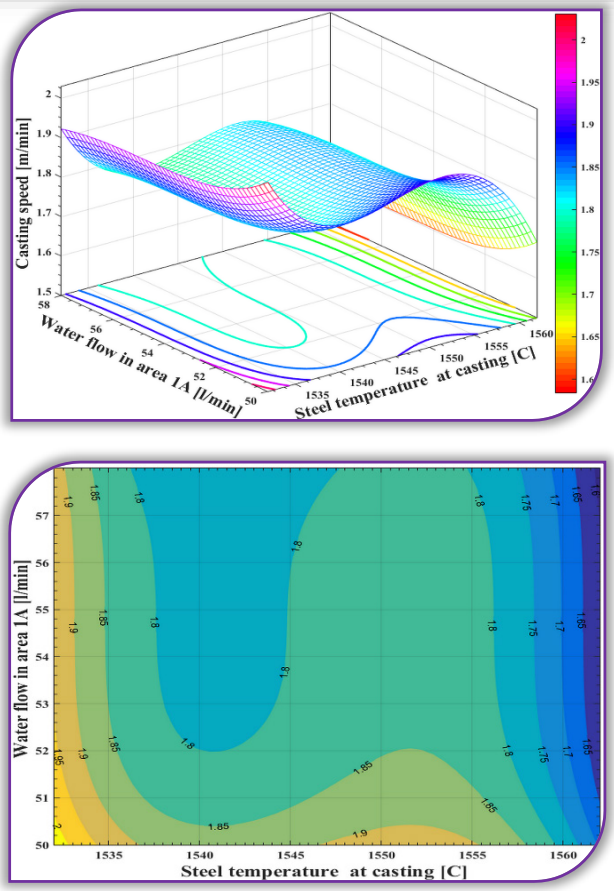

Figure 3. Casting speed= f(Steel temperature at casting, Water flow in area 1A, equation 3)

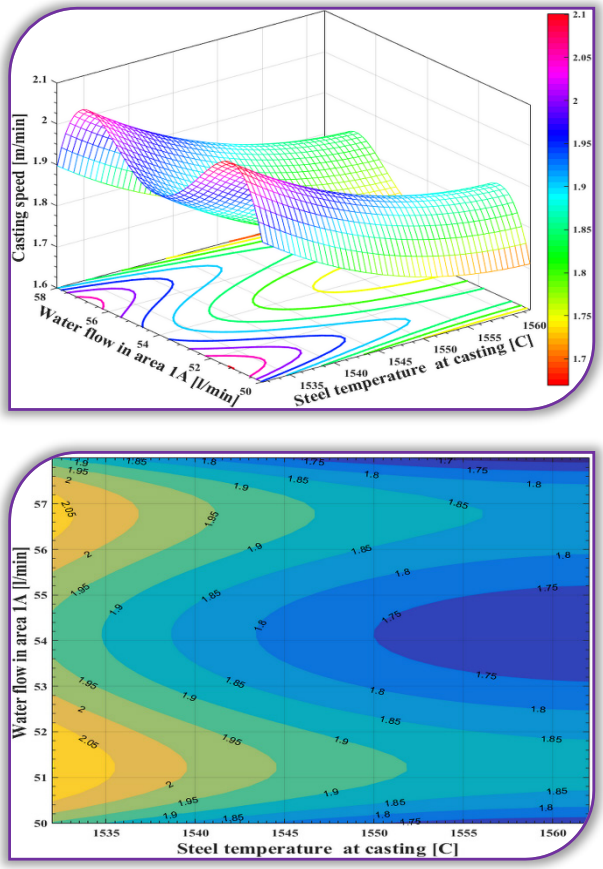

Figure 2. Casting speed= f (Steel temperature at casting, Water flow in area 1A, equation 2)

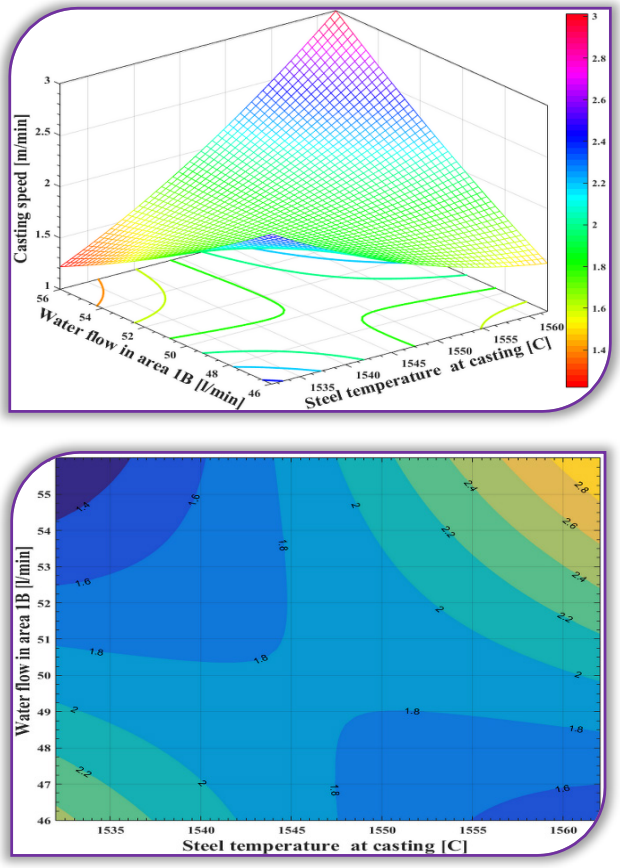

Figure 4. Casting speed= f (Steel temperature at casting, Water flow in area 1B, equation 1)

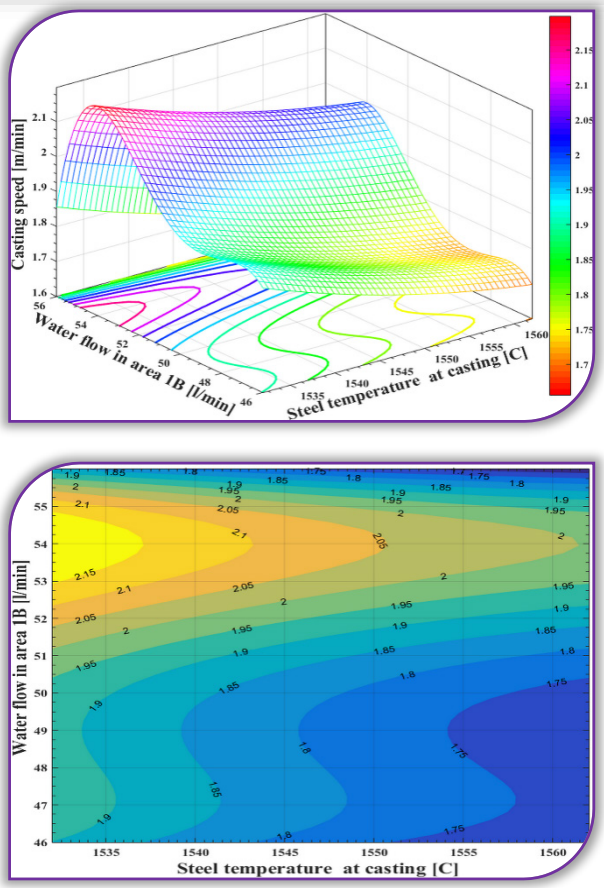

Figure 5. Casting speed= f (Steel temperature at casting, Water flow in area 1B, equation 2)

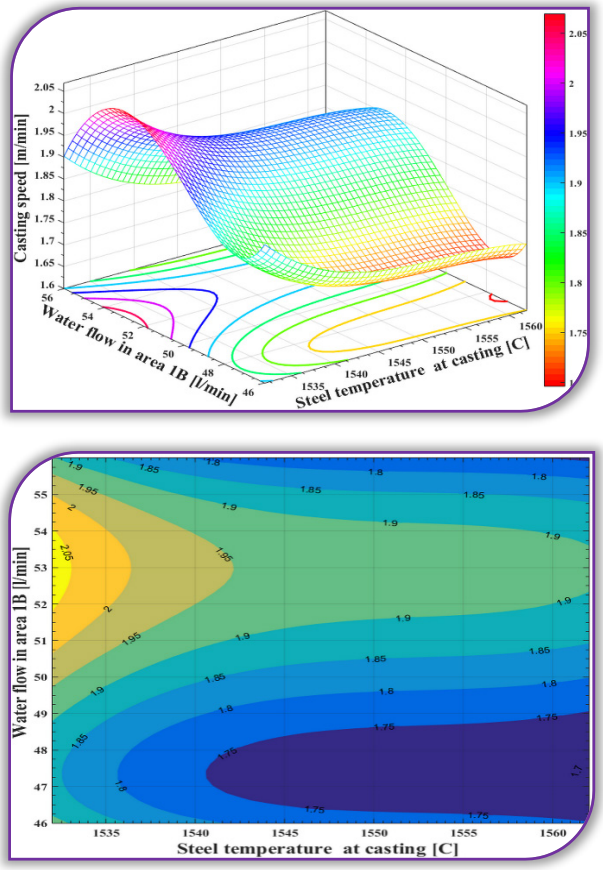

Figure 6. Casting speed= f (Steel temperature at casting, Water flow in area 1B, equation 3)

$$z_1 = 0.00039\,x^2 + 0.00344\,y^2 + 0.00264\,xy + 1.35823\,x + 3.72223\,y + 1153.39115 \quad (1)$$
$$R^2 = 0.5287$$

$$z_2 = 7.52129\,x + 0.00460\,x^2 + 14.07756\,y^2 + 0.52186\,y^3 + 0.00724\,y^4 \quad (2)$$
$$R^2 = 0.61243$$

$$z_3 = 11890 + 48574\log(x) + 66145\log(x)^2 + 300000\log(x)^3 + 16829/y + 92059/(y^2) + 16786/(y^3) \quad (3)$$
$$R^2 = 0.5441$$

$$z_1 = 0.00065\,x^2 + 0.00258\,y^2 + 0.00925\,xy + 47158\,x + 14.56371\,y + 2274.28489 \quad (4)$$
$$R^2 = 0.71748$$

$$z_2 = 1.59968\,x + 0.00092\,x^2 + 3.71578\,y^2 + 0.14897\,y^3 + 0.00223\,y^4 \quad (5)$$
$$R^2 = 0.79421$$

$$z_3 = 21424 + 87475\log(x) + 11905\log(x)^2 + 54000\log(x)^3 + 44161/y + 22154/(y^2) + 36930/(y^3) \quad (6)$$
$$R^2 = 0.70210$$

$$z_1 = 0.00023\,x^2 + 0.0253\,y^2 + 0.00013\,xy + 0.7328\,x + 2.7963\,y + 627.2682 \quad (7)$$
$$R^2 = 0.76230$$

$$z_2 = 36.6474\,x + 0.0239\,x^2 + 70.4148\,y^2 + 2.7289\,y^3 + 0.0396\,y^4 + 0.0002\,y^5 \quad (8)$$
$$R^2 = 0.86142$$

$$z_3 = 78060 + 31882\log(x) + 43407\log(x)^2 + 197000\log(x)^3 + 17588/y + 88439/y^2 + 14811/y^3 \quad (9)$$
$$R^2 = 0.79973$$

$$z_1 = 0.00063\,x^2 + 0.00037\,y^2 + 0.00755\,x\,y + 2.3735\,x + 11.6326\,y + 2150.4986 \quad (10)$$
$$R^2 = 0.6831$$

$$z_2 = 8.3524\,x + 0.0054\,x^2 + 13.7375\,y^2 + 0.4916\,y^3 + 0.0066\,y^4 \quad (11)$$
$$R^2 = 0.6212$$

$$z_3 = 44677 + 18249\log(x) + 24848\log(x)^2 + 113000\log(x)^3 + 38611/y + 21071/(y^2) + 38268/(y^3) \quad (12)$$
$$R^2 = 0.55463$$

Table 1. Data used for the graphical representations

Steel cast. Temp. [C]	Water flow in area: [l/min]				Casting speed [m/min]
	1A	1B	2	3	
1562	50	48	50	52	1.7
1551	50	48	50	52	1.7
1548	50	48	50	52	1.7
1546	52	50	52	54	1.9
1551	50	48	50	52	1.75
1552	53	48	52	55	1.7
1550	55	46	54	55	1.7
1546	56	49	53	58	1.73
1551	53	51	53	55	1.7
1546	53	50	52	54	1.8
1544	52	50	52	54	1.85
1540	58	56	58	60	1.85
1549	50	48	50	52	1.75
1546	56	53	56	58	1.85
1532	53	51	53	55	2.05
1551	56	50	50	52	1.88
1556	54	49	52	54	1.95

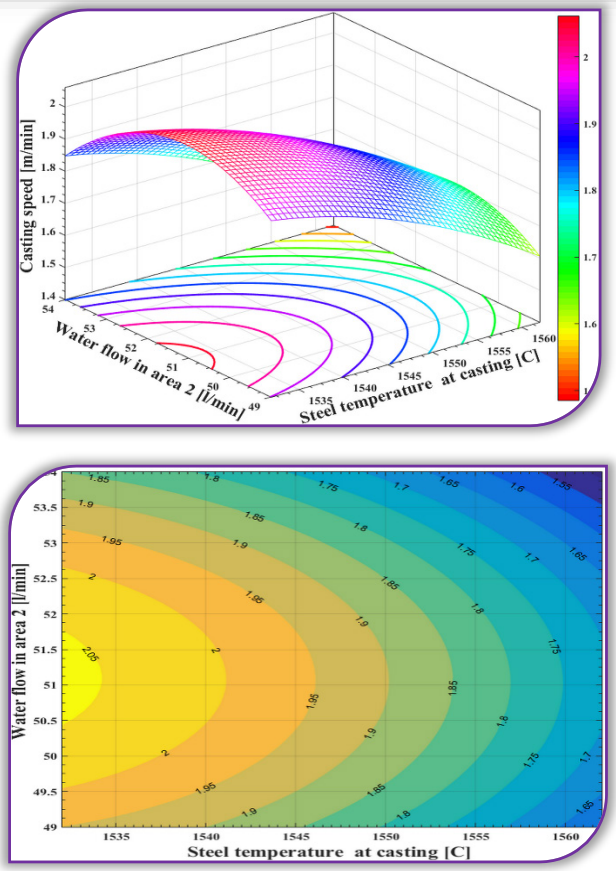

Figure 7. Casting speed= f (Steel temperature at casting, Water flow in area 2, equation 1)

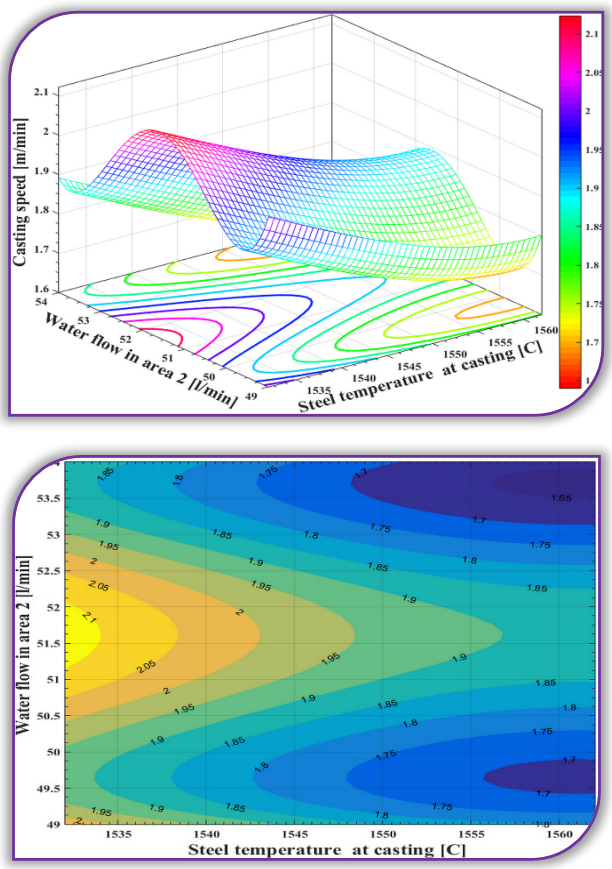

Figure 8. Casting speed= f (Steel temperature at casting, Water flow in area 2, equation 2)

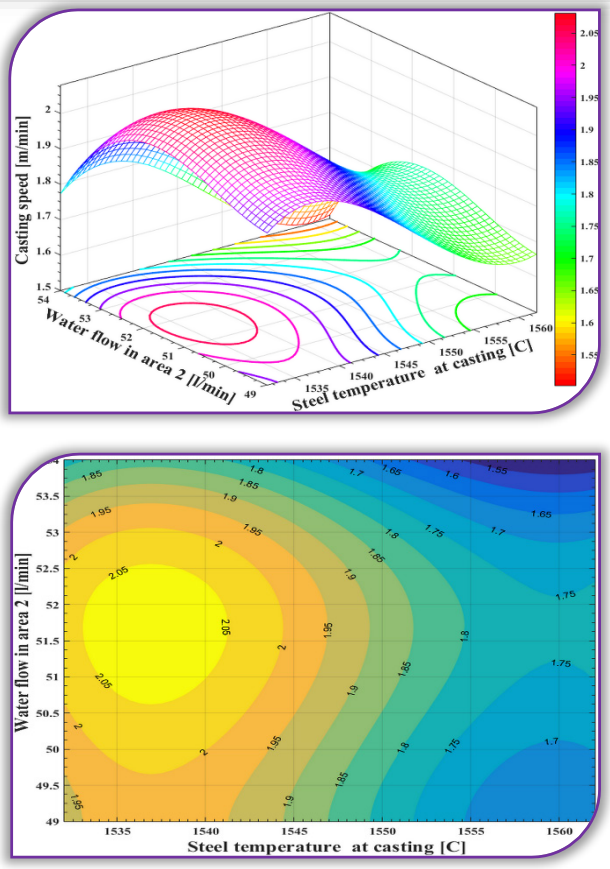

Figure 9. Casting speed=f(Steel temperature at casting, Water flow in area 2, equation 3)

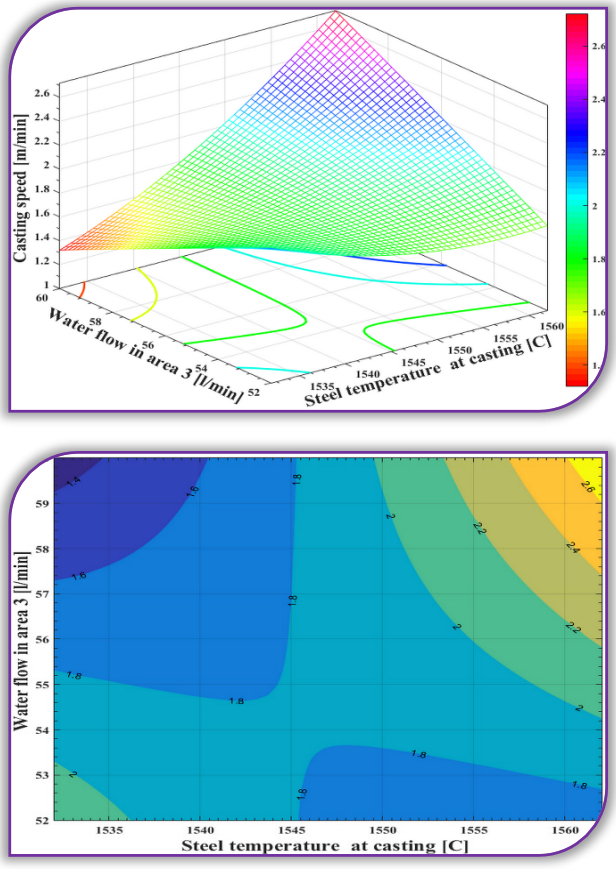

Figure 10. Casting speed=f(Steel temperature at casting, Water flow in area 3, equation 1)

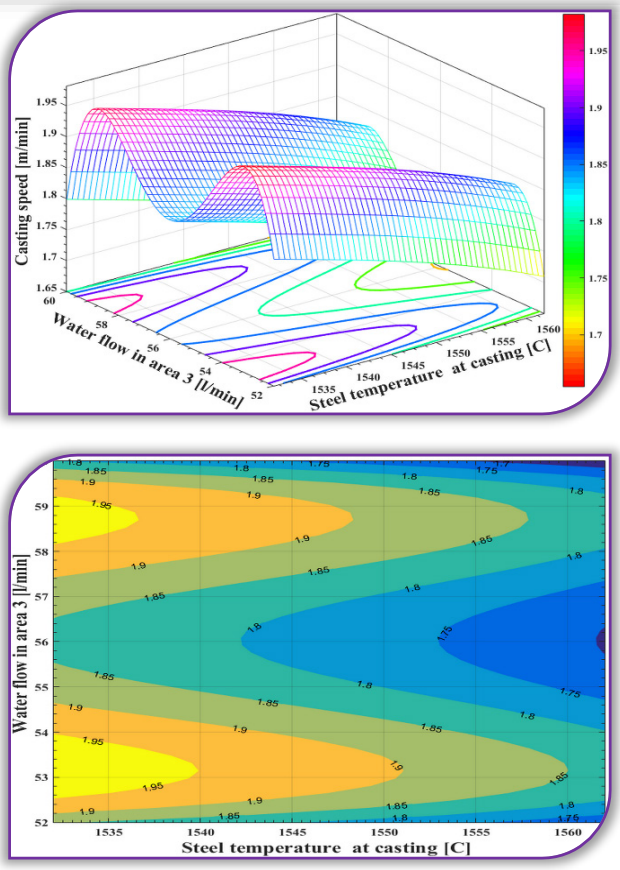

Figure 11. Casting speed=f(Steel temperature at casting, Water flow in area 3, equation 2)

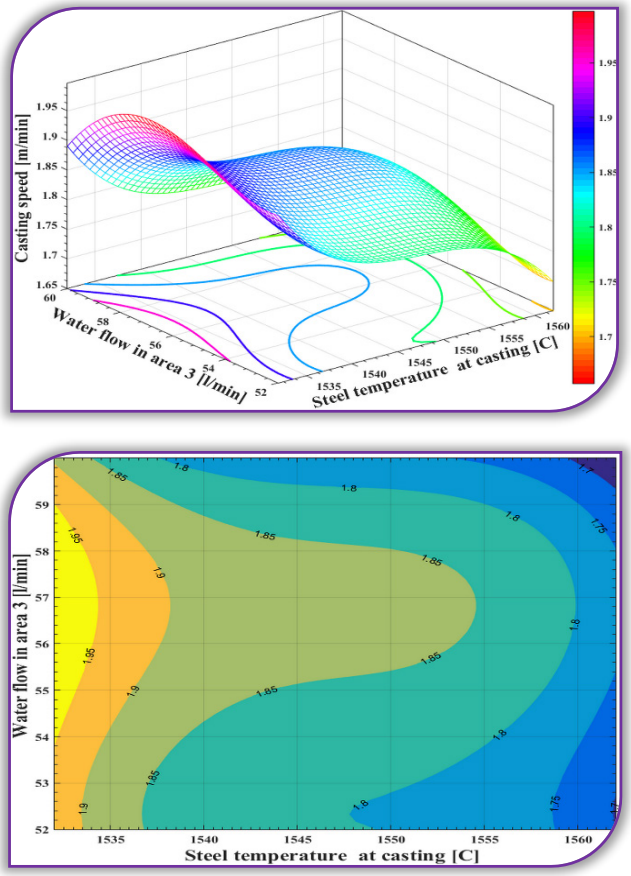

Figure 12. Casting speed= f(Steel temperature at casting, Water flow in area 3, equation 3)

TECHNOLOGICAL ANALYSIS OF THE RESULTS

After all the data gathering from the industrial experiments and then implementing them in the computing program MATLAB were obtained four groups of double correlation, using three types of correlation equations. All correlations obtained are presented as analytical and graphical representations in a technological meaning.

Regarding the casting temperature, graphs confirm that an increase in temperature causes a reduction in casting speed, which ensures optimum removal of heat from the system liquid steel-crystallizer, in the system crystallizer-cooling water, namely the system performing water-cooling from the secondary zone.

All four groups of data contain three types of correlations each and the influence of temperature has the same effect in all of them.

For example, Figure s 7, 8 and 9 establish that:

» in Figure 7 steel is at a temperature of 1550C and the flow rate of cooling water from zone 2 is 51l/min., the casting speed is 1.9m/min, and in Figure 8 is the same 1.9m/min;

» Figure 9 at the same values as Figure 7 has the casting speed of 1,95m/min, a difference of 2.62% compared to the two cases above, so in terms of practice imperceptible;

» mentioned that all four groups of data containing three types of correlations each similar results are obtained

CONCLUSIONS

Based on the research conducted the results obtained can be summarized as follows:

≡ between the parameters for the secondary cooling of the casting installation and the speed of the continuous casting of steel can be established technological correlations expressed analytically and graphically;

≡ based on graphical representations the casting speed can be chosen in advance depending on the temperature of the steel casting and water flow;

≡ the results can be used in practice for casting 180mm blanks.

Bibliography

[1.] Ioan Romulus Vasile, Turnarea continua a semifabricatelor rotunde: Notiuni teoretice minimale și notite din experienta proprie, Editura „Neutrino”, 2013

[2.] Nicolae, A., Ioana, A., Predescu C., Sandu, I.F., Sohaciu, M., Calea, G.G., Conducerea optimă a cuptoarelor cu arc electric, Ed. Fair Partners, Bucuresti, 2002.

[3.] Instrucțiuni tehnologice de lucru la cuptorul EBT, SC AcelorMittal SA Hunedoara, 2006.

[4.] Nica, Ghe., Socalici, A., Ardelean E., Hepuț, T., Tehnologii pentru îmbunătățirea calității oțelului, Ed. Mirton, Timișoara, 2003.
[5.] Drăgoi, F., Cercetări privind reducerea conținutului de gaze din oțelurile elaborate și tratate pe fluxul tehnologic E.B.T. – L.F., teză de doctorat, Universitatea Politehnica Timișoara, 2012.
[6.] Geantă, V., Procese și tehnologii de obținere a oțelurilor de înaltă puritate prin tratare în afara cuptorului. Teză de doctorat, Universitatea Politehnica București, 1998.
[7.] Schuster, M., Perfecționări în tehnica turnării continue cu implicații privind calitatea semifabricatelor, reducerea consumului de metal și creșterea productivității instalațiilor, Gazeta Tehnico Științifică, ICEM, nr.3/1980.
[8.] Butnariu, I., Geantă, V., Turnarea continuă a semifabricatelor de oțel, Editura Tehnică, București, 2000.
[9.] Ardelean, E., Hepuț, T., Ardelean, M., Turnarea continuă a oțelului, Editura Politehnica, Timișoara, 2001.
[10.] Popa E., Cercetari privind influența proceselor fizico-chimice-metalurgice ce au loc la interfețele cristalizor-zgură-oțel lichid, Ed. Politehnica Timișoara,2009
[11.] Lascuțoni A., Cercetări privind modelarea matematică a regimului termic al oțelului lichid la nivelul oală de turnare- distribuitor-cristalizor, Teză de doctorat, Universitatea Politehnica Timișoara 2014
[12.] Ardelean, E., Hepuț,T., Ardelean, M., Socalici, A., Abrudean, C., Optimizarea proceselor la turnarea continuă a oțelului, Editura CERMI, Iași, 2007
[13.] Ardelean, E., D., Turnarea semifabricatelor de oțel, Editura Mirton, Timișoara, 2004

ACTA Technica CORVINIENSIS
BULLETIN OF ENGINEERING
ISSN:2067-3809

ACTA TECHNICA CORVINIENSIS
– Bulletin of Engineering
Tome IX [2016], Fascicule 4 [October – December]
ISSN: 2067 – 3809

[1.]Peter SZUCHY

BASIC FAILURE POSSIBILITIES USING FINITE ELEMENT METHOD OF AUTODESK INVENTOR 2012 STRESS ANALYSIS

[1.]Department of Technology, Faculty of Engineering, University of Szeged, Mars tér7, Szeged, HUNGARY

Abstract: Teaching Finite Element Method (FEM) with Autodesk Inventor 2012, Statics and Strength of Materials we have collected a lot of sample how the lack of Statics knowledge and/or accurate FEM knowledge leads to incorrect results during stress analysis of Inventor. Our students use the 3D model part of the software really well but the application of Stress Analysis brings very often mistakes. Wrew are going to introduce the two most common problems that we could meet recently during the students' practice: choosing false constraints and leaving out of consideration the buckling.
Keywords: Finite Element Method, constraint, buckling

INTRODUCTION

Coaching of Autodesk Inventor, three dimensional model designing software has been executed for years on the Faculty of Engineering, University of Szeged. We have worked with Inventor 2012, thus our experiments are the widest with this version. Most of the student enjoy the creative job, discovering this playful way of self-realization.

It is good to see as their curiosity pursues them ahead on the self-supporting development. The playfulness recoils and the first mistakes are made as they reach the Stress simulation and its necessary knowledge from Statics or Strength of Materials.

The general steps of a FEM software are the following:

1. Preparing of 3D geometric model.
2. Characterising of the raw material.
3. Determination of constraints and loads.
4. Mesh settings, calculation, and valuation of the results.

Though mesh setting knowledge is a key skill in the process, in a beginner's work the most problems occur at the last two steps: determining the constraints and valuating the results.

INTRODUCTION OF Autodesk Inventor 2012 Stress Analysis

Autodesk Inventor 2012 is a user-friendly software for 3D simulation, really suitable for self-learning. It has a Stress Analysis module that usesFinite Element Method (FEM). For its use the user does not need to have deep knowledge in the math of FEM, but it is essential to have and use wellthe knowledge of Statics and Strength of Materials. The followings are recommended by the Manual [1.]: Inventor 2012 Stress Analysis is designed for estimation of deformation, stress, natural frequencies in linear static problems. It does not substitute physical testing, only identifies areas of the highest stress and deformation reducing the numbers of required physical tests. Its application is limited in the following situations:

- Non-linear material features.
- Non-linear effects (e.c.: buckling)
- Dynamic loading effects.
- Thermal influence.
- Large deformation compared to the part's dimensions.

When somebody has these circumstances further analysis is recommended.

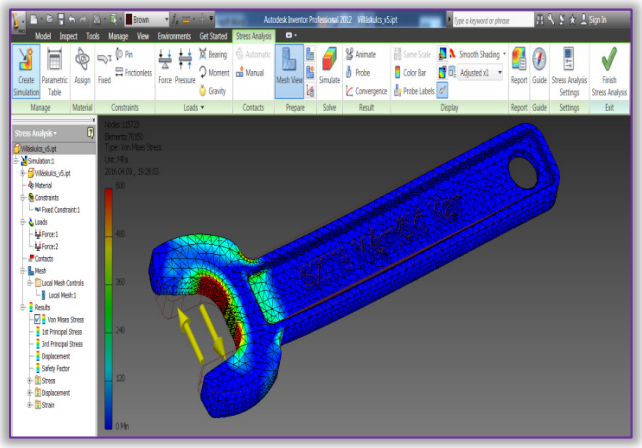

Figure 1. Stress Analysis environment of Autodesk Inventor 2012

The Autodesk Inventor 2012 has a really useable environment for Stress Analysis [Figure 1]. The Panels lead the user through the steps of analysis in logical way: Managing the simulation, setup of Materials, Constraints, Loads, Contacts, preparing Mesh and calculation, Simulation, visualizing and analysing of Result.
The beginning two steps are easy to do - even if setting Material well needs advancedknowledge. The first problem occurs at setting the constraints.

CONSTRAINT SETTING FAILURES

For setting the constraints the possibilities are the following in Inventor 2012:

1. Fixed constraint, k=6 or less, as custom needs, ("k" is the number of constraints, how many degree of freedom is tied down.)
2. Pin constraint, k=5 or 4.
3. Frictionless Constraint, k=1.

The first problem can occur if the user does not constrain fully the model and the simulation cannot be run. Often happens it when Pin and Frictionless constraints were used in combination. In this case there is a chance to set the Detect and eliminate rigid body modes when weak springs are automatically added without influencing the result [Figure 2]

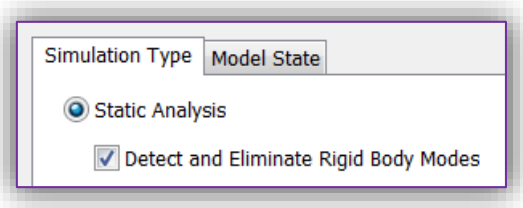

Figure 2. Preventing under constrain

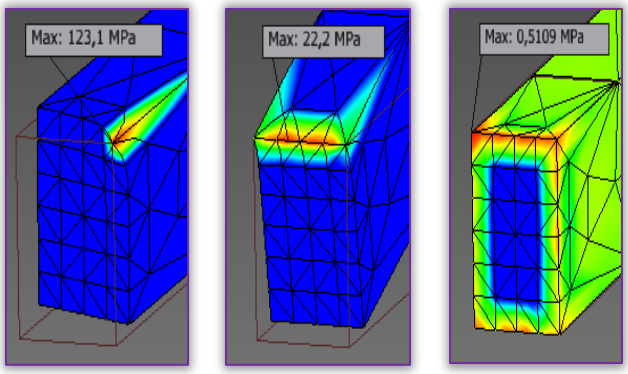

Figure 3. Pulled bar with a fixed constraint applied on: 3.a. upper right point (left), 3.b. upper edge (middle), 3.c. closing surface (right)

The second problem comes forward if the user adds the constraint to a geometry that has no surface (vertex, edge). In this case the stress in the surroundings of applied constrain will be extremely high because of the force/surface rate. Figure 3. shows a pulled bar, where fix constrain is applied on the upper right corner [3.a.], then on the upper edge [3.b.] and in the end on the whole closing surface [3.c.]. The probe labels show the maximum stress values. (Mesh settings also influencethe results.)
The previous problems are almost childish, easy to find and avoid them, but the following example isnot so obvious. Over-constraining the model can show lower stresses than they are in truth, thus it can lead to undersizing. The following example is a stress analysis of a home-made wrench [Figure 4].

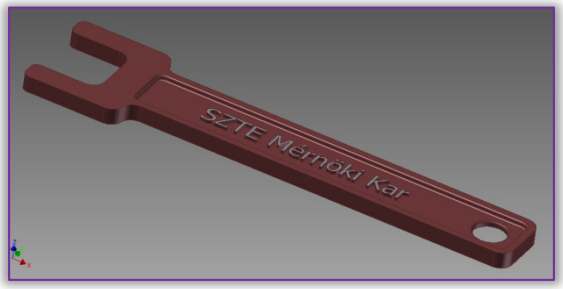

Figure 4. Home-made wrench

During the simulation two fixed constraints are put on the inner surfaces of the wrench [Figure 5]. 300 N Force is added to the end of wrench, Embossed text is excluded, than we run the simulation and analyze the result [Figure 6]. It is visible that the maximum stress occurs on both side of the neck.

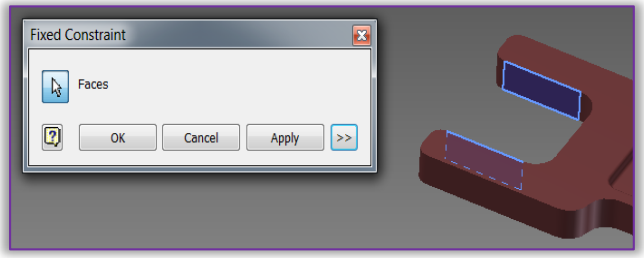

Figure 5. Fixed constraints added on the inner surfaces of fork

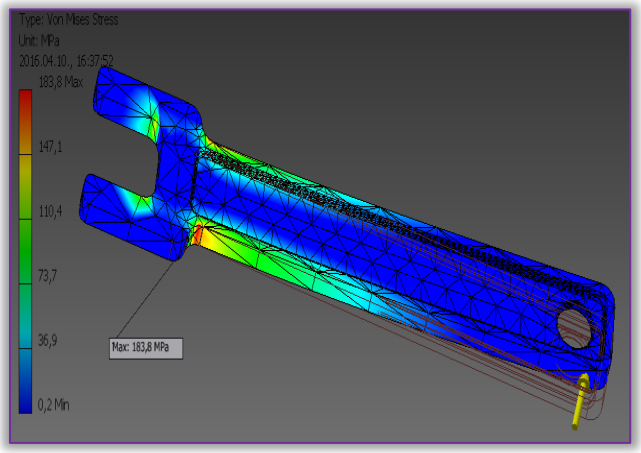

Figure 6. Maximum stresses are on the neck fixing the forks together

As we analyze the result it turns out that on the inner side of the fork's tines the image of stress is not too high, its escalation is narrow and does not correspond to the theoretical stress distribution learned in Strength of Materials [4]. Running a Local Mesh Control the result is not better. What is the problem? As we put two fixed constraints on

both tines of the fork, we fixed the two tines to each other, so they could not move independently, they strengthen each other. With these constraints we can analyze the stress only in the neck of the wrench. For better result in the tines there are several way to analyze, for example we can change the places of the constraint and the load [Figure 1.], or we can put a screw-nut between the tines, using fixed constraint to the nut.. The problem is similar to a simple bar that is constrained on both ends and loaded on the middle. If two fixed constraints are used on both ends of the bar, there will occur normal and shearing forces in the constraints and in the bar as well [Figure 7]. If one of the fixed constraints is replaced to a Frictionless constraint, the normal forces disappear [Figure 8]. The structure is more rigid in the first case.

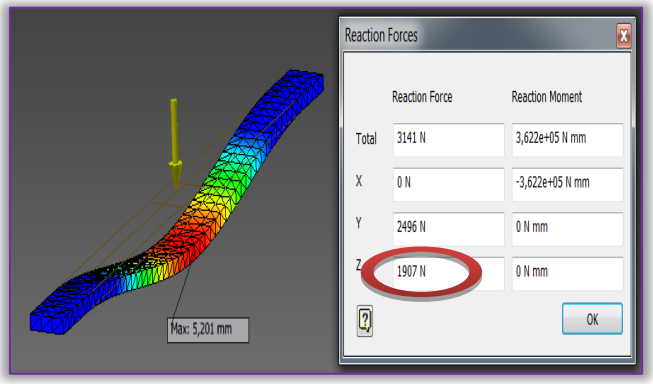

Figure 7. Bended bar with two Fixed constraints on both ends. Normal and shearing forces appear

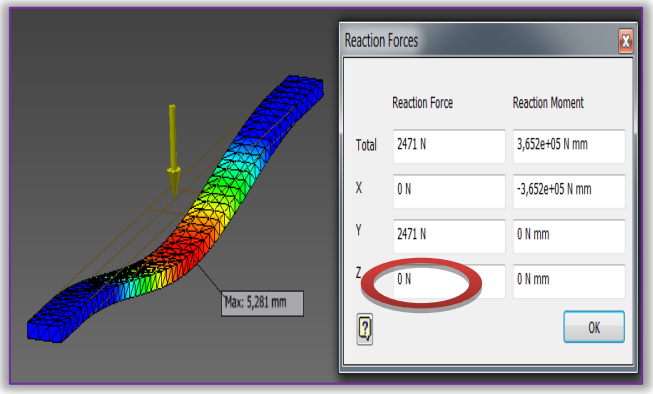

Figure 8. Bended bar with one Fixed and one Frictionless constraint. Only shearing forces appear

The same failure can be made at stress analysis of vehicle under-carriage. If somebody adds only the combination of Fixed or Pin constraints to the connecting points of wheel suspension without any Frictionless constraint, the structure will be over-constrained and it gets more than real rigidity.

BUCKLING

A bar compressed theoretically exactly in the center of mass axis has no buckling. For producing it we need some moment from unpunctuality or from the surroundings. Let's make a calculation for critical compressing force for buckling in case of a 40x100x3000 mm bar, fixed on one ending section, pressed on the other end (β=2) [3]. (The equations are well-known, I concentrate on the calculation):

$$A = 40\ \text{mm} \cdot 100\ \text{mm} = 4000\ \text{mm}^2 \quad (1)$$

$$I_2 = \frac{(40\ \text{mm})^3 \cdot 100\ \text{mm}}{12} = 533333\ \text{mm}^4 \quad (2)$$

$$i_2 = \sqrt{\frac{533333\ \text{mm}^4}{4000\ \text{mm}^2}} = 11{,}547\ \text{mm} \quad (3)$$

$$\lambda = \frac{2 \cdot 3000\ \text{mm}}{11{,}547\ \text{mm}} = 519.6\ \ (\beta = 2) \quad (4)$$

$$\sigma_{\text{critical}} = \frac{\pi^2 \cdot E}{\lambda^2} = \frac{\pi^2 \cdot 210 \cdot 10^3 \text{MPa}}{519{,}6^2} \quad (5)$$

$$\sigma_{\text{critical}} = 7{,}68\ \text{MPa} \quad (6)$$

$$F_{\text{critical}} = 7{,}68\ \text{MPa} \cdot 4000\text{mm}^2 \quad (7)$$

$$F_{\text{critical}} = 30{,}7\ \text{kN} \quad (8)$$

Without using coefficient of safety!

If the effect of buckling is not considered, the supposed allowable pressing force (F_{supposed}) from the permissible stress ($\sigma_{perm} := 150MPa$) is:

$$F_{\text{supposed}} = 150\text{MPa} \cdot 4000\text{mm}^2 = 600\text{kN} \quad (9)$$

What a difference! The Manual of Inventor 2012 [1] declares that it does not handle the buckling, but many students forget it or even do not know it. Let us see what happens, if we make a stress analysis for the compression of the above mentioned bar.

After modelling the bar we put a fixed constraint on one of the ends, 200kN Force on the other one. Figure 9.a. shows the replacement of the bar. If we double the load, the strain doubles as well, without any sign of buckling. Perhaps an above mentioned moment is missing. Let us add M=1 Nm moment to the loaded section. Figure 9.b. shows the result, and it is visible that replacement does not changed.

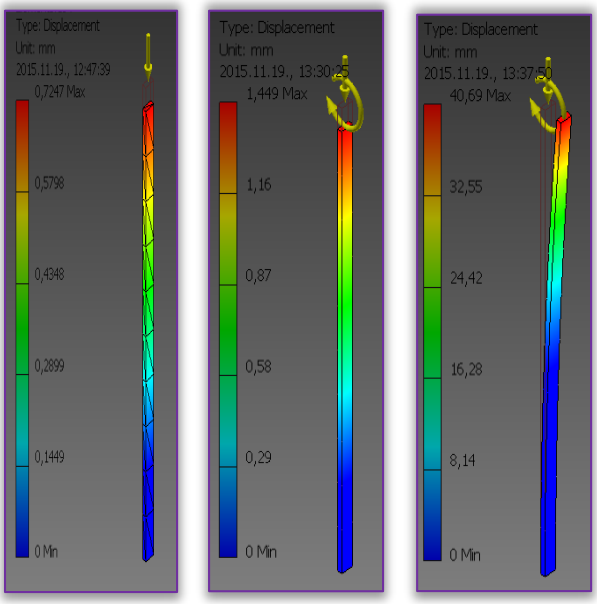

Figure 9. a. (left) Load: $F_{\text{normal}} = 200\text{kN}$, b. (middle) Load: $F_{\text{normal}} = 400\text{kN}, M = 1\text{kNm}$, c. (right) Load: $F_{\text{normal}} = 400\text{kN}, M = 1000\text{kNm}$

Increased the Moment to 1000 Nm Figure 9.c. shows the replacements. The loaded end section has moved lateral around 40 mm from its original position. The loading force is more than 10 times higher than the theoretical critical force, beside it there is inducing moment, but there is no collapse. The Manual was right. I heard this problem from students designing truss (compressed members) and driving (bearer-bar).

CONCLUSIONS

I have introduced the basic failure possibilities using Autodesk Inventor 2012 Stress Simulation. Their emergences come rather from the moderate knowledge of Statics and Strength of Material then Finite Element Method. The easiest problems, like forces, constraints without surfaces applied on, are simply to be avoided. The developer of the software declares that buckling is not considered during the FEM simulation, but people can forget it and do not calculate it plus on pushed elements. The hardest problem to find is the false constraining. Over-constraining can show more rigidity and less stress than it is indeed. False constraints can cause false results as well. How can we find the false results of FEM? Not accepting the result at once, always being suspicious and using our engineering mind: can it be true? The real answers arrive after the execution at the first tests, but with good practice we can reduce the number of the false tests.

Bibliography

[1.] Autodesk Inventor Professional 2010, Simulation, Autodesk, Inc., 462B1-050000-CM06A, June 2009.
[2.] OrbánFerenc, FEM Lectures 2014/15, Univerity of Pécs, Technical and Information Faculty, Machine construction Institute
[3.] BíróIstván: Strenth of materials, Lecture notes, University of Szeged, Technical Faculty, Szeged, 2009.
[4.] M. CsizmadiaBéla – NádoriErnő: Statics, National Coursebook Publisher, Budapest, ISBN 978-963-19-2850-1,
[5.] KovácsÁdám – UjJózsef: Basics of Finite Element Methods, Publisher of Technical University, 2007.
[6.] PáczeltIstván – SzabóTamás – Baksa Attila: Basics of Finite Element Methods, HEFOP lecture notes (electronic form, supported by: HEFOP 3.3.1-P.-2004-09-0102/1.0 tender), 2007.
[7.] KovácsÁdám - MoharosIstván - OldalIstván – SzekrényesAndrás: FINITE ELEMENT METHOD, University notes (electronic form), 2011. ISBN 978-963-279-539-3, TÁMOP-4.1.2-08/2/A/KMR-2009-0029 tender

ACTA Technica CORVINIENSIS
BULLETIN OF ENGINEERING
ISSN:2067-3809

ACTA TECHNICA CORVINIENSIS
– Bulletin of Engineering
Tome IX [2016], Fascicule 4 [October – December]
ISSN: 2067 – 3809

[1.]Kemal Çağatay SELVI, [2.]Önder KABAŞ

BENDING AND SHEARING PROPERTIES OF SOME STANDARD CARNATION (dianthus caryophyllus l.) VARIETIES STEM

[1.] Ondokuz Mayıs University, Faculty of Agriculture,
Department of Agriculture Machinery and Technologies Engineering, Samsun, TURKEY
[2.]Akdeniz University Vocational School of Technical Science,
Department of Machinery and Metal Technology, Antalya, TURKEY

Abstract: In this study, some engineering parameters such as strength and deformation were determined for five standard varieties of Carnation stem. The experiments were conducted on samples selected from carnation greenhouses in Antalya. Strength parameters consisted of maximum and bio yield force in shearing, shearing and bio yield stress, maximum energy in maximum force, maximum energy in bio yield point and modulus of elasticity. Deformation parameters are also maximum bio yield deformation and maximum breaking dilatation. The tests were conducted at five moisture contents (89.90, 88.65, 90.08, 98.54 and 88.94% (dry basis) for five different varieties (Toldo, Betsy, Jack, Loris and Naxsos), respectively. It was found that, except bending stress, shearing force, bio yield force, bending force, shearing stress, bio yield stress, energy in bio yield point, and energy in shear point were statistically different at $P < 0.05$ whereas breaking dilatation and bio yield deformation were statistically different at $P < 0.001$.
Keywords: carnation; shearing force; bending force; dianthus; harvest; cutting comp

INTRODUCTION

Growing flowers for cutting in the world began in the beginning of the 20th century and it has become an important commercial activity in many developed and developing countries, especially after the end of World War II. The total production land for ornamental plants reached about 610.000 ha. It is known that there are more than 50 countries in the world producing flowers for cutting. The most important producers of the European Union are Italy, Netherland and Spain. The countries of the European Union's produce 47 % of the total cut flower production in the world. Carnations are among the most extensively grown cut flower in the world [2].

The carnation has been commercially grown in Turkey as a cut flower crop since 1945. The cut flower production area in Turkey mostly includes carnation (43 %), followed by rose (12.5 %) and gladiolus (12 %). In Turkey, the most important export production of cut flowers is the carnation consisting of 89 % of Turkey's cut flower export. The numbers of carnation exported in 2009 were 296,218,547 stems and the amount of money obtained was 21,828,260 USD [1].

Prasada and Gupta [17] studies showed that with increasing cutting rate from 200 to 1000 mm/min the shear strength of maize stalk decreased from 3.63 to 2.10 MPa. The average values of shear strength and shear energy of grasses were reported 16 MPa and 12 mJ mm^{-2}, respectively by McRandal and McNulty [13]. Kushwaha et al., [12] investigations revealed that the average value of shear strength of wheat straw was in the range of 8.6 to 13.0 MPa. Persson [16] believes that the bevel angle of blade to be effective on force and energy of cutting process of agricultural materials. When there was no problem of stalk holding versus cutting blade, Persson [16] recommends using smooth blade for cutting of grasses due to the lower force and energy requirement. Most studies on the mechanical properties of plants have been done during their development using breakdown criteria (force, stress and the effect of shearing velocity, energy) and the Young's modulus (Annoussamy et al., [3]; Hirai et al., [9]). Khazaei et al., [17] reported that with increasing cutting rate from 20 to 200 mm min^{-1} the shear strength of pyrethrum stalk decreased. The maximum values of shear force and energy for cutting of hemp were 243 N and 2.1 J, respectively [5]. Ince et al. [10] reported that the maximum shear stress and specific shear energy of sunflower stalks were 1.07 MPa and 10.08 mJ mm^{-2}, respectively. The

physical properties of the cellular material are important for cutting, compression, tension, bending, density and friction [19-21].

Literature survey showed that there was no detailed study concerning the same engineering parameters (shear strength and shear energy) of the carnation stem. This study was carried out in determining strength parameters such as maximum force and bio yield force in shearing, shearing and bio yield stress, maximum energy in maximum force, maximum energy in bio yield point, modulus of elasticity and deformation parameters such as maximum bio yield deformation, maximum breaking dilatation of the carnation stem and different varieties of carnation. The obtained data would be useful in designing and developing harvesting equipment for the carnation.

MATERIAL AND METHODS

Seedling of five carnation varieties (Dianthus caryophyllus L. cv.' Toldo, Betsy, Jack, Loris and Naxos, which is a standard type) were planted on 01 June 2010 in plots (1.25 m long and 1.0 m wide) with a plant density of 32 plants m^{-2} (with four rows), and each plot contained 40 plants. Carnations were grown following regular farmer practices and randomly harvested manually from a plastic greenhouse in a field located southern Antalya, Turkey. During cutting tests, samples were stored in plastic bags in a refrigerator to keep them from drying further. Plants from October, 2010-harvest season were used in all the experiments.

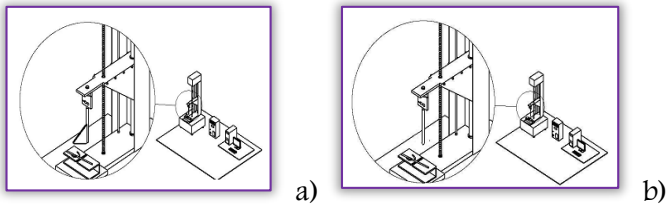

a) b)

Figure1. Computer-aided (a) cutting and (b) bending system's equipment

All of the tests were done at the Biological Test Devices, Laboratory of Agriculture Machinery, Akdeniz University, Antalya, Turkey. Carnations were harvested at moisture contents of 89.90 %, 88.65%, 90.08%, 98.54% and 88.94% (d.b.) in five varieties (Toldo, Betsy, Jack, Loris and Naxsos), respectively. In order to determine the variable of carnation, cutting apparatus was used (Figure 1a). The cutting and bending system had three main components: a stable forced and moving platform (slot, knife), a driving unit and a strain-gauge load cell (Figure 2).

The diameter of the specimen was measured by micrometer, and the specimen was weighed, oven-dried at 102°C for 24 h and then weighed again to determine the moisture content. The samples were for each carnation varieties; the 30 samples were randomly selected from the harvested carnations varieties. The average and SD values of the cross-sectional dimensions of carnation stem were 5.2±0.3, 5.8±0.2, 6.1±0.3, 5.6±0.3 and 4.8±0.2 mm, in five varieties (Toldo, Betsy, Jack, Loris and Naxsos), respectively.

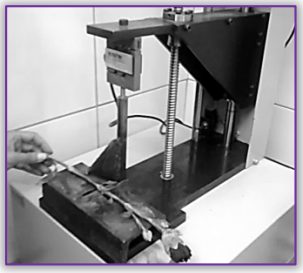

Figure 2. Cutting of carnation stem

There are three methods of positioning a cutting edge relative to counter edge defined as perpendicular, oblique and oblique variable for these studies. In the present study, perpendicular cutting was employed, since most researchers have used this method to determine the cutting forces of biological materials [10-11, 20]

The sliding plate was loaded at the range of 30 mm min^{-1} and, as for shear test, a strain-gauge load cell measured the applied force and a force-time record obtained up to the specimen failure. The shearing stress τ in MPa was calculated based on Eq. (1) and also reported by previous studies [5-7-10,14].

$$\tau = F_{smax} / A \quad (1)$$

where, F_{smax} was the maximum shearing force of curve, N; A was the wall area of the specimen at the failure cross-sections, mm^2. The knife displacement was computed and the forces versus displacement curves were plotted for each stem diameter.

To determine modulus of elasticity, the stems were arranged with major axis of the cross-sections in the horizontal plane and placed on the slot. A strain gage load cell measured the bending force and a force time record obtained up to the failure of the specimen (Figure 1b).

Most specimens were slightly elliptical in cross-section and second moment of area in bending about a major axis (I_b) was calculated based on equation (Eq. (2)), [7-8]:

$$I_b=\pi/4[ab^3-(a-t)(b-t)^3] \quad (2)$$

Where "a" is the semi major axis of the cross–section in mm, "b" is the semi minor axis of the cross-section in mm and "t" is the mean wall thickness in mm. Modulus of elasticity was assessed using a three–point bending test similar to those described by previous studies (Figure 1b) [14].

The modulus of elasticity, E, was calculated from the expression obtained for a simply supported beam located at its center (Eq. (3)), [6-20]:

$$E=F_bI^3/48\delta I_b \quad (3)$$

where, F_b was the applied load, N; I was the distance between the metal supports, mm; δ was the

deflection at the specimen center, mm; and I_b the second moment of area, in mm^4.

A sample force-displacement curve of the carnation stem was similar to that for straight cut against a counter shear reported (Figure 3) [20]. The curve explained three sections: A, B and C, representing compression only, compression and cutting and cutting only, respectively. In section A, the force increased from zero at the moment of initial contact between the knife and the stem, and then decreased due to the failure in stem structure. The compression continued in section B along with cutting as the knife moved. When the force reached its peak point, pure cutting took place in section C and the force dropped as the cutting was completed.

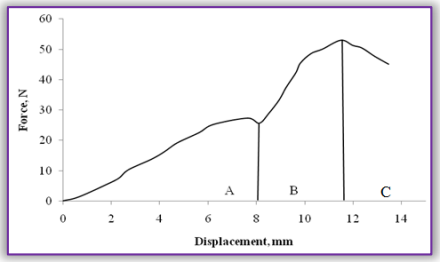

Figure 3. The force versus displacement curve for carnation

The bio yield forces, bio yield stress, bio yield deformation and maximum breaking dilatation were calculated by using the force curves [4-5-7,10]. Maximum energy in maximum force and maximum energy in bio yield point were calculated as the area (evaluated by numerical integration) beneath the entire force displacement. Maximum breaking dilatation is described as the rate of the total dilation to first length of the carnation stems. Bio yield deformation and maximum breaking dilatation were calculated by using computer program.

RESULT AND DISCUSSION

The initial moisture content of the samples were 89.90 %, 88.65%, 90.08%, 98.54% and 88.94% (d.b.) in five varieties (Toldo, Betsy, Jack, Loris and Naxsos), respectively. The results with respect to mechanical characteristics of carnation varieties together with statistical analysis are presented Tables 1 and 2. It was found that, except bending stress, shearing force, bio yield force, bending force, shearing stress, bio yield stress, energy in bio yield point, and energy in shear point were statistically different at $P < 0.05$ whereas breaking dilatation and bio yield deformation were statistically different at $P < 0.001$ (Table 1). These differences are due to different mechanical, physical and physiological properties of stem varieties. This information is very useful for selecting suitable equipment design [18]. Also work performance and efficiency productivity and quality as well as user comfort and safety of work can be improved [15].

Table 1. Variance analyzes results with respect to mechanical characteristics of carnation varieties

Source of variation	d.f.	Characteristics (variable)									
		Shearing force (N)	Bioyield force (N)	Bending force (N)	Shearing stress (MPa)	Bioyield stress (MPa)	Bending Stress (MPa)	Energy in bioyield point (J)	Energy in shear point (J)	Breaking dilatation (mm)	Bioyield def. (mm)
Replication	9										
Varieties (V)	4	***	***	***	***	***	N.S.	***	***	*	*
Error (V)	36										
Total	49										

N.S.: Not significant, * Sinificant at P<0,05, *** Sinificant at P<0,001

Table 2. The average values of mechanical characteristics in carnation varieties

Mechanical Characteristics	Betsy	Loris	Toldo	Jack	Naxos
Shearing force (N)	43.34 c*	55.65 b	53.24 b	74.47 a	38.57 c
Bio yield force (N)	17.94 b	39.84 a	23.93 b	40.60 a	14.30 b
Bending force (N)	7.74 b	11.40 a	8.12 b	10.98 a	6.55 b
Shearing stress (MPa)	6.25 b	8.29 ab	8.05 ab	9.37 a	7.77 ab
Bio yield stress (MPa)	2.51 b	5.93 a	3.57 ab	5.22 ab	2.88 ab
Bending stress (MPa)	1.12	1.71	1.23	1.39	1.32
Energy in bio yield point (J)	38.62 c	108.34 ab	87.70 b	131.46 a	20.57 b
Energy in shear point (J)	140.36 c	264.14 a	212.25 b	266.49 a	123.78 c
Breaking dilatation (mm)	10.85 b	11.23 b	12.84 a	11.44 ab	11.06 b
Bio yield deformation (mm)	6.99 ab	7.78 ab	8.16 ab	8.57 a	6.42 b

*Different letters show different means according to Duncan test results at 5 % confidence interval.

The highest shearing force, bio yield force, bending force, shearing stress, energy in bio yield point, and energy in shear point, and bio yield deformation were obtained Jack variety (Table 2). Selection of suitable cutting apparatus and equipment plays an important role on shearing cutting force requirements. According to our results the cutting properties of carnation stems varied as a function of the variety.

As can be seen in Table 2, average values for shearing force were 43.34, 55.65, 53.24, 74.47 and 38.57 N for varieties of Betsy, Loris, Toldo, Jack and Naxos, respectively and average value of bending force were 7.74, 11.40, 8.12, 10.98 and 6.55 N for varieties of Betsy, Loris, Toldo, Jack and Naxos, respectively. The maximum value of energy in shear point was 266.49 J for Jack stems, among the five varieties investigated and the minimum value was 123.78 J for Naxos.

The maximum value of shearing and bio yield force was 74.47 N and 40.60 N for Jack stems, among

the five varieties investigated and the minimum value was 123.78 N and 14.30 N for Naxos but the maximum value of bending force (11.40 N) was obtained at Loris and the minimum value of its (6.55 N) was obtained at Naxos. The highest shearing, bio yield and bending stress (9.37, 5.93 and 1.71 MPa, respectively) were obtained at Jack variety for shearing and bio yield stress and Loris variety for bending stress. The lowest shearing, bio yield and bending stress (6.25, 2.51 and 1.12 MPa, respectively) were found at Betsy variety.

The highest breaking dilatation was obtained for Toldo while the lowest was for the Betsy variety and the highest bioyield deformation was obtained for Jack while the lowest was for the Naxos variety. The highest shearing and bioyield stress (9.37 and 5.93 MPa) were obtained at variety of Jack and Loris, respectively, the lowest shearing and bioyield stress (6.25 and 2.51 MPa) were obtained at variety of Betsy.

The study results showed that there is significant difference between mean values of mechanical characteristics of carnation based on the variety. Study results could be considered in designing the prototype or realization of a good cutting.

CONCLUSIONS

Variety of carnation is the important factor affecting shearing force, bio yield force, bending force, shearing stress, bio yield stress, energy in bio yield point, and energy in shear point, Breaking dilatation and bio yield deformation of the carnation stem.

Shearing force, bio yield force, bending force, shearing stress, bio yield stress, energy in bio yield point, and energy in shear point, were statistically different at $P < 0.05$ among the studied varieties. Breaking dilatation and bio yield deformation were statistically different at $P < 0.001$, among the studied varieties.

There was no significant difference among the bending stress of Betsy, Loris, Toldo, Jack and Naxos. Jack variety with 74.47 and 40.60 N had the highest shearing and bioyield force and highest energy in bioyiled and shearing point with 266.49 and 131.46 J, respectively, among the studied varieties.

As a result, it was showed that, the Shearing force, bio yield force, bending force, shearing stress, bio yield stress, energy in bio yield point, and energy in shear point are related to carnation stems' physical and mechanical properties.

Acknowledgements

This study was partly supported by the Department of Agriculture Machinery, Akdeniz University and Batı Akdeniz Agricultural Research Institute. Antalya, Turkey

References

[1.] AIB (2010) Cut Flower Export Report. Republic of Turkey Prime Ministry, Undersecretariat for Foreign Trade Antalya Exporter Union. Antalya, Turkey.
[2.] AIPH (2007) International Statistics Flowers and Plants. Volume 55, Ed. by Florian Heinrichs, Belgium.
[3.] Annoussamy. M, Richard. G, Recou. S, Guerif. J, Change in mechanical properties of wheat straw due to decomposition and moisture. App. Eng. Agric., 16(6): 657-664. (2000)
[4.] Chattopadhyay. P.S, Pandey. K.P, Mechanical properties of sorghum stalk in relation to quasi-static deformation. J. Agric. Eng. Res., 73: 199–206. (1999)
[5.] Chen. Y, Louis. J, Gratton. L.J, Power requirements of hemp cutting and conditioning. Biosys. Eng., 87(4): 417-424. (2004)
[6.] Crook. M.J, Ennos. A.R, Stalk and root characteristics associated what lodging resistance in poor winter wheat cultivars. J. Agric. Sci., 126: 167–174. (1994)
[7.] Galedar. M.N, Tabatabaeefar. A, Jafari. A, Sharifi. A., Rafiee. S, Bending and shearing characteristic of Alfalfa stalks. Agricultural Engineering International The CIGR Journal, Manuscript FP 08 001. Vol. X. (2008)
[8.] Gere. J.M, Timoshenko. S.P, Mechanics of Materials. 4th edn. (PWS Publishing, Boston 1997)
[9.] Hirai. Y, Inoue. E, Mori. K, Hashiguchi K, Analysis of reaction horses and posture of a bunch of crop stalks during reel operations of a combine harvester. Agricultural Engineering International the CIGR J., Manuscript FP 02-002, Vol. IV. (2002)
[10.] Ince. A, Ugurluay. S, Güzel. E, Özcan. M.T, Bending and shearing characteristics of sunflower stalk residue. Biosystems Eng. 92(2): 175-181. (2005)
[11.] Khazaei. J, Rabani. H, Golbabaei. F, Determining the shear strength and picking force of pyrethrum flower. Iranian J. Agric. Sci. 33(3): 433-444. (2002)
[12.] Kushwaha. R.L, Vashnav. A.S, Zoerb. G.C, Shear strength of wheat straw. Can. Agric. Eng., 25(2): 133-142. (1983)
[13.] Mcrandal, D.M, Mcnulty. P.B, Mechanical and physical properties of grasses. Trans. ASAE, 23(4): 816-821. (1980)
[14.] Mohsenin, N.N, Physical Properties of Plant and Animal Materials. (Gordon and Breach Sci, New York 1970).
[15.] Paivinen. M, Heinimaa. T, The effects of different hand tool blade coatings on force demands when cutting wood. International Journal of Industirial Ergonomics. 32 (2203). 139-146. (2003).
[16.] Persson. S, Mechanics of cutting plant material. (ASAE Publications, Michigan, 1987).
[17.] Prasada. J, Gupta. CB, Mechanical properties of maize stalks as related to harvesting. J.Agric. Eng. Res., 20(1): 79-87. (1975)
[18.] Sessiz. A, Esgici. R, Özdemir. G, Eliçin. A.K, Pekitkan. F.G, Cutting properties of different grape varieties. Agriculture &, Foresttry. Vol. 6 Issue 1:211-216. Podgorica. (2015)
[19.] Shaw. M.D, Tabil. L.G, Compression, relaxation and adhesion properties of selected biomass grinds. Agricultural Engineering International the CIGR Journal, Manuscript FP 07- 006, Vol. IX. (2007)
[20.] Srivastava. A.K, Goering. C.E, Rohrbach. R.P, Buckmaster. D.R, Engineering Principles of Agricultural Machines. 2nd ed. ASABE, St. Joseph, MI. (2006)
[21.] Yiljep. Y.D, Mohammed. U.S, Effect of knife velocity on cutting energy and efficiency during impact cutting of sorghum stalk. Agricultural Engineering International the CIGR Journal, Manuscript PM, 05-004, Vol. VII. (2005)

ACTA TECHNICA CORVINIENSIS
– Bulletin of Engineering
Tome IX [2016], Fascicule 4 [October – December]
ISSN: 2067 – 3809

[1.]Olutosin O. ILORI, [2.]D.A. ADETAN, [3.]L.E. UMORU

EFFECT OF CUTTING PARAMETERS ON THE SURFACE ROUGHNESS GENERATED DURING FACE MILLING OF PEARLITIC DUCTILE IRON WITH CEMENTED CARBIDE TOOL

[1.]Department of Mechanical Engineering, Adeleke University, Ede, NIGERIA
[2.]Department of Mechanical Engineering, Obafemi Awolowo University, Ile-Ife, NIGERIA
[3.]Department of Material Science and Engineering, Obafemi Awolowo University, Ile-Ife, NIGERIA

Abstract: This study examined the effect of cutting parameters on the surface roughness generated during face milling operation ofa pearlitic ductile iron using cemented carbide tool. The pearlitic ductile iron used for the study was prepared from scraps of ferrous metals using 100 kg rotary furnace at the Engineering Materials Development Institute (EMDI), Akure, Nigeria. Four cutting parameters were considered for the study, namely; cutting speed, feed rate, depth of cut and cutting fluid flow rate. The experimentation was based on Taguchi's design approach. The data collected were subsequently subjected to analysis of variance.The average surface roughness of machined surfaces, increased as depth of cut increased. The effect of increase in feed rate and cutting speed was to reducethe average surface roughness, though not statistically significant. On the other hand, surface roughness decreased significantly with increase in cutting fluid flow rate and depth of cut. The average surface roughness value was highest at zero fluid flow rate and lowest at the flow rate of 4 l/min. The study concluded that out of all four cutting parameters investigated, the cutting fluid flow rate had most considerable positive influence on the surface roughness of a machined pearlitic ductile iron.
Keywords: surface roughness, cutting parameters, face milling, pearlitic ductile iron

INTRODUCTION

Surface integrity is the sum of all elements that describe the conditions existing on the surface of a finished hardware. It is built up by the geometrical values of the surface such as surface roughness and the physical properties such as residual stresses, hardness and structure of the surface layers (Field and Kahles, 1971). These properties are critical to the functionality of machined components. Thus, a good understanding of surface generation mechanisms can be used to optimize machining processes and thereby improve component functionality.

The demand for high quality and fully automated production focuses attention on the surface condition of the product, especially the roughness of the machined surface, because of its effect on product appearance, function, and reliability. For these reasons, it is important to maintain consistent tolerances and surface finish (Hayajneh et al., 2007). Moreover, the quality of the machined surface is useful in diagnosing the stability of the machining process, where a deteriorating surface finish may indicate workpiece material non-homogeneity, progressive tool wear, cutting tool chatter, etc. Surface roughness affects several functional attributes of parts, such as wearing, heat transmission, and ability of holding a lubricant, coating, or resisting fatigue. Hence, the desired surface finish is usually specified and the appropriate processes are selected to obtain the required quality.

A number of factors influence the final surface roughness in end milling operation (Hayajneh et al., 2007). Factors such as spindle speed, feed rate and depth of cut that control the cutting operation can be setup in advance. However, factors such as tool geometry, tool wear, and chip formation, or the material properties of both tool and workpiece are uncontrolled.

Numerous investigations have been conducted to determine the effect of parameters such as feed rate, tool nose radius, cutting speed and depth of cut on surface roughness in turning operations (Thiele and Melkote, 1999). These investigations show consistently that the surface roughness is predominantly a function of the feed rate. Arunachalam et al. (2004) studied the surface

roughness generated when facing age hardened Inconel 718 using cubic-boron-nitride (CBN) cutting tools as a function of cutting speed, depth of cut and coolant. They reported that the values of surface roughness decreased with increase in the cutting speed, the coolant used generated good surface roughness that is free from deposited built-up edges and lower depth of cut resulted in better surface roughness. Also, Hayajneh et al. (2007) studied the effect of machining parameters (spindle speed, cutting feed rate and depth of cut) on the surface roughness in the end milling process. They observed that cutting feed rate is the most dominant factor that influenced the surface finish of the machined workpiece significantly.

Kuram et al. (2010) investigated the effect of different types of cutting fluid and cutting parameters on surface roughness and thrust force during drilling of AISI 304 austenitic stainless steel using HSS tool. They reported that increase in the spindle speed decreased the surface roughness value and the thrust force value; an increase in the feed rate increased the surface roughness and the thrust force values. They also observed that the cutting fluids used were effective in reducing surface roughness and thrust force as spindle speed increased at the lowest feed rate. Zhang et al. (2007) conducted a research on surface roughness optimization in an end-milling operation using the Taguchi design method. Yusuf et al. (2010) also conducted a research on the effect of cutting parameters on the surface roughness of titanium alloys using end-milling process.They employed the Taguchi design method to optimize the surface roughness quality in a computer numerical control (CNC) end mills. Their experimental results indicated that spindle speed is the most significant factor affecting the surface roughness quality and tool life, followed by type of end mills tool, feed rate and depth of cut in that order.

Rech and Moisan (2003) studied the influence of feed rate and cutting speed on the surface roughness of case-hardened 27MnCr5 steel in hard turning. In their study, the feed rate was the main parameter that influenced the surface roughness compared to the influence of cutting speed. The hard turning process is interesting with regards to its capacities to produce a low surface roughness during a long cutting time. Gunnberg et al. (2006) studied the influence of cutting parameters like tool rake angle, tool nose radius, cutting speed, cutting depth and feed rate on surface topography during hard turning of 18MnCr5 case carburized steel using poly cubic-boron-nitride (PCBN) cutting tool inserts. They reported from their study that the surface roughness values were mainly influenced by the feed rate and tool nose radius. Also, Jacobson et al. (2002) examined the effect of cutting speed on surface roughness in the hard turning of bainite steel B8. They reported that increase in the cutting speed increased the surface roughness. At low cutting speed the surface roughness was found to be minimum.

This study examined the effect of some machining parameters on the surface roughness generated in the face milling of locally produced pearlitic ductile iron.

EXPERIMENTAL PROCEDURE

Material Preparation

The pearlitic ductile iron used for this study was cast at Engineering Materials Development Institute (EMDI), Akure, Ondo state, Nigeria, using a rotary furnace of 100 kg capacity designed and built by the Institute.

Small sample of castings obtained was appropriately ground and polished with the SBT Model 900 and Metaserv 2000 grinder/ polisher with emery paper grits 60, 120, 240, 320, 400 and 600, for metallographic examination. The etchant was prepared from 2% nitric acid and 98% alcohol (Nital). Nikon Eclipse ME600 metallurgical microscope of x200 magnification was used to carry out the microstructural examination. The micrograph (Figure 1) shows ductile iron containing nodular graphite in a matrix of pearlite with small amount of ferrite at 500 magnification (500x).

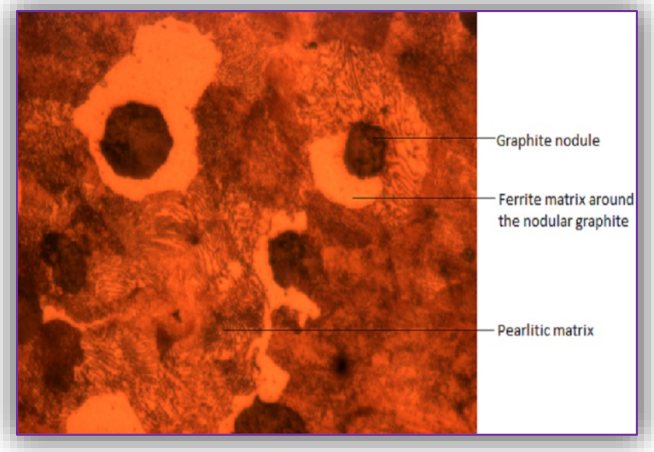

Figure 1: Micrograph of as-cast Pearlitic Ductile Iron showing Graphite Nodules (x500)

The chemical composition of the pearlitic ductile iron as obtained with EDS (Energy Dispersive Spectrometer) analysis is shown in Table 1; its mechanical properties were obtained using Nano-indenter and are shown in Table 2. Table 1 shows that the material is iron rich with 93.17% iron, 3.6% carbon, 2.9% silicon, 0.25% manganese, 0.025% sulphur, 0.01% magnesium and 0.045% phosphorus. This is similar to ASTM A536 100-70-03 specification for pearlitic ductile iron. Castings of the pearlitic ductile iron which were retrieved

from the moulds after cooling to room temperature were sectioned with a power hacksaw. All sectioned castings were subjected to annealing heat treatment by heating to temperature of 650°C, holding at this temperature for four hours and furnace-cooling to relieve all residual stresses induced during the casting process.

Table 1: The Chemical Composition of the Pearlitic Ductile Iron

Elements	% (Weight)
C	3.6
Si	2.9
Mn	0.25
S	0.025
Mg	0.01
P	0.045
Fe	93.17

Table 2: The Mechanical Properties of the Pearlitic Ductile Iron

Properties	Value (Unit)
Brinell HardnessAverage	277
Tensile Strength	690 MPa
Yield Strength	483 MPa
Elongation	3 %

Table 3: Combination of the Cutting Parameters used for Experimentation

Experimental Run	Factors			
	Depth of Cut (mm)	Feed Rate (mm/rev)	Cutting Speed (rev/min)	Cutting Fluid Flow Rate (l/min)
1	0.2	10	200	0.0
2	0.2	20	600	1.0
3	0.2	30	1000	2.0
4	0.2	40	1400	3.0
5	0.2	50	1800	4.0
6	0.4	10	600	2.0
7	0.4	20	1000	3.0
8	0.4	30	1400	4.0
9	0.4	40	1800	0.0
10	0.4	50	200	1.0
11	0.6	10	1000	4.0
12	0.6	20	1400	0.0
13	0.6	30	1800	1.0
14	0.6	40	200	2.0
15	0.6	50	600	3.0
16	0.8	10	1400	1.0
17	0.8	20	1800	2.0
18	0.8	30	200	3.0
19	0.8	40	600	4.0
20	0.8	50	1000	0.0
21	1.0	10	1800	3.0
22	1.0	20	200	4.0
23	1.0	30	600	0.0
24	1.0	40	1000	1.0
25	1.0	50	1400	2.0

Face milling tests

The face milling tests were carried out at Engineering Materials Development Institute (EMDI), Akure, Ondo State, Nigeria, using cemented carbide cutting tool (Grade YG6 and Type 4160511) and soluble oil as cutting fluid. A 3-axis CNC vertical machining centre (PRODIS PDC-650H machine centre) with spindle speed up to 10,000 rpm and power output of 15kVA was used for the test. Four cutting parameters were considered for the experimentation, namely; depth of cut, feed rate, cutting speed and cutting fluid flow rate. Five levels were assigned to each parameter. Taguchi's experimental design approach was used to drastically reduce the number of experimental runs required because it uses special design of orthogonal arrays to study the entire parameter space with a small number of experiments. Table 3 shows the levels of cutting parameters considered and how they were combined in accordance with Taguchi's design to obtain the 25 experimental runs used for this study.

Nano-indenter with Atomic Force Microscope (AFM) compartment was used to examine the surface roughness of the machined parts without indentation (see Appendix). The data collected were subjected to analysis of variance (ANOVA).

RESULTS AND DISCUSSION

The values of surface roughness generated during the face milling operation at various combinations of values of cutting parameters used in this study are presented in Table 4.

Table 4: Effect of the Cutting Parameters on the Surface Roughness Generated during Face Milling of the Pearlitic Ductile Iron

Depth of Cut (mm)	Feed Rate (mm/rev)	Cutting Speed (rev/min)	Cutting Fluid Flow Rate (l/min)	Surface Roughness RMS (nm)
0.2	10	200	0	101.78
0.2	20	600	1	66.25
0.2	30	1000	2	49.63
0.2	40	1400	3	20.07
0.2	50	1800	4	18.98
0.4	10	600	2	64.47
0.4	20	1000	3	30.41
0.4	30	1400	4	21.73
0.4	40	1800	0	102.92
0.4	50	200	1	90.28
0.6	10	1000	4	40.05
0.6	20	1400	0	107.77
0.6	30	1800	1	95.71
0.6	40	200	2	56.91
0.6	50	600	3	50.47
0.8	10	1400	1	97.66
0.8	20	1800	2	69.66
0.8	30	200	3	61.39
0.8	40	600	4	51.13
0.8	50	1000	0	132.85
1.0	10	1800	3	75.16
1.0	20	200	4	47.00
1.0	30	600	0	154.70
1.0	40	1000	1	101.94
1.0	50	1400	2	96.26

Statistical analysis established that the effect of feed rate and cutting speed were not significant on the surface roughness. ANOVA and Duncan multiple range test established that depth of cut and cutting fluid flow rate have statistically significant influence on the average surface roughness generated (Table 5).

Table 5: ANOVA for Surface Roughness

Factors	Degree of freedom	Sum of squares	Mean square	Variance	Percentage contribution (%)
Depth of Cut	4	5856.032	1464.008	54.11	19.06
Feed rate	4	794.590	198.647	7.34	2.59
Cutting speed	4	1202.059	300.515	11.11	3.91
Cutting fluid flow rate	4	22875.625	5718.906	211.32	74.44
Residual (error)	8	216.451	27.061	-	-
Total	24	30728.306	-	-	-

Effect of feed rate on surface roughness

Effect of feed rate on the surface roughness generated during face milling operation was not statistically significant. Figure 2 shows how the surface roughness varies with feed rate at the average cutting speed, cutting fluid flow rate and depth of cut values of 1000 rev/min, 2 l/min and 0.6 mm respectively; it shows no definite trend.

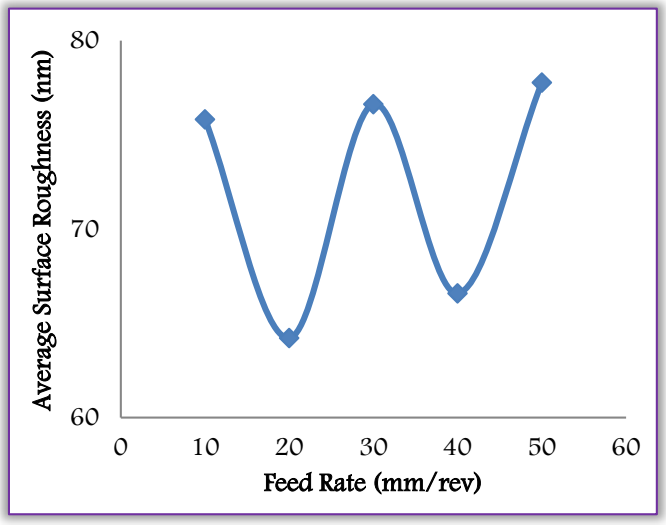

Figure 2: Observed variation of average Surface Roughness with feed rate

It is obvious from the Figure that the variation observed is merely a random one that may be due to experimental error. Grzesik and Zak (2012) stated that for higher feed rate, surface roughness produced by oblique turning is substantially lower than that generated by lower feed rate. Their observation was thought to be due to high milling cutter vibration and tool wear rate caused by low feed rate. This disagreed with reports of Navas et al. (2012), Bajic et al. (2008), Rech and Moisan (2003), and Capello et al. (1999) who reported increase in the surface roughness as feed rates increased. They emphasized that feed rate is the main factor influencing the surface roughness, due to the geometrical relations between the feed, tool nose radius and roughness in turning operations. However, in machining operations, other cutting parameters also influence surface roughness, because of the material behavior under large deformations.

Kuram et al. (2010) also reported that an increase in the feed rate increased the surface roughness values since an increase in feed rate increased the materials removal rate. Also, Hughes et al. (2004) showed that an increase in feed rate resulted in a larger surface roughness value due to more feed marks. Similarly, Thiele and Melkote (1999), and Franco et al. (2004) also stated that the more the increase in the values of feed, the more the surface deteriorates in face milling with round insert cutting tools. These observations are at variance with the result of this study perhaps because the feed rate values used in this work are much larger than those used in the earlier studies.

Effect of cutting speed on surface roughness

Figure 3 illustrates the variation in the surface roughness with increase in cutting speeds at average depth of cut, feed rate and cutting fluidflow rate values of 0.6 mm, 30 mm/rev and 2 l/min respectively. The variation has no definite trend and it is therefore not statistically significant.

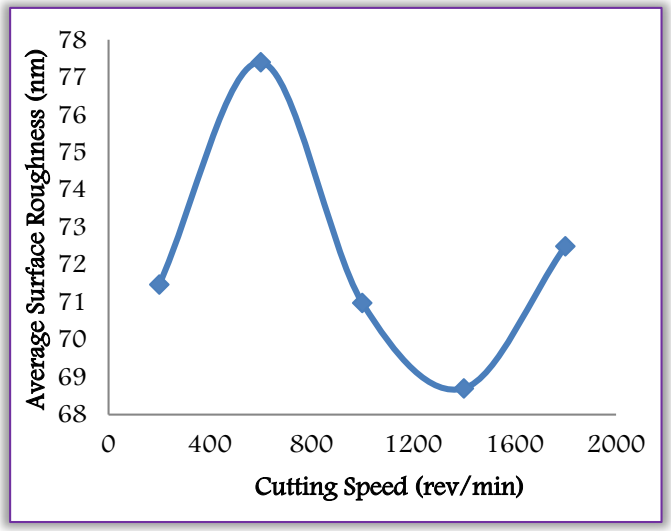

Figure 3: Variation of average Surface Roughness with cutting speed

The average surface roughness increased as cutting speed increased from 200 – 600 rev/min and decreased between cutting speeds of 600 and 1400 rev/min. As cutting speed increased beyond 1400

rev/min, the surface roughness increased again. Across all speeds, the range of surface roughness variation is quite narrow (68.69 – 77.40 nm) and appears more or less like a random variation; indeed, ANOVA established that it is statistically insignificant at 5% significance level. Lopez de lacalle et al. (2000) reported that with the increase of cutting speed, surface roughness value first increased and then decreased with the tool wear progression in milling using hard solid mills. On the other hand, Uyaner et al. (2012) observed in machining of ADI (Austempered Ductile Iron) that the surface roughness values decreased with increasing cutting speed until a limit (1400 rev/min) when it started to increase. This appears to agree perfectly with the results observed in this study in the speed range, 600 – 1800 rev/min.

The observed increase in the surface roughness as speed increased from 1400 – 1800 rev/min could be attributed to the possible increase in tool wear at high cutting speeds. The temperature in the cutting area increased with increasing cutting speed and for a cutting process maintained at a raised temperature, the strength of the built-up edge is reduced. The temperature on the tool face also played a major role with respect to the size and stability of the built-up edge (Uyaner et al., 2012). An earlier study by Yigit et al. (2008) on the effect of cutting speed on the performance of multilayer-coated cutting tools when turning nodular cast iron reported a similar trend. Bajic et al. (2008) who modeled machined surface roughness in face milling process alsoreported that minimum surface roughness could be achieved by setting the cutting speed as high as possible. This was inconsistent with the trend observed by Rech and Moisan (2003) who reported from their experimental study on the turning of case-hardened steel that cutting speed has a small influence on finishing operations. Furthermore, Axinte and Dewes (2002) who studied high speed milling of hot worked tool steel also reported that the values of surface roughness increased when cutting speed increased. They notted that this is contrary to what would normally be expected because higher cutting speeds generally give lower roughness due to avoidance of built-up edge effect. As no built-up edge was seen on the cutting tool and workpiece, the increase, according to them, was due to increased unbalance of the cutting tool inserts at high cutting speed, with possible vibrations in the milling cutter and tool wear.

The seemingly irreconcilable inconsistencies in the results reported by various researchers is probably a pointer to the fact that the integrity of the surface generated in machining operations may depend largely on the workpiece and tool material types. The complex material-variable physico-chemical interactions between the workpiece and tool at the elevated temperatures associated with high speed machining operations is perhaps a significant determinant of the properties of the workpiece surface generated.

Effect of depth of cut on surface roughness

Figure 4 shows the effect of depth of cut on the surface roughness of machined workpieces at the average feed rate, cutting speed and cutting fluid flow rate values of 30 mm/rev, 1000 rev/min and 2 l/min respectively. The surfaces of machined samples became significantly rougher as depth of cut increased. This result agrees with the observations of Uyaner et al. (2012).

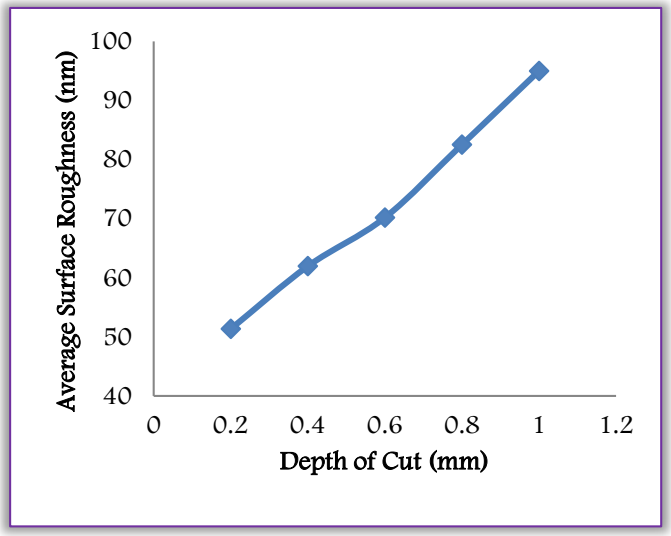

Figure 4: Effect of Depth of Cut on Average Surface Roughness

The result is also consistent with an earlier report by Arunachalam et al. (2004) who studied the residual stress and surface roughness generated when facing age hardened Inconel 718. Sosa et al. (2007) also observed that roughness increased as depth of cut increased in machining of thin wall ferritized ductile iron plates. This is probably because increased cutting force and tool wear results from the increase in depth of cut.

The increased cutting forces cause several changes in the shapes of both tool and workpiece and probably change the location (position) of tool/workpiece thereby affecting cutting quality (Uyaner et al., 2012) and increasing workpiece surface roughness. On the other hand, Bajic et al. (2008) reported from modeling of machined surface roughness that depth of cut has a negligible influence on surface roughness.

Figure 5 illustrates the variation in surface roughness with depth of cut at various levels of fluid flow rate. It reveals that the upper and lower limits of the range of variation in surface roughness observed in this study decreased with increase in fluid flow rate. For instance, at fluid flow rate of 0

l/min (dry cutting), the roughness value increased from 101.78 – 154.70 nm as depth of cut increased from 0.2 – 1.0 mm. At fluid flow rate of 4 l/min (wet cutting), the roughness value increased from 18.98 – 47 nm as depth of cut increased from 0.2 – 1.0 mm.

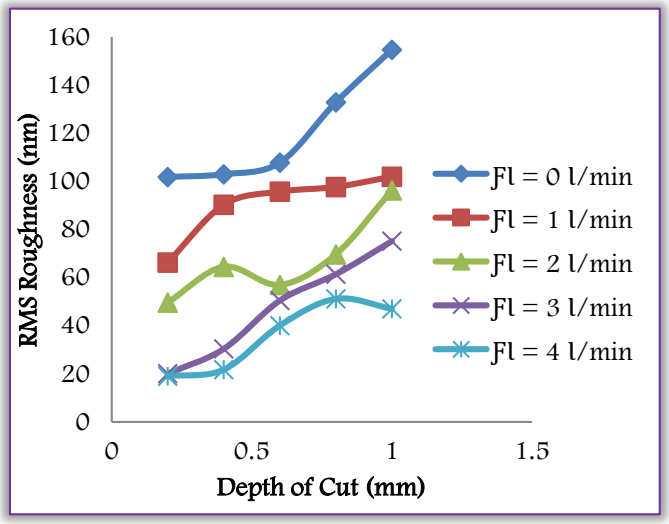

Figure 5: Effect of Depth of Cut on Surface Roughness at various levels of Cutting Fluid Flow Rate

Effect of cutting fluid flow rate on surface roughness

Figure 6 shows the effect of cutting fluid flow rate on the surface roughness of machined surfaces at average depth of cut, feed rate and cutting speed values of 0.6 mm, 30 mm/rev and 1000 rev/min respectively.

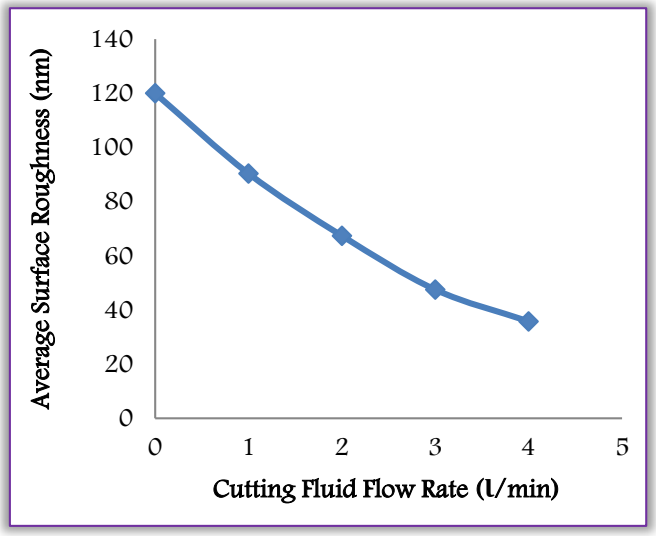

Figure 6: Effect of Cutting Fluid Flow Rate on Average Surface Roughness

The surface roughness decreased significantly with increase in cutting fluid flow rate at 5% significance level. The average surface roughness value was highest at fluid flow rate of 0 l/min (dry machining) and lowest at the flow rate of 4 l/min. This shows that machining at dry condition increased the surface roughness thereby generating a poor surface finish while machining at wet conditions reduced surface roughness thereby producing a good surface finish. It is observed from Figure 6 that the average surface roughness decreased from 120.00 – 35.78 nm as cutting fluid flow rate increased from 0 – 4 l/min. This agreed with Arunachalam et al. (2004) who reported that low values of surface roughness were obtained when coolant was used while dry cutting resulted in high values of surface roughness. The higher values of surface roughness in dry cutting were due to the built-up edges deposited over the machined surface and the higher temperature involved. But as the cutting fluid was applied, the surface roughness values dropped because of the reduction in the temperature on the machined surface during machining and this result in a smoother finish. The use of cutting fluid also generates good surface that is free from deposited built-up edges (Arunachalam et al., 2004).

Zhou et al. (2012) observed that machined surfaces produced using cutting fluid were superior to corresponding surfaces generated under dry cut condition. Kuram et al. (2010) also found that vegetable based (sunflower) cutting fluid reduced the surface roughness effectively in machining process.

Dhar et al. (2006) reported that the cutting performance of minimum quantity lubrication (MQL) machining was better than that of dry machining because it provided better surface finish in cutting process. It provided the benefits by reducing the cutting temperature which improved the chip – tool interaction and maintains sharpness of the cutting edges.

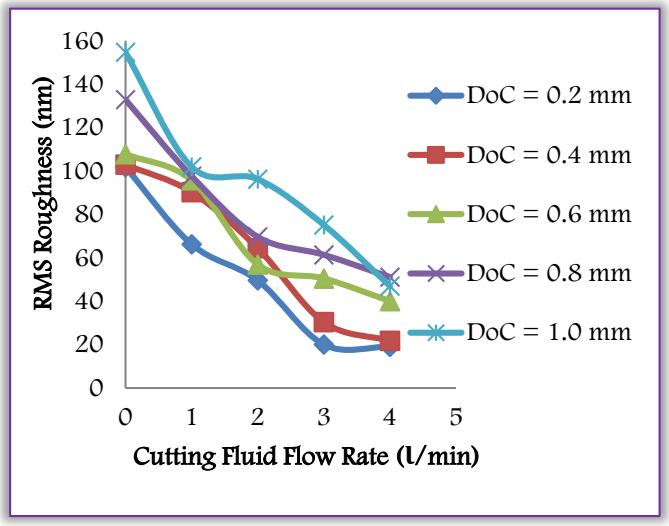

Figure 7: Effect of Cutting Fluid Flow Rate on Surface Roughness at various levels of Depth of Cut

Figure 7 shows how the surface roughness varies with fluid flow rate at various levels of depth of cut, the other parameter that had significant effect on the surface roughness. It shows that the upper and lower limits of the range of variation in surface

roughness with fluid flow rate increased with increase in depth of cut. For instance, at depth of cut of 0.2 mm, surface roughness decreased from 101.78 – 18.98 nm as cutting fluid flow rate increased from 0 – 4 l/min while at depth of cut of 1.0 mm, roughness decreased from 154.70 – 47.00 nm as fluid flow rate increased from 0 – 4 l/min.

On the contrary, Yusuf et al. (2010) stated that coolant did not significantly affect the surface roughness quality during machining. Ezugwu et al. (2007) also observed that surface roughness was not affected by coolant pressure. However, these observations could hardly be scientifically explained.

CONCLUSIONS

The study concluded that all the four (4) cutting parameters studied have some effect on surface roughness of the pearlitic ductile iron face-milled with cemented carbide cutting tool. The surface roughness was statistically significantly affected by cutting fluid flow rate and depth of cut while the effect of feed rate and cutting speed on the surface roughness were not statistically significant ($p \leq 0.05$). The implication of these findings is that in order to enhance the surface integrity and produce good surface finish thus reducing tooling cost in high-speed face milling operations in manufacturing industries, thecutting fluid flow rate must be strongly considered.

References

[1.] Arunachalam, R. M., Mannan, M. A. and Spowage, A. C. (2004). Residual stress andsurface roughness when facing age hardened Inconel 718 with CBN and ceramic cutting tools. International Journal of Machine Tools & Manufacture. 44, pp. 879–887.

[2.] Axinte, D. A. and Dewes, R. C. (2002). Surface integrity of hot work tool steel after high speed milling-experimental data and empirical models. Journal of materials processing Technology. 127, pp. 325 – 335.

[3.] Bajic, D., Lela, B. and Zivkovic, D. (2008). Modeling of machined surface roughness and Optimization of cutting parameters in face milling. Metalurgija: 47 (2008) 4, pp. 331-334.

[4.] Dhar, N. R., Kamruzzaman, M. and Ahmed, M. (2006). Effect of minimum quantity lubrication (MQL) on tool wear and surface roughness in turning AISI-4340 steel. Journal of Materials Processing Technology. 172, pp. 299–304

[5.] Ezugwu, E. O., Bonneya, J., Silvab, R. B. D. and Cakir, O. (2007). Surface integrity of finished turned Ti–6Al–4V alloy with PCD tools using conventional and high pressure coolant supplies. Int. J. Machine Tools Manuf. 47, pp. 884–891.

[6.] Field, M. and Kahles, J. (1971). Review of surface integrity of machined components,Ann. CIRP 20 (2), pp. 153–163.

[7.] Franco, P., Estrems, M. and Faura, F. (2004). Influence of radial and axial runouts on surface roughness in face milling with round insert cutting tools. International Journal of Machine Tools & Manufacture 44, pp. 1555–1565

[8.] Grzesik, W. and Zak, K. (2012). Surface Integrity generated by oblique machining of Steel and Iron parts. Journal of Materials Processing Technology. 212, pp. 2586–2596.

[9.] Gunnberg, F, Escursell, M. and Jacobson, M. (2006). The influence of cuttingparameters on residual stresses and surface topography during hard turning of 18MnCr5 case carburized steel. Journal of Materials Processing Technology. 174, pp. 82–90.

[10.] Hayajneh, M. T., Tahat, M. S. and Bluhm, J. (2007). A Study of the Effects ofMachining Parameters on the Surface Roughness in the End-Milling Process. Jordan Journal of Mechanical and Industrial Engineering, Volume 1, Number 1, Sep., ISSN 1995-6665, pp. 1 – 5.

[11.] Hughes, J. I., Sharman, A. R. C. and Ridgway, K. (2004). The effect of tool edge preparation on tool life and workpiece surface integrity. Proc. Inst. Mech. Eng., Part B: J. Eng. Manuf. 218, pp. 1113–1123.

[12.] Jacobson, M., Dahlman, P. and Gunnberg, F. (2002). Cutting speed influence onsurface integrity of hard turned bainite steel. Journal of Materials Processing Technology 128, pp. 318–323.

[13.] Kuram, E., Ozcelik, B., Demirbas, E. and Şık, E. (2010). Effects of the Cutting FluidTypes and Cutting Parameters on Surface Roughness and Thrust Force. Proceedings of the World Congress on Engineering 2010 Vol. II, June 30 - July 2, London, U.K.

[14.] Lopez de lacalle, L. N., Perez, J. I., Llorente, J. and Sanchez, J. A. (2000). Advanced cutting conditions for the milling of aeronautical alloys. J. Mater. Proc. Technol. 100, pp. 1–11.

[15.] Navas, V. G. O. and Bengoetxea, I. (2012). Effect of cutting parameters in the surface residual stresses generated by turning in AISI 4340 steel. International Journal of Machine Tools & Manufacture 61, pp. 48–57.

[16.] Rech, J. and Moisan, A. (2003). Surface integrity in finish hard turning of casehardened steels. International Journal of Machine Tools & Manufacture 43, pp. 543–550.

[17.] Sosa A. D., Echeverri, M. D., Moncada, O. J. and Sikora, J. A. (2007). Residual stresses, distortion and surface roughness produced by grinding thin wall ductile iron plates. International Journal of Machine Tools & Manufacture 47, pp. 229–235

[18.] Thiele, J. D. and Melkote, S. N. (1999). Effect of cutting edge geometry and workpiece hardness on surface generation in the finish hard turning of AISI 52100 steel. Journal of Materials Processing Technology 94, pp. 216 – 226.

[19.] Uyaner, M., Akdemir, A., Yazman, S. and Saglam, H. (2012). The effects of cutting speed and depth of cut on machinability characteristics of Austempered ductile iron. Journal of

manufacturing science and engineering, 134 (2), pp. 10-13.
[20.] Yigit, R., Celik, E., Findik, F. and Koksal, S. (2008). Effect of cutting speed on the performance of coated and uncoated cutting tools in turning nodular cast iron. Journal of materials processing technology: 204, pp. 80–88.
[21.] Yusuf, K., Nukman, Y., Yusof, T. M., Dawal, S. Z., Yang, H. Q., Mahlia, T. M. I. andTamrin, K. F. (2010). Effect of cutting parameters on the surface roughness of titanium alloys using end milling process. Scientific Research and Essays: Vol. 5(11), pp. 1284-1293.
[22.] Zhou, J. M., Bushlya, V. and Stahl, J. E. (2012). An investigation of surface damage in the high speed turning of Inconel 718 with use of whisker reinforced ceramic tools. Journal of Materials Processing Technology: 212, pp. 372– 384.

ACTA Technica CORVINIENSIS
BULLETIN OF ENGINEERING
ISSN:2067-3809

ACTA TECHNICA CORVINIENSIS
– Bulletin of Engineering
Tome IX [2016], Fascicule 4 [October – December]
ISSN: 2067 – 3809

[1.]Noémi DARIDA, [2.]József GÁL

WASTEWATER TREATMENT IN HÓDMEZŐVÁSÁRHELY

[1.]Budapest University of Technology and Economics, Faculty of Civil Engineering, Budapest, HUNGARY
[2.]University of Szeged, Faculty of Engineering, Szeged, HUNGARY

Abstract: The contamination of our living waters is a serious environmental issue in every corner of our world. The main polluting sources are the industry, the agriculture and the general population in their everyday life. In the protection of our living waters, the mainly used technology is the wastewater treatment, whose main objective is to prevent the contaminants from seeping into the water's environment. With the continuous growth of the urbanization, both the developed and the underdeveloped countries' way of life are modified so the wastewater gets collected in increasing quantities. Although the concentration of pollutants may appear in very different degrees, in certain cases severely concentrated pollutions may occur. Wastewater being produced in such big quantities must not be irrigated to the soil in the hopes of using its nutrient content. Thus, the purification of wastewater required proper engineering mainly because the load surpasses the self-cleaning ability of the water. The consequence of such demand resulted in the establishment of different artificial cleansing methods varying in complexity and specialty – mechanical and biological treatments.
Keywords:wastewater, wastewater treatment, Hódmezővásárhely

INTRODUCTION

All the people should know that all the used water in every home goes down through drains and through sewage collection system to wastewater treatment plants. We have to clean our wastewater before it returns to the environment. This wastewater can contain municipal sewage (which comes from households), agricultural wastewater, institutional and industrial wastewater. An average Hungarian person contributes 90-160 litres of wastewater each day. It depends on where they live; in small, in big cities or on ranches. [2] [4]

GENERALLY ABOUT WASTEWATER TREATMENT

There are three phases of cleansing wastewater: primary treatment, secondary treatment and sludge treatment.

The first is primary treatment, which means a physical removal of floatable and settleable solids. One task of primary treatment is to remove large objects (such as stones or sticks) with scum removal and grit removal and then comes a settling tank to settle out settleable solids. Essentially primary treatment is a mechanical removal.

The essence of secondary treatment is biological removal of dissolved solids. This typically utilizes biological treatment processes, in which microorganisms convert non-settleable and settleable solids.

There are two parts of biological treatments: aeration and sedimentation. Activated sludge can be circulated between these tanks. Then the treated effluent flows back to the environment. By chance, it can be disinfected before release.

From primary and from secondary treatment as well comes sludge to treat with various technologies such as thickening, dewatering and digestion. Then we can use it or disposal it. [1] [2] [4]

SEWAGETREATMENT PLANT IN HÓDMEZŐVÁSÁRHELY

Hódmezővásárhely is located in South-East Hungary, on the Great Plain, in the county of Csongrád. This city has the second biggest area in the country. Until the middle of the 20th Century it was one of the most highly populated town.

Already in the 90's almost the whole city had sewage collection system. Therefore, the city needed a better and more effective sewage treatment plant.

Namely, this wastewater is predominantly from municipal sources (households and small industry from Mártély) it is called sewage and its treatment is called sewage treatment.

This new sewage treatment plant was built in 1994 with new – those days – modern technology, called 2AB by the UTB Company (Figure 1), which had 15.000 m3/d cleansing capacity. This plant works at nowadays as well and has earned a recognition from the Hungarian Hydrological Corporation. [5]

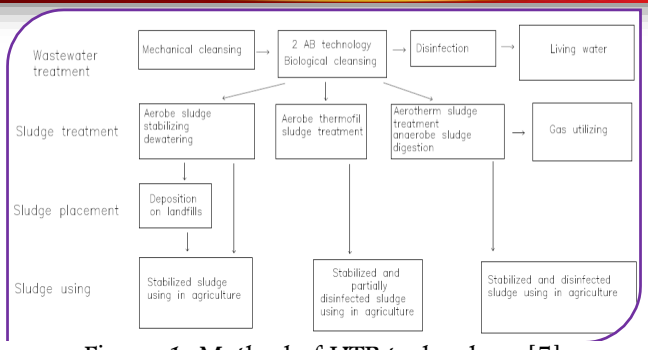

Figure 1. Method of UTB technology [5]

Features of this plant:

» needs small area
» does not have bad smell
» has low energy-using
» has low operating costs
» can save energy by the biogas utilizing
» uses digestion
» has no denitrification and phosphorremoval.

At that time a lot of cities used this technologies: Martfű, Ercsi, Écs, Gyömrő, Ibrány, Jánossomorja, Kópháza, Soltvadker, Recsk-Parád-Mátraderecske, Szerencs and Szilvásvárad. [5]

Figure 2. Present sewage treatment plant in Hódmezővásárhely [7]

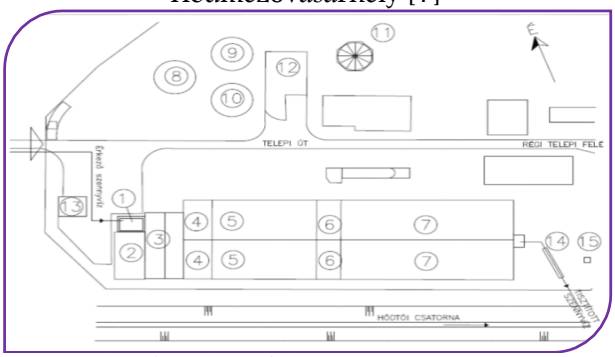

Figure 3. The site plan of the sewage treatment plant in Hódmezővásárhely [6]. Content: wastewater receiver, scum removal, grit removal, 2AB oxidation ponds, primary treatment, 2AB sedimentation, primary treatment, 2ab oxidation ponds, secondary treatment, 2ab sedimentation, secondary treatment, sludge-thickener, digestion tank, sludge tank, gas tank, aerothermal building, sniffed sewage pre-treater, parshall-channel [3] [6]

The population of Hódmezővásárhely has reached 44 795 in 2015. [10] Sewage treatment has two parts in this plant. (Figure 2, Figure 3) The first part is waterline, which contains two phases: mechanical and biological treatment. The second part of cleansing is sludge line, which means the second phase, the sludge treatment. The 72% of the sewage system of Hódmezővásárhely is combined storm drains and sewers. The rain goes instantly through sewage system to treatment plant. Other wastewaters come from a small industry (from Mártély) and from separated ranches as sniffed sewage. The process of treatment flows like on the following picture.

CONCLUSIONS

Although the treatment plant of this city was built in the '90's, it is still an effective and properly maintained plant. However, the renovation of Hódmezővásárhely's treatment plant is scheduled we would like to believe that a reclaimed water, (which means potable water) will not be so futuristic idea and we can recycle all our used water not just in big cities, but all around the world. The technology is not enough, people living in environment of waste water treatment plant have individual feeling about it as well. Although smell can sometimes appear is not dangerous for human life people have sensitive feeling about bad smell. Expansion of town Hódmezővásárhely is very fast, so new buildings are closer to the plant. It means inhabitants require against high tech technology during renewing waste water treatment plant is getting stronger. It makes a typical situation how to find technical and social solutions for best and more comfortable sustainable life.

References

[1.] Fazekas B., Kárpáti Á., Kovács Zs. (2014): Szennyvíztisztítás korszerű módszerei, Veszprém: Pannon Egy. Környezetmérnöki Intézet, http://nbn.urn.hu/
[2.] *** Wastewater treatment, Water Environment Federation, WEF_ww_curriculum.pdf, 2015
[3.] *** A hódmezővásárhelyi szennyvíztisztító telep Próbaüzemi Kezelési Utasítása és Működési Szabályzata, Hódmezővásárhely, (2015)
[4.] Öllős G. (1992): Szennyvíztisztítás, BME MTI, Budapest
[5.] *** Az United Technologies Bureau Kft., UTB technológia ismertető kiadványa (1994)
[6.] *** A hódmezővásárhelyi szennyvíztisztító telep technológiai leírásai, kézirat, Hódmezővásárhely (1994)
[7.] Harmat Péter magán képgyűjteménye (2015)
[8.] Hódmezővásárhely Megyei Jogú Város Polgármesteri Hivatal Városfejlesztési- és Építéshatósági Iroda adatai alapján, Hódmezővásárhely, (2016)

ACTA TECHNICA CORVINIENSIS
– Bulletin of Engineering
Tome IX [2016], Fascicule 4 [October – December]
ISSN: 2067 – 3809

[1.]Cristina Daniela PACURAR, [2.]Teodor HEPUŢ

MATHEMATICAL MODELING ON THE LOAD METAL OF THE ELECTRIC ARC FURNACE

[1-2.] University Politehnica Timisoara, Faculty of Engineering Hunedoara, Hunedoara, ROMANIA

Abstract: In research conducted, it was considered analyze the fabric of electric arc furnaces on several dimensions, but especially the removal of liquid steel, one of the main technical and economic indicators in the steel industry.This indicator depends on several factors aids and specifically: structure and the quality of the metal load, the degree of preparation of the content of materials accompanying non-metallic, unit of elaboration, the technology of elaboration, etc. the load has been composed of eight metallic components, in some cases with great differences from the point of view of quality. The data obtained have been processed in the programs of MATLAB calculation using the three types of equations, results obtained being presented both graphically and analytical. Based on results obtained has opted for an optimum structure of the load.
Keywords:steel industry, electric arc furnace, liquid steel, MATLAB calculation

INTRODUCTION

Currently steel industry shows interest in two units for steelmaking, namely: oxygen converter and electric arc furnaces.

The purpose of this paper is to understand the actual working conditions and performance of the EAF, determine the best technical and economic choices in order to achieve the performance targets making a correlation of data obtained by applying mathematical models of experimental design that is currently most modern tool used in optimization problems.

It contributes to the achievement of important clarifications on the relationship between variables, parameter estimation links, testing different ways of practical action, determining the optimal level of controlled variables and model behavior of the variation factors. For optimal management of processes it is necessary to know the characteristics of mathematical models of these processes.

STUDY OF THE PROBLEM

Industrial experiments conducted mainly aimed at determining correlations between structure loads double metal components respectively stake (%) and removal of liquid steel (%). To analyze the fabric of metal were followed a total of 30 batches of steel produced at a steel mill elective equipped with an electric arc furnace type EBT, which have the capacity 100t, a facility type LF and a casting plant continues with 5-wire Bloom is molded preforms (270x240mm).

During the development was monitored carefully load structure, its status in terms of dimensional presentation of the content of slag both bark from inside, mostly on slag heaps, but also commercially. Also appreciated was prepared visual quality scrap E1, E2, E5, E100, scrap derived from internal cassation, in terms of the levels of rust, nonferrous metals, earth. The analysis was conducted for 30 batches of steel and experimental results were processed in Matlab computer programs, using three types of equations.

MATHEMATICAL DATA MODELING

The data processing was made in the computing program MATLAB, using three types of correlation equations. The results are presented both analytical and graphical form, each correlation being analyzed technologically indicating optimal values for the independent parameters. The analysis conducted shows a comparison between the results obtained by three types of equations for each correlation.

» Equation 1:

$$z_1 = a_{(1)}\, x^2 + a_{(2)}\, y^2 + a_{(3)}\, x\, y + a_{(4)}\, x + a_{(5)}\, y + a_{(6)}$$

» Equation 2:

$$z_2 = a_{(1)} + a_{(2)}\, x + a_{(3)}\, x^2 + a_{(4)}\, x^3 + a_{(5)}\, y + a_{(6)}\, y^2 + a_{(7)}\, y^3 + a_{(8)}\, y^4 + a_{(9)}\, y^5$$

» Equation 3:

$$z_3 = a_{(1)} + a_{(2)}\, \log(x) + a_{(3)}\, \log(x)^2 + a_{(4)}\, \log(x)^3 + a_{(5)}/y + a_{(6)}/(y^2) + a_{(7)}/(y^3) + a_{(8)}/(y^4) + a_{(9)}/(y^5)$$

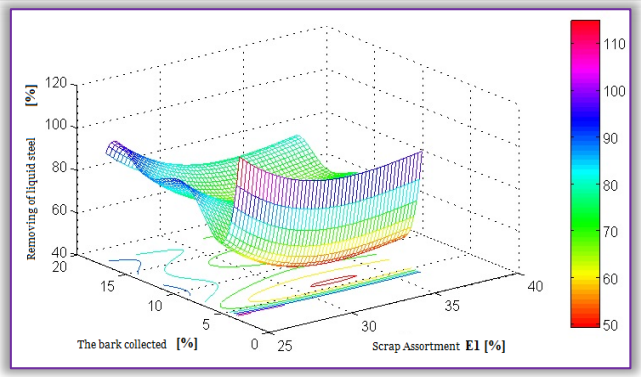

a)

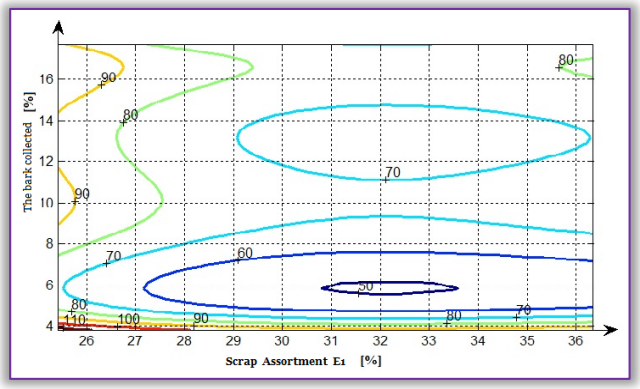

b)

Figure 1.Variation of removal of liquid steel depending on scrap iron assortment E1 and the bark collected
a) spatial representation; b) Curved level, projection in the horizontal plane

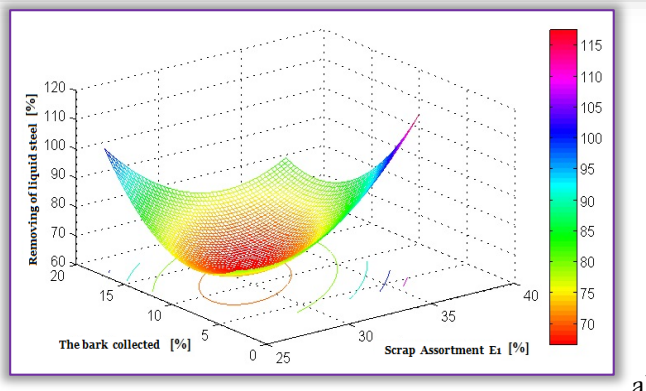

a)

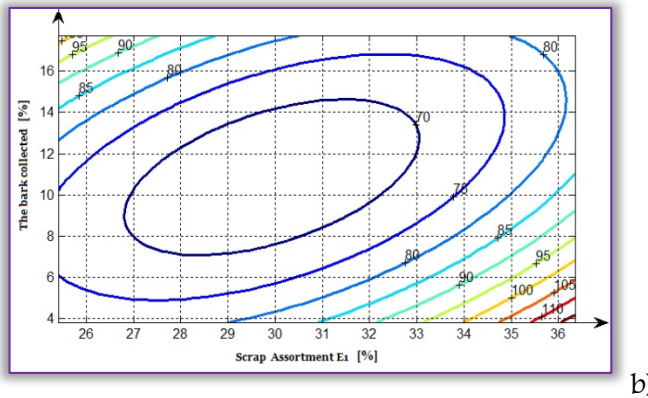

b)

Figure 3. Variation of removal of liquid steel depending on scrap iron assortment E1 and the bark collected.
a) spatial representation; b) Curved level, projection in the horizontal plane

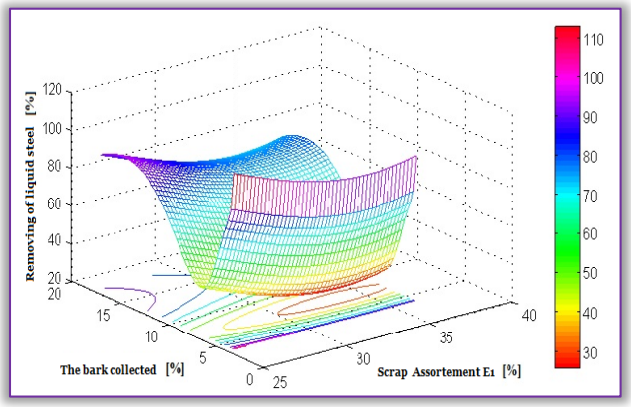

a)

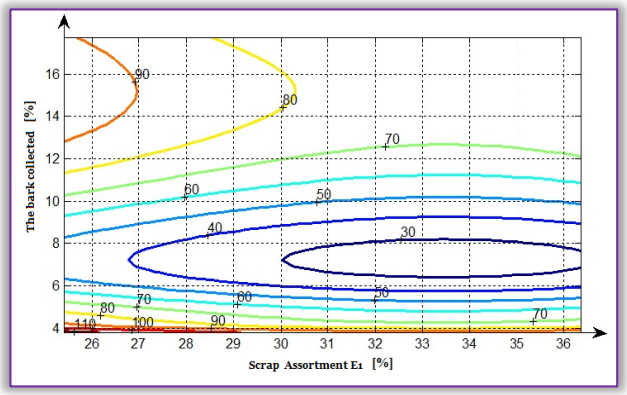

b)

Figure 2.Variation of removal of liquid steel depending on scrap iron assortment E1 and the bark collected
a) spatial representation; b) Curved level, projection in the horizontal plane

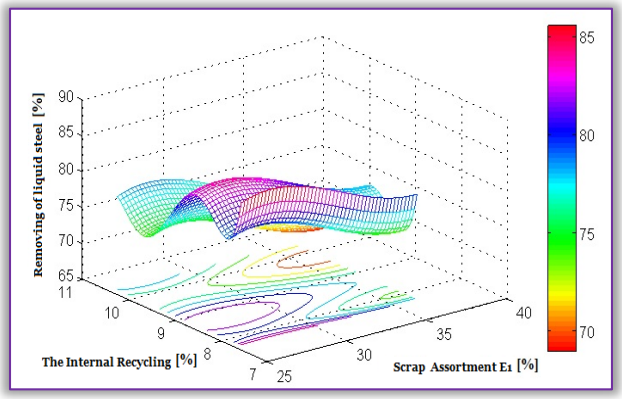

a)

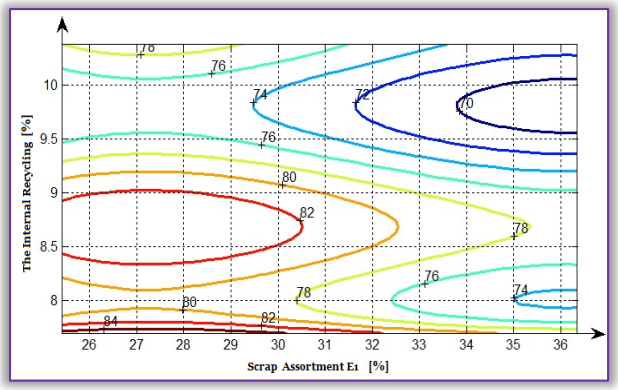

b)

Figure 4. Variation of removal of liquid steel depending on scrap iron assortment E1 and the internal recycling
a) spatial representation; b) Curved level, projection in the horizontal plane

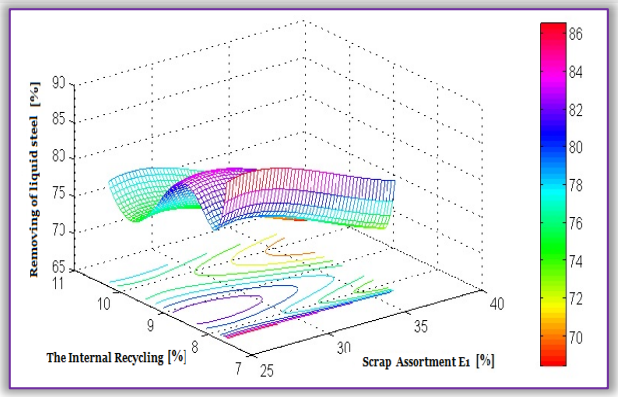

a)

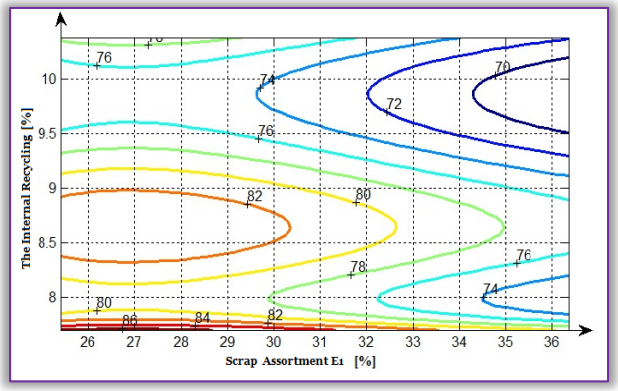

b)

Figure 5. Variation of removal of liquid steel depending on scrap iron assortment E1 and the internal recycling. a) spatial representation; b) Curved level, projection in the horizontal plane

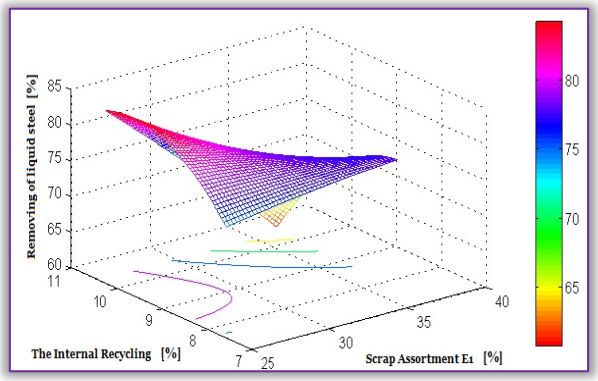

a)

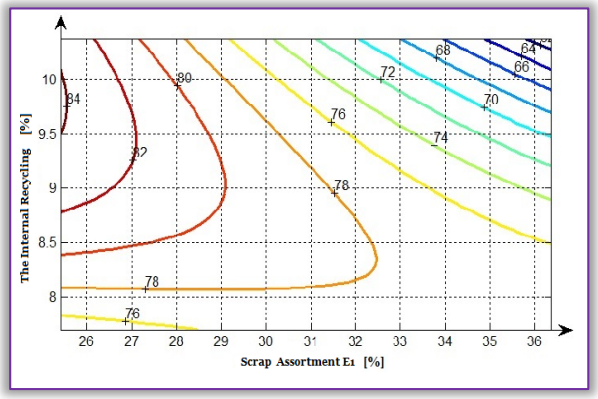

b)

Figure 6. Variation of removal of liquid steel depending on scrap iron assortment E1 and the internal recycling a) spatial representation; b) Curved level, projection in the horizontal plane

$$z_1 = 2055.978 - 96.9298\,x + 2.7087\,x^2 - 0.0249\,x^3 - 464.043\,y + 94.1492\,y^2 - 8.9908\,y^3 + 0.4089\,y^4 - 0.0071\,y^5. \quad R^2 = 0.7901 \tag{1}$$

$$z_2 = -22618.34 + 20449.93\log(x) - 6253.52\log(x)^2 + 634.44\log(x)^3 + 225.83/y - 350566.31/(y)^2 + 2426.70/(y)^3 - 7737.716/(y)^4 + 9333.687/(y)^5 \quad R^2 = 0.7608 \tag{2}$$

$$z_3 = 0.45469\,x^2 + 0.31039\,y^2 - 0.370718\,xy - 23.19604\,x + 4.359415\,y + 390.12349 \quad R^2 = 0.54409 \tag{3}$$

$$z_1 = 334772.217 + 49.527\,x - 1.595\,x^2 + 0.016\,x^3 - 183952.436\,y + 40233.530\,y^2 - 4383.805\,y^3 + 237.957\,y^4 - 5.148\,y^5 \quad R^2 = 0.2290 \tag{4}$$

$$z_2 = -121884.628 + 8276.466\log(x) - 2372.550\log(x)^2 + 225.896\log(x)^3 + 5437.035/y - 1043.316/(y)^2 + 9933.190/(y)^3 - 4691.719/(y)^4 + 8801.122/(y)^5 \quad R^2 = 0.2326 \tag{5}$$

$$z_3 = -0.012\,x^2 - 2.125\,y^2 - 0.8751\,x\,y + 7.757\,x + 63.881\,y - 309.054 \quad R^2 = 0.4078 \tag{6}$$

$$z_1 = 243166.294 - 30.104\,x + 2.690\,x^2 - 0.072\,x^3 - 134334.481\,y + 29605.198\,y^2 - 3251.290\,y^3 + 177.9344\,y + 3.8823\,y^5 \quad R^2 = 0.4540 \tag{7}$$

$$z_2 = 113101.143 - 633.699\log(x) + 277.959\log(x)^2 - 39.387\log(x)^3 - 4786.051/y + 8096.734/(y)^2 - 6808.853/(y)^3 + 2846.182/(y)^4 - 4734.095/(y)^5 \quad R^2 = 0.5163 \tag{8}$$

$$z_3 = 0.1104\,x^2 - 1.7666\,y^2 - 0.1475\,x\,y - 1.5058\,x + 30.2430\,y - 36.9735 \quad R^2 = 0.2208 \tag{9}$$

$$z_1 = 7486.588 + 158.4922\,x - 5.32198\,x^2 + 0.05885\,x^3 - 477216.852\,y + 121097.401\,y^2 - 15321.1660\,y^3 + 966.4518\,y^4 - 24.3154\,y^5 \quad R^2 = 0.3822 \tag{10}$$

$$z_2 = -7969.4302 + 52952.9294\log(x) - 15602.9092\log(x)^2 + 1530.9533\log(x)^3 + 2926.0360/y - 4634.981/(y)^2 + 3659.408/(y)^3 - 1440.451/(y)^4 + 2261.2983/(y)^5 \quad R^2 = 0.3620 \tag{11}$$

$$z_3 = 0.0788\,x^2 + 1.2697\,y^2 + 0.3408\,x\,y - 8.317\,x - 26.4914\,y + 304.8916 \quad R^2 = 0.5272 \tag{12}$$

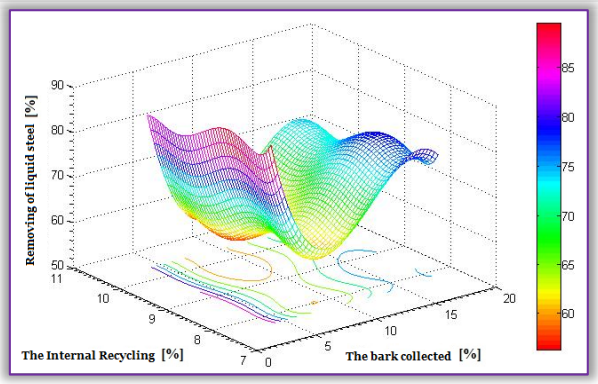

a)

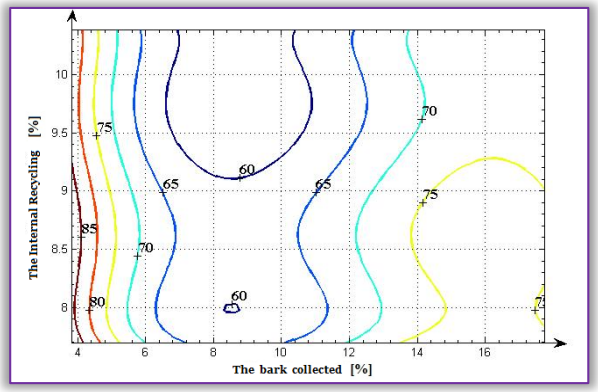

b)

Figure 7. Variation of removal of liquid steel depending on bark collected and the internal recycling
a) spatial representation; b) Curved level, projection in the horizontal plane

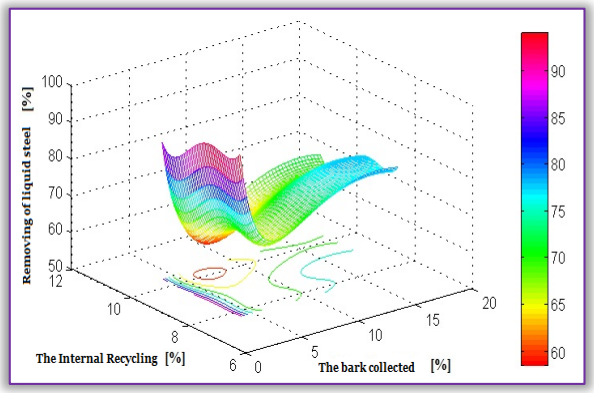

a)

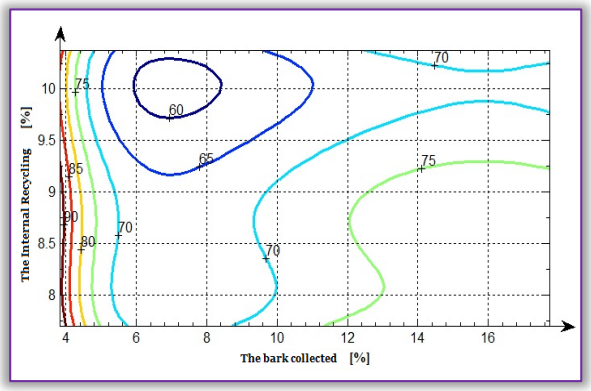

b)

Figure 8. Variation of removal of liquid steel depending on bark collected and the internal recycling
a) spatial representation; b) Curved level, projection in the horizontal plane

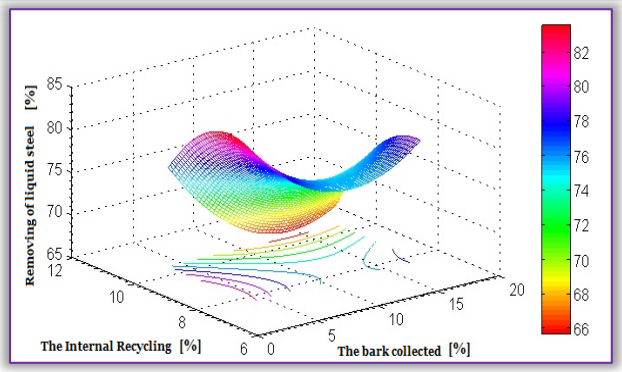

a)

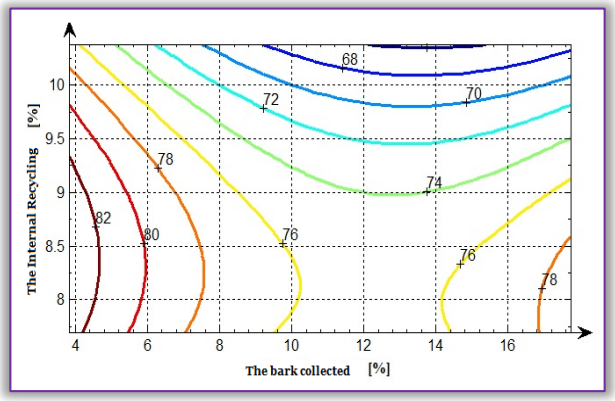

b)

Figure 9. Variation of removal of liquid steel depending on bark collected and the internal recycling
a) spatial representation; b) Curved level, projection in the horizontal plane

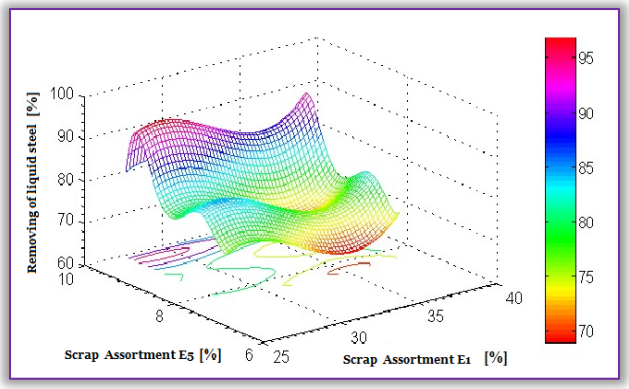

a)

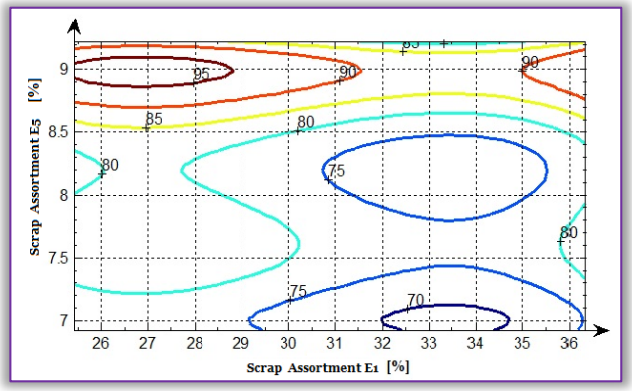

b)

Figure10. Variation of removal of liquid steel depending on scrap iron assortment E1 and E 5 scrap iron assortment. a) spatial representation; b) Curved level, projection in the horizontal plane

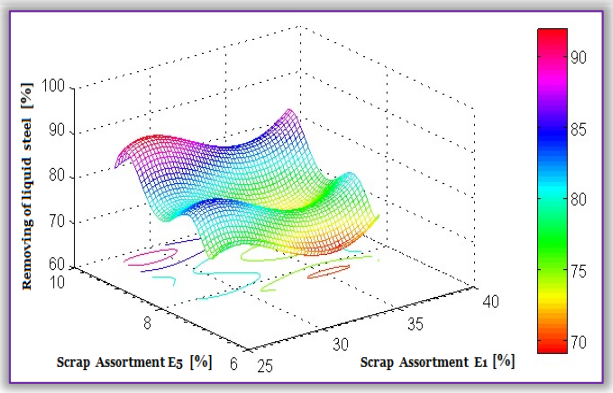

a)

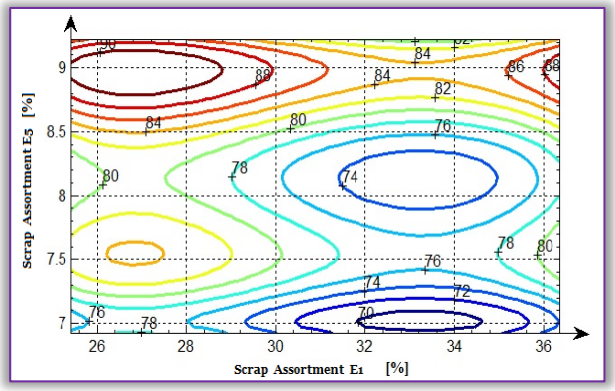

b)

Figure 11. Variation of removal of liquid steel depending on scrap iron assortment E1 and E 5 scrap iron assortment. a) spatial representation; b) Curved level, projection in the horizontal plane

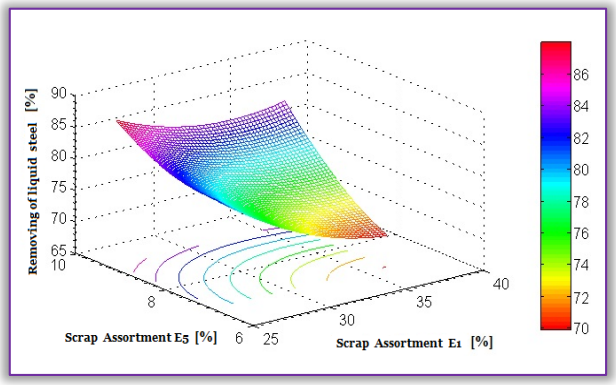

a)

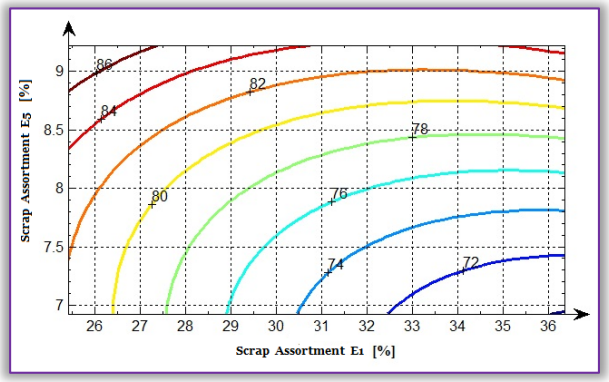

b)

Figure 12. Variation of removal of liquid steel depending on scrap iron assortment E1 and E 5 scrap iron assortment. a) spatial representation; b) Curved level, projection in the horizontal plane

TECHNOLOGICAL ANALYSIS OF THE RESULTS

Regarding the quality of the load on the basis of the representations received for the duration of the session tracking we found that from the point of view of quality load has not been of the highest quality in the sense that prevailed from the point of view of quantitative old iron gently (Baler) and metal rugs from internal and external, fact confirmed also by the values obtained for the removal of liquid steel. In particular, the quality of the barks metal,both under the aspect of the content of iron and granulometrically is less appropriate.

From the graphic representations obtained from the processing of personal data in the MATLAB program can be established the proportions of the components in the load in order to obtain a specific value for removing of liquid steel, respectively choose load component taking into account and the quantity of available varieties concerned the possibilities of supply.

The results obtained after the three types of equations used in the course of correlations are fairly close to the example:

» in Figure 4, Figure 5 and Figure6 to a content of 30 % and 10% values for removing of liquid steel are 74% and 76.2%; a difference of 3,03% compared to the other values (value permissible practically) regardless after which we analyze the technological point of view is significantly;

» in Figure 7,Figure8 and Figure9 to a content of 14 % and 10%. The values for the removal of liquid steel are 70%; 68 % and 69 %, a difference of 1.4 percent as compared to the other (value permissible practically) regardless after which we analyze the technological point of view is significant.

In the same way can be analyzed and the other correlation.

CONCLUSIONS

In the analysis of the results obtained in the research can be concluded the following:

» the quality of the metal load has not been of the highest quality and reflected in the values obtained for the removal of liquid steel;

» from representations of curves by level in the projection surface can choose values for load metal composition, must be considered and the possibilities for supply of raw materials;

» it requires the use of a metal load of top quality, which will lead to a reduction in the specific consumption of energy, which will be found in lower degree of environmental pollution.

References

[1.] Hepuţ, T., Nica, G., Socalici, A., Ardelean, E., The faults on the bullion and half-finished products

made of steel, Editura Politehnica, Timişoara, 2001.
[2.] Constantin, N., Research contract no. 233/2006: Integrated technology of obtaining energy sources used non-standard technological as raw materials in the preparation of the steel.
[3.] Aloman, A., et al., Treatyofmaterials science and engineering, vol.I,Fundamentals ofmaterials science, AGIR 2006.
[4.] Bacinschi, Z., et al., Treatyofmaterials science and engineering, vol.II Theoreticalandobtainengineeringmetallic materials, AGIR 2007.
[5.] Vacu, S. et al - Elaborarea oţelurilor aliate, vol. I, Bucharest, Editura Tehnică [Technical Publisher], 1980.
[6.] *** Prospective scenarios on energy efficiency and CO2 emissions in the Iron & Steel industry, JRC;
[7.] Vacu, S. et al - Elaborarea oţelurilor aliate, vol. II, Bucharest, Editura Tehnică [Technical Publisher], 1983.
[8.] Rău, A., Cosma, D., Ilin, Gh. - Elaborarea oţelului în cuptoare electrice cu arc, Bucharest, Editura Tehnică [Technical Publisher], 1967.
[9.] Rău, A., Tripşa, I., Metalurgia oţelului, Bucharest, E.D.P., 1981.

ACTA Technica CORVINIENSIS
BULLETIN OF ENGINEERING
ISSN:2067-3809

ACTA TECHNICA CORVINIENSIS
– Bulletin of Engineering
Tome IX [2016], Fascicule 4 [October – December]
ISSN: 2067 – 3809

[1.]Laura TOMA, [1.]Gheorghe VOICU, [1.]Gigel PARASCHIV, [2.]Valentin VLĂDUȚ,
[1.]Mirela DINCĂ, [2.]Iulian VOICEA, [1.]Nicoleta UNGUREANU, [1.]Georgian MOICEANU

THE INFLUENCE OF THE TEMPERATURE ON BIOGAS PRODUCTION IN A SMALL CAPACITY PLANT

[1.]University Politehnica of Bucharest, ROMANIA
[2.]INMA Bucharest, ROMANIA

Abstract: Biological fermentation represents one of the waste recycling technologies that can with stands a higher degree of waste capitalisation. It can be applied on wastes with a high organic content and it is possible to obtain a gaseous fuel (biogas) with different uses: heating, cooking, electricity generation, the leftover residues that represents a non-polluting material can be used with great results in agriculture as fertilizer.A number of factors including the type and composition of the substrate, temperature, pH, moisture content and the structure of the bioreactor influence the yield of biogas. Temperature has a major influence in biogas production obtain by anaerobic digestion. The temperature effect on biogas quantity obtain in a small capacity plant was studied in this paper. Experiments were done at a temperature of 25°C, 35°C, respectively 45°C.
Keywords: temperature, anaerobic digestion, biogas

INTRODUCTION

Biological fermentation represents one of the waste recycling technologies that can withstands a higher degree of waste capitalisation. It can be applied on wastes with a high organic content and it is possible to obtain a gaseous fuel (biogas) with different uses: heating, cooking, electricity generation, the leftover residues that represent a non-polluting material can be used with great results in agriculture as fertilizer.

Biogas represents a gaseous mixture composed of methane (max. 80%), carbon dioxide (min. 20%) along with small quantities of hydrogen (H_2), hydrogen sulfide (H_2S), mercaptans and water vapors [5].

Microorganisms that can live only in environments lacking of oxygen are responsible for anaerobic fermentation. The four stages of organic wastes decomposition are hydrolysis, acidogenesis, acetogenesis and methanogenesis [1, 3].

The organic decomposable matter, in natural systems in which it can be found, is the bearer of a varied and active microflora. This mixed microflora ensures specific metabolic compounds for metanobacteria development.

A number of factors including the type and composition of the substrate, temperature, pH, moisture content and the structure of the bioreactor influence the yield of biogas. Some studies have shown that the substrate concentration at the outlet of the fermenter depends on the substrate concentration entering the bioreactor [10].

In the literature, a series of experiments were conducted on the effect of temperature on anaerobic fermentation process.Although, the process is well known in mesophilic and thermophilic domains, the current state of knowledge on biomethanisation process development in psychrophilic domain is not so developed. In nature, it was observed that methane can be obtained at temperatures between 0 and 97°C. There are sufficient experimental evidences that methane can be produced at temperatures below 20°C due to the existence of psychrophilic methanogenic bacteria in the medium [4].

Anaerobic bacteria, especially metanogenic, are sensitive to medium conditions. Many researchers evaluate the performance of an anaerobic system based on biogas production because mehanogenesys represents a limit in anaerobic treatment. Methanogenic organisms are very vulnerable and have a very low rate of growth therefore requires careful maintenance

and monitoring of environmental conditions. A change in temperature or substrate concentration can lead to stopping the production of biogas [7].
Many researchers have observed that temperature has a significant influence on bacterial community, kinetic processes but also on the yield of methane. In the process of anaerobic digestion, low temperatures reduce the microbial culture, slow the rate of decomposition of the substrate and reduce production of biogas.On the other hand, higher temperatures result in reduced yield of biogas due to the volatile gas produced by the volatile acids such as ammonia that suppresses the activity of methanogenic bacteria.
In general, the process of anaerobic digestion, carried out in order to obtain biogas, takes place at mesophilic temperatures. Process development in the mesophilic domain is more stable and require less energy consumption.Experiments have shown that the optimum temperature for anaerobic fermentation process is 35°C, with a retention time in the fermenter of 18 days.In addition, a temperature in the range 35 - 37°C is considered optimal for the production of methane, and the changeover from the mesophilic to thermophilic temperature may cause a decrease in biogas production.
However, the thermophilic temperature presents a number of advantages, such as faster speed decomposition of the organic fraction, a higher production of biogas and the destruction of pathogens present in the substrate [5].
Anaerobic digestion of the substrate in order to obtain the biogas can be inhibited when changes in temperature exceed 1°C/day. To maintain a stable process, studies shown that changes in temperature should be less than 0.6°C/day [2].

MATERIAL AND METHOD

Experimental research presented in this paper aimed to analyze the influence of substrate temperature on biogas production and have been conducted on a small capacity pilot plant (Fig. 1) belongs to the Department of Biotechnical Systems, Faculty of Biotechnical Systems Engineering from the University „Politehnica" of Bucharest [8].
The system has four main parts, namely:

- Food compartment consists of biomass preparation system and a pump that transfers the material in the reactor;
- anaerobic digester;
- gas pipelinewith relative treatment systems;
- a tank where the gas is stored prior to use.

In the stirring tank, the fermented material with water and a number of feed substances is inserted (Table 1).
Each batch introduced into the tank is mixed with the water and feeding substances for 1 hour.

Table 1. Quantities of substances necessary for fermentation [8]

No.	Substance	Symbol	Quantity, g/100 L
1.	Glucose	$C_6H_{12}O_6$	6000
2.	Ammonium phosphate	$(NH_4)_2HPO_4$	91.1
3.	Ammonium chloride	NH_4Cl	56.6
4.	Potassium chloride	KCl	8
5.	Ferric chloride	$FeCl_3$	10
6.	Magnesium chloride	$MgCl_2 \cdot 6H_2O$	20
7.	Aluminum chloride	$AlCl_3 \cdot 6H_2O$	2.2
8.	Calcium chloride	$CaCl_2 \cdot 2H_2O$	2
9.	Magnesium sulphate	$MgSO_4 \cdot H_2O$	0.5
10.	Zinc chloride	$ZnCl_2$	0.04
11.	Ammonium molybdate	$(NH_4)_6MoO_{24} \cdot 4H_2O$	0.2

The material is separated into a liquid phase and a solid phase. Partially fermented liquid fraction is pumped from the stirring tank to the fermentation reactor with a piston pump which is operated from the console.
Fermentation reactor is hermetically sealed to preserve substrate anaerobic conditions throughout the fermentation process. Inside the fermenter takes place temperature and pH control of the liquid sample. The liquid must have a pH around 7 (neutral), and if necessary is adjusted using acid or base solution contained in the two containers. It should be noted that during the process, the pH tends to became acidic and, hence, needs to be monitored.

Fig. 1 - Small capacity plant for biogas production [8]

The sample subjected to fermentation is heated by a heating element. Fermented mass is taken by means of a pump from the bottom or the top of the reactor, where it is further heated by resistance.
Biogas production process begins after about a day. Before arriving in the storage tank, the gas passes through a series of treatment systems, namely activated carbon filter, drier filter and

carbon dioxide separator. The amount of biogas can be read directly from the gas meter or from the console.

Finally, the biogas is stored in the storage reservoir that consists of four stacked rubber rooms with 120 liter capacity, suitable for biogas storage at atmospheric pressure.

Before connecting the storage tank to the corresponding valve, it is recommended to remove the air contained in the tank. When the ball was emptied, biogas flow sand fills it completely maintaining atmospheric pressure.

For the study was used the same substrate composed of the manure and feeding substances with a C/N ratio of 20.4 (Table 2), the pH waskept constant, and there tention time was one week (from the moment the imposed working parameters are reached) for the three experiments [8].

Table 2. Composition and parameters of substrate[9]

Substrate	Quantity, kg	C/N Ratio	Drymatter, %	Umidity, %
Pigmanure	2	13	13.5	86.5
Cattlemanure	3	25	14	86
Water	150	-	-	-

Organic materials used as a substrate was weighed and placed in the mixing and homogenization tank. Then, the tank was filled with an amount of 150 L of water for fluidization of the substrate because the homogenisation of the substrate in the fermenter is done by recirculation. The substrate was kept under these conditions for two days during which the substrate partially disintegrates in water and begin the bacteria development needed in process of fermentation.

After two days, feeding substances were added in the resulting liquid, in the specified amounts by the plant manufacturer. All of these were mixed using the mixer inside the tank for one hour.

The feeding pump was powered from the control panel in order to transfer the liquid substrate in the fermenter. After filling the digester, the temperature and pH were kept constant automatically throughout the fermentation process. The liquid substrate was re-circulated to reach the required temperature and pH.

The data acquisition system was started to record the biogas flow, temperature and pH changes that occur during fermentation after the liquid meets the required conditions.

RESULTS

The values recorded during the experiments are shown in Table 3 and in Figures 2, 3 and 4 is represented the change in the production of biogas for the temperatures of 25°C, 35°C and 45°C.

Table 3. The biogasquantities for the studied temperatures [8]

Time, h	Biogas production, m³/h		
	for 25°C	for 35°C	for 45°C
4	0	0	0
8	0	0	0.0017
12	0	0.001	0.0025
16	0	0.0013	0.0036
20	0.001	0.002	0.0051
24	0.001	0.0026	0.0072
28	0.0013	0.0034	0.0089
32	0.0016	0.005	0.012
36	0.0016	0.0071	0.017
40	0.0025	0.0084	0.016
44	0.0031	0.014	0.019
48	0.0042	0.012	0.021
52	0.005	0.015	0.018
56	0.0046	0.018	0.019
60	0.0051	0.02	0.022
64	0.006	0.022	0.024
68	0.007	0.021	0.022
72	0.009	0.024	0.024
76	0.011	0.027	0.023
80	0.013	0.027	0.021
84	0.012	0.029	0.022
88	0.015	0.03	0.024
92	0.014	0.031	0.02
96	0.015	0.03	0.019
100	0.015	0.029	0.021
104	0.014	0.032	0.018
108	0.014	0.031	0.017
112	0.013	0.029	0.018
116	0.0125	0.027	0.0185
120	0.013	0.028	0.017
124	0.0125	0.026	0.015
128	0.011	0.027	0.0155
132	0.011	0.025	0.014
136	0.01	0.022	0.0145
140	0.011	0.024	0.0132
144	0.01	0.021	0.0139
148	0.009	0.02	0.0128
152	0.0084	0.022	0.012
156	0.0076	0.019	0.0125
160	0.007	0.016	0.012
164	0.0069	0.016	0.0115
168	0.006	0.015	0.011

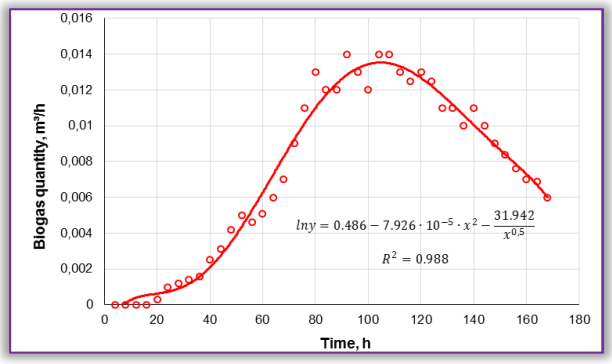

Fig. 2 –Variation of biogas production at 25°C

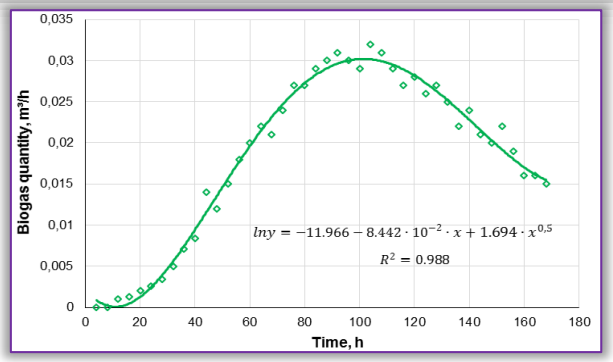

Fig. 3 - Variation of biogas production at 35°C

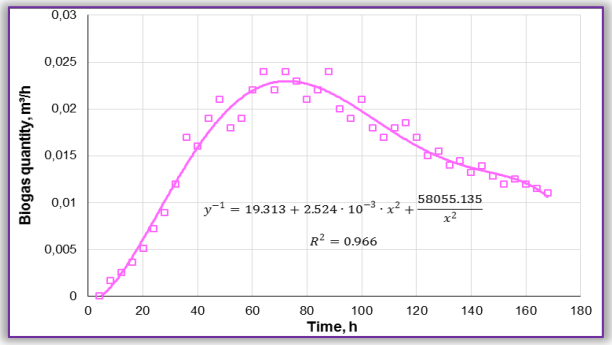

Fig. 4 - Variation of biogas production at 45°C

Experimental data, obtained from the fermentation of a mixture of pig and cattle manure at different temperatures, in the pilot plant RE-biomass with continuous hydraulic stirred cylindrical digester, respectively 25°C, 35°C and 45°C, shows an increasing variation up to a certain moment in the process of fermentation, respectively a decreasing variation in the second part of the test that lasted for approximately 170 hours.

The maximum curve of the biogas production process are recorded after about 110 hours with a value of approximately 0.013 m³/h for the temperature of 25°C; at the end of the test period, the production of biogas records a value of 0.0065 m³/h.

For a temperature of 45°C, the maximum of the biogas production curve is recorded after about 75 hours of fermentation, with a value of about 0.023 m³/h, at theend of the test range, the value is about 0.011 m³/h, which shows that the fermentation process is not over, as in the first case.

The highest biogas production was recorded for the temperature of 35°C after about 100 hours of operation with a maximum value of 0.03 m³/h, but at theend of the test range, the amount of biogas production is at 0.015 m³/h and again the fermentation process is incomplete, being possible the continue.

The variation laws of the biogas production have been identified after the mathematical regression analysis of the data using TableCurve 2D software.

The variation laws of biogas production, for the tests done to determine the effect of temperature on the biogas production that shows the best correlation with the experimental data, are exponential or hyperbolic having a correlation coefficient R^2 of over 0.966.

CONCLUSIONS

Anaerobic digestion is affected by many factors and the results obtained in this work have shown that the temperature is among the most important. In experiments was used the same substrate, the pH waskept constant and the analyzed temperatures were of 25, 35 and 45°C.

The maximum amount of biogas was obtained at 35°C with a total value of 0.7798 m³. Total biogas production values, for the other two temperatures, were 0.3249 m³, for the temperature of 25°C, respectively, 0.6394 m³, for the temperature of 45°C.

References

[1.] Al Seadi Teodorita, D. Rutz, H. Prassl, M. Köttner, T. Finsterwalder, S. Volk, R. Janssen, A. Ofiţeru, M. Adamescu, F. Bodescu, D. Ionescu (2008), Biogazul–ghid practic, ghid elaborate în cadrul proiectului BiG>East (EIE/07/214/SI2.467620)

[2.] Apples L., Assche A.V., Willems K., Degreve J., Impe J.V., Dewil R. (2011), Peracetic acid oxidation as an alternative pre-treatment for the anaerobic digestion of waste activated sludge, Bioresource Technology, no. 102, pp. 4124 – 4130

[3.] Arsova L. (2010), Anaerobic digestion of food waste: Current status, problems and an alternative product, University of Columbia

[4.] Dhaked R.K., Singh P., Singh L., Biomethanation under psychrophilic conditions, Waste Management, vol. 30, pp. 2490-2496, 2010

[5.] Khalid A., Arshad M., Anjum M., Mahmood T., Dawson L. (2011) - The anaerobic digestion of solid organic waste, Waste Management, vol. 31, pp. 1737–1744

[6.] Păunescu I., Paraschiv G.(2006), Instalaţii pentru reciclarea deşeurilor, Editura AGIR

[7.] Real Olvera J., Lopez-Lopez (2012), Biogas production from anaerobic treatment of agro-industrial wastewater, Biogas, InTech, 91-112

[8.] Toma M.L. (2015), Cercetări privind procesul de obţinere a biogazului în instalaţii de mică capacitate. Teză de doctorat. Universitatea Politehnica din Bucureşti

[9.] Vintilă T., Nikolic V. (2009), Integrarea fermentaţiei anaerobe şi captare a metanului în managementul dejecţiilor într-o fermă de vaci de lapte, Institutul de Biotehnologii Aplicate, IBA Timişoara

[10.] Zainol N. (2012), Kinetics of biogas production from banana stem waste, Biogas, InTech, 395-408

ACTA TECHNICA CORVINIENSIS
– Bulletin of Engineering
Tome IX [2016], Fascicule 4 [October – December]
ISSN: 2067 – 3809

[1.]Jimit R. PATEL, [2.]G. M. DEHERI

ON THE PERFORMANCE OF A JENKINS MODEL BASED FERROFLUID SQUEEZE FILM IN CURVED ROUGH ANNULAR PLATES CONSIDERING THE SLIP EFFECT

[1-2.]Department of Mathematics, Sardar Patel University, Vallabh Vidyanagar, Anand, Gujarat, INDIA

Abstract: An endeavour has been made to study the effect of slip velocity on the Jenkins model based ferrofluid lubrication of a squeeze film in curved rough annular plates when the upper surface is described by a hyperbolic function while the lower surface is determined by an expression involving secant function. The roughness effect is analyzed by adopting the stochastic model of Christensen and Tonder while Beavers and Joseph's slip model is deployed to evaluate the influence of slip velocity. The pressure distribution is obtained after solving the associated stochastically averaged Reynolds type equation. Then the load carrying capacity is calculated. The results presented in graphical forms confirm that while the effect of transverse roughness is in general adverse, the magnetization results in sharply increased load carrying capacity. This investigation indicates that the effect of transverse roughness can be minimized to a large extent by the Jenkins model based ferrofluid lubrication. However, for any type of improvement in the performance characteristics the slip parameter is required to be reduced. Lastly, this paper also underlines the crucial role of the aspect ratio especially, when higher negative values of skewness and variance are involved, even if, the curvature parameters are chosen suitably.
Keywords: Annular plates, Roughness, Slip velocity, Jenkins model, Magnetic fluid

INTRODUCTION

Nowadays, many fascinating materials have been attracting the investigators and scientists due to their physical properties and technological usage. One of smart materials is magnetic fluid which is not available free state in nature, but are synthesized. One of the important properties of the magnetic fluid is that they can be retained at a desired location by an external magnetic field. Due to this main property, Ferrofluids have variety of applications in the field of sciences and engineering. Owing to the wide application and property of the magnetic fluids, many researchers have used ferrofluid as a lubricant in different physical geometry of bearing systems. Sinha et al. (1993) discussed the effect of ferrofluid lubrication on cylindrical rollers. Ram and Verma (1999) dealt with the performance of porous inclined slider bearing using ferrofluid lubrication. Osman et al. (2001) investigated the static and dynamic characteristics of magnetized journal bearings lubricated with ferrofluid. Shah and Bhat (2005) worked on the effect of ferrofluid lubrication on a squeeze film between curved annular plates considering rotation of magnetic particles. Deheri et al. (2006) examined the performance of circular step bearings under the presence of a magnetic fluid. Ahmed and Singh (2007) discussed the effect of porous-pivoted slider bearing with slip velocity using ferrofluid. Urreta et al. (2009) studied the effect of hydrodynamic bearing lubricated with magnetic fluids. Patel et al. (2010) investigated the performance of a short hydrodynamic slider bearing in the presence of magnetic fluids. Patel et al. (2012) analyzed the effect of hydrodynamic short journal bearings lubricated with magnetic fluids. All the above investigations have established that the performance of the bearing system gets enhanced due to magnetization.

In the above studies, most of the investigations dealt with no-slip boundary conditions. Beavers and Joseph (1967) obtained the interface between a porous medium and fluid layer in an experimental study and introduced a slip boundary condition at the interface. Salant and Fortier (2004) discussed the numerical analysis of a slider bearing with a heterogeneous slip/no-slip surface. Wu et al. (2006) analyzed the effect of low friction and high load support capacity of slider bearing with a mixed slip surface. Ahmed and Singh (2007) dealt with the performance of magnetic fluid lubrication of porous-pivoted slider bearing with slip velocity.

Wang et al. (2012) numerically analyzed the performance of the radial sleeve bearing with combined surface slip. In all of the above mentioned study, it was obtained that effect of slip remained vital for modifying the bearing performance.

The smoothness of the bearing surfaces were assumed in all the above investigations. But it is almost not possible because, the bearing surfaces could be rough through the manufacturing process and the impulsive damages. Sometimes, even the contamination of the lubricant causes roughness. Many methods have been proposed to find the effect of surface roughness on the performance characteristics of squeeze film bearings. Christensen and Tonder (1969a, 1969b, 1970) modified the stochastic theory of Tzeng and Saibel (1967) to study the effect of surface roughness in general. Quite a good number of research papers (Nanduvinamani et al. (2003), Chiang et al. (2004), Bujurke et al. (2007), Patel et al. (2009), Shimpi and Deheri (2010), Patel and Deheri (2011), Abhangi and Deheri (2012)) adopted the model of Christensen and Tonder (1969a, 1969b, 1970) to study the effect of roughness in different types of bearing systems.

Patel and Deheri (2013) analyzed the performance of a ferro fluid based squeeze film in rotating rough curved circular plates resorting to Shliomis model. It was found that the adverse effect of roughness could be reduced considerably at least in the case of negatively skewed roughness with a suitable choice of curvature parameters. Patel and Deheri (2014) investigated the effect of different porous structures on the performance of a Shliomis model-based magnetic squeeze film in rotating rough porous curved circular plates. It was concluded that the adverse effect of transverse roughness could be compensated by the positive effect of magnetization in the case of negatively skewed roughness, suitably choosing the rotation ratio and the curvature parameters. Patel and Deheri (2014) dealt with the combined effect of slip velocity and surface roughness on the performance of Jenkins model based magnetic squeeze film in curved rough circular plates. It was obtained that the Jenkins model modified the performance of the bearing system as compared to Neuringer-Rosensweig model, but this model provided little support to the negatively skewed roughness for overcoming the adverse effect of standard deviation and slip velocity, even if curvature parameters were suitably chosen.

This paper aims to analyze the effect of slip velocity and roughness on the Jenkins model based ferrofluid lubrication of a curved rough annular squeeze film bearing.

ANALYSIS

Figure 1 shows the squeeze film bearing configuration of two annular plates each of inside radius b and outside radius a. Here, the upper plate and lower plate are considered as in curved geometry and r is the radial coordinate.

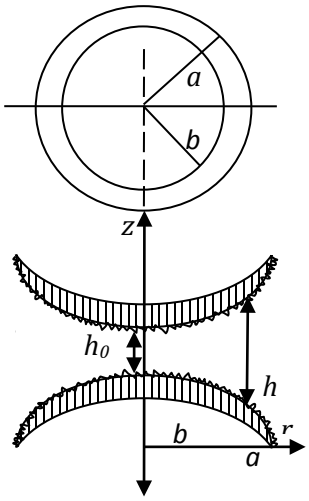

Figure 1. Configuration and geometry of the bearing system

It is assumed that bearing surfaces are transversely rough in the present study. In view of the model for stochastic theory of Christensen and Tonder (1969a, 1969b, 1970), the thickness h of the lubricant film is

$$h = \bar{h} + h_s \qquad (1)$$

where $\bar{h}$ stand for the mean film thickness and h_s represents the deviation from the mean film thickness characterizing the random roughness of the bearing surfaces. h_s is decided by the probability density function

$$f(h_s) = \begin{cases} \frac{35}{32c^7}\left(c^2 - {h_s}^2\right)^3, -c \le h_s \le c \\ 0 \quad , \text{ elsewhere} \end{cases}.$$

wherein c denotes the maximum deviation from the mean film thickness. The mean α, the standard deviation σ and the parameter ε, which is the measure of symmetry of the random variable h_s, are adopted as in the theory of Christensen and Tonder (1969a, 1969b, 1970).

In 1972, Jenkins developed a simple model to state the flow of a magnetic fluid. Later on, it was found that Jenkins model was not only a generalization of the Neuringer- Rosensweig model but also modified both the pressure and the velocity of the magnetic fluid.

Using Maugin's theory, equations of the steady flow turns out to be (Jenkins (1972) and Ram and Verma (1999))

$$\rho(\bar{q}.\nabla)\bar{q} = -\nabla_p + \eta\nabla^2\bar{q} + \mu_0(\bar{M}.\nabla)\bar{H} + \frac{\rho A^2}{2}\nabla \times \left[\frac{\bar{M}}{M} \times \{(\nabla \times \bar{q}) \times \bar{M}\}\right] \qquad (2)$$

together with

$$\nabla.\bar{q}=0,\nabla\times\bar{H}=0,\bar{M}=\bar{\mu}\bar{H},\nabla.(\bar{H}+\bar{M})=0$$

(Bhat (2003). where ρ indicates the fluid density, $\bar{q}$ stand for the fluid velocity in the film region, $\bar{H}$ is external magnetic field, $\bar{\mu}$ denotes magnetic susceptibility of the magnetic fluid, p represents the film pressure, η denotes the fluid viscosity, μ_0 indicates the permeability of the free space, A indicates a material constant and $\bar{M}$ denotes magnetization vector. From equation (2) one establishes that Jenkins model is a generalization of Neuringer- Rosensweig model with the extra term

$$\frac{\rho A^2}{2}\nabla\times\left[\frac{\bar{M}}{M}\times\{(\nabla\times\bar{q})\times\bar{M}\}\right]$$
$$=\frac{\rho A^2\bar{\mu}}{2}\nabla\times\left[\frac{\bar{H}}{H}\times\{(\nabla\times\bar{q})\times\bar{H}\}\right] \quad (3)$$

which modifies the velocity of the fluid.

Let (u,v,w) to be the velocity of the fluid at any point (r,θ,z) between two solid surfaces, with OZ as axis. With the usual assumptions of hydrodynamic lubrication theory and recalling that the flow is steady and axially symmetric, the equations of motion are

$$\left(1-\frac{\rho A^2\bar{\mu}H}{2\eta}\right)\frac{\partial^2 u}{\partial z^2}=\frac{1}{\eta}\frac{d}{dr}\left(p-\frac{\mu_0\bar{\mu}}{2}H^2\right) \quad (4)$$

$$\frac{1}{r}\frac{\partial}{\partial r}(ru)+\frac{\partial w}{\partial z}=0 \quad (5)$$

Solving the equation (4) under the boundary conditions, $u=0$ when $z=0,h$, one arrives at

$$u=\frac{z(z-h)}{2\eta\left(1-\frac{\rho A^2\bar{\mu}H}{2\eta}\right)}\frac{d}{dr}\left(p-\frac{\mu_0\bar{\mu}}{2}H^2\right) \quad (6)$$

Replacing the value of u in equation (5) and integrating it with respect to z over the interval $(0,h)$, one finds the Reynolds type equation for film pressure, as

$$\frac{1}{r}\frac{d}{dr}\left(\frac{h^3}{\left(1-\frac{\rho A^2\bar{\mu}H}{2\eta}\right)}r\frac{d}{dr}\left(p-\frac{\mu_0\bar{\mu}}{2}H^2\right)\right)=12\eta\dot{h_0} \quad (7)$$

It is considered that the upper plate lying along the surface determined by (Bhat (2003), Abhangi and Deheri (2012), Patel and Deheri (2013))

$$z_u=h_0\left[\frac{1}{1+\beta r}\right];\ b\le r\le a$$

approaches with normal velocity $\dot{h_0}$ to the lower plate lying along the surface governed by

$$z_l=h_0[\sec(\gamma r^2)-1];\ b\le r\le a$$

where β, γ and h_0 indicate the upper plate's curvature parameter, lower plate's curvature parameter and the centre film thickness respectively. Therefore, the mathematical expression for the film thickness $h(r)$ is defined by (Bhat (2003), Abhangi and Deheri (2012), Patel and Deheri (2014))

$$h(r)=h_0\left[\frac{1}{1+\beta r}-\sec(\gamma r^2)+1\right];\ b\le r\le a$$

In view of the theory of Christensen and Tonder (1969a, 1969b, 1970), the stochastic averaging of the differential equation (7), under the usual hypothesises of hydro-magnetic lubrication yields (Bhat (2003), Prajapati (1995), Patel et al. (2009)), the modified Reynolds type equation,

$$\frac{1}{r}\frac{d}{dr}\left(\frac{g(h)}{\left(1-\frac{\rho A^2\bar{\mu}H}{2\eta}\right)}r\frac{d}{dr}\left(p-\frac{\mu_0\bar{\mu}}{2}H^2\right)\right)$$
$$=12\eta\dot{h_0} \quad (8)$$

where

$$H^2=K(r-b)(a-r),G=\left(\frac{4+sh}{2+sh}\right)$$
$$g(h)=(h^3+3h^2\alpha+3(\sigma^2+\alpha^2)h+3\sigma^2\alpha+\alpha^3+\varepsilon)G.$$

The following dimensionless quantities are introduced as

$$\bar{h}=\frac{h}{h_0}=\left[\frac{1}{1+BR}-\sec(CR^2)+1\right],R=\frac{r}{b},\bar{\varepsilon}=\frac{\varepsilon}{h_0^3},$$
$$P=-\frac{h_0^3p}{\eta b^2\dot{h_0}},B=\beta b,C=\gamma b^2,k=\frac{a}{b},\bar{s}=sh_0$$
$$\mu^*=-\frac{K\mu_0\bar{\mu}h_0^3}{\eta\dot{h_0}},\bar{A}^2=\frac{\rho A^2\bar{\mu}b\sqrt{K}}{2\eta},$$
$$\bar{\sigma}=\frac{\sigma}{h_0},\bar{\alpha}=\frac{\alpha}{h_0}, \quad (9)$$

Using equation (9), equation (8) reduces to,

$$\frac{1}{R}\frac{d}{dR}\left(\frac{g(\bar{h})}{\left(1-\bar{A}^2\sqrt{(R-1)(k-R)}\right)}R\frac{d}{dR}\left(P-\frac{1}{2}\mu^*(R-1)(k-R)\right)\right)=-12 \quad (10)$$

where

$$g(\bar{h})=(\bar{h}^3+3\bar{h}^2\bar{\alpha}+3(\bar{\sigma}^2+\bar{\alpha}^2)\bar{h}+3\bar{\sigma}^2\bar{\alpha}+\bar{\alpha}^3+\bar{\varepsilon})\bar{G},$$
$$\bar{G}=\left(\frac{4+\bar{s}\bar{h}}{2+\bar{s}\bar{h}}\right)$$

Under the boundary conditions

$$P(1)=P(k)=0 \quad (11)$$

one can derive the solution of equation (10), for the dimensionless pressure distribution, as

$$P=\frac{\mu^*}{2}(R-1)(k-R)$$
$$-6\int_1^R\frac{R}{g(\bar{h})}\left(1-\bar{A}^2\sqrt{(R-1)(k-R)}\right)dR$$

$$+6\frac{\int_1^k \frac{R}{g(\bar{h})}\left(1-\bar{A}^2\sqrt{(R-1)(k-R)}\right)dR}{\int_1^k \frac{1}{Rg(\bar{h})}\left(1-\bar{A}^2\sqrt{(R-1)(k-R)}\right)dR}$$

$$\int_1^R \frac{1}{Rg(\bar{h})}\left(1-\bar{A}^2\sqrt{(R-1)(k-R)}\right)dR \quad (12)$$

The non-dimensional load carrying capacity of the bearing system then, is obtained as

$$W=-\frac{h_0^3 w}{2\pi\eta b^4 \dot{h}_0}=\frac{\mu^*}{24}(k+1)(k-1)^3$$

$$+3\int_1^k \frac{R^3}{g(\bar{h})}\left(1-\bar{A}^2\sqrt{(R-1)(k-R)}\right)dR$$

$$-3\frac{\left[\int_1^k \frac{R}{g(\bar{h})}\left(1-\bar{A}^2\sqrt{(R-1)(k-R)}\right)dR\right]^2}{\int_1^k \frac{1}{Rg(\bar{h})}\left(1-\bar{A}^2\sqrt{(R-1)(k-R)}\right)dR} \quad (13)$$

RESULTS AND DISCUSSION

A scrutiny of equation (13) suggests that the dimensionless load carrying capacity gets increased by

$$\frac{\mu^*}{24}(k+1)(k-1)^3$$

in comparison with the conventional lubricant based bearing system. The increased load is caused due to the fact that the magnetization enhances the viscosity of the lubricant. Further, one can easily notice that the expression found in equation (13) is linear with respect to the magnetization parameter. Consequently, an increase in the magnetization would result in increased load carrying capacity. This is reflected in figures 2-8. As can be seen the load carrying capacity rises sharply. The effect of standard deviation appears to be nominal while the effect of skewness is almost negligible on the distribution of load carrying capacity with respect to the magnetization.

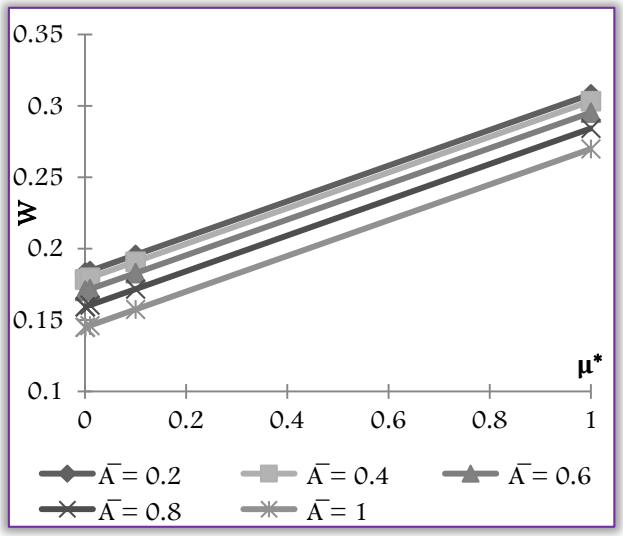

Figure 2. Variation of Load carrying capacity with respect to μ^* and $\bar{A}$.

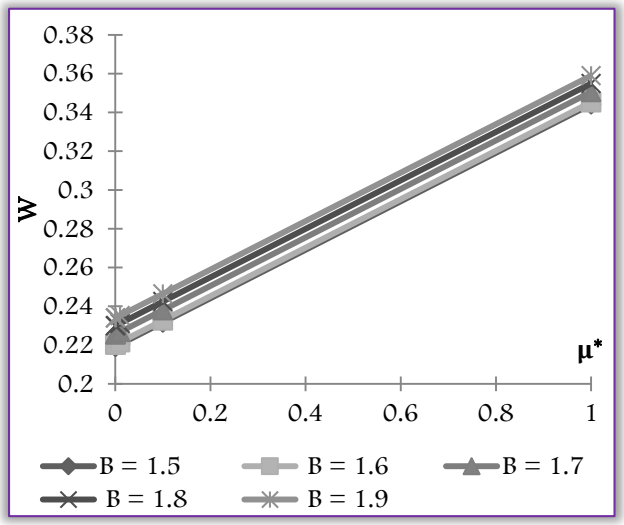

Figure 3. Variation of Load carrying capacity with respect to μ^* and B.

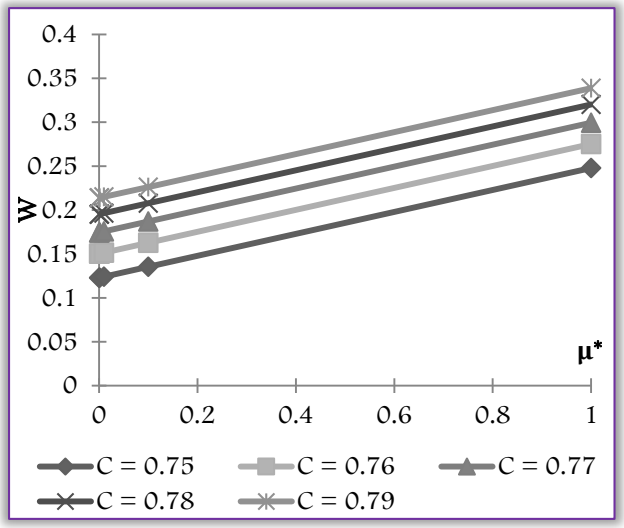

Figure 4. Variation of Load carrying capacity with respect to μ^* and C.

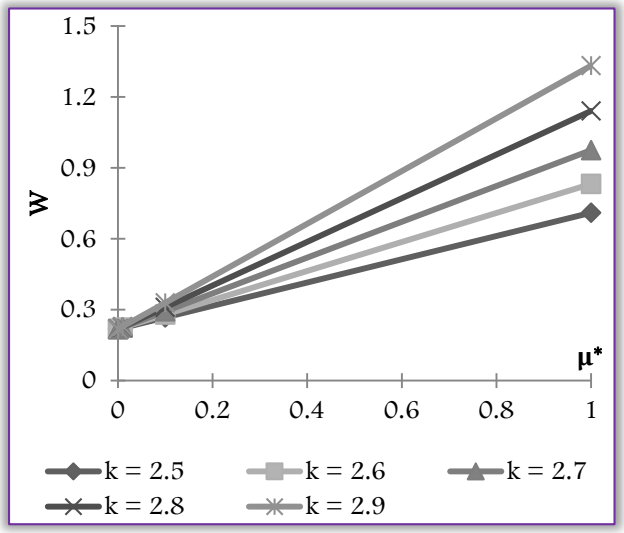

Figure 5. Variation of Load carrying capacity with respect to μ^* and k.

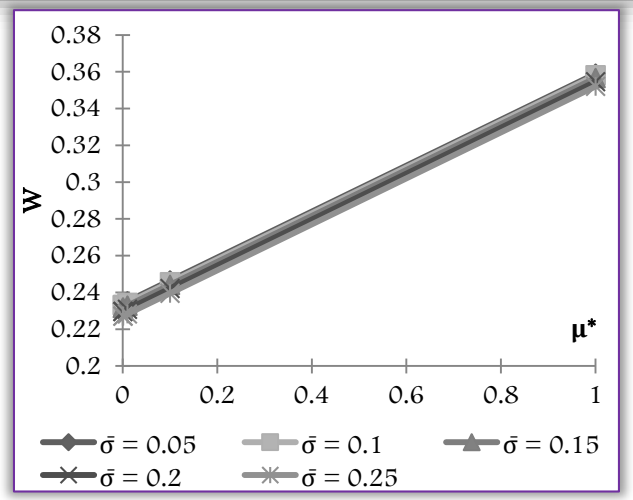

Figure 6. Variation of Load carrying capacity with respect to μ^* and $\bar{\sigma}$.

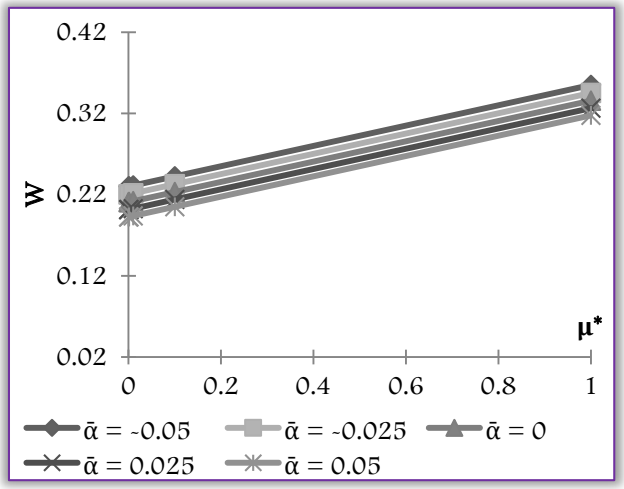

Figure 7. Variation of Load carrying capacity with respect to μ^* and $\bar{\alpha}$.

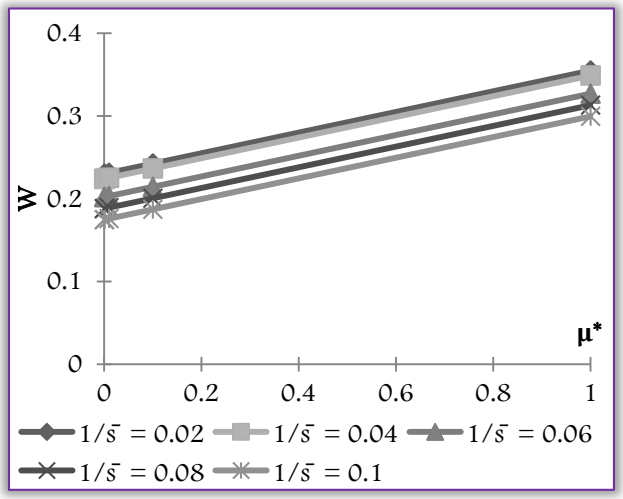

Figure 8. Variation of Load carrying capacity with respect to μ^* and $1/\bar{s}$.

The fact that the material constant parameter causes decreased load carrying capacity can be obtained from figures 9-14. Here the effect of standard deviation is negligible while the effect of skewness is nominal. Further, the effect of aspect ratio remains negligible up to the value of material constant parameter 0.4 (Figure 11).

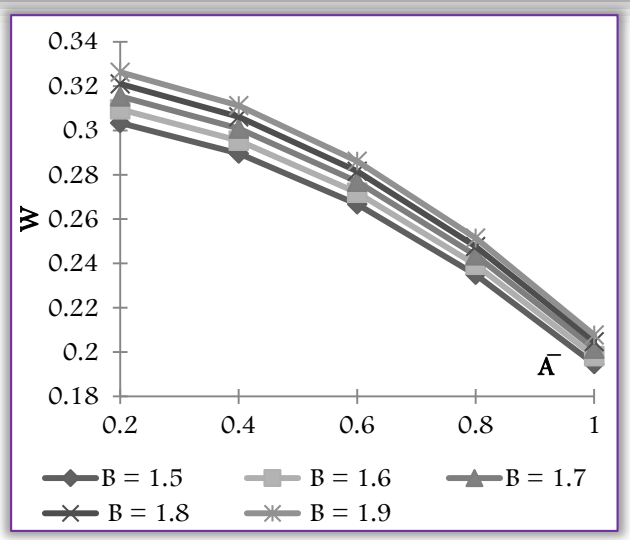

Figure 9. Variation of Load carrying capacity with respect to $\bar{A}$ and B.

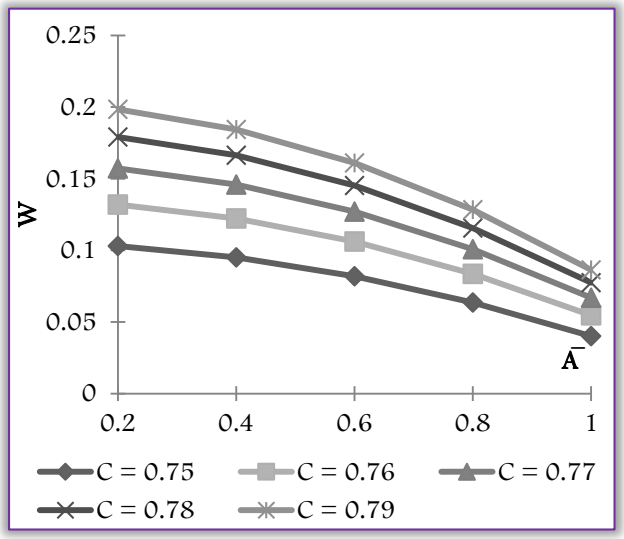

Figure 10. Variation of Load carrying capacity with respect to $\bar{A}$ and C.

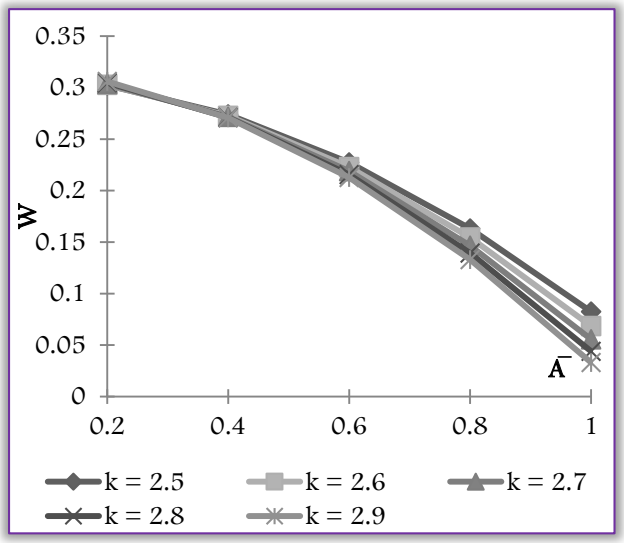

Figure 11. Variation of Load carrying capacity with respect to $\bar{A}$ and k.

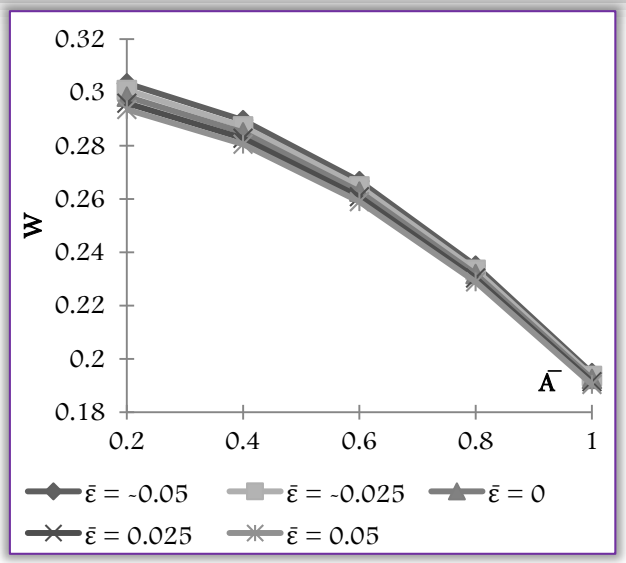

Figure 12. Variation of Load carrying capacity with respect to $\bar{A}$ and $\bar{\varepsilon}$.

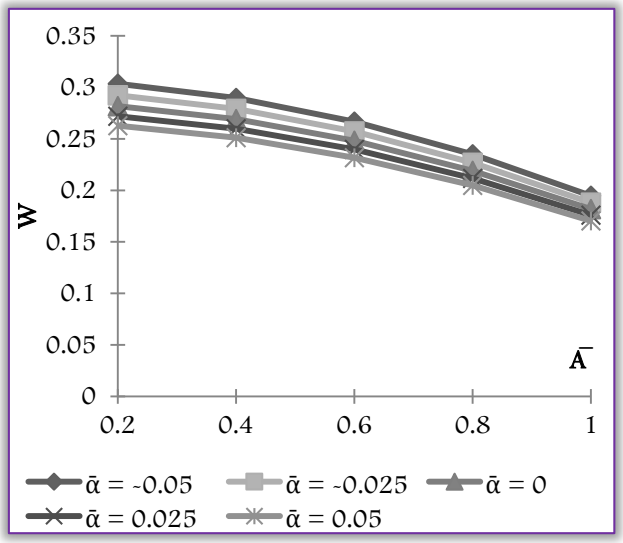

Figure 13. Variation of Load carrying capacity with respect to $\bar{A}$ and $\bar{\alpha}$.

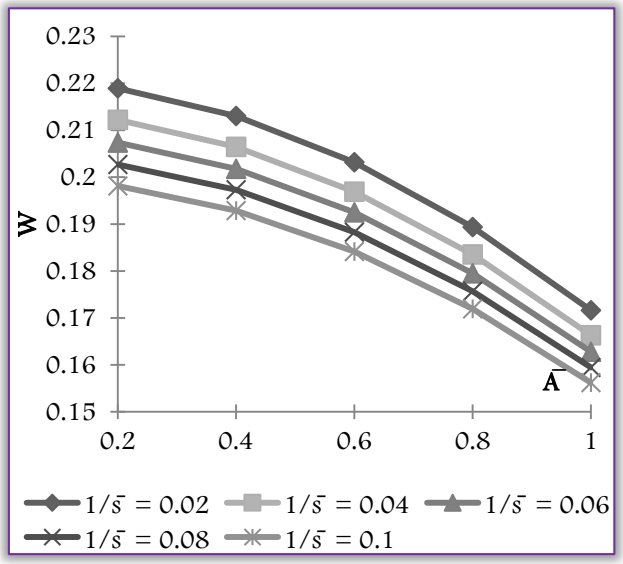

Figure 14. Variation of Load carrying capacity with respect to $\bar{A}$ and 1/$\bar{s}$.

The effect of curvature parameters is described in figures 15-24. It is observed that the load carrying capacity increases with increasing values of the upper plate's curvature parameter. However, the lower plate's curvature parameter follows the path of the upper plate's curvature parameter which is mostly contrary to the other geometrical shapes of the curved surface (Patel and Deheri (2013,2014)). Therefore, for designing this type of bearing system the ratio of curvature parameters must be judiciously chosen to overcome the effect of slip velocity (Figures 20, 24). This can be explained mathematically as the trigonometric function sec is even in nature. Here also, the effect of aspect ratio turns out to be nominal. Further, the effect of skewness can be also regarded when the lower plate's curvature parameter is more then 0.78.

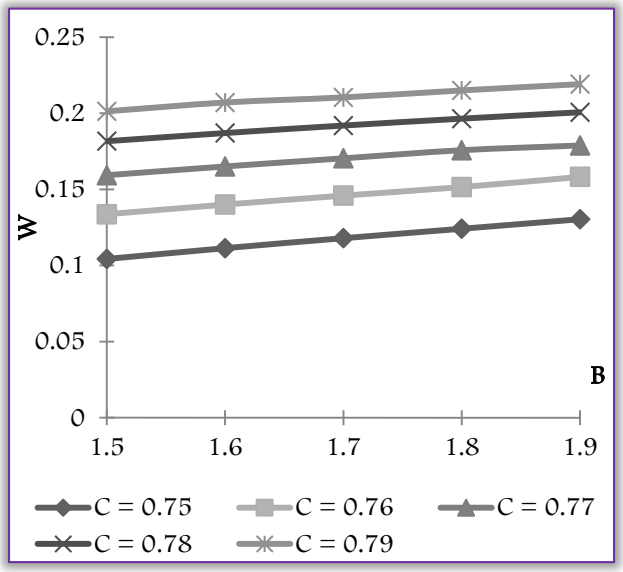

Figure 15. Variation of Load carrying capacity with respect to B and C.

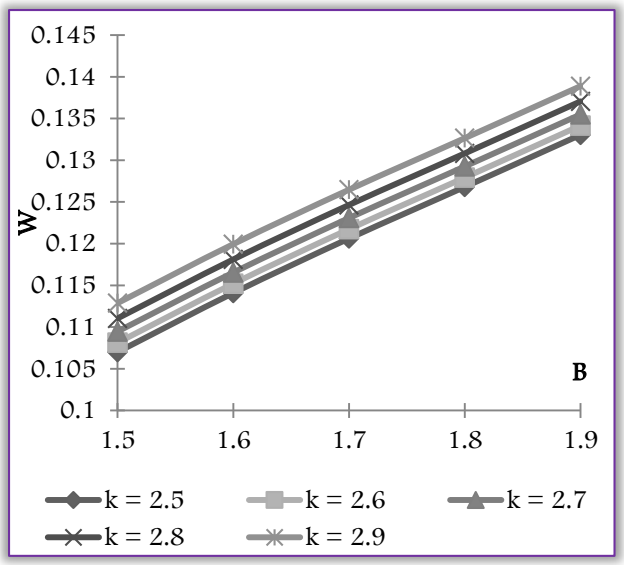

Figure 16. Variation of Load carrying capacity with respect to B and k.

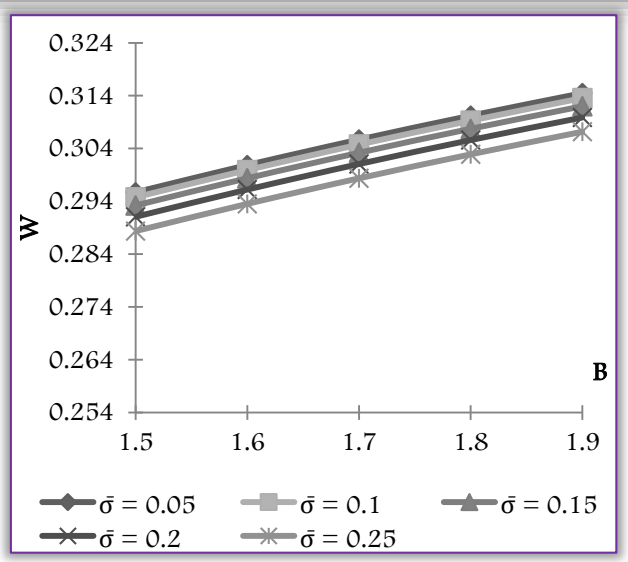

Figure 17. Variation of Load carrying capacity with respect to B and $\bar{\sigma}$.

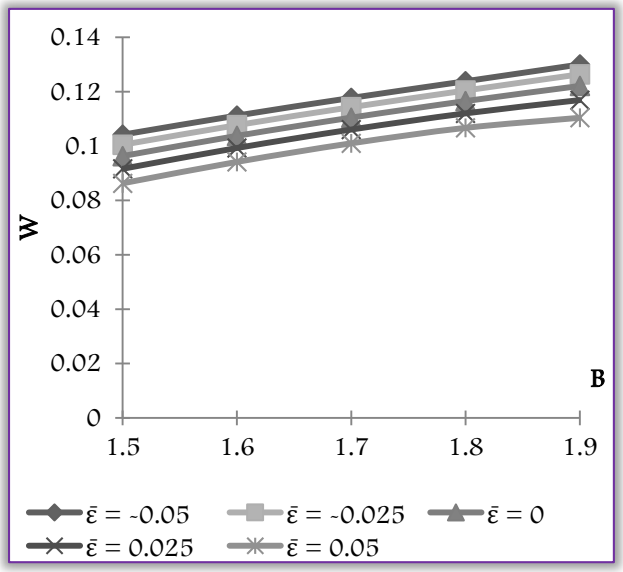

Figure 18. Variation of Load carrying capacity with respect to B and $\bar{\varepsilon}$.

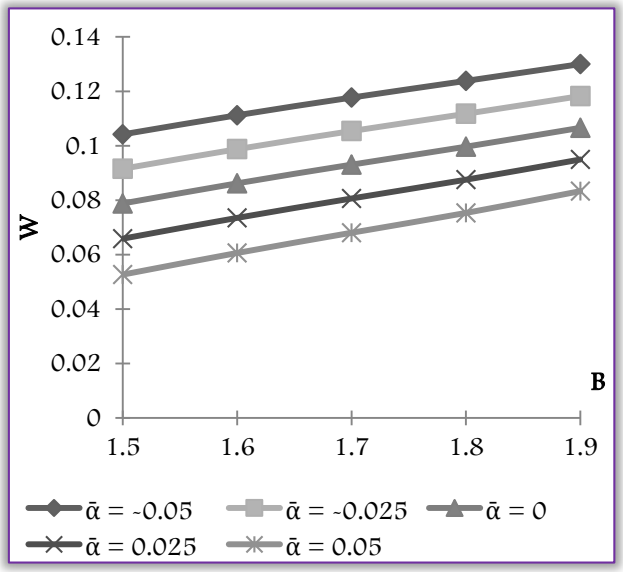

Figure 19.Variation of Load carrying capacity with respect to B and $\bar{\alpha}$.

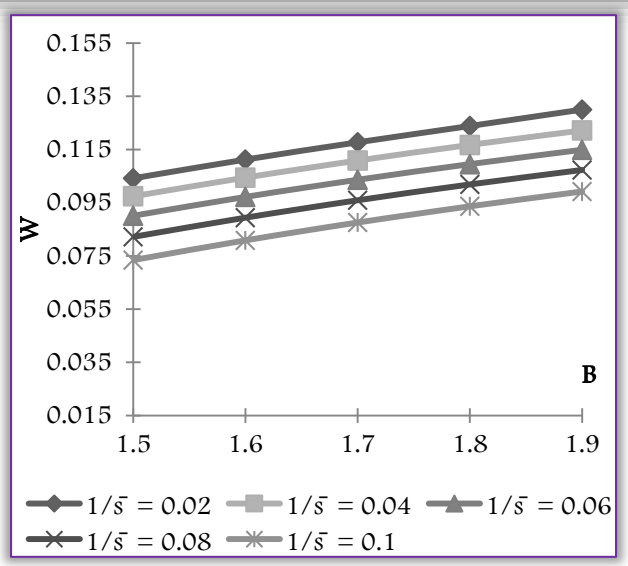

Figure 20. Variation of Load carrying capacity with respect to B and $1/\bar{s}$.

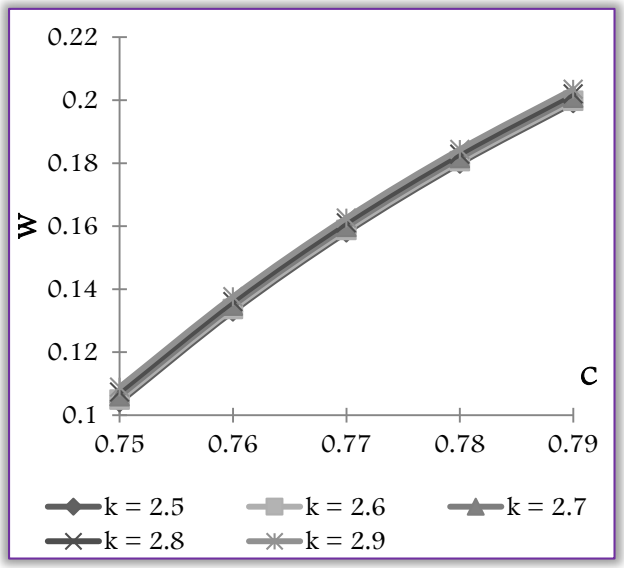

Figure 21. Variation of Load carrying capacity with respect to C and k.

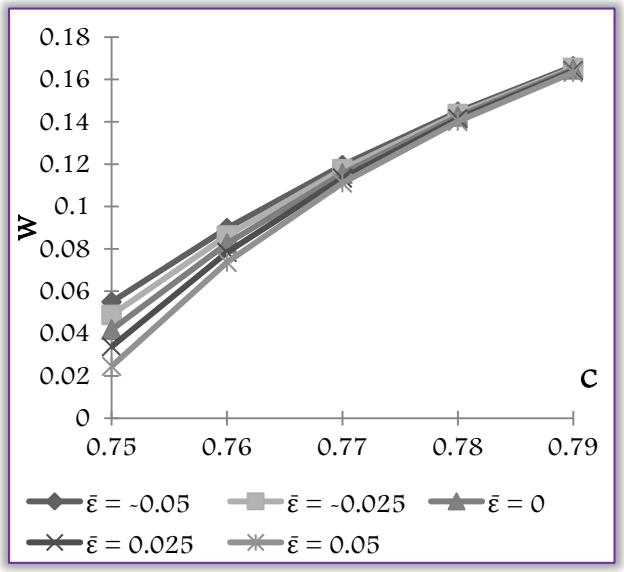

Figure 22. Variation of Load carrying capacity with respect to C and $\bar{\varepsilon}$.

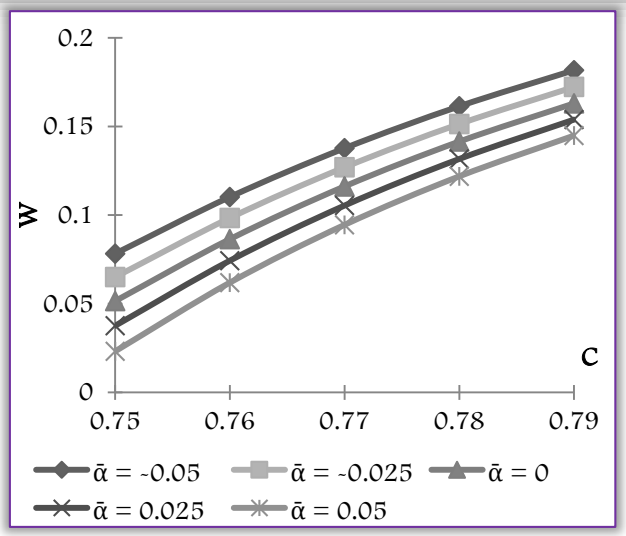

Figure 23. Variation of Load carrying capacity with respect to C and $\bar{\alpha}$.

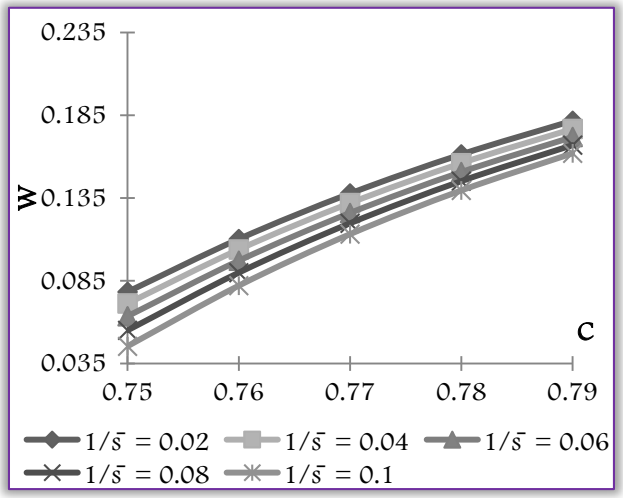

Figure 24. Variation of Load carrying capacity with respect to C and $1/\bar{s}$.

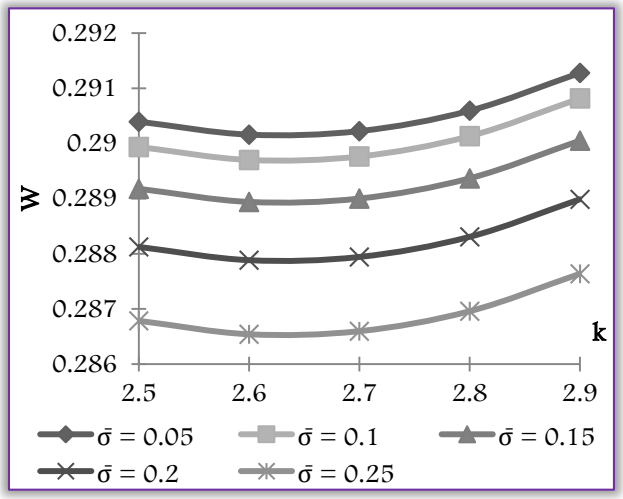

Figure 25. Variation of Load carrying capacity with respect to k and $\bar{\sigma}$.

The effect of aspect ratio k on the performance of this type of bearing system is found from Figures 25-28. It is manifest that the load carrying capacity increases owing to the increasing values of the aspect ratio. Therefore, this study underlines the crucial role of the aspect ratio to improve the performance characteristics of the bearing system.

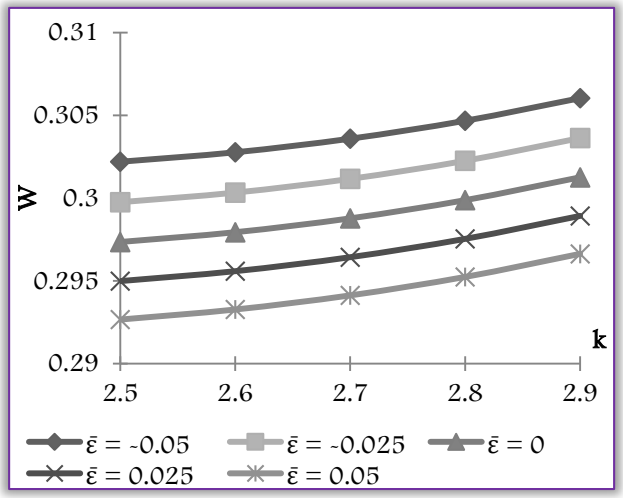

Figure 26. Variation of Load carrying capacity with respect to k and $\bar{\varepsilon}$.

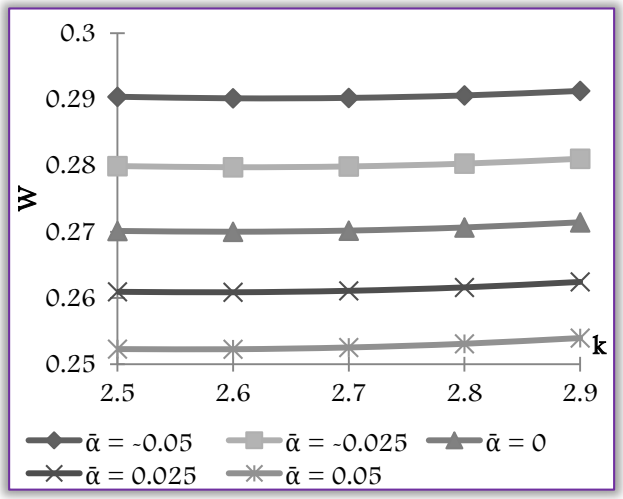

Figure 27. Variation of Load carrying capacity with respect to k and $\bar{\alpha}$.

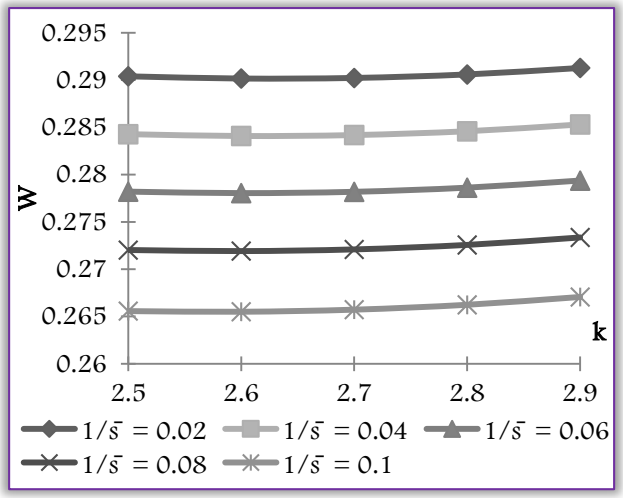

Figure 28. Variation of Load carrying capacity with respect to k and $1/\bar{s}$.

The effect of roughness is presented in figures 29-34. It is noticed that the standard deviation brings down the load carrying capacity while the negatively skewed roughness increases the load

carrying capacity, same being case of variance (-ve). Therefore, this combined positive effect can be channelized to improve the performance of the bearing system. It is clear that slip has a good amount of effect. This effect gets compounded further in the case of standard deviation.

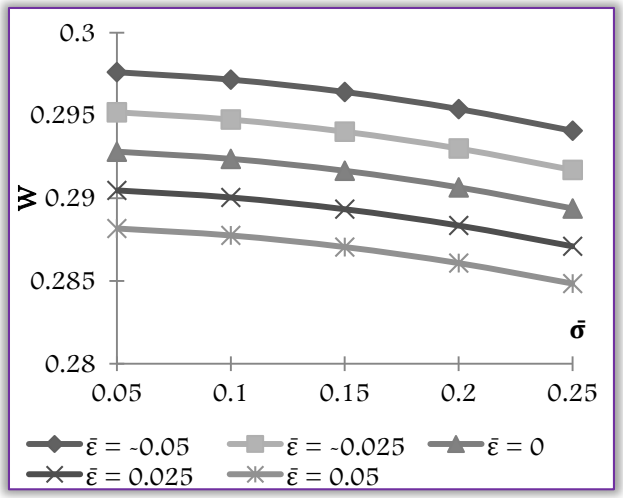

Figure 29. Variation of Load carrying capacity with respect to $\bar{\sigma}$ and $\bar{\varepsilon}$.

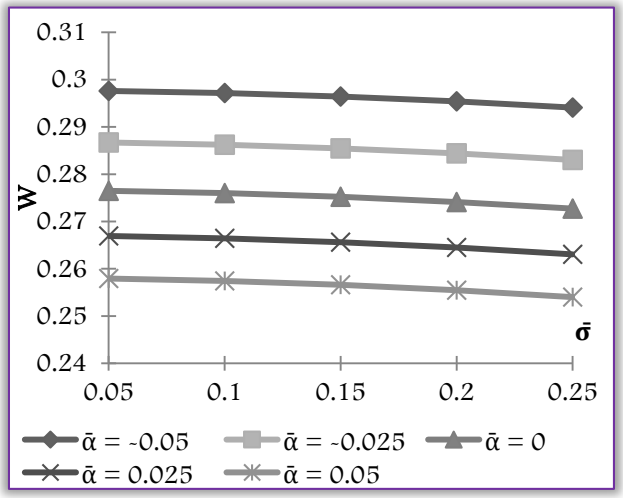

Figure 30. Variation of Load carrying capacity with respect to $\bar{\sigma}$ and $\bar{\alpha}$.

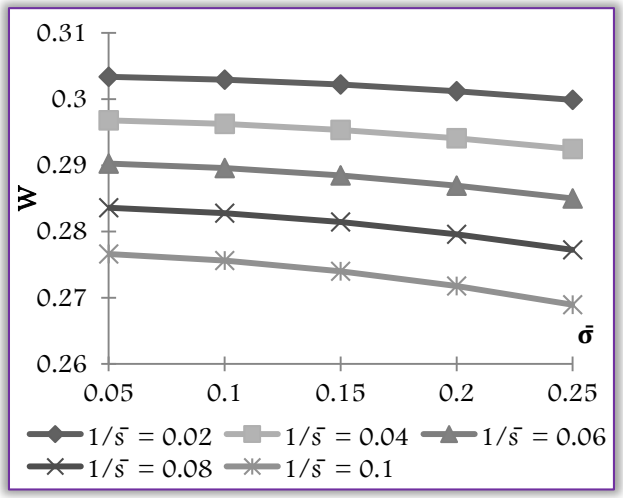

Figure 31. Variation of Load carrying capacity with respect to $\bar{\sigma}$ and $1/\bar{s}$.

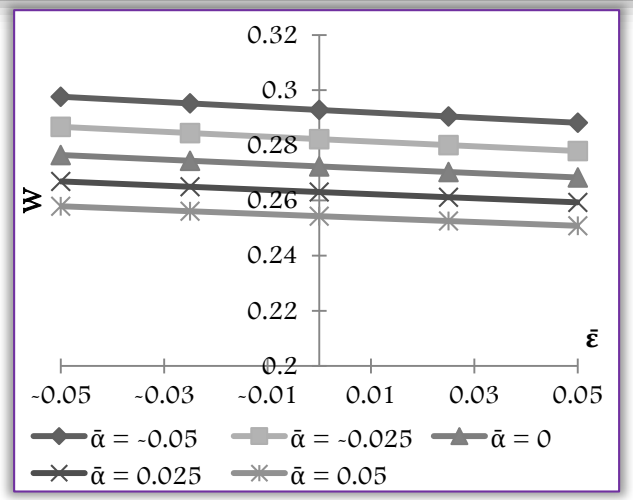

Figure 32. Variation of Load carrying capacity with respect to $\bar{\varepsilon}$ and $\bar{\alpha}$.

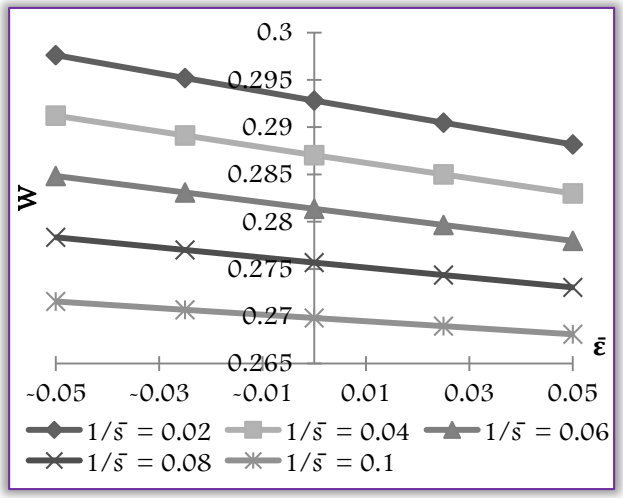

Figure 33. Variation of Load carrying capacity with respect to $\bar{\varepsilon}$ and $1/\bar{s}$.

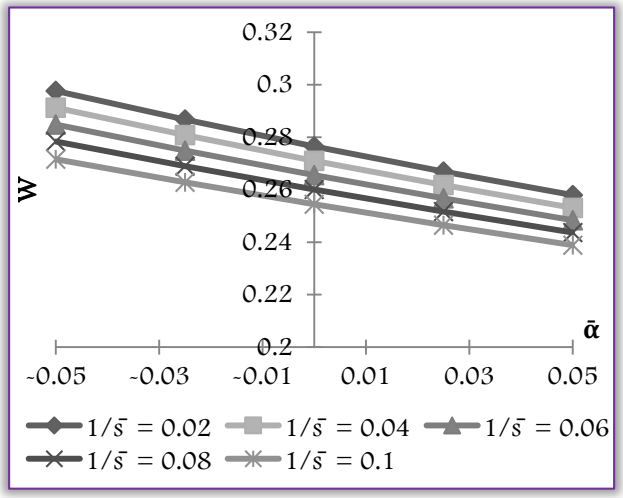

Figure 34. Variation of Load carrying capacity with respect to $\bar{\alpha}$ and $1/\bar{s}$.

There are ample proofs to certify that for any type of improvement in the bearing performance characteristics the slip parameter is required to be kept at reduced level. It is also established from this study that Jenkins model modifies the performance of the bearing system as compared to the case of

Neuringer-Rosensweig model based magnetic fluid flow.

A close glance at the graphs indicates that the Jenkins model based magnetic fluid flow goes to a large extent in minimizing the effect of standard deviation when the slip is at minimum at least in the case of variance (-ve) when negatively skewed roughness is involved.

CONCLUSION

It is visibly clear that the Jenkins model modifies and improves the performance of the bearing system in compensation with the case of Neuringer-Rosensweig model. As the slip parameter causes reduced load carrying capacity, this article makes it mandatory that the roughness must be accounted for while designing the bearing system even if the ratio of curvature parameters is suitably chosen. Further, this article confirms that Jenkins model based magnetic fluid flow may present a better option for the design aspects when the slip velocity is minimized. Lastly, this type of bearing system supports a good amount of load even when there is no flow, which is unlikely, in the case of conventional lubricants based bearing system.

References

[1.] Sinha, P., Chandra, P. and Kumar, D., "Ferrofluid lubrication of cylindrical rollers with cavitation," Acta Mechanica, 98, 27-38, 1993.

[2.] Ram, P. and Verma, P.D.S., "Ferrofliuid lubrication in porous inclined slider bearing," Indian Journal of Pure and Applied Mathematics, 30(12), 1273-1281, 1999.

[3.] Osman, T.A., Nada, G.S. and Safar, Z.S., "Static and dynamic characteristics of magnetized journal bearings lubricated with ferrofluid," Tribology International, 34(6), 369-380, 2001.

[4.] Shah, R.C. and Bhat, M.V., "Ferrofluid squeeze film between curved annular plates including rotation of magnetic particles," Journal of Engineering Mathematics, 51, 317-324, 2005.

[5.] Deheri, G.M., Patel, H.C. and Patel R.M., "Performance of magnetic fluid based circular step bearings," MECHANIKA, 57(1), 22-27, 2006.

[6.] Ahmad, N. and Singh, J.P., "Magnetic Fluid lubrication of porous-pivoted slider bearing with slip velocity," Journal of Engineering Tribology, 221, 609-613, 2007.

[7.] Urreta, H., Leicht, Z., Sanchez, A., Agirre, A., Kuzhir P. and Magnac, G., "Hydrodynamic bearing lubricated with magnetic fluids," Journal of Physics: Conference Series, 149(1), Article ID 012113, 2009.

[8.] Patel, R.M., Deheri, G.M. and Vadher, P.A., "Performance of a Magnetic Fluid-based Short Bearing," Acta Polytechnica Hungarica, 7(3), 63-78, 2010.

[9.] Patel, N.S., Vakharia, D.P. and Deheri, G.M., "A Study on the Performance of a Magnetic-Fluid-Based Hydrodynamic Short Journal Bearing," ISRN Mechanical Engineering, 2012, Article ID 603460, 2012.

[10.] Beavers, G.S. and Joseph, D.D., "Boundary conditions at a naturally permeable wall," Journal of Fluid Mechanics, 30, 197-207, 1967.

[11.] Salant, R.F. and Fortier, A.E., "Numerical Analysis of a Slider Bearing with a Heterogeneous Slip/No-Slip Surface," Tribology Transactions, 47(3), 328-334, 2004.

[12.] Wu, C.W., Ma, G.J., Zhou, P. and Wu, C.D., "Low Friction and High Load Support Capacity of Slider Bearing With a Mixed Slip Surface," Journal of Tribology, 128(4), 904-907, 2006.

[13.] Wang, L.L., Lu, C.H., Wang. M. and Fu, W.X., "The Numerical Analysis of the Radial Sleeve Bearing With Combined Surface Slip," Tribology International, 47, 100–104, 2012.

[14.] Christensen, H. and Tonder, K.C., "Tribology of rough surfaces: stochastic models of hydrodynamic lubrication," SINTEF, Report No.10, 69-18, 1969a.

[15.] Christensen, H. and Tonder, K.C., "Tribology of rough surfaces: parametric study and comparison of lubrication models," SINTEF, Report No.22, 69-18, 1969b.

[16.] Christensen, H. and Tonder, K.C., "The hydrodynamic lubrication of rough bearing surfaces of finite width," ASME-ASLE Lubrication Conference, Cincinnati. OH., Paper no. 70-lub-7, 1970.

[17.] Tzeng, S.T. and Saibel, E., "Surface roughness effect on slider bearing lubrication," ASLE Trans., 10(3), 334-348, 1967.

[18.] Naduvinamani, N.B., Fathima, S.T. and Hiremath, P.S., "Hydrodynamic lubrication rough Slider bearings with couple stress fluids," Tribology International, 36(12), 949-959, 2003.

[19.] Chiang, H.L., Hsu, C.H. and Lin, J.R., "Lubrication performance of finite journal bearings considering effects of couple stresses and surface roughness," Tribology International, 37(4), 297–307, 2004.

[20.] Bujurke, N.M., Naduvinamani, N.B. and Basti, D.P., "Effect of surface roughness on the squeeze film lubrication between curved annular plates," Industrial Lubrication and Tribology, 59(4), 178–185, 2007.

[21.] Patel, H.C., Deheri, G.M. and Patel, R.M., "Magnetic fluid-based squeeze film between porous rotating rough circular plates," Industrial Lubrication and Tribology, 61(3), 140-145, 2009.

[22.] Shimpi, M.E. and Deheri, G.M., "Surface roughness and elastic deformation effects on the behavior of the magnetic fluid based squeeze film between rotating porous circular plates with concentric circular pockets," Tribology in Industry, 32(2), 21-30, 2010.

[23.] Patel, N.D. and Deheri, G.M., "Effect of surface roughness on the performance of a magnetic fluid based parallel plate porous slider bearing with slip velocity," J. Serb. Soc. Comput. Mech., 5(1), 104-118, 2011.

[24.] Abhangi, N.D. and Deheri, G.M., "Numerical modeling of squeeze film performance between rotating transversely rough curved circular plates under the presence of a magnetic fluid lubricant," ISRN Mechanical Engineering, 2012, Article ID 873481, 2012.
[25.] Patel, J.R. and Deheri, G., "Shliomis model based magnetic fluid lubrication of a squeeze film in rotating rough curved circular plates," Caribbean Journal of Science and Technology, 1, 138-150, 2013.
[26.] Patel, J.R. and Deheri, G., "Shliomis model-based magnetic squeeze film in rotating rough curved circular plates: a comparison of two different porous structures," Int. J. of Computational Materials Science and Surface Engineering, 6(1), 29 - 49, 2014.
[27.] Patel, J.R. and Deheri, G., "Combined Effect of Surface Roughness and Slip Velocity on Jenkins Model Based Magnetic Squeeze Film in Curved Rough Circular Plates," International Journal of Computational Mathematics, 2014, Article ID 367618, 2014.
[28.] Jenkins, J.T., "A theory of magnetic fluids," Arch. Rational Mech. Anal., 46(1), 42-60, 1972.
[29.] Bhat, M.V., Lubrication with a Magnetic fluid, India: Team Spirit (India) Pvt. Ltd, India, 2003.
[30.] Patel, J.R. and Deheri, G., "Shliomis Model Based Ferrofluid Lubrication of Squeeze Film in Rotating Rough Curved Circular Disks with Assorted Porous Structures," American Journal of Industrial Engineering, 1(3), 51-61, 2013.
[31.] Patel, J.R. and Deheri, G., "Theoretical study of Shliomis model based magnetic squeeze film in rough curved annular plates with assorted porous structures," FME Transactions, 42(1), 56-66, 2014.
[32.] Prajapati, B.L., On Certain Theoretical Studies in Hydrodynamic and Electro-magneto hydrodynamic Lubrication, Ph.D. Thesis, S.P. University, Vallabh Vidya-Nagar, Gujarat, India, 1995.

ACTA Technica CORVINIENSIS
BULLETIN OF ENGINEERING
ISSN:2067-3809

ACTA TECHNICA CORVINIENSIS
– Bulletin of Engineering
Tome IX [2016], Fascicule 4 [October – December]
ISSN: 2067 – 3809

ACTA TECHNICA CORVINIENSIS – BULLETIN OF ENGINEERING. Fascicule 1 [JANUARY–MARCH]

ACTA TECHNICA CORVINIENSIS – BULLETIN OF ENGINEERING. Fascicule 2 [APRIL–JUNE]

ACTA TECHNICA CORVINIENSIS – BULLETIN OF ENGINEERING. Fascicule 3 [JULY–SEPTEMBER]

ACTA TECHNICA CORVINIENSIS – BULLETIN OF ENGINEERING. Fascicule 4 [OCTOBER–DECEMBER]

ACTA Technica CORVINIENSIS
BULLETIN OF ENGINEERING

ISSN:2067-3809

ACTA TECHNICA CORVINIENSIS
– Bulletin of Engineering
Tome IX [2016], Fascicule 4 [October – December]
ISSN: 2067 – 3809

MANUSCRIPT PREPARATION – GENERAL GUIDELINES

Manuscripts submitted for consideration to **ACTA TECHNICA CORVINIENSIS – Bulletin of Engineering** must conform to the following requirements that will facilitate preparation of the article for publication. These instructions are written in a form that satisfies all of the formatting requirements for the author manuscript. Please use them as a template in preparing your manuscript. Authors must take special care to follow these instructions concerning margins.

BASIC INSTRUCTIONS AND MANUSCRIPT REQUIREMENTS

The basic instructions and manuscript requirements are simple:

- Manuscript shall be formatted for an A4 size page.
- The all margins (top, bottom, left, and right) shall be 25 mm.
- The text shall have both the left and right margins justified.
- Single-spaced text, tables, and references, written with 11 or 12-point Georgia or Times Roman typeface.
- No Line numbering on any pages and no page numbers.
- Manuscript length must not exceed 15 pages (including text and references).
- Number of figures and tables combined must not exceed 20.
- Manuscripts that exceed these guidelines will be subject to reductions in length.

The original of the technical paper will be sent through e-mail as attached document (*.doc, Windows 95 or higher). Manuscripts should be submitted to e-mail: redactie@fih.upt.ro, with mention **"forACTA TECHNICA CORVINIENSIS – Bull. of Eng."**.

STRUCTURE

The manuscript should be organized in the following order: Title of the paper, Authors' names and affiliation, Abstract, Key Words, Introduction, Body of the paper (in sequential headings), Discussion & Results, Conclusion or Concluding Remarks, Acknowledgements (where applicable), References, and Appendices (where applicable).

THE TITLE

The title is centered on the page and is CAPITALIZED AND SET IN BOLDFACE (font size 14 pt). It should adequately describe the content of the paper. An abbreviated title of less than 60 characters (including spaces) should also be suggested. Maximum length of title: 20 words.

AUTHOR'S NAME AND AFFILIATION

The author's name(s) follows the title and is also centered on the page (font size 11 pt). A blank line is required between the title and the author's name(s). Last names should be spelled out in full and succeeded by author's initials. The author's affiliation (in font size 11 pt) is provided below. Phone and fax numbers do not appear.

ABSTRACT

State the paper's purpose, methods or procedures presentation, new results, and conclusions are presented. A nonmathematical abstract, not exceeding 200 words, is required for all papers. It should be an abbreviated, accurate presentation of the contents of the paper. It should contain sufficient information to enable readers to decide whether they should obtain and read the entire paper. Do not cite references in the abstract.

KEY WORDS

The author should provide a list of three to five key words that clearly describe the subject matter of the paper.

TEXT LAYOUT

The manuscript must be typed single spacing. Use extra line spacing between equations, illustrations, figures and tables. The body of the text should be prepared using Georgia or Times New Roman. The font size used for preparation of the manuscript must be 11 or 12 points. The first paragraph following a heading should not be indented. The following paragraphs must be indented 10 mm. Note that there is no line spacing between paragraphs unless a subheading is used. Symbols for physical quantities in the text should be written

in italics. Conclude the text with a summary or conclusion section. Spell out all initials, acronyms, or abbreviations (not units of measure) at first use. Put the initials or abbreviation in parentheses after the spelled-out version.
The manuscript must be writing in the third person ("the author concludes... ").

FIGURES AND TABLES

Figures (diagrams and photographs) should be numbered consecutively using Arabic numbers. They should be placed in the text soon after the point where they are referenced. Figures should be centered in a column and should have a figure caption placed underneath. Captions should be centered in the column, in the format "Figure 1" and are in upper and lower case letters.
When referring to a figure in the body of the text, the abbreviation "Figure" is used Illustrations must be submitted in digital format, with a good resolution. Table captions appear centered above the table in upper and lower case letters.
When referring to a table in the text, "Table" with the proper number is used. Captions should be centered in the column, in the format "Table 1" and are in upper and lower case letters. Tables are numbered consecutively and independently of any figures. All figures and tables must be incorporated into the text.

EQUATIONS & MATHEMATICAL EXPRESSIONS

Place equations on separate lines, centered, and numbered in parentheses at the right margin. Equation numbers should appear in parentheses and be numbered consecutively. All equation numbers must appear on the right-hand side of the equation and should be referred to within the text.

CONCLUSION

A conclusion section must be included and should indicate clearly the advantages, limitations and possible applications of the paper. Discuss about future work.

ACKNOWLEDGEMENTS

An acknowledgement section may be presented after the conclusion, if desired. Individuals or units other than authors who were of direct help in the work could be acknowledged by a brief statement following the text. The acknowledgment should give essential credits, but its length should be kept to a minimum; word count should be <100 words.

REFERENCES

References should be listed together at the end of the paper in alphabetical order by author's surname. List of references indent 10 mm from the second line of each references. Personal communications and unpublished data are not acceptable references.

Journal Papers: Surname 1, Initials; Surname 2, Initials and Surname 3, Initials: Title, Journal Name, volume (number), pages, year.
Books: Surname 1, Initials and Surname 2, Initials: Title, Edition (if existent), Place of publication, Publisher, year.
Proceedings Papers: Surname 1, Initials; Surname 2, Initials and Surname 3, Initials: Paper title, Proceedings title, pages, year.

ACTA Technica CORVINIENSIS
BULLETIN OF ENGINEERING

ISSN:2067-3809

Edited by:

ADVANCED MATERIALS CENTER "ProENGINEERING" Hunedoara
FACULTY OF ENGINEERING HUNEDOARA
UNIVERSITY POLITEHNICA TIMISOARA

with kindly supported by
the Associate Editor:

GENERAL ASSOCIATION OF ROMANIAN ENGINEERS (AGIR)
– branch of HUNEDOARA

Editor / Technical preparation / Cover design:

Assoc. Prof. Eng. KISS Imre, PhD.
UNIVERSITY POLITEHNICA TIMISOARA,
FACULTY OF ENGINEERING HUNEDOARA
ADVANCED MATERIALS CENTER "ProENGINEERING" Hunedoara

Commenced publication year:

2008

ACTA Technica CORVINIENSIS
BULLETIN OF ENGINEERING

ISSN:2067-3809